# Bio-Geochemistry of ovarian cancer : Role of selenium nanoparticles in treatment and copper isotopes in detection of ovarian cancer.

Benoit Toubhans

# THÈSE

Pour obtenir le grade de

**DOCTEUR DE L'UNIVERSITE GRENOBLE ALPES**

**préparée dans le cadre d'une cotutelle *entre la Communauté Université Grenoble Alpes* et Swansea University**

Spécialité : **Sciences de la Terre, de l'Univers et de l'Environnement** Arrêté ministériel : le 6 janvier 2005 – 25 mai 2016

Présentée par


## Benoit TOUBHANS


Thèse dirigée par **Prof. Laurent CHARLET** et **Prof. Steve R CONLAN** codirigée par **Dr. Lewis W FRANCIS et Dr. Alexandra T GOURLAN**

préparée au sein des **Laboratoires Institut des Sciences de la Terre (ISTERRE) et Center for NanoHealth (CNH)** dans **les Écoles Doctorales Terre, Univers, Environnement (TUE) et College of Medicine**

# Bio-Géochimie du Cancer : Utilisation des Nanoparticules de Sélénium dans le traitement et des Isotopes du Cuivre dans la détection des cancers ovariens

Thèse soutenue publiquement le **11 Septembre 2020** ,
devant le jury composé de :

**Mr Claude VERDIER,** DR, Laboratoire Interdisciplinaire de Physique (CNRS, Université Grenoble Alpes), Président

**Mr Philipp RATHERT,** DR, Institut für Biochemie und Technische Biochemie (Universität Stuttgart), Rapporteur

**Mr David HUGHES,** Lecturer, Assistant Professor, School of Biomolecular and Biomedical Science (University College Dublin), Rapporteur

**Mme Nathalie VIGIER,** DR, Laboratoire d'Oceanographie de Villefranche (CNRS, Université Paris 6), Examinatrice

**Professeur Laurent CHARLET,** Professeur, ISTerre (Université Grenoble Alpes), Directeur de Thèse

**Professeur Steve R CONLAN,** Professor, Center For Nanohealth (Swansea University), Directeur de Thèse

**Mr Lewis W FRANCIS**, Assistant Professor, Center For Nanohealth (Swansea University), Co-Directeur de Thèse

**Mme Alexandra T GOURLAN,** MC, ISTerre (Université Grenoble Alpes), Co-Directrice de Thèse

# Bio-Geochemistry of ovarian cancer: Role of selenium nanoparticles in treatment and copper isotopes in detection of ovarian cancer.

**Benoit Toubhans**

**Cotutelle**

Université Grenoble Alpes Institut des Sciences de la Terre (ISTerre), Equipe Géochimie 4D
Ecole Doctorale : TUE (Terre Univers Environnement)

Swansea University, Center for Nanohealth, RGBO group
PhD School: College of Medicine

## Acknowledgments

I would like to thank the Université Grenoble Alpes, the doctoral school TUE and Swansea University Medical School for the funding during the three years of my PhD. They allowed me to fulfil this PhD between Swansea and Grenoble in the best conditions sharing my time between the two labs. I would like to thank all technicians, secretary and doctoral school administrators for their helpful support when I was going through the different administrative challenges.

I'd like to thank my PhD directors. Laurent that trusted me in the first place, trusted the fact that even after 3 years into a teaching program I would still be able to adapt to the research world. Steve that decided since the beginning to set recurrent meeting that helped me a lot in leading my research to high scientific standards allowing publications. Lewis that was their everyday for 3 years, supporting and helping me at any time, correcting my clumsy English writings with the same patience everytime. I can't be more grateful for all what you did for me. Alexandra for the MITI bursary we obtained that released a lot of pressure on my research expenses for those three years.

I'd like to thank the post-doc dream team of the RGBO Jetzi, Seydou, Marcos, Andrea, without you the lab wouldn't be the same.

Dorine and Antoine for hosting me in Lyon every time I had to go to the ENS for my experiments. Martina, Francesca, Carla, Roberto, Claudia, Dom for those numerous diners we cooked altogether during the hard winter months in Swansea. Andrew for being an amazing roommate as well as an amazing friend, slowing your Texan English to teach me few English tricks. Jacques, Tobias, Josefine, Ellie, Maor, Cyril, Amber, Irène and Axel for all that support during my first year as the only biologist in ISTerre.

Corentin, Aurélie, Nelson, who pushed me to come to Grenoble, it changed everything for me and allowed me to have this PhD opportunity.

It wouldn't be possible to make those acknowledgments complete without thanking Victor. More than a friend, I can't be more grateful for all you have done for me in the past 8 years, we've grown up together in many ways. Amongst all the trips we did together, you came with me around the UK when I was going to Swansea because everybody knows the shortest way to go to Wales is through John O'Groats. You were the first supporting me in my decision to go back to research for this PhD, finishing what I started when I joined the ENS.

I finally would like to thank my family for supporting me for those 28 years so far. My mother who keeps worrying about me because she wouldn't accept not doing enough for her children, I'm fine mum, and my father whose experience always proved to be right, both being guides in the decision I had to make through the years.

## Abstract

Ovarian cancer is the seventh most common cancer in women with five-year survival rates of less than 45%, and only 20% of cases are detected at early stages of the disease. Major challenges still exist to treat this lethal disease.

The development of new drugs that target better cancer cells and reduce side effects is highly needed. Selenium at high doses has been shown to act as a cytotoxic agent, with potential applications in cancer treatment. However, clinical trials have failed to show any chemotherapeutic value of selenium at safe and tolerated doses (<90 μg/day). To enable the successful exploitation of selenium for cancer treatment, I evaluated inorganic selenium nanoparticles (SeNP), and found them effective in inhibiting ovarian cancer cell growth. In both SKOV-3 and OVCAR-3 ovarian cancer cell lines SeNP treatment resulted in significant cytotoxicity. The two cell types displayed contrasting nanomechanical responses to SeNPs, with decreased surface roughness and membrane stiffness characteristic of OVCAR-3 cell responses. In SKOV-3, cell membrane surface roughness and stiffness increased, both are properties associated with decreased metastatic potential. Very excitingly I made the novel discovery that SeNPs dramatically increase histone methylation at three histone marks, namely H3K4, H3K27 and H3K9. This effect was partially blocked by pharmacological agents that blocked histone methyltransferase (HMT) function. Gene expression profiling of SeNP treated cells through RNA sequencing demonstrated that Se caused upregulation and downregulation of HMTs expression suggesting one mechanism for its ability to alter histone methylation. Further interrogation of RNA seq data showed the SeNPs impact on the expression of genes linked to hallmarks of cancer such as DNA repair activation, ROS response, extracellular matrix organization. The beneficial effects of SeNPs on ovarian cancer cell death appear to be cell type dependent, and due to their low in vivo toxicity, offer an exciting opportunity for future cancer treatment.

Finally, following on from recent studies in breast and colorectal cancer patients revealing that measurement of circulating copper isotopes ($^{63}Cu/^{65}Cu$ ratio) can be related to cancer development I investigated this in biosamples from ovarian cancer patients (blood and tissue). A significant decrease in copper isotopic ratios in the serum of cancer donors was observed demonstrating the potential effectiveness of $^{63}Cu/^{65}Cu$ for the blood-based detection of ovarian cancer.

## Résumé

Le cancer des ovaires est le septième cancer le plus commun chez les femmes dont le taux de survie à 5 ans est en deçà de 45% et dont le taux de détection des premiers stades de développement est inférieur à 20%. Avant d'arriver à un traitement, de nombreux défis restent à relever.

Le développement de nouveaux traitements ciblant spécifiquement les cellules cancéreuses en réduisant les effets secondaires liés au traitement est nécessaire. Pour cela, le Sélénium a été étudié et a démontré à forte doses d'être efficace contre les cellules cancéreuses in vitro. De plus, les essais cliniques ont montré que l'utilisation de doses tolérables de sélénium (<90µg/jour) n'avait pas d'effet thérapeutique contre le cancer. Le développement de nouvelles formes de sélénium afin d'augmenter les doses administrées est donc nécessaire afin d'atteindre l'effet thérapeutique souhaité. Au cours de cette thèse j'ai mesuré l'effet de formes agrégées de sélénium appelées nanoparticules et démontré leur capacité à inhiber la croissance de cellules cancéreuses ovariennes. Dans les lignées cellulaires cancéreuses ovariennes SKOV-3 et OVCAR-3, le traitement aux SeNPs a déclenché la mort cellulaire. La mesure des propriétés nanomécaniques de ces deux lignées cellulaires après traitement a démontré un effet différent des SeNPs en fonction du type cellulaire. Les cellules OVCAR-3 ont vu diminuer leur rugosité de surface ainsi que leur rigidité cellulaire alors que les cellules SKOV-3 ont augmenté leur rigidité et leur rugosité, ces deux caractéristiques étant liées à une diminution de leur potentiel métastatique. De plus, le traitement aux SeNPs a augmenté de manière considérable la méthylation de trois lysines de l'histone 3 H3K4, H3K27 et H3K9. Cette méthylation a pu être bloquée par l'utilisation d'inhibiteurs de méthyltransférases spécifiques de ces marqueurs. L'étude du profil d'expression des deux lignées cellulaires après traitement a démontré le fait que le sélénium induit des modifications d'expression des méthyltransférases nous permettant de suggérer un mécanisme d'action du sélénium. De plus les SeNPs ont démontré leur impact sur l'expression marqueurs cancéreux comme l'activation de la réparation de l'ADN, la réponse aux espèces réactives de l'oxygène, la réorganisation de la matrice extracellulaire. L'effet des SeNPs semble dépendant du type cellulaire cependant leur bonne tolérabilité in vivo offre de bonnes perspectives d'utilisation en tant que traitement du cancer.

Enfin, dans la continuité de récentes études sur le cancer du sein le cancer colorectal s'intéressant à la mesure des isotopes du cuivre (rapport $^{63}Cu/^{65}Cu$) et démontrant leur potentiel dans la détection du développement de ces cancers, j'ai pu mesurer le contenu isotopique de biopsies et de prélèvements sanguins issus de patientes atteintes de cancers ovariens. J'ai pu mesurer une diminution significative du rapport des isotopes du cuivre dans le sérum des patientes cancéreuses en comparaison avec des témoins sains démontrant l'efficacité de détection des cancers par la mesure des isotopes du cuivre dans le sang.

# Contents


**INTRODUCTION** **1**

**I. Ovarian cancer** **1**

1. The disease 1
2. Biomechanical process during cancer progression 6
3. Current diagnostics and new developments 7
4. 'Classic' Ovarian Cancer treatments 10
5. 'New' Ovarian Cancer treatments 11
6. Nanomedicines and Ovarian Cancer 11

**II. Epigenetics** **16**

1. Definition 16
2. Transcription activation mark (H3K4) 19
3. Transcription repression mark (H3K27) 20
4. Heterochromatin mark (H3K9) 21
5. Current knowledge of the effect of epigenetics in ovarian cancer 22

**III. Selenium in cancer treatment** **24**

1. Dietary window of selenium and metabolism 24
2. Low dose of selenium triggers ROS scavenging 27
3. High doses of selenium are cytotoxic 30
4. Effect of selenium on epigenetic mechanisms 33
5. Selenium Nanoparticles 33

**IV. Objectives** **37**

**SELENIUM NANOPARTICLES TRIGGERS ALTERATIONS IN OVARIAN CANCER CELLS BIOMECHANICS** **38**

**I. Presentation of the article** **38**

**II. Article** **40**

**SELENIUM NANOPARTICLES INDUCE GLOBAL HISTONE METHYLATION CHANGES IN OVARIAN CANCER CELLS** **52**

**I. Presentation of the article** **52**

**II. Article** **55**

**CU ISOTOPE RATIOS ARE MEANINGFUL IN OVARIAN CANCER DIAGNOSIS** **77**

**I. Presentation of the article** **77**

**II. Article** **80**

**CONCLUSION AND PERSPECTIVES** **87**

**I. Conclusions** **87**

**II. Perspectives** **88**

**REFERENCES** **93**

# Introduction

## I. Ovarian cancer

### 1. The disease

Cancer is characterized by an abnormal and uncontrolled growth of cells[1]. This transformation is due to genomic instability and specific gene mutations that have been linked to cancer cells being able to adapt to, and regulate, their local micro environment[1]. Tumorigenic processes are distinct and have been well characterised, exhibiting hallmarks linking to biological functions that are unique to cancer cells[1] (Figure 1). Cancer cells have a unique ability to sustain proliferative signalling by activation of growth factors expression, evade growth suppressors notably p53 (signalling DNA damages) mutation, activate invasive and metastatic processes, enable replicative immortality, induce angiogenesis to increase oxygen and nutrient availability, and resist cell death by circumventing apoptosis[2]. In addition, cancer cells have been shown to deregulate their energy metabolism and avoid the immune cell surveillance mechanisms[1].

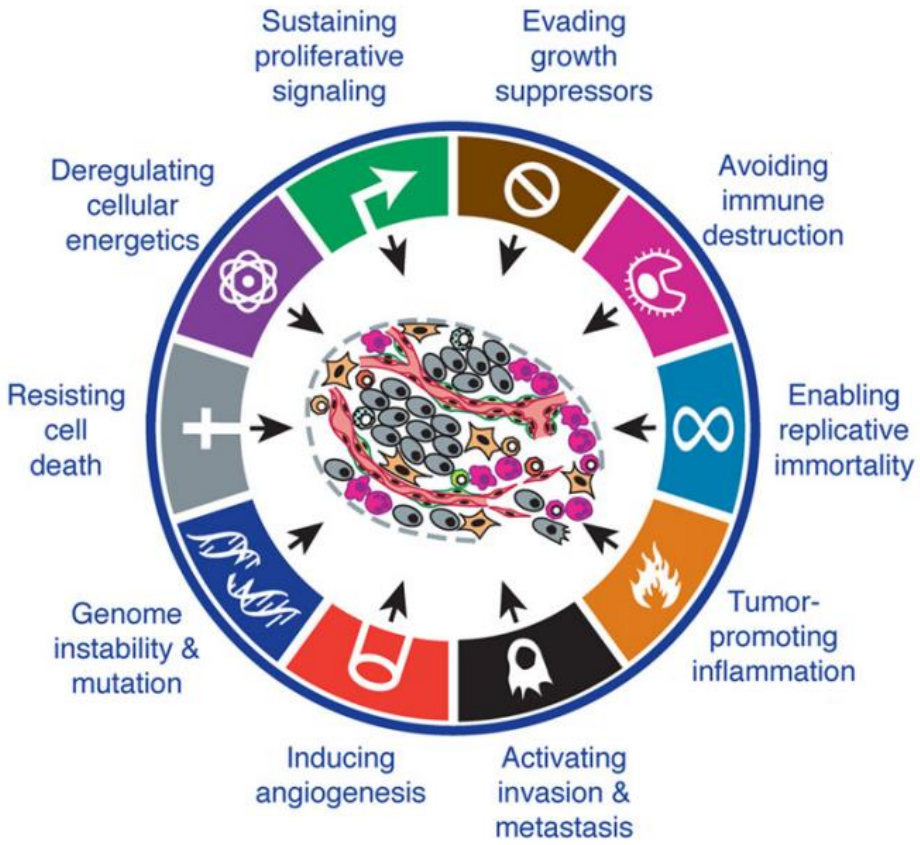


***Figure 1 Hallmarks of cancer***[1]

*Cancer cells are cells that divide without control and resist to cell death due to genomic instability. The growth of tumours can lead to induced angiogenesis responsible for metastatic dissemination.*

## i. Epidemiology

Ovarian cancer is the most common cancer in women with 295,400 cases in 2018 and the 6th most lethal with 184,800 mortalities reported worldwide that year[3]. The incidence has been increasing during the last decade with 1.3% of the women in the UK and 3.8% in France being affected by the disease[4]. Ethnicity has been correlated with the prevalence with 1.64 times more black women than other ethnic groups developing ovarian cancer.

Different symptoms of early stage such as abdominal and pelvic pain, irregular menarche, change in bowels habits and increase urinary frequency[5] have been identified however these are not specific to ovarian cancer. More severe symptoms are often indicating that ovarian cancer has developed. Survival rates of late detection drops with only 35% of UK patients surviving within 5 years[6] whereas the early detection lead to an 90% chance of survival[4,7].
Despite the fact that the survival rate have been increasing in the last 20 years due to better detection and development of new chemotherapies (PARP inhibitors for example), amongst the high grade carcinomas ovarian cancer remains the deadliest gynaecological cancer (35% survival rate) compared to an 80% 5-years survival for breast cancer, 70% for endometrial cancer and 60% for cervical cancer[8,9].

## ii. High Grade Serous Ovarian Cancer (HGSOC)

### Risk Factors

Ovarian cancer most often affects women between the ages of 75 and 80 years [10,11]. Two hypotheses have been suggested to explain the development of High Grade Serous Ovarian Cancer (HGSOC). Firstly ovulation creates a lesion of the ovarian epithelium that needs to be repaired. This highly inflammatory microenvironment may lead to DNA damage, replication errors and malignant transformations[12,13]. Incessant ovulation with an early menarche has been related to an increase prevalence of low grade ovarian cancer[14,15].

Secondly, the development of Ovarian Cancer has been related to the onset of menopause. During menopause the ovaries are unable to respond to hormonal stimuli stopping the feedback of gonadotropins[16]. The higher level of oestrogen compared to progesterone then results in higher oestrogen exposure by ovarian epithelial cells increasing the risk to develop ovarian cancer[5,17].

Obesity is another risk factor due to high androgens which can be converted into oestrogen in adipose tissue by aromatase[11,17,18]. A decrease in blood sex hormone binding globulins can also result in an increase in the relative amount of free oestrogen. Finally, the use of hormonal therapy such as infertility drugs (gonadotropin releasing-hormone antagonists or clomiphene)[16,17] have been determined as risk factors.

Hereditary factors are also linked to an overall 5% to 10% [17] risk of developing OC when one immediate relative has had OC . This is due to the inherited mutation of *BRCA* genes which increases the chance to develop OC for women of the age of 70 with *BRCA1* mutation by 63%

and by 27% for *BRCA2* mutation[19]. *BRCA1* and *2* are involved in DNA repair, maintenance of genome stability and function as tumour suppressors[20]. The use of progesterone-based oral contraceptives for at least 4 years has been related to a decrease of ovarian cancer risk by 50% in women with a *BRCA* mutation[21] by blocking ovulation. Genetic mutations are not limited to *BRCA1/2* genes inducing instability in genome[22] with deficiencies in homologous recombination, impairing the repair of the DNA also reported[23]. Several suppressor genes and oncogenes have been associated with ovarian cancer. P53 and mismatch repair (*MMR*) or double strand break repair system (*CHEK, RAD1*) mutations have also been related to cancer development[4,11,17].

Finally, epigenetic modifications have also be related to malignant development and progression of ovarian cancer. Hypermethylation of *BRCA1* and *2* promoters has been related to a decrease in the efficacy of DNA repair of spontaneous mutations in ovarian epithelial cells[24]. Hypermethylation of CpG islands have been found to be related with tumour development in comparison with normal tissues[25].

**Metastasis**

Cancer metastasis is the leading cause of cancer death accounting for 90% of ovarian cancer cases[26]. Ovarian cancer has a unique mode of development, disseminating locally in the peritoneal cavity and rarely beyond[27,28]. Peritoneal dissemination occurs by movement of ovarian cancer cells in the peritoneal fluid (also called ascites)[29]. Dissemination happens either when the tumour has grown extensively in the organ and caused rupture of the ovary surface or when tumour arises from the surface of the ovary. This dissemination is accompanied by molecular alterations in cells and notably through a cadherin switch involving overexpression of E-cadherin (Figure 2), and activation of N-cadherin expression which is a mesenchymal marker and vimentin expression[30]. Moreover the phenotype of the cells is modified as they undergo an epithelial to mesenchymal transition [26,31].
Once in the peritoneal cavity, ovarian cancer cells undergo two different paths. Isolated cells undergo anoikis as they lost interaction with extracellular matrix and other cells while multicellular aggregates[32] formed in the peritoneal cavity form spheroids that can seed in multiple distal sites. The invasion of secondary sites is facilitated by the remodelling of the extracellular matrix of the mesothelial lining at these locations by matrix metalloproteases.

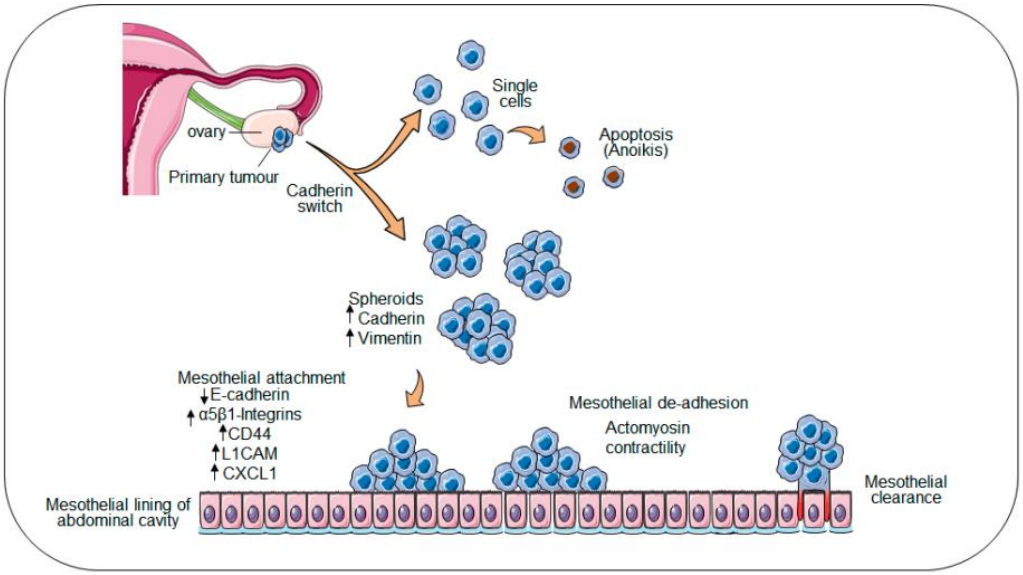


***Figure 2: Modification of the membrane expression profile of the cells in the primary tumour to their dissemination[30].***
*Dissemination of ovarian cancer cells from the primary tumour to the peritoneal cavity through ascitic fluid is accompanied with cadherin switch allowing the formation of spheroids which can land on the mesothelial lining of the abdominal cavity. This attachment leads to a second set of modifications of the cellular properties in their interactions with other cells and cancer cells acquire the ability to go through the peritoneum.*

The colonisation of secondary sites involves the interaction between ovarian cancer cells and mesothelium cells of the peritoneal cavity[28] switching the cancer cells from a proliferative to an invasive phenotype that is translated by an increase of integrin expression[33].

The adhesion of the spheroids on the surface of the mesothelium causes a decrease of E-cadherin and increase of CD44[34,35]. This docking triggers the expression of fibronectin by the mesothelium increasing the interaction with the integrin of the cancer cells[36]. CD44 and L1CAM are crucial for secondary tumour formation[35]. Blocking CD44 or L1CAM expression has been shown to reduce mesothelial adhesion[37] (Figure 2). Once docked the spheroids initiate infiltration and spread to surrounding tissues.

The dissemination through the peritoneum is a passive mechanism involving the circulation and accumulation of ascitic fluid[27]. In comparison with the surrounding environment of other solid tumours, the malignant ascitic fluid accumulating in the peritoneal cavity during ovarian cancer progression is uniquely constituted forming of highly inflammatory environment due to macrophage activation[38]. The circulation of ascitic fluid transports the spheroids allowing them to spread and attach throughout the peritoneal cavity forming nodules mainly on the omentum but also on the diaphragm, liver or lungs[23,39]. The ascitic fluid is constantly changing with the evolution of the pathology and plays a major role in tumour progression, spheroid formation, tumour dissemination. For example, lysophosphatic acid which is present in ascites or ovarian cancer patients promotes motility and invasiveness of cancer cells via induction of expression of metalloproteases that modify the extracellular matrix of the mesothelium[33]. Moreover the

increase of CXCL12 released by epithelial ovarian tumoral cells in the ascitic fluid acts as autocrine and paracrine stimulation inducing increased expression of integrins by ovarian cancer cells leading to increased migratory potential. Finally after cancer cell implantation, synthesis of pro-inflammatory TNF-α by ovarian cancer cells stimulates endothelial cells[40] to secrete interleukins enhancing angiogenesis at metastatic tumour sites. The accumulation of ascitic fluid is not well understood but it is thought that vascular endothelial growth factor (VEGF) is involved[41]. VEGF promotes angiogenesis inducing in vitro the formation of confluent microvascular endothelial cells that invade collagen gels and form capillary structures. Its overexpression has been detected in some cancer patients and allow the creation of a more favourable environment for the new implant.

## iii. Different forms of Ovarian Cancer

Ovarian cancer cells can originated from cells of ovarian epithelial surfaces[42], from the epithelium of distal fallopian tubes [43] or from peritoneal cavity epithelium[26]. Epithelial ovarian cancer is the most common tumour type accounting for 90% of the cases[44]. They are separated in 2 categories depending on the pathway of tumorigenesis (Histotypes are detailed in figure 3).

Type I is comprised of low grade serous, endometrioid, mucinous and clear cell carcinomas originating from lesions in the ovary[45]. They are slow growing tumours and characterized by a stable genome and do not carry a p53 mutation, however they have a mutation in KRAS gene, which is involved in the RAS/MAPK pathway controlling cell growth, proliferation or maturation[45].

Type II are high grade serous or undifferentiated carcinomas and carcinosarcomas. They are fast growing tumours with a high metastatic potential and a low level of detection. They represent about 75% of the Epithelial Ovarian Cancer diagnosis[46,47].

Recent studies have been suggesting that High Grade Serous Ovarian Cancer originate from the distal end of fallopian tubes before crossing the surface epithelium of the ovary[43]. They are characterized by the absence of architecture and dysmorphic nuclei[48]. Other features include high nuclear to cytoplasmic ratio, atypic mitotic figures[49], high mitotic/apoptotic rates[50] and a high Ki-67 protein concentration[51].

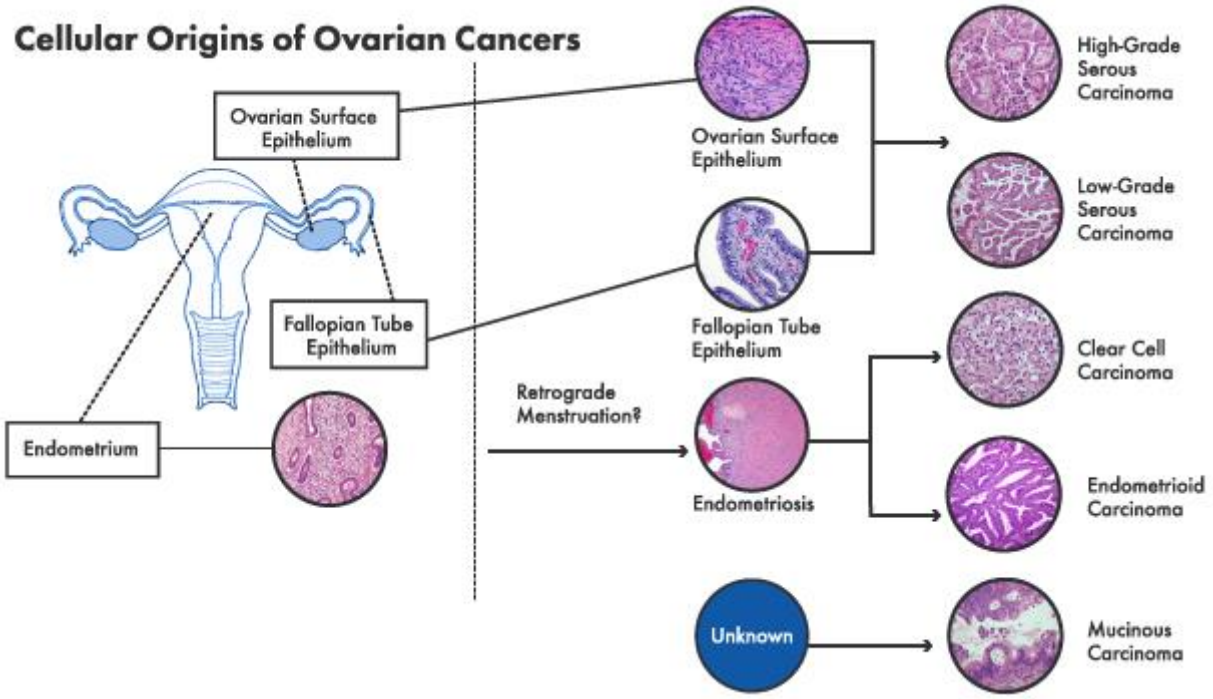


***Figure 3*[52]*: Histopathology of ovarian cancer***

*Ovarian cancer is defined by any any primary malignant tumour initiating from the ovary, the endometrium or from fallopian tubes. More than 85% of ovarian cancers are carcinomas, meaning they are derived from epithelium. Amongst them 70-74% are High Grade Serous Carcinoma, 3-5% are Low-Grade Serous Carcinoma, 10 to 26% are Clear Cell Carcinoma, 2-6% are Mucinous Carcinoma and 7-24% are Endometrioid Carcinoma.*

# 2. Biomechanical process during cancer progression

Dissemination of cancer cells following Epithelial to Mesenchymal Transition (EMT) is sustained by modification of cell-cell, cell-matrix interactions and cytoskeleton modifications. The cell cytoskeleton is formed of actin filaments, microtubules and intermediate filaments that all influence cell morphology[53]. These different structures interact with each other providing mechanical stability of cells. The effect of chemical drugs targeting cytoskeleton been used to reveal the role of each type of fibre in cell elasticity. For example the depolymerization of actin fibres resulted in rounder cells related to softening of the cells[54].

Invasive properties in HEY/HEYA8 ovarian cells have revealed that modified morphology is linked to cytoskeleton modifications increased the migration capacity of these cells[55–57]. Such observations are not directly applicable to in vivo mechanisms as in the tumour environment cell-cell contacts and extracellular matrix are strongly affecting cell stiffness[58–61]. Notably during the metastatic process, the cells acquire motility and increased deformability. Those morphological changes influence cell stiffness[55].

The adhesion of cells to the extra cellular matrix is a key property that has important functions in cell physiology. Indentation experiments in breast epithelial cancer cells have shown that matrix stiffness dictates intracellular mechanical state of those cells[62]. Moreover the comparison

between cirrhosis tissue and hepatocellular carcinoma tissue did not show any stiffness differences suggesting the hardness of the liver is increased during carcinogenesis[63].

Such modifications are studied using instruments, such as the atomic force microscope (AFM) which can measure nanomechanical changes. The measure of a force necessary to indent a cell (Young's modulus) in different cancerous cells such as breast[64,65], prostate[64,66], ovaries[67], or kidney[58] cancer has been shown to be less than their normal counterparts. It appears that modification of the Young's modulus can indicate the transition to a cancerous state for individual cells.

# 3. Current diagnostics and new developments

**Current diagnostics**

Different symptoms of early stage ovarian cancer have been identified, however, they are not specific to ovarian cancer, including abdominal and pelvic pain, irregular menarche, change in bowels habits and increased urinary frequency[5]. These benign gastrointestinal and gynaecological problems are often symptoms attributed to stomach or colon diseases.

The familial history of cancers plays an important role in deciphering the cancer risk. Importantly it can be related to the presence of an inherited mutation in the germline such as a BRCA genes mutation[68].

Ovarian cancer detection is currently based on circulating cancer antigen 125 (CA-125) glycoprotein concentrations as is has been shown to be elevated in 50% of cases with early stage ovarian cancer[69], but is also increased in pregnancy and endometriosis and other benign clinical conditions[70], which reduces its specificity. The lack of specificity and sensitivity of current early detection biomarkers severely impacts screening efficacy[71,72]. Population screening is also limited due to the rarity of the disease, and therefore cost implications related to such testing. However CA-125 remains an effective approach for sequentially monitoring the response to chemotherapy from patients and detecting relapse[208].
Transvaginal ultrasonography (TVU) is used in addition with CA-125 to screen symptomatic patients to detect ovarian cancer and rule out the false positives caused by weak or absent CA-125 signal. TVU enables precise imaging of the ovaries and helps to identify simple cysts, complex pelvic masses and solid tumours. However, only a fraction of metastatic tumours reach a sonographically-detectable size which may lead to false negatives in the detection of early-stage ovarian cancers[74].

Additionally, magnetic resonance tomography imaging (MRI) can be used when the other two tests give opposing results. The low spatial resolution of ovarian cancer hinders the detection of small tumours[75]. If the result of the diagnostic test raises suspicions, surgical approaches are adopted depending on the stage of the tumours[76].
The staging system (Table 1) for ovarian cancer is derived from the International Federation of Gynaecology and Obstetrics[77].

***Table 1:*** *Summary of the international staging system for ovarian carcinomas.*

| **Stage1** | **Limited to ovary or ovaries** |
|---|---|
| IA | One ovary, surface involvement or rupture |
| IB | Both ovaries, surface involvement or rupture |
| IC | Malignant ascites |
| **Stage II** | **Pelvic extension** |
| IIA | Involvement of the uterus or the fallopian tubes |
| IIB | Involvement of the other pelvic organs (bladder, rectum) |
| **Stage III** | **Involvement of the upper abdomen or lymph nodes** |
| IIIA | Microscopic peritoneal metastases outside pelvis |
| IIIB | Macroscopic peritoneal metastases , 2cm diameter |
| IIIC | Macroscopic peritoneal metastases >2cm diameter |
| **Stage IV** | **Distant organ involvement** |
| IVA | Pleural effusion with positive cytology |
| IVB | Metastases to extra-abdominal sites |

**Development of a new blood-based biomarker**

Stable and radioactive isotopes have been used in earth science in numerous fields (paleoclimate, paleocirculation, chemical evolution of earth, pollution). Recent improvements of Multi-Collector Inductively Coupled Plasma Mass Spectrometry (MC-ICP-MS), thermic ionization (TIMS) and isotopic ratio mass spectrometry (IRMS) allowed new measurements of small isotopic elemental variations. While those techniques were common in archaeology, they have recently been used in human and animal medicine[78–81]. Alkaline earth metals such as Calcium and Magnesium and the transition elements Iron, Copper, and Zinc have been studied due to their functional roles in biology and because their turnover rates in the body are relatively short.

Dietary intake of copper in human needs to be around between 1 and 3mg/day[82,83]. A portion is absorbed by the intestinal cells, after being reduced from $Cu^{2+}$ to $Cu^{+}$ by the membrane protein STEAP[84], through the CTR1 transporter. In cells, chaperons ATOX1 or COX17[85,86] bind to copper $Cu^{+}$ and deliver copper to different organites where it is used as cofactor of cytochrome c oxidase in mitochondria, or the superoxide dismutase SOD1 that catalyses the scavenging of ROS producing oxygen and hydroperoxide. Copper is transported through the intestinal cells and delivered to the blood through the ATP7A copper transporter[85]. Copper is then transported in blood by the ceruloplasmin to the liver[87]. The liver is the main site of copper accumulation, controlling concentrations in blood[88]. Liver synthesizes ceruloplasmin[89] which can transport up to seven copper[90] atoms due to a methionine rich domain and cysteine-histidine domains. Excess copper is excreted in the duodenum or in urine via the kidneys. Demands of copper in organs depend on their metabolic functions such as mitochondrial content and activity. For example in muscles, the high amount of mitochondria increase the demand of copper for cytochrome c function. This transmembrane protein contains 2 copper centres[91]. Their functions are to transport electrons from the soluble cytochrome c to the oxygen that is reduced into water.

Modifications of Cu concentration and relative abundance of Cu isotopes (fractionation) have been linked to modified metabolic processes (oxidative phosphorylation, hypoxia) or in

angiogenesis, and thus to health and disease[92]. In different cancers it has been shown that copper is required for angiogenic processes[93], stimulating proliferation and migration of endothelial cells[94]. In the liver tissue of colon tumour bearing mice, gene expression the copper transporters ceruloplasmin, and CTR1 and ATP7B was increased significantly, which can explain elevated copper serum levels[95] and suggesting its potential use as a diagnostic marker of cancer. Isotopic ratio between heavy isotope $^{65}Cu$ and the light isotope $^{63}Cu$ has been measured in different healthy and human materials[96] (Table 2).

***Table 2*** *[96] Cu isotope composition in blood and bones of human samples*

| Material | $\delta^{65}$Cu Variation (‰) | Average $\delta^{65}$Cu (‰, 2SD) |
|---|---|---|
| Healthy women serum | −0.80~0.04 | −0.28 ± 0.41 |
| Healthy men serum | −0.64~0.06 | −0.28 ± 0.40 |
| Healthy womenerythrocytes | −0.04~0.80 | 0.46 ± 0.47 |
| Healthy menerythrocytes | 0.23~0.91 | 0.67 ± 0.36 |
| Healthy womentotal blood | −0.52~0.32 | 0.00 ± 0.41 |
| Healthy mentotal blood | −0.21~0.43 | 0.16 ± 0.33 |
| Cancer patients (HCC) serum | −0.66~0.47 | −0.02 ± 0.54 |
| Control group serum | −0.39~0.38 | 0.10 ± 0.45 |
| Cancer patients (HCC) red blood cell | −0.07~0.92 | 0.51 ± 0.56 |
| Control group red blood cell | 0.57~1.24 | 0.88 ± 0.44 |
| Breast cancer patients serum | −1.45~0.12 | −0.51 ± 0.52 |
| Colorectal cancer patients serum | −0.65~0.04 | −0.29 ± 0.30 |
| Aging men blood | | 0.68 ± 0.49 |
| Control group (Young men) | | 0.67 ± 0.36 |
| Postmenopausal women | | 0.71 ± 0.54 |
| Control group (Premenopausal women) | | 0.43 ± 0.48 |
| Liver | | −0.26 ± 0.22 |
| Vegetarian female blood | −0.75~−0.29 | −0.51 ± 0.46 |
| Vegetarian male blood | −0.22~0.23 | −0.07 ± 0.52 |
| Omnivorous female blood | −0.14~0.17 | −0.02 ± 0.34 |
| Omnivorous male blood | −0.28~0.09 | −0.05 ± 0.41 |
| Russian and Yakut blood | −1.37~−0.22 | −0.68 ± 0.62 |
| Archeological women bones | | −0.20 ± 0.25 |
| Archeological men bones | | −0.11 ± 0.16 |

*Cu isotope data were obtained by MC-ICP-MS and expressed as $\delta^{65}Cu$ (‰) notation with a comparison between $^{65}Cu/^{63}Cu$ ratio of the samples with the ratio of the Cu standard solution and calculated by the formula :*

$$\partial^{65}Cu = \left[ \frac{\left(^{65}Cu/^{63}Cu\right)\text{sample} - \left(^{65}Cu/^{63}Cu\right)\text{ref}}{\left(^{65}Cu/^{63}Cu\right)\text{ref}} \right] \text{x}10^{3}$$

Cu is more concentrated in erythrocytes compared with serum (Table 2). Moreover Cu isotopic composition is lower in serum (-0.28**‰**) and higher in erythrocytes (0.46 to 0.67**‰**). To explain this difference, it has been suggested that enrichment of $^{65}Cu$ in red blood cells is due to the strong binding of $^{65}Cu$ with nitrogen of histidines and sulphurs of cysteines of the superoxide dismutase 1 or ceruloplasmin inducing enrichment of $^{63}Cu$ in the serum[97,98]. Although Cu is more concentrated in serum in women relative to men [79,99], the slight isotopic enrichment in women blood compared to men ($\delta^{65}Cu_{men}$ = -0.24 ± 0.36 **‰** and $\delta^{65}Cu_{women}$ = -0.28 ± 0.40 **‰**) shows that sex does not affect copper fractionation in humans [97].

The potential of measuring the variability of copper isotopes as a new diagnostic tool for cancer detection has been evaluated in colorectal and breast cancer patient serum. For all patients a decrease of $^{65}Cu$ concentration was observed[100] and related with an increase of tumour $^{65}Cu$ concentration. By following the evolution of the isotopic composition over time a faster shift

of $\delta^{65}$Cu was correlated with a more severe tumour, and with the CA15-3 (MUC1 blood concentration) marker. A decrease by 0.25‰ in serum of breast cancer patients, 0.14‰ [100] in colorectal cancer patients and 0.5‰ in cirrhosis patients[101] has been measured. Moreover, this shift in Cu isotopic composition has also been observed on other mammals such as dogs[80] and felines[81].

So far no direct link has been established between the increase of the copper concentration in the blood and the modifications of the isotopic compositions. However the analysis of tumour and peri-tumoral hepatocarcinoma cells has highlighted an increase of $\delta^{65}$Cu by 0.5 to 1‰ in tumour cells[102].
Moreover hypoxic growth of primary tumour cells have revealed the same type of shift of the $\delta^{65}$Cu[79,102]. These results suggest that $\delta^{65}$Cu ratio could be a cancer marker candidate for detection of Ovarian Cancer.

# 4. 'Classic' Ovarian Cancer treatments

Ovarian cancer treatment depends on disease stage. If the tumours are confined to one ovary (type Ia), the surgical removal of one ovary is performed[103]. If both ovaries have developed tumours (stage Ib), platinum and taxane (cisplatin and paclitaxel) treatment is given. Treatment for stage II and above where cancer has spread beyond the ovaries, involves chemotherapy and surgical reduction of the tumour mass[104,105]. The timescale for medical intervention depends on the size of the tumours. A high tumour load involves chemotherapy treatment before surgery[106]. Intravenous or more recently intraperitoneal delivery of platinum based chemotherapy with paclitaxel infusion can be used[105,106]. In the case of severe side effects of the treatment, the use of liposomal doxorubicin can also be used[107]To gauge treatment efficacy, the monitoring of CA-125 levels and physical examination are performed[108].

A major obstacle in the use of chemotherapy to treat ovarian cancer is its high recurrence rate (70%) due to the development of resistance to platinum treatment within 18 months which reduces dramatically the survival rate[19]. Resistance to treatment is defined by patients not responding to treatment or relapse within 6 months after first treatment[109]. The recurrence is due to the multiplication of subpopulation of cells that have adapted to the chemotherapy[110,111]. In most cases this is due to acquired resistance to chemotherapy via overexpression of drug efflux pump[35,112] . Restoration of BRCA genes in subpopulations of tumour cells thus regaining more effective DNA repair capabilities results in enhanced resistance to chemotherapy[20,113]. BRCA gene mutation is therefore both a risk factor for ovarian cancer development due to the lack of repair of DNA breakage, but also a risk factor if it is unregulated in ovarian cancer cells which can overcome chemotherapy.

To overcome the acquired resistance to treatment, Paclitaxel has been developed and is considered as the standard for platinum resistant ovarian cancer. Paclitaxel blocks cell division by binding to beta-tubulin that stabilize microtubules which leads to cell death[104]. However, like platinum treatment, taxane based chemotherapy induces oxidative stress and selects cancer

cell populations that resist treatment. The side effects of chemotherapy are a reduced immunity, gastrointestinal disruption, neuropathy and breathing difficulties[114].

The development of more specific and less harmful treatments is highly needed in order to target specific cancer cell populations allowing better life preservation and quality of life[103]

# 5. 'New' Ovarian Cancer treatments

New therapeutics have been developed that are more effective against ovarian cancer than platinum and taxane based treatments, and can be used as second line treatments. Olaparib and Veliparib, PARP inhibitors, have shown good efficacy in 50% of HGSC patients[23] carrying BRCA1 and 2 mutations[5,116]. The inhibition of PARP leads to accumulation of single strands breaks and unrepaired forks in DNA. PARP inhibitors have been proven to selectively kill cells with defects in DNA repair pathway[116]. PARP inhibitors are preferentially used in treatment of recurrent, BRCA-associated ovarian cancer patients but can also be used in maintenance following platinum-based chemotherapy for recurrent epithelial ovarian cancer[117].

Antibody therapies targeting human epithelial growth factor receptor 2 (HER2) and folate receptor[118,119] have been developed which block signalling that drives cell proliferation. Recent use of Trastuzumab (Herceptin) in ovarian cancer, a therapeutic monoclonal antibody directed against HER2, which is overexpressed in some ovarian cancer patients and related with poor prognosis[120] has raised good hopes. However only 6.7% of advanced ovarian carcinomas overexpresses HER2[121] therefore only a limited number of patients would benefit from this treatment.

# 6. Nanomedicines and Ovarian Cancer

**Definition**

Nanomedicines include a range of nanomaterials and nanosize biological entities (e.g. exosomes and antibody drug conjugates) that have been 'engineered' and are applied to cancer treatment. In some cases nanocarriers have been developed to transport drugs in order to overcome the low solubility, low stability or strong side effects of classic chemotherapy[122]. Nanocarriers have specific properties such as their size, high surface/volume ratio, physical or chemical specificities, while loading drugs into nanocarriers improves the pharmacokinetic and dynamic profiles of drugs enhancing therapeutic index by increasing accumulation to tumour sites [123]. Other nanomedicines use intrinsic properties of nanomaterials to elicit an anti-cancer effect. For example, gold nanoparticles have been used for local thermal ablation of tumour due to the ability of such particles to be manipulated by magnetic fields of radio frequency to generate heat locally[124].

**Passive targeting**

Nanocarriers/nanoparticles can be passively targeted to tumour sites via the so called EPR (Enhanced Permeability and Retention) effect to deliver pharmacologically active compounds. The EPR effect involves the accumulation of drugs in the tumour sites due to the movement of particles from the circulatory system through 'leaky' intratumoral blood vessels[125] with fenestrated endothelium allowing the passive transport of the nanomedicines through gaps in the vessels. The main limitations of passive targeting are heterogeneity[126] of the tumours impacting delivery of the drugs, interstitial pressure, extracellular matrix secreted by tumours and accumulation of nanocarriers to other organs. The escape from the opsonization by the immune system is also important to prevent the clearance of the drug before it has any effect on tumours.

**Active targeting**

Actively targeted nanomedicines are directed to tumours via high affinity ligand attached to their surfaces, selectively binding to a receptor of the targeted cells. Targeting moieties can include sugars, proteins, antibodies, and oligonucleotides. The targeting molecule needs to be stable in the blood in order to deliver specifically the nanocarrier to a tumour. The particle is still reliant on the passive EPR effect to reach the tumour, but then targets the tumour once escaped from the neovascular system[126]. Once at the tumour site, cancer cells can internalise the nanocarriers allowing the accumulation of drugs.

**Diversity of nanocarriers in cancer care**

Various type of nanomedicine have been developed and tested in clinical trials including drug conjugates, lipid based nanocarriers, polymer-based nanocarriers or inorganic nanoparticles.

Drug conjugates are defined as binding of the drug of interest with antibodies, peptides or polymers. Polymer HPMA (hydroxypropyl methacrylamide) drug conjugates are passive targeting nanocarriers based on the EPR effect that have been used due to the high biocompatibility of HPMA. Conjugated with oxaliplatin such nanomedicines have reached phase 2 clinical trials for recurrent ovarian cancer patients with equal or superior efficacy than oxaliplatin alone and demonstrating excellent tolerability with low accumulation in liver[127].

Active targeting such as antibodies drug conjugates (ADCs) have been developed against specific receptors overexpressed on cancer cell membrane such as HER2 (Human Epidermal growth factor Receptor 2) in breast cancer and in some ovarian cancers. Herceptin has been in clinical use and proved its efficacy as adjuvant in conjugation with emtansine inhibiting microtubule polymerisation increasing Herceptin efficacy.

Lipid based nanocarriers such as liposomes or micelles are able to transport greater amounts of drug in comparison with ADCs and use the EPR effect to accumulate tumour tissue. Paclitaxel loading lipid nanoparticles have been used in ovarian cancer and proved equivalent to Paclitaxel infusions in phase 2 trials, and effectively reduced side effects[128]. Despite the ability of liposomes nanocarriers to concentrate drugs, they do not actively target tumours. However functionalisation of liposomes with anti HER2, anti EGFR, anti VEGFR2 antibodies has been

developed, and overcame the multidrug resistance in xenograph mouse models and in breast and gastric cancer patients[129–131]

Polymer based nanocarriers include protein or peptide nanocarriers, polymers such as PEGylation or sugars. Albumin (BSA) based nanocarriers are mainly used due to its high bioavailability and stability in blood. Albumin coated particles/conjugates allow increased solubility of the chemotherapeutic drugs such as paclitaxel. A major drawback is the immunogenicity induced by this kind of coating leading to opsonization. Glycan nanocarriers such as chitosan based nanoparticles have been used for loading gemcitabine resulting in increased uptake by intestinal cells compared to free oral gemcitabine improving the stability of the drug in preclinical trials[132]. Chitosan coated nanocarriers are uptaken by endocytosis after binding to the phospholipids of the membrane. With a pKa of 6.5 for its primary amine groups, chitosan is highly soluble at acidic pH allowing the swelling of the chitosan nanostructure leading to the leak of drug of interest through the nanoparticle to the cells[133].

Inorganic nanoparticles are made of different materials and used for variety of applications including theragnostic. For example MRI studies have been using superparamagnetic iron oxide nanoparticles to image tumours[134]. Moreover iron oxide nanoparticles are used for their magnetic properties to induce thermal ablation[135] (magnetic hyperthermia). Gold nanoparticles are also extensively used in the synthesis of nanocarriers. Pegylated gold nanoparticles binding TNF-α to deliver necrosis factor to solid tumours have been tested in phase one clinical trial but hasn't reached the next stage yet[136].

**Development of nanocarriers for ovarian cancer treatment**

Nanocarriers such as those described above have been developed in both in vitro and in vivo ovarian cancer models (summarised in table 3), with several progressing to clinical trials (summarised in table 4).

***Table 3:*** *In vitro and in vivo nanocarrier development in ovarian cancer models (adapted from [126]).*

| **Passive targeting nanocarriers** | **System** | **Drug** | **Description** | **Model** |
|---|---|---|---|---|
| | Nanoparticles | Cisplatin<br>Paclitaxel | Poly ethylene glycol (PEG) based polymer | SKOV-3<br>A2780<br>Female athymic mice |
| | Polymeric nanocarriers | Cisplatin<br>Paclitaxel | Chitosan | A2780 |
| | Lipid based nanocarriers | Cisplatin<br>Paclitaxel<br>Doxorubicin | Phosphatidylcholine, and cholesterol PEG | OVCAR-3<br>A2780<br>SKOV-3 |
| | Polymeric micelle | Paclitaxel<br>Doxorubicin | Pegylated liposomes, poly-ethylene based, polystyrene based | CAOV-3<br>SKOV-3 |
| | Nanocapsule | Cisplatin<br>Paclitaxel | DOPC based or alginic core shell | OVCAR-3<br>Female nude mice |
| | Dendrimer | Cisplatin<br>Paclitaxel | Polyamidoamine dendrimers | SKOV-3<br>A2780,<br>female athymic nude mice |
| | Hydrogel | Paclitaxel | Hyaluronic acid based hydrogel | SKOV-3,<br>Female BALB/cmice |
| | Polymer-drug conjugate | Doxorubicin | PolyL-lysine citramide and DOX copymer | SKOV-3,<br>Female BALB/cmice |
| **Active targeting nanocarriers** | **Targeted receptor** | **Carrier system** | **Description** | **Model** |
| | Folate receptor | AuNP<br>Liposome<br>NP | PEG conjugated AuNP<br>Phosphatidylcholine-PEG-cholesterol<br>Folicacid-PEG-chitosan<br>Paclitaxel-glucose | SKOV-3<br><br>OVK18<br>OVCAR-3 |
| | Luteinizing hormone releasing hormone receptor | Nanogel<br>Magnetic NP | PEG based + cisplatin<br>Iron-platinum-PEG copolymer | A2780 |
| | HER2 rceptor | Polymeric NP<br>Dendrimers | Paclitaxel loaded poly lactic acid PEG NP<br>Polyamidoamine dendrimers | SKOV-3<br>OVCAR-3 |
| | Transferrin receptor | Micelles | Tf PEG-PE micelles | A2780 |
| | Integrin receptors | NP | Cyclic pentapeptide containing gemcitabine hydrochlorine | SKOV-3 |
| | CA125 | Liposome | Chain of anti CA25 fused to streptavidin | OVCAR-3 |
| | Angiogenesis | NP | SilicaNP loaded with candesartan | SKOV-3 |
| | Magnetic NP | NP | Carboplatin Fe3O4NP | A2780 |

*SKOV-3, A2780, OVCAR-3, CAOV-3 cited in the table are commercial ovarian cancer cell lines.*

**Table 4:** *Nanocarriers under clinical trials (from searchtrials.com)*
When typing Nanoparticles in Ovarian Cancer in clinicaltrials.gov, we summed up the actual drugs in test in clinical trial.

| Name | Chemotherapeutic agent | Description | Number of patients | Clinical trial phase | Goal / Effect |
|---|---|---|---|---|---|
| PIPAC | Paclitaxel | Albumin (nab) shell covering paclitaxel Pressurized intraperitoneal aerosol | Recruiting | Phase 1 | Single-agent activity and a favourable toxicity profile |
| Paclitaxel-Albumin Stabilized NP | Intraperitoneal injection of Paclitaxel | Albumin shell covering paclitaxel | 27 | Phase 1 | Determine the potential pharmacokinetic advantage of the nanoparticles Determine the favorable ratio of nab-paclitaxel (Abraxane) concentration in the peritoneal cavity vs. plasma |
| Paclitaxel-Albumin Stabilized NP | Blood infusion of Paclitaxel | Albumin shell covering paclitaxel | 51 | Phase 2 | 30% of reduction of tumour size |
| CriPec | Docetaxel | Polymeric NP loading docetaxel (analogue of paclitaxel) | 27 | Phase IIa in Pt-resistant patients | Inhibit VEGF, cell cycle arrest in G2/M, Inhibit microtubule disassembly. |
| IMX10 | Curcumin Doxorubicin | Curcumin Doxorubicin encapsulated NP | 70 | Phase 1 | Coupling the role of curcumin as a signal transducer, activator of transcription Stat3, NFkB to doxorubicin which is antineoplasic |
| EGEN-001 | Doxorubicin | IL12 based immunotherapeutic coupled with pegylated liposomal doxorubicin | 16 | Phase 1 | Stimulate immune system, stop tumour growth Increased cell death in comparison with separated drugs |
| CRLX101 | Bevacizumab | Camptothecin in nanoparticle (structure not detailed) | 63 | Phase 2 | Would inhibit together distinct step along HIF-> CAIX->VEF-VEGFR2 pathway. CRLX101 inhibits HIF1α hypoxia inductible transcription factor and HIF1α associated resistance to VEGFR inhibitors. |
| 9-ING41 | | Single agent therapy | 350 | Phase 2 | GSK3b inhibitor |

# II. Epigenetics

## 1. Definition

Epigenetics refers to reversible[137] chemical modifications of chromatin organization and structure[138] that result in alterations in gene expression profiles, cellular function, and which are in some cases heritable. These chromatin related epigenetic mechanisms allow cells to modify gene expression in response to chemical and environmental stimuli for example. Distinct mechanisms of epigenetic alterations include DNA methylation, histone acetylation, methylation or phosphorylation, and microRNA (miRNA) expression and regulation[138]. These mechanisms (except miRNA) are affected by enzyme families that transfer or remove small chemical moieties that function as activating and repressing 'marks' from histones or DNA, that are then recognised by regulatory proteins that control transcription.

**Histone structure and modifications**

Epigenetic changes can result in aberrant oncogene activation or inactivation of tumour suppressor genes, allowing cancer progression[137]. DNA is packaged in the nucleus, wound around nucleosomes that are composed of segments of 147 base pairs of DNA wrapped around a histone core, comprising of 2 copies of histones 2A, 2B, 3 and 4[57,58]. These 14kDa basic proteins are positively charged due to high numbers of lysine and arginine amino acids, enabling them to bind to the negatively charged DNA. Sequences of nucleosomes are then organized in a relatively open and uncompacted form, termed euchromatin associated with open, active chromatin regions or more densely packed, closed chromatin, termed heterochromatin which is associated with silent or inactive gene expression. Chromatin compaction is controlled by combinations of post translational modification of histones tails [141]. The main histone modifications include methylation, acetylation, phosphorylation or ubiquitination[142] to lysines and arginines, present in the histone tails (Figure 4). The different modifications are controlled by enzyme families such as methyltransferases or demethylases, acetylases or deacetylases[139,141,143].

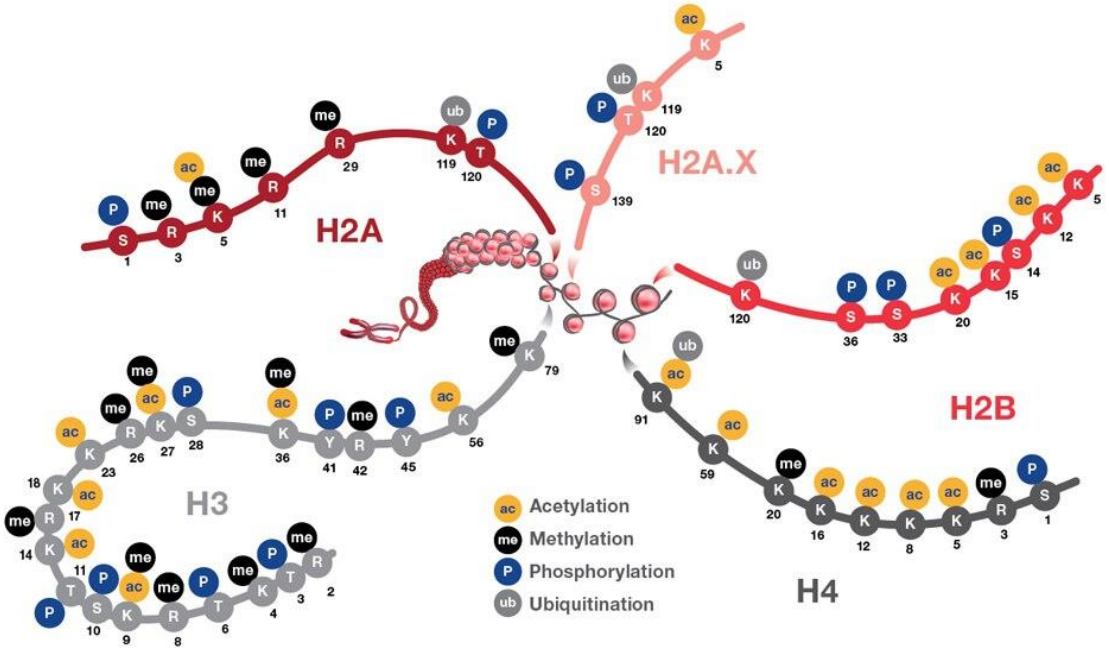


***Figure 4*: Main post translational modification sites of the histones affecting epigenetics.** *Nucleosomes are composed of segments of 147 base pairs of DNA wrapped around a histone core, comprising of 2 copies of histones 2A, 2B, 3 and 4*[57,58]*. These 14kDa basic proteins are positively charged due to high numbers of lysine and arginine amino acids, enabling them to bind to the negatively charged DNA. The post translational modifications of the histone on the amino acids of their N-terminal end, also called tail, induce modifications in gene expression by altering chromatin structure and recruiting transcription factors. These modifications activate or inactivate transcription, induce chromosome packaging or recruit factors for DNA repair.*

**Histone methylation**

Histone H3 consists of a main globular domain and a long N-terminal tail that contains 6 sites of modifications for methylation that have different consequences on chromatin compaction and genetic expression. The methylation sites are constituted of lysines (K) or arginines (R) and their methylation is catalysed by a range of different histone methyltransferases (HMT) (Figure 5).

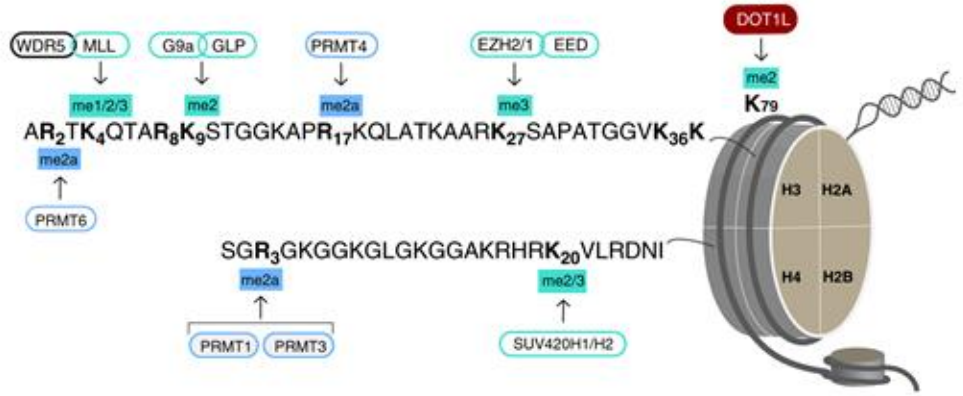


***Figure 5 : Enzyme responsible for histone tails methylation***[144]

*Histones H3 and H4 are part of the nucleosomes and their N terminal domain (tails) can be modified through the activity of different methyltransferases using S-adenosylmethionine (SAM) methyl donor.*

The number of methyl groups that can be added to each lysine (K) or arginine (R) is controlled by the HMT which can transfer up to 3 methyl to each post-translational modification site (Figure 5, 6). The PRDM/SMYD family of HMTs family catalyse the addition of one to three methylation of H3K4[145], where as enhancer Zeste Homolog 2 (EZH2) can mediate the addition of one to three methylation on H3K27[146], and G9a (EHMT2) is able to mediate the addition of one or two methylation on H3K9[143].

Methylation of lysines and arginines is mediated by the transfer of a methyl from SAM by HMTs (Figure 6). The product of this reaction is a methylated lysine/arginine and S-adenosylhomocystein (SAH) which is cleared into homocysteine and recycled into methionine through remethylation by Betaine Homocysteine MethylTransferase (BHMT) (Figure 6).

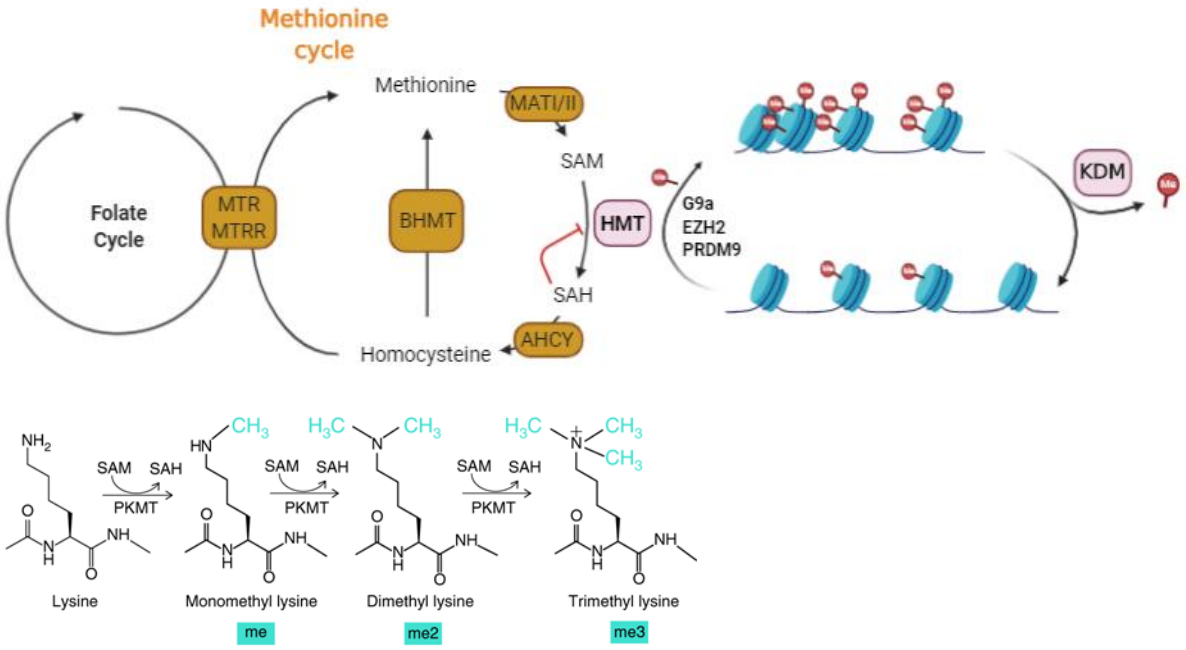


***Figure 6 : Histone lysine methylation***[144]
*SAM methyl donor can transfer up to 3 methyl groups onto lysines or arginines in histone by methyltransferase enzymes (HMTs). The methyl group changes the interaction of the histone tails with the DNA and modulating the binding of transcription factor hence the DNA expression.*

# 2. Transcription activation mark (H3K4)

The methylation of H3K4 has been shown to result in gene activation[141,142,147] (Figure 7). H3K4me3 is highly enriched near the Transcription Start Sites.[148], and appears to be an epigenetic signature in tumour-suppressor genes in normal cells[147]. Genetic domains covered by H3K4me3 are broader (>4kb) in genes controlling cell-type specific functions in normal cells, where transcription is increased[147,149]. The shortening of broad H3K4me3 in cancers is associated with repression of tumour suppressors. Patient studies have demonstrated that decreased levels of H3K4me3 are associated with poor prognostic factors in lung and kidney cancers[150,151].
H3K4 methylation is mediated by SET1 complex which is composed of methyltransferase and seven subunits[152]. The PR/SET domain gene family (PRDM) encodes for 19 zinc-finger domain containing proteins involved in gene expression regulation modifying chromatin structure through methyltransferase activity or recruitment of chromatin remodelling complex[153,154]. While PRDMs have been mainly identified as tumour suppressors, some family members have been associated with mutations, epigenetic silencing or overexpression in multiple cancer types. PRDMs have two isoforms differing by the presence of a PR domain with the short isoform being oncogenic[153].

SMYD histone methyltransferases have also been implicated in cancer development with increased expression of SMYD3 in ovarian cancer inducing high H3K4me3[155]. SMYD3 is

known to interact with RNA Pol II and H3K4me3, and functions as a selective transcriptional amplifier for oncogenes. A meta-analysis of 1474 patients from 10 clinical studies accross different cancers indicated that lower levels of H3K4me2 were characteristic of shorter overall survival, whereas patients with lower level of H3K4me3 expression had a longer overall survival[149] and raises the importance of investigating patterns of H3K4 methylation on prognosis of patients with malignant tumours.

# 3. Transcription repression mark (H3K27)

H3K27me is regulated by EZH2 a catalytic component of polycomb repressive complex 2 (PRC2). Through H3K27me2 and H3K27me3, EZH2 represses gene expression (Figure 7), triggering the differentiation or maintenance of stem cell self-renewal capacity [156–158]. The expression of EZH2 increases in prostate cancer, esophageal squamous cell carcinoma, and breast cancer[159160 161]. EZH2 knockdown often leads to reduced invasive potential of cancer cells[1,2]. H3K27 methylation has also been related to increased DNA breaks, since EZH2 is found in PRC2 complex that is recruited to damage sites through PARP activity (poly ADP-ribose polymerase) where it increased H3K27 methylation [163–165]. The induction of apoptosis by staurosporine lead to PARP cleavage and increased H3K27me in osteosarcoma cells[166]. EZH2 accumulates in promoters of actively transcribed genes inducing repression upon DNA damage by recruiting remodelling factors, which may facilitate repair of DNA lesions and organize response to DNA damage[167].

# 4. Heterochromatin mark (H3K9)

The H3K9me2 or 3 marks are catalysed by the G9a (EHMT2) methyltransferases[168] . The position of these marks are important in their role in chromatin expression. H3K9me2 and 3 have been associated with gene silencing and heterochromatin[169] (Figure 7) when they accumulate in the 5'UTR regions of genes. In contrast increase of H3K9me3 within the body of a gene has been linked to active gene expression. H3K9me2 is rarely found within silenced genes[170]. H3K9me2 has been described as a repressive mark and has been located within LaminB1 bound regions (nuclear periphery, nuclear lamina, associated with inactive genes). LaminB1 regions are areas of low gene expression indicating that Lamin B1 rich regions represents a repressive chromatin environment. H3K4me3 and RNAPol II are also absent from LaminB1 regions which strengthens the idea of H3K9me2 being a repressive mark that separates active and inactive genes[171].

G9a is highly expressed in different cancers such as hepatocellular carcinoma[172], colorectal cancer[173] and breast cancer[174]. The knockdown of G9a induced apoptosis and growth inhibition with increased cell population in sub-G1 phase [143,175]. Moreover, G9a downregulation induced centrosome disruption and chromosomal instability leading to cell senescence in prostate cancer cells[176].

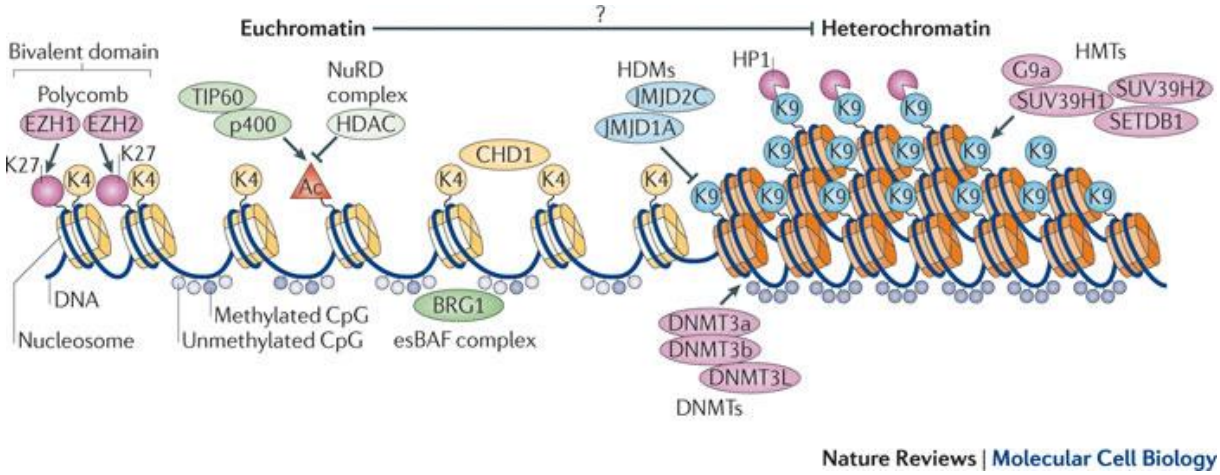


***Figure 7[177]: Histones methylation regulating the euchromatin and heterochromatin forms.*** *Among the different histones marks described in the literature, we focus here on three important ones. H3K4me3 has been described as translational activation mark and H3K27me3 and H3K9me3 have been described as repressive marks. The methylation is orchestrated by different regulators which are specific of each mark. Addition of methylation is permited by histone methyltransferase (HMT) while methyl removal is mediated by histone demethylase (HDM). H3K9 is methylated by G9a, SUV39H1/2 or SETDB1 and lead to chromatin condensation, e.g. hetetochromatin. The JMJD family of HDMs remove methyl from H3K9 leading to decondensation of the chromatin. In euchromatin, the marks H3K4 and H3K27 are respectively modified by SET1 complex (SMYD or PRDM families) and EZH1/2 Polycom complex. These marks are present on the histones and the balance between both leads to activation or repression of the transcription.*

# 5. Current knowledge of the effect of epigenetics in ovarian cancer

Recent studies of ovarian cancer cell populations identified sub-populations that are stem-cell like nature[178]. This is supported by the presence of the methylation bivalent chromatin mark H3K4/H3K27 at the transcription start site of silenced genes[179]. This mark is required for silencing of developmental genes which keeps cells in a stem cell nature conducive to the formation of tumours.

The balance between the different epigenetic marks has been linked to the aggressiveness of the ovarian cancer[179]. In high grade serous ovarian tumours H3K4me3 and H3K27me3 marks at transcription start sites are specific for malignancy progression[179]. The overexpression of EZH2 lead to H3K27me3 mediated gene silencing driving tumorigenesis in subpopulation of cells.

Following treatment with chemotherapy, subsequent development resistance to treatment by ovarian cancer cells is prevalent[4,72], with specific populations of cancer cells thought to retain pluripotent embryonic stem cell-like features, with high H3K4me3 and H3K27me3 repressing transcription factor networks and subsequent patterns of gene expression[180]. In platinum-resistant PEO4 cell lines (derived from malignant effusion from the peritoneal ascites), the presence of the bivalent mark (H3K4me3 and H3K27me3) or repressive H3K27me3 mark were generally expressed at a lower level than in PEO1 platinum-sensitive cell lines.

In ovarian cancer spheroids, SMYD3 expression was elevated[155] and associated with increased H3K4 methylation. A knockdown of SMYD3 decreased spheroid invasion and adhesion associated with a downregulation of integrin family members. Patients with high SMYD3 expression have been related with ovarian cancer cells proliferation[181].
In OVCAR-3 cells, H3K27me3 relates to the development of resistance to cisplatin and tumour progression[179]. However in human studies, the expression of H3K27me3 was lower in ovarian cancer tissues than in normal tissues[182]. This has also been observed in clinical studies comparing different ovarian cancer (cystadenomas, borderline tumour or carcinomas) where between 30 to 50% of cases displayed a decrease in H3K27me3 mark expression[183]. The use of inhibitors of PRC2 like metformin caused reduced methylation of H3K27, reducing cancer cells proliferation and migration, and triggering apoptosis[184]. In SKOV-3 cells, when epithelial to mesenchymal transition was triggered by TGF-β, EZH2 expression was reduced leading to reduced H3K27me3[162]. Moreover, the inhibition of EZH2 triggered EMT-like changes in SKOV-3 cells. EZH2 is thought to be required for the maintenance of epithelial phenotype in ovarian cancer cells[162]. During metastatic process, cells undertake the EMT. However in ovarian cancer, after dissemination from primary tumour site, cells adopt epithelial phenotype to adhere to the mesothelium. EZH2 is thought to facilitate this process during tumour metastasis, as it is overexpressed, tilting the balance EMT/MET in favour of MET[162].

G9a overexpression has been identified as a marker of aggressiveness and can promote the peritoneal metastasis[185]. Knockdown of G9a expression suppressed prometastatic cellular

activities including adhesion, migration and invasion in cell lines. It significantly attenuated the development of ascites and tumour nodules in a peritoneal dissemination model[185]. The expression levels of G9a were higher in metastasis in comparison with primary tumours. The expression of G9a is correlated with late stage of ovarian cancer, predicting a shorter survival in patients expressing high levels of G9a[185].

# III. Selenium in cancer treatment

## 1. Dietary window of selenium and metabolism

**Dietary window**

The amount of Selenium (Se) in food and thus in the diet is highly dependent on the amount of Se in soil and water which is regionally dependent[186]. The optimal dose range of Se intake in human nutrition is narrow and has been shown to be between 100 and 200 µg/day (Figure 8) [187,188]. In contrast, consumption of over 1500 µg/day of Se can induce single and double strand DNA breaks[189] that progressively worsen with increasing dose leading to selenosis[190191] characterised in acute phase by necrosis and haemorrhage resulting from capillary damage and in chronic poisoning by degenerative and fibrotic changes of the liver and skin[192].

To prevent adverse effects due to excessive intake of selenium, the USA Institute of Medicine set a tolerable upper intake level of selenium at 400µg/day[193]. The consumption of selenium between 200 and 400µg/day has been shown to be protective against liver necrosis by increasing glutathione peroxidase and thioredoxin reductase levels[194]. The role of selenium in ROS protection lead to the study of the effect of supranutritional doses of selenium (>200µg) in cancer. While doses of selenium between 200 and 400µg/day[186,195] of selenium were shown as protective, doses above 400µg/day were shown to have a strong inhibitory effect on cancer cells growth and impaired cancer development in vitro and in vivo. Various organic (selenomethionine, methylseleninic acid) and inorganic (selenite, selenate) selenium forms have been tested over the years allowing to describe different biological activities highlighting the need of better characterisation of toxicology of each selenium species[193,196–198]. Those studies raise the challenge of the definition of the dietary window of selenium.

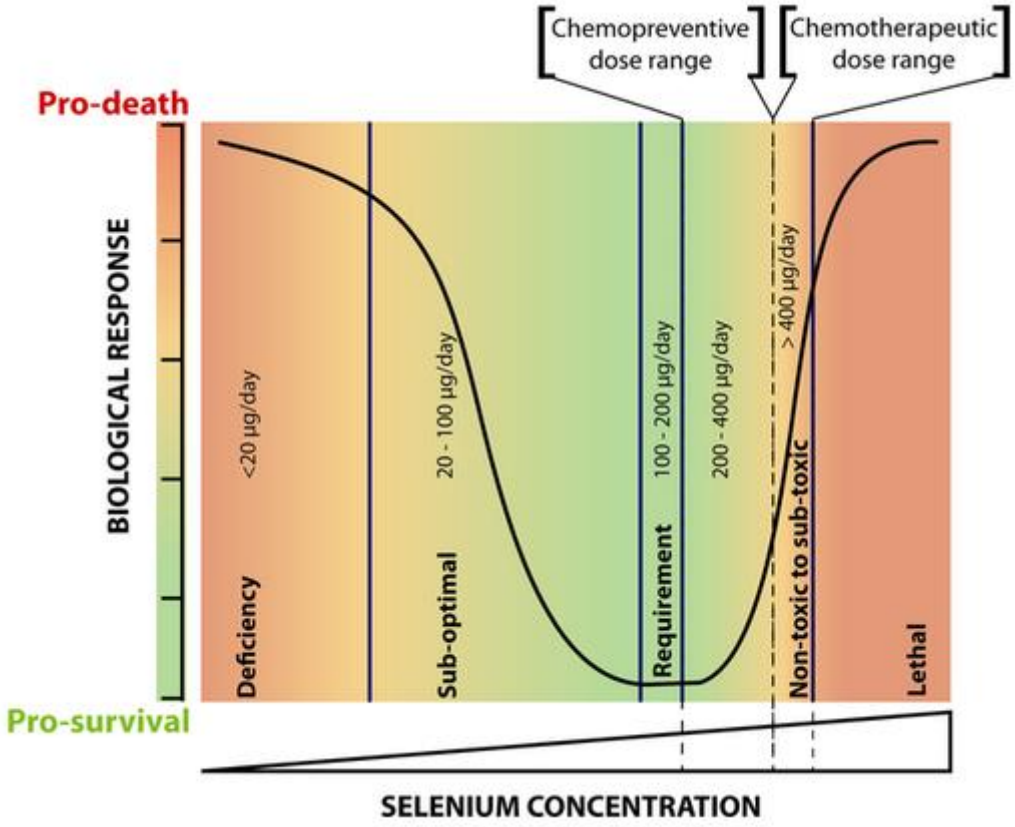


***Figure 8 : Dietary range of selenium in human diet***[199]

*Selenium is a nutrient with a narrow dietary range with a requirement of 100 to 200 µg of selenium per day. Under this intake selenium deficiency can cause diseases, notably Kashin-Beck disease which is a skeletal disorder due to necrosis of the growth plates of bones and joint cartilage. Above this dietary window, selenium may prevent cancer development up to 400µg per day however becomes toxic above this dose. Selenosis is an intoxication to selenium characterized by nail and hair loss which can lead to death.*

**Cell Metabolism**

Assimilation of selenium in human nutrition occurs through different mechanisms. As elemental selenium 0 is insoluble, it is not likely to cross the cell membrane[200]. To transit through the gut wall, selenium can enter the cells as selenite ($SeO_3^{2-}$) using sulphate transporters[200]. Moreover, phosphate transporters can also be involved in selenium transport. Selenite uptake kinetics have been correlated with phosphate uptake kinetics[201]. While high affinity phosphate transporters are not affected by the presence of selenite *in vitro*, low affinity phosphate transporters poorly discriminate selenite from phosphate, enabling selenite to enter cells when phosphate concentration increases[201]. Once inside the body, selenate and selenite can be directly transported to other cells through blood transport bound to proteins[202] and/or transformed into selenocysteine in intestinal cells[203]. Selenoaminoacids (selenomethionine and selenocysteine) from food are transported through the bloodstream to the liver (Figure 9) where they are incorporated into selenoprotein P (SELENOP) that is then transported to cells requiring Se through blood. SELENOP is a secreted glycoprotein that bind to glycosaminoglycans using heparin of endothelial cell membrane. SELENOP have antioxidant properties and the numerous selenocysteines it transports is a source of selenium for the cells absorbing it by endocytosis. In

the cells, selenium spontaneously reacts with other compounds producing organic selenium metabolites such as selenides ($R_2Se$), diselenide ($R_2Se_2$) and selenols ($RSeH$)[204] (Figure 9). Selenite is metabolized by glutathione (GSH) or glutathione reductase as a seleno-di-glutathione (GS-Se-SG) which can be utilised by cells as an antioxidant in the presence of reactive oxygen species[195,205,206]. However, seleno-di-diglutathione has a short lifetime due to its catabolism by glutathione reductase[207], which results in its conversion back to selenide ($H_2Se$) and GSH.

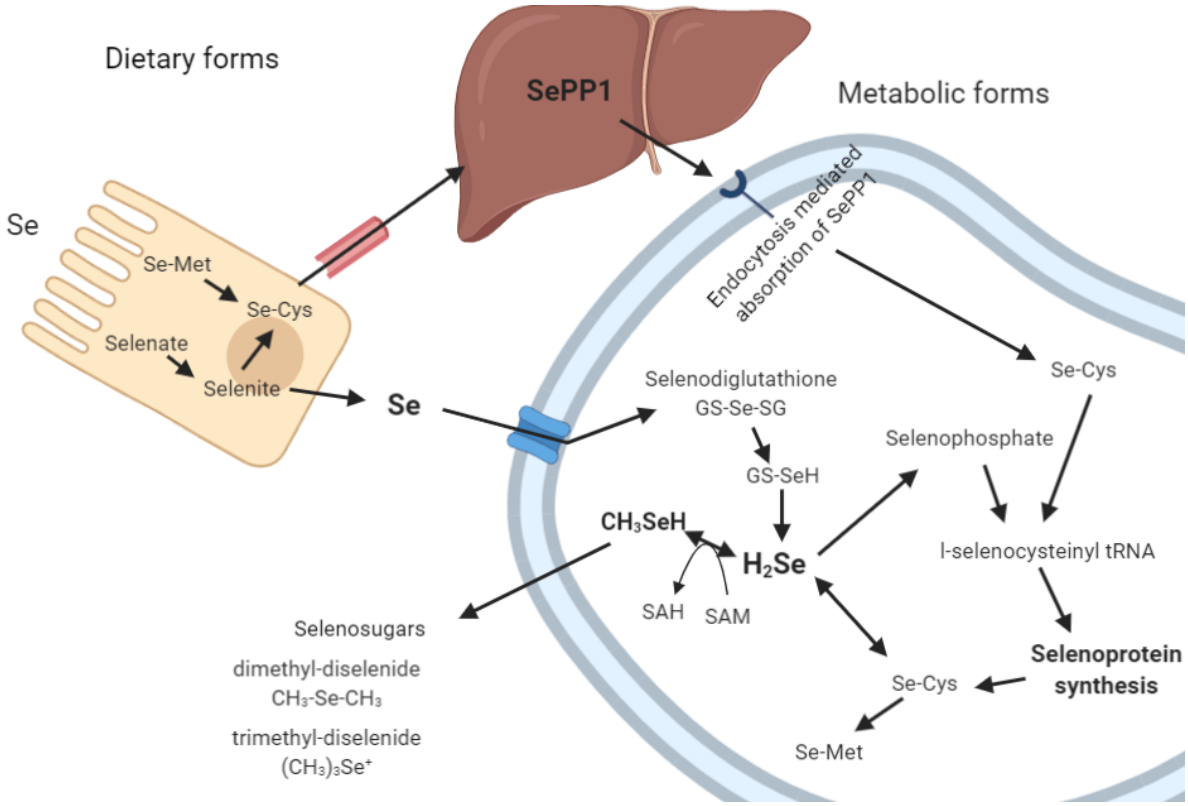


***Figure 9 : Dietary and metabolic forms of selenium in cells***[203,208]
*Selenium from diet (as selenite or seleno amino acids) enters intestinal epithelial cells and is transported through the blood to the liver where its involved in synthesis of the SePP1 or seleno-sugars. Those selenium forms are circulating forms and are distributed to organs where they are involved in selenoprotein synthesis. Selenium can be methylated via the methyl donor SAM into dimethylselenium which is volatilized through lungs or into trimethylselenium in kidneys where it is then excreted through the bladder. Selenium as selenite can also circulate in the blood and be absorbed in organs through sulphate or phosphate transporters. Once in the cells, selenium is metabolized through the glutathione system leading to the production of $H_2Se$ that can either enter the pathway for synthesis of selenocysteine or be methylated and excreted.*

The proximity between sulphur (S) and selenium (Se) allows for substitutions in organic molecules to occur, especially in proteins such as selenomethionine, which is randomly included in proteins or selenocysteine, the 21$^{st}$ amino acid[209]. This seleno amino acid is inserted into proteins in the same way as serine; each selenoprotein is synthetized by a selenoprotein

mRNA that contains a UGA codon and a unique SElenoCysteine Insertion Structure (SECIS). The Selenocysteine-Serine tRNA is used for the integration of the selenocysteine into the amino acid sequence that forms selenoproteins[204,205]. This system produces a group of around 25 identified proteins in the human proteome[210] that are mainly involved in antioxidant and anti-inflammatory activities[211].

Modifications of the level of selenium in the cells has been shown to influence selenoprotein activity and production[1,2]. Thioredoxine reductase for example, which contain selenocysteines, is present in the cytosol (TrxR1, thioredoxin glutathione reductase TGR-TrxR3) and the mitochondria (TrxR2). These proteins are involved in the reduction of oxidized thioredoxins, can catalyse NADPH, control ascorbate levels and regulate metabolism[212]. Glutathione peroxidases (GPX) are found in the cytosol and mitochondria (GPX1), extracellular matrix (GPX3), and embryonic cells (GPX4)[212,213]. GPXs have been shown to protect cells against oxidative damage by reducing lipo hydroperoxides and hydrogen peroxide[212]. GPX1 is known to be highly sensitive to selenium content and oxidative conditions in cells. Selenoprotein P meanwhile, is a selenocysteine rich secreted glycoprotein is endocytosed[214] through ApoER2 receptor by cells that subsequently break down the protein and use selenium as SeCys, therefore regulating Se distribution in the body[212]. Importantly, selenoproteins in combination with vitamin C, E beta-carotenes, has been proven to enhance the control of free radicals, protecting cellular functions[215,216].

Selenium is also involved in the biosynthesis of diverse molecular components that are required for important cellular functions, from deoxyribonucleoside triphosphates (dNTPs) for DNA, to the reduction of oxidized proteins and/or membranes, to roles in diverse regulation mechanisms such as redox, apoptosis, immunomodulation, thyroid hormones and the formation of methyl donor compound[217] (S/Se adenosylmethionine). Selenium, is therefore an important trace element which is fundamental to human health.

# 2. Low dose of selenium triggers ROS scavenging

As a naturally occurring element with both nutritional and toxicological properties, selenium deficiency has been linked to cancer development. Indeed, a meta-analysis of the epidemiological literature shows that selenium deficiency is linked with higher cancer development risk[218]. Cancer risk is 2 to 6 times lower when blood serum selenium concentrations are between 100 and 400 ng/mL; corresponding to a consumption of 55 to 200 µg/day of selenite[219]. However a stratified analysis of SELECT results based on genotype examining the nutritional prevention of prostate cancer, with a group of men taking 200µg of selenium per day over a period of 7 years, showed a no effect of Selenium and Vitamin addition for cancer prevention compared to the treated group[220]. Moreover, analysis of randomized controlled trials has failed to show any beneficial effect of Se supplements in reducing cancer risk in humans[193].

Major impacts of different selenium forms on human health are currently not well understood. This is mainly due to the lack of knowledge in requirements of the different selenium forms for

therapeutic application. In vitro and murine model studies have focused on the treatment of various cancer cell models with selenite ($SeO_3^{2-}$, the most toxic form of free selenium), MethylSelininic Acid (MSA) or SeMet. It appears that at levels below 5µM most forms of selenium tend to have a protective effect against DNA damages and ROS production[221,222,223–225]. However above 10µM studies have shown a strong inhibitory and cytotoxic effect of different forms selenium leading to cell cycle arrest and ROS production leading to mitochondria or DNA damages triggering cell-type dependent cell death[225,226,44–50]. Several mechanisms have been suggested to explain the effect of selenium in cancer therapy depending on the concentration of treatment applied to the cell culture and murine models (summarised in Table 2).

***Table 2 : Main effects of different dietary forms of selenium on cancer cell lines and in vivo models.***

| Cells | Selenium form | Dose | Effect | Ref |
|---|---|---|---|---|
| PC3 Prostate cancer | Methylseleninic acid | 10µM for 12h | Reducing DNA damage | [221,222] |
| LNCaP Prostate Cancer | Selenite | 1µM | | |
| Whole blood | Selenite | 30nM | | |
| Mouse embryonic fibroblasts | Selenomethionine | 10µM 15h | Improving DNA repair | [234–236] |
| Human fibroblast | | 10µM 24h | | |
| LNCap Prostate cancer | Selenite | 30nM 72h | | |
| MCF7 Breast cancer | | 30nM 72h | | |
| Human Blader Cancer Cell | Selenite | 10µM 12h | Increasing DNA damage | [225,226] |
| Glioma cells | | 7µM 24h | | |
| Rat pancreatic islets | Selenite | 30nM 1 to 6 days | Reduction of oxidative stress by increase of selenoproteins expression | [223–225] |
| Prostate cancer LnCaP | | 1.5µM 6h | | |
| Glioma cells | | 1µM 24h | | |
| Glioma cells | Selenite | 7µM 24h | Induce ROS production | [225,226] |
| Human bladder cancer cells RT-112 | | 10µM 12h | Mitochondria damages | |
| Prostate cancer PC3 LNCaP and Du145 cells | Selenite | 1µM | Alteration of DNA methylation for tumour suppressor genes | [213,217] |
| DU145 prostate cancer | Selenomethionine | | Cell cycle arrest in G1 | [227–229] |
| HT1080 | | | Cell cycle arrest in G2 | |
| Fibrosarcoma cells | Methylseleninic acid | 5µM | Altering functions of cyclins (C, D1 cyclin-dependent kinases (1, 2, 4) and protein kinases AKT | |
| TM6 mammary hyperplastic epithelial cell | | | | |
| SW982 Synovial sarcoma | Selenite | 10µM | Induce apoptosis | [230–233] |
| | | 2.5µM 5d | | |
| LNCaP Prostate cancer | | | | |
| OVCAR-3 Ovarian cancer | | 10µM 72h | | |
| Glioblastoma | | 5µM 24h | | |
| RT-112 Blader cancer | Selenite | 10µM 24h | Necroptosis | [226,237] |
| PC3 Prostate cancer | | | | |
| Glioma cells | Selenite | 7µM 12h | Autophagy | [225] |

# 3. High doses of selenium are cytotoxic

## i. Effect of selenium on ROS production

Reactive oxygen species (ROS) are free radicals formed within cells during oxidation processes that are characterized by one or more unpaired electrons[238]. The major ROS found in cell systems are superoxide (O2°-), hydroxyl radical (HO°) and nitric oxide (NO°). These transitory but highly reactive species are implicated in cellular reactions as second messengers at physiological concentrations[238]. When ROS concentrations increase in cells, a range of cellular damage can be induced such as lipid oxidation, DNA and protein damage[239]. The control of ROS concentration is mediated by antioxidant molecules such as vitamins (A, E, C), peptides (Glutathione GSH) and proteins (GPx, TRx). In cancer, high metabolic activity, cellular signalling and mitochondrial dysfunction elevate ROS levels[238]. Supplementation with selenium in human studies have failed to prove beneficial chemopreventive effects[193]. However in cells, low doses of selenium have been proven to decrease the amount of ROS[225], with higher doses inducing levels of ROS[223,225]. As a result, two parameters for ROS production need to be studied; the time of exposure with selenium and the concentration of the selenium species used (Figure 8).

In vitro, glutathione spontaneously reacts with selenite ($SeO_3^{2-}$) to form various selenocompounds: selenodiglutathione (GS-Se-SG), glutathioselenol (GS-Se-), hydrogen selenide ($HSe^-$) and elemental selenium ($Se^0$) [240] through reduction by thiols and NADPH-dependent reductases (Figure 10). This leads to an oxidized inactive thioredoxin system by oxidation of structural cysteine[241] and depletion of NADPH[242]. Hydrogen selenide is known to quickly and spontaneously react with dioxygen to form elemental selenium $Se^0$, water, and ROS (Figure 10). It can also react with sulphur forming intramolecular disulphide bonds that have been related with inactivation of voltage sensors in the mitochondrial permeability transition pore[243]. Moreover $H_2Se$ promotes inhibition of heme containing enzymes belonging to respiratory chain[244,245]. This reaction leads to leakage of electrons which react with oxygen forming superoxide ions (ROS). This formation of ROS is then amplified by mitochondria[246].

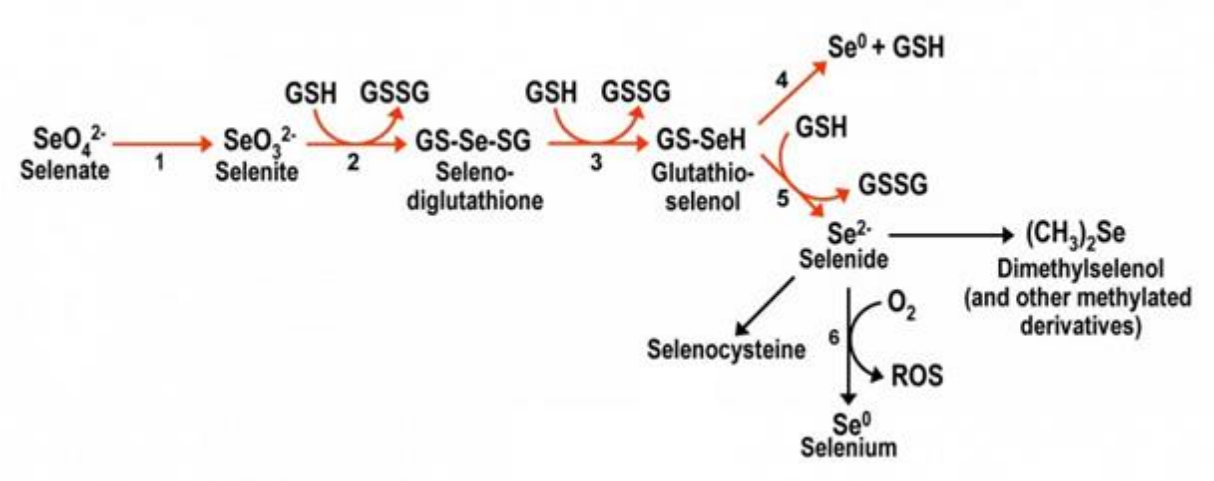


***Figure 10 : Effect of selenium on ROS production*** [247]

*Selenate is transformed into selenite in cells under redox conditions. Selenite interacts with the glutathione system and is processed into selenide. The reaction of selenite with oxygen liberates ROS and aggregates of Se°. Selenide can also be used in selenocystein production and can be eliminated through a methylation process.*

## ii. Effect of selenium on cell death

**Apoptosis**

Apoptosis is a regulated suicide mechanism that is involved in development and defence of multicellular organisms and can occur via two (intrinsic and extrinsic) pathways[248]. The extrinsic pathway is initiated by attachment of a ligand to the death receptor on cell membrane activating caspase 8 inside the cells. The intrinsic pathway is initiated within the cell through caspase 9 and caspase 3 due to DNA damage or internal stress, such as mitochondria membrane leakage[249]. BCL-2 family proteins regulate this pathway, controlling the release of the mitochondrial cytochrome c which activates the caspases (Figure 11).

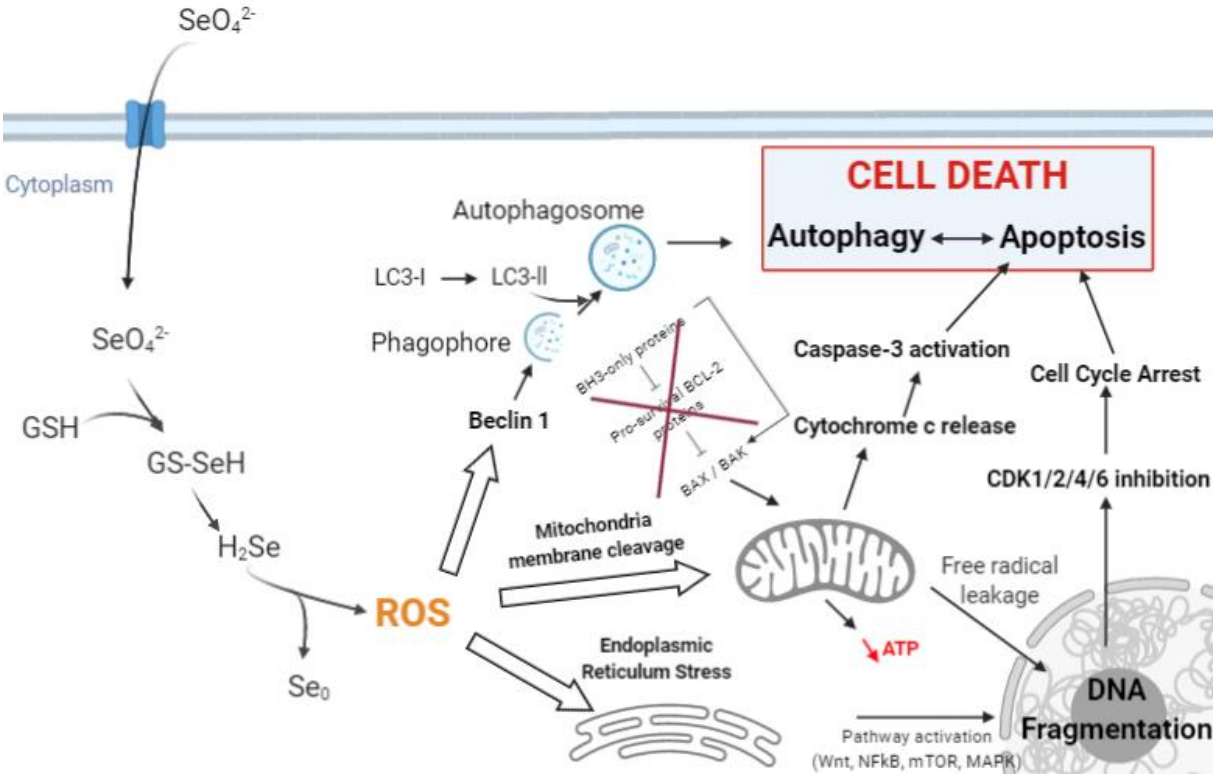


***Figure 11 : Effect of selenium on cell death***[250–253]
*Selenite triggers the production of ROS which leads to DNA, ER and mitochondrial damage triggering apoptosis. The accumulation of ROS can trigger the activation of Beclin-1 which triggers the autophagy in cells.*

In normal conditions, the mitochondrial respiratory chain reduces oxygen into water, however, intermediaries of this reaction produce ROS[239]. With the greater metabolic rates of cancer cells, this ROS production is increased. Treatment of cells with cytotoxic doses of selenium induces mitochondrial damage through an overproduction of ROS in the cytosol[254]. The increase of mitochondrial permeability following selenium treatment has been measured by the decrease of Bcl-xl prosurvival family proteins[255], the increase of pro-apoptosis Bad family proteins[256], and the liberation of the cytochrome c from the mitochondrial membrane[255]. The leakage of ROS in the cytosol saturates the redox management systems such as glutathione or thioredoxin reductase[257] and induces *in vivo* chromosome fragmentation and DNA phosphodiester bond break via $O_2$ dependent reactions[244,258]. Downstream effects of DNA damage and mitochondrial membrane disruption include the activation of the caspase 3, and the increase of cleaved PARP (poly (ADP-ribose) polymerase, a polymerase activated by single strand DNA)[259]. Resultant cell death then inhibits tumour growth[260].

**Autophagy**

Autophagy, related to cell survival, is a cellular process characterized by the formation of autophagosomes including cytoplasmic contents, such as proteins and organelles, in response to starvation or oxidative stress[238,261,262]. The formation of autophagosomes is initiated by the formation of protein complex ULK, PI3K (which contains Beclin-1) and ATG5-ATG12. The fusion of autophagosomes with lysosomes induces degradation of the autophagosome content[262] (Figure 11). Selenite treated cancer cells have been shown to display increased levels

of autophagy [230,263,264]. In colon cancer cells, 10 µM selenite induced ROS-related DNA damages leading to p53 (protein signalling DNA damages) mediated apoptosis in HCT116. However, in p53 Knock Out HCT116, autophagy was triggered through selenite treatment[250]. In both cell lines, when autophagy was inhibited, the apoptotic response to treatment was increased suggesting that the autophagic response is actually a defence mechanism against selenite treatment[263]. This is also supported by the fact that cell death decreased following autophagy activation in these cells[264]. This crosstalk was mediated via BCL-2 family proteins that are bound to Beclin-1 under normal conditions, which is cleaved by apoptotic caspases[262]. This prosurvival autophagy activation against selenite treatment phenotype has not been shown for all cancer cells. In glioma cells 7 µmol/L of selenite triggered autophagy that lead to increased cell death[225] through ROS overproduction, suggesting that the type of cell death is dependent on the cancer cell line.

# 4. Effect of selenium on epigenetic mechanisms

Cell and murine models have both revealed that selenium triggers DNA methylation modifications through dose dependent DNA methyltransferases (DNMT) activation/inhibition[207,217]. Se deficiency have been reported to inhibit liver expression of enzymes involved in the one-carbon metabolism [207,217]. Low doses of selenium increase DNA methylation while higher doses decrease levels of methylation of promoters[217] through modification of the activity of DNMTs.

The effect of selenite and methylseleninic acid on H3K9 modifications has been measured in prostate cancer cell lines. In LNCap prostate cancer cells, treatment with 1.5µM of selenite for 7 days reduced the activity of histone deacetylases either by binding to the catalytic site of the enzyme or by modifying cysteine residues in HDAC proteins leading to increased acetylated H3K9. Investigators have also measured a decreased amount of H3K9me in this cell line. Overall this induced the activation of gene expression. Decreased methylation of histone might be due to a decrease of the DNMT1 following selenium treatment as inhibition of DNMT by 5-aza-dC has been shown to result in decrease of H3K9 methylation[265]. This was concomitant with decrease of the DNA methylation on promoter of tumour suppressor genes. In glioblastoma spheroids, LN229 cells were treated with 2.5µM selenite resulting in a 30% reduction in of H3K9 methylation in comparison to control, whereas treatment of U87 (O(6)-methyguanine-DNA-methyltransferase (MGMT) negative cells) with 10µM selenite treatment increased the methylation of H3K9 [233], and methylseleninic acid (MSA) inhibited DNMT1 expression and decreased methylation of H3K9[266].

# 5. Selenium Nanoparticles

The toxicity of selenium is critically dependent on its redox state and concentration making it difficult to use in pharmacology. Selenium in solution has been extensively studied in different cancer cell types overall showing induction of redox functions at low doses[212,267] and apoptosis at higher doses[268] depending on the form of selenium and the type of cells used.

Preclinical and clinical studies have suggested a protective effect of selenium against prostate cancer[220] however higher (>90µg/day) didn't prove any chemotherapeutic effect. Higher doses of aqueous selenium are toxic and lead to selenosis[190,269]. To overcome the limitations of high dose systemic toxicity the use of selenium in the form of nanoparticles (SeNPs) has been initiated, with initial promising results including preferential uptake by cancer cells in comparison with normal cells[257,270]. Similarly to the aqueous selenium studies, SeNPs demonstrate an antioxidant activity in cancer cell lines[208] at low doses and demonstrating cytotoxic effect at higher doses. Moreover, SeNPs reduced toxicity of selenium up to four times in mouse models[271] in comparison with selenium in solution and the toxic effect on livers have been significantly reduced[272]. A major drawback of bare SeNPs appears to be the poor cellular intake, which has been overcome by conjugation to stabilizing and targeting ligands on the exterior surface of the nanoparticles[271–275].

**Coated SeNPs**

In order to increase the reactivity, bioavailability and stability of SeNPs but also to control their size, different coatings can be added during the process of synthesis. The addition of proteins (albumin), oligosaccharides (sucrose) and polysaccharides (chitosan) at different concentrations or at different times of preparation of the SeNPs influences size, morphology and stability[276] of the NPs in liquid dispersion[277].

In early 2000's SeNPs were synthesized in presence of different concentrations of albumin (BSA). It appeared that the higher the concentration of BSA, the smaller the nanoparticles[274,278]. The albumin bind the selenium through interaction by the cysteines as Cys-S-Se[274,279]. It allows the stability of the nanoparticles which would aggregate as micro particles in absence of proteins.

BSA-SeNPs have been proven to be 7-fold less toxic than selenite in mice with respectively 113 and 14mg Se/kg body weight to reach toxic doses. However in hepatic cancer cells (HepG2) no differences have been measured in growth inhibition between selenite and SeNP treatment after 72h of 25µM of Se[279] while GPx and TRx were upregulated. BSA allow stabilization of the nanoparticles and doesn't elicit toxic biological responses as well as being largely available. However non specific binding of albumin to other proteins inhibit their functions disturbing cellular processes. While paving the way for selenium nanoparticles study, BSA-SeNPs effect on cancer cells have been barely studied.

The use of chitosan for SeNP coating results in the nanoparticles having the ability to bind cell membrane phospholipids via exposed $NH_3^+$ groups[280]. Compared to bare SeNPs, chitosan coated SeNPs are better internalized by cancer cells through endocytosis[281,282]. In mouse model, chitosan coated SeNPs were 10 fold less toxic than aqueous selenite with a 50% mouse mortality of 24 mg selenite/g of body mass and 250 mg/g of bodymass chistosan-SeNPs/g[276].

Cancer cell specific properties can also be used to enable the targeting of SeNPs. The overexpression of folate receptor (vitamin B9) in different cancer tumours (kidney, liver, skin, lung)[164,165] has been used in order to specifically target cancer cells. In 4TI breast cancer cells, folic acid ($C_{19}H_{19}N_7O_6$) modified SeNPs increased cell mortality by 68% compared to bare

SeNPs[285]. Moreover, folic acid targeting of coated SeNPs induced apoptosis[285–287] in liver HepG2, osteosarcoma MG-63 and kidney HK-2 cells. In mouse models SeNP-folate decreased the tumour growth rate[285].

Interestingly chitosan and folate combined coatings resulted in targeting folate receptor and negatively charged membrane[286]. After internalization, when pH increase above 6.5, the amino groups of chitosan become positively charged and chitosan precipitate which induce an increased intracellular drug accumulation[288].

**SeNPs combined with chemotherapy**

Classic chemotherapy increases the oxidative stress in cancer cells but also in other normal cells. The preclinical and clinical studies using inorganic selenium supplements increased the antioxidant capacities of the cells[193,197]. Recent studies conjugated SeNPs with chemotherapeutics such as paclitaxel (PTX) or cisplatin, have any combined (additive or synergistic) cytotoxic effect[254,289,290] against cancer cells. Further development is needed to investigate the low impact of these treatment toward normal cells.

Paclitaxel has been loaded on 20-100 nm SeNPs by adsorption on pluronic F-127 detergent. The NPs demonstrated an anti-proliferative activity against lung (A549), breast (MCF7) and cervical (Hela) cancer cells[289]. Cell cycle analysis demonstrated a G2/M arrest in a dose dependent manner of SeNP-PTX leading to apoptosis due to ROS induced mitochondrial membrane disruption and activation of caspases without deciphering whether SeNPs or PTX had this effect. PTX-SeNPs used on these cancer cell types showed a greater cytotoxic effect at much lower concentrations than treatment with SeNPs or PTX alone and is thought to decrease the side effects of the different drugs[289].

Cisplatin the most widely used treatment in ovarian cancer causes side effects including nephrotoxicity and genotoxocity mediated via activation of the inflammatory pathway due to high oxidative stress in cells[204]. SeNPs reduced cisplatin toxicity against reproductive system in Wistar rats[290]. SeNP-cisplatin also reduced toxicity in mice against osteoblasts[291], thyroid gland[292], intestinal cells[293,294] by limiting nuclear and mitochondrial damages and apoptosis In brain and hepatocytes SeNP-cisplatin reduced the number of pro-apoptotic B-cells[295].

Building a more comprehensive approach of the effect of selenium nanoparticles in cancer models, we decided to review the literature in order to describe the different type of SeNPs that have been synthesized and used as treatment toward cancer cells or tumour bearing mice since the beginning of the 21$^{st}$ century. Table 3 sums up the main outcomes of those trials.

***Table 3:*** *2000 to 2020 selenium nanoparticle preparations and effect in cancer cells.*

| NP Type | Size | Shell | Model | Outcomes | Ref |
|---|---|---|---|---|---|
| SeO2 in vitamin C | NC | None | HeLa cercical cancer cells MDA-MB-231 breast cancer cells | Cell cycle arrest in S phase | 296 |
| Nano Se | 40 to 90nm | None | MCF-7 breast cancer (ERα+) MDA-MB-231 (ERα-) | SeNP induce cell death expression Bax/Cytc in ERα+ cells. Scavenging ROS | 297 |
| Nano Se | 5 to 200nm | BSA | In vitro ROS scavenging | Better free radical scavenging efficiency for lower size NP | 274,279 |
| Nano Se | 36 to 90nm | BSA | GST/GPx activity measurement in mice liver/blood | Size effect of NanoSe as chemopreventive | 278 |
| Nano Se | 20-60nm | BSA | Mice | Lower toxicity than selenomethionine with increase selenoenzyme producton | 272 |
| Folic Acid modified SeNPs | 70nm | Folic Acid | MCF-7 breast cancer cells | Antiproliferative, Mitochondria-dependent apoptosis | 287 |
| Light and heavy Chitosan on synthesized SeNP | 50 to 103nm | Chitosan | BABLC-3T3 skin cells Caco2 viscera cells | Inhibit ROS Production (GPx increase). Chitosan stabilize NP | 276 |
| Sialic Acid coated SeNPs | 70-170nm | Sialic Acid | HeLa Cervical cancer cells | Apoptosis and increased uptake | 298 |
| Transferrin conjugated doxorubicin loaded SeNP | 130nm | Transferrin Doxorubicin (DOX) | MCF-7 breast HepG2 hepatocellular carcinoma A375 melanoma HUVEC umbilical vein endothelial cancer cells | Cytotoxicity against cancer cells through apoptosis (p53 activation, ROS overproduction) | 256 |
| 5FU surface functionalized SeNP | 70nm | 5-fluorouracil | A375 human melanoma | subG1 arrest apoptosis (casp9) due do DNA damages Mitochondrial disruption | 269,299 |
| Paclitaxel charged SeNP | 74nm | Paclitaxel | A549 lung MCF7 breast HeLa cervical HT29 colon cancer cells | G2/M arrest apoptosis (casp3) Mitochondrial disruption | 289 |

# IV. Objectives

Hypothesis: Selenium nanoparticles accumulate in ovarian cancer cells and limit the growth of these cells more effectively then free forms of selenium that display inherent in vivo toxicity. Moreover the use of copper isotopes ratio in blood and samples are informative in Ovarian Cancer early detection.

Main objectives:

1. Determine the effects of selenium nanoparticles on ovarian cancer cells by investigating nanoparticle accumulation, cell death, cytotoxicity, migration of cancer cells.
2. Characterise the effects of selenium nanoparticles on cell biomechanics to understand if selenium impairs metastatic potential by affecting cytoskeleton.
3. Determine the molecular process triggered by selenium nanoparticles in ovarian cancer cells to understand underlying mechanisms of action
4. Evaluate $^{65}Cu/^{63}Cu$ ratios ($\delta^{65}Cu$) in serum samples from cancer patients as a potential complementary ovarian cancer biomarker.

# Selenium Nanoparticles triggers alterations in ovarian cancer cells biomechanics

# I. Presentation of the article

Metastasis is the leading cause of cancer death in 90% of ovarian cancer cases[26]. The ability to limit this process is paramount in the treatment of ovarian cancer, where metastasis seems to be triggered by the accumulation of highly inflammatory peritoneal ascitic fluid, which contains growth factors that can induce epithelial to mesenchymal transition (EMT). In addition to these biochemical factors, the sheer stresses that cells are exposed to as a result of ascitic fluid circulation, may help tumour cell dispersion[27]. EMT is defined by the loss of cellular polarity, modifying their interactions with neighboring cells while gaining migratory and invasive properties. During this process, cells exhibit modified mechanical properties as a result of altered architectural changes of their cytoskeleton[2, 53]. Principal cytoskeletal components such as actin microfilaments, intermediate filaments and microtubule polymer networks play important roles in locomotion and cell integrity, influencing cell adherence, interactions with other cells and motility[58-60].

With Ovarian cancer motility and mechanical transformation being a central theme to both local and distal metastasis, selenium nanoparticle effect on ovarian cancer cell lines, SKOV-3 and OVCAR-3 biomechanical properties were assessed in vitro. SKOV-3 are metastatic epithelial cancer cells originally derived from the ascitic fluid. OVCAR-3 are also epithelial cancer cells, however are derived from slow growing adenocarcinoma and are associated with resistant phenotypes. Expression of EMT markers in SKOV-3 and OVCAR-3 cell were assessed using western blotting, alongside cellular morphology, membrane roughness and mechanical properties (elasticity and adhesion), in the presence and absence of selenium nanoparticles coated with BSA and chitosan. BSA is used in nanoparticles synthesis for its ease of use and high bioavailability and stability in blood. However, it can non selectively bind to proteins impairing cellular functions. Chitosan is highly soluble when pH<6.5 thanks to the positive charges of the nitrogen groups and the coating disaggregate allowing the drug release[133]. Free selenite was used as a control to show evidence for the increased efficacy and uptake of selenium nanoparticles.

Dissemination of cancer cells following EMT is sustained by modification of cell-cell, cell-matrix interactions and cytoskeleton modifications. Such modification can be studied using nanomechanical tool such as atomic force microscopy. Atomic Force Microscopy is composed of a mobile cantilever on which a laser detects its deflection through its interaction with the surface studied. While the cantilever is moving, the surface elasticity and roughness impacts the way the cantilever bends. This is detected by the laser receptor which translates the properties of the material studied into force curves using the Hertz model allowing the estimation of Young's Modulus (force necessary to indent into the cells). Literature data demonstrate[53,56,300] that cellular elasticity is strongly correlated with cell cytoskeleton.

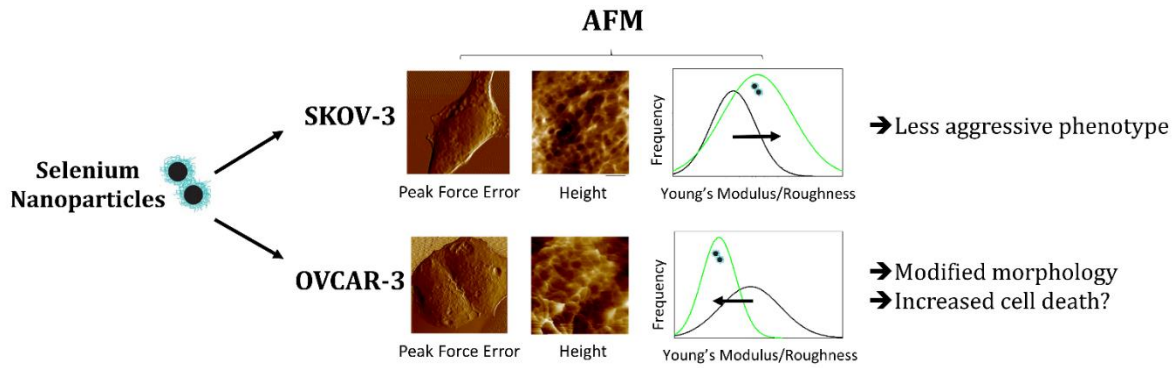


**Graphical Abstract: Selenium nanoparticles triggers nanomechanic properties modifications in ovarian cancer cell lines**

*Treatment of high grade serous ovarian cancer cells OVCAR-3 and SKOV-3 with coated selenium nanoparticles highlighted two opposite behavior depending on the aggressiveness of the cell type. Biomechanical modifications in metastatic SKOV-3 and aggressive OVCAR-3 assessed by Atomic Force Microscopy measurement led us to decrease the metastatic potential of SKOV-3 cells and decrease viability of OVCAR-3 cells.*

We assessed the EMT markers and the mechanical properties of SKOV-3 and OVCAR-3 using AFM before and after treatment with selenite or coated selenium nanoparticles (see Figure above). SeNP penetration in SKOV-3 and OVCAR-3 ovarian cancer cells was assessed by measuring the levels of selenoprotein transcript GPX1 after treatment. It appeared that selenium can't affect EMT markers in the two different ovarian cancer cell lines. The analysis of nanomechanical parameters revealed opposite phenotype between SKOV-3 and OVCAR-3 after treatment with SeNPs. While SKOV-3 increased stiffness and roughness, OVCAR-3 became more elastic and softer. In addition we acquire we hypothesized the SeNPs are effective for cell proliferation inhibition but in different mech anisms depending on the cell type. We tried to elucidate those mechanisms in the following part constituted by the paper entitled "Selenium nanoparticles induce global histone methylation changes in ovarian cancer cells".

# II. Article

This paper is Published in Nanomedicine: Nanotechnology, Biology and Medicine
**https://www.sciencedirect.com/science/article/pii/S154996342030112X**

## Selenium nanoparticles trigger alterations in ovarian cancer cell biomechanics.

Benoit Toubhans[1,2] (PhD Student) Salvatore Andrea Gazze[1](Dr) Caroline Bissardon[3] (Dr), Sylvain Bohic[3,4](Dr) Alexandra T. Gourlan[2](Dr) Deyarina Gonzalez[1](Pr) Laurent Charlet[2](Pr) R. Steven Conlan[1] (Pr) and Lewis W. Francis[1] (Dr).

**Affiliations:**
[1]Center for NanoHealth**, Swansea University Medical School**
[2]ISTerre **Université Grenoble Alpes**
[3]Inserm, UA7, Synchrotron Radiation for Biomedicine (STROBE), **Université Grenoble Alpes**
[4]ID16A Beamline, **ESRF, The European Synchrotron**

The authors declare no conflict of interest.

ELSEVIER

Nanomedicine: Nanotechnology, Biology, and Medicine
29 (2020) 102258

nanomedicine
Nanotechnology, Biology, and Medicine

nanomedjournal.com

# Selenium nanoparticles trigger alterations in ovarian cancer cell biomechanics

Benoit Toubhans[a,b,*], Salvatore Andrea Gazze[a], Caroline Bissardon[c], Sylvain Bohic[c,d], Alexandra T. Gourlan[b], Deyarina Gonzalez[a], Laurent Charlet[b], R. Steven Conlan[a], Lewis W. Francis[a]

[a]Centre for NanoHealth, Swansea University Medical School, Swansea, UK
[b]ISTerre Université Grenoble Alpes, Grenoble, France
[c]Inserm, UA7, Synchrotron Radiation for Biomedicine (STROBE), Université Grenoble Alpes, Grenoble, France
[d]ID16A Beamline, ESRF, The European Synchrotron, Grenoble, France

Revised 22 May 2020

**Abstract**

High dose selenium acts as a cytotoxic agent, with potential applications in cancer treatment. However, clinical trials have failed to show any chemotherapeutic value of selenium at safe and tolerated doses (<90 μg/day). To enable the successful exploitation of selenium for cancer treatment, we evaluated inorganic selenium nanoparticles (SeNP), and found them effective in inhibiting ovarian cancer cell growth. In both SKOV-3 and OVCAR-3 ovarian cancer cell types SeNP treatment resulted in significant cytotoxicity. The two cell types displayed contrasting nanomechanical responses to SeNPs, with decreased surface roughness and membrane stiffness, characteristics of OVCAR-3 cell death. In SKOV-3, cell membrane surface roughness and stiffness increased, both properties associated with decreased metastatic potential. The beneficial effects of SeNPs on ovarian cancer cell death appear cell type dependent, and due to their low *in vivo* toxicity offer an exciting opportunity for future cancer treatment.


*Key words:* Selenium; Nanoparticles; Nanomechanics; Ovarian Cancer; Metastasis

Selenium (Se) is an essential trace element, obtained primarily through the diet as selenium containing amino acids,[1] however it has a narrow safe range of exposure and becomes toxic at levels above the recommended dietary intake (30-90 μg/day). Selenoproteins are implicit in human health due to their antioxidant activity and are associated, for example, with anti-inflammatory, and antiviral properties.[2] Selenocysteine (SeCys) is present in Se containing proteins, predominantly glutathione peroxidase (GPX) in the liver, and is involved in reactive oxygen species (ROS) scavenging through its redox function.[3] GPX reduces lipid hydroperoxides in alcohols and reduces free hydrogen peroxide to water.

Observational studies revealed that Se can inhibit cancer cell growth. This effect occurs through increasing ROS-mediated necrosis in prostate cancer,[4] autophagy in colorectal cancer,[5] and apoptosis in skin, breast, and liver cancer.[6] However, a meta-analysis of randomized controlled trials, >25,000 patients, failed to show any significant effect of Se dietary supplementation in reducing the incidence of colorectal, skin, lung, bladder or prostate cancer.[7] High supplementation levels induced toxicity limiting the utility of Se containing compounds as potential chemotherapeutic agents.[8] To overcome the toxicity associated with soluble Se, Se-nanoparticles (SeNPs) have been synthesized and evaluated for their anticancer properties. Both free-SeNPs[9] and encapsulated-SeNPs[10] are effective in reducing cancer cell proliferation *in vitro*. Furthermore, SeNPs appear to be effective and well tolerated *in vivo* [11], enabling Se to be used effectively at doses that would be toxic if administered as soluble Se.

Ovarian cancer is the seventh most common cancer in women with five-year survival rates of less than 45%,[8] and only 20% of cases are detected at early stages of the disease.[12] The ovarian micro-environment cancer is highly inflammatory, and the use of

The authors declare no conflict of interest.

*Corresponding author at: Centre for NanoHealth, Swansea University Medical School.
*E-mail address:* 970914@swansea.ac.uk. (B. Toubhans).

https://doi.org/10.1016/j.nano.2020.102258

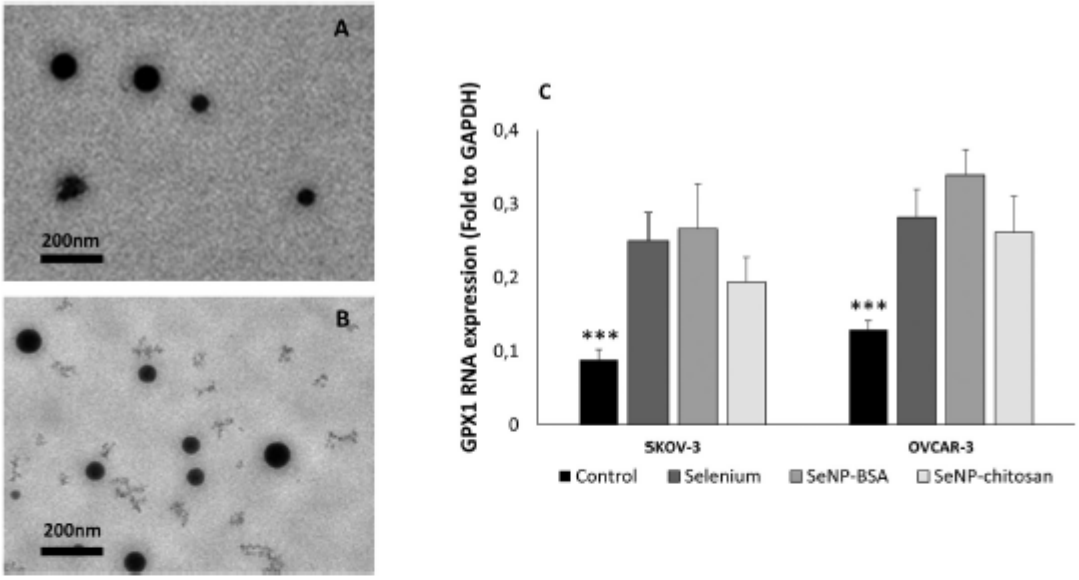


Figure 1. **SeNP characterization and internalization**. Representative TEM images of the SeNP-BSA (A) and SeNP-chitosan (B). Images have been taken with x23000 magnification. Treatment for 48 h with sublethal doses of selenite, SeNP-BSA and SeNP-chitosan resulted in significant alteration (C) in SKOV-3 (left) or OVCAR-3 (right) cells expression of GPX1. In untreated SKOV-3 relative GPX1 expression levels were respectively 0.08 +/− 0.01 for control, 0.25 +/− 0.03 for selenite, 0.26 +/− 0.06 SeNP-BSA, 0.19 +/− 0.03 for SeNP-Chitosan. Same pattern have been observed in OVCAR with 0.13 +/− 0.01 for control, 0.28 +/− 0.03 for Selenite, 0.34 +/− 0.03 SeNP-BSA, 0.26 +/− 0.05 SeNP-Chitosan. All measurement representative of a minimum 3 biological repeats.

antioxidant supplements has been correlated with a decreased risk of cancer development[13], possible due to the form of selenite used in supplements forming endogenous SeNPs that inhibit glycolysis, causing mitochondrial dysfunction, autophagy and cytoskeletal depolymerisation.[14]

Tumor metastasis in advanced ovarian disease is the leading cause of death and is an inherently mechanical process where these properties are known to be altered.[16,17] The acquisition of invasiveness by tumor initiating cells is accompanied by the loss of the epithelial features and the gain of a mesenchymal phenotype, termed epithelial to mesenchymal transition (EMT).[15] Chemotherapeutic drugs have been shown to modify such cellular biomechanical features, through architectural changes to the cell cytoskeleton.[18] Similarly cellular cytoskeletal components such as actin microfilaments, intermediate filaments, and microtubule polymer networks play determinant roles in cellular mechanical properties, locomotion, while regulating cellular integrity during differentiation.[18] Modifications to those networks influence cytoadherence, migration, invasion and tumor metastasis.[19,20]

Here, we assessed the anticancer activity of protein (BSA) and carbohydrate (chitosan) surface coated SeNPs in two distinct high grade serous ovarian cancer cell lines, OVCAR-3 and SKOV-3. Both SeNPs were significantly more cytotoxic than soluble Se in OVCAR-3 cells at high doses (>40µg/mL), but similar to soluble Se with SKOV-3 cells, which were more sensitive to Se treatment than OVCAR-3 cells, highlighting the differences between cell types. Further analysis revealed SKOV-3 cells exhibited stable EMT markers and decreased motility, and interestingly, an increase cell surface roughness and cellular stiffness. In contrast OVCAR-3 cells displayed a decrease in cellular stiffness indicative of altered cytoskeletal dynamics that, alongside decreased vimentin expression levels and autophagy, can be interpreted as sensitization toward apoptosis.[5,6,21] It appears that reduction in cell viability following SeNP exposure occurs through different mechanisms that result in contrasting perturbations in cellular mechanics in serous ovarian cancer subtypes. SeNPs may therefore offer the potential for pan-cancer treatments, not least in ovarian cancer, that is a complex and multifaceted disease with a very poor prognostic outcome.

## Methods

### *Cell culture*

The OVCAR-3 (ATCC, Rockville, MD, USA) ovarian cancer cells were cultured in RPMI-1640 (Sigma-Aldrich, Gillingham, UK) supplemented with 20% bovine serum albumin (BSA, Sigma-Aldrich, UK), 5 µg/mL insulin (Sigma-Aldrich, Gillingham, UK), and 1% penicillin-streptomycin (v/v) solution (Sigma-Aldrich, UK). The SKOV-3 (ATCC, Rockville, MD, US) ovarian cancer cells were cultured in McCoy's 5A (Sigma-Aldrich, Gillingham, UK) supplemented with 10% bovine serum albumin (BSA, Sigma-Aldrich, UK), and 1% penicillin-streptomycin (v/v) (Sigma-Aldrich, Gillingham, UK). Cells were maintained at 37°C and 5% $CO_2$ and routinely passaged using 0.25% trypsin - 0.1% EDTA (v/v).

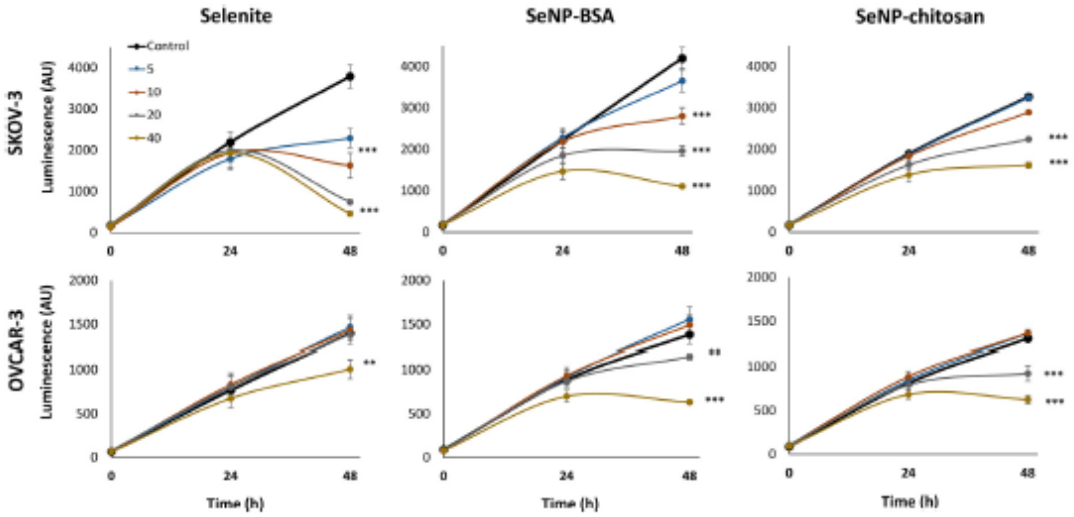


Figure 2. **SeNP cytotoxicity.** Ovarian cancer cells SKOV-3 (top) and OVCAR-3 (bottom) were grown in the presence of Selenite, BSA coated selenium nanoparticles or chitosan coated selenium nanoparticles over 48 h and monitored for cellular cytotoxicity. Both cell lines were treated for 48 h with an increasing range of concentration from 0 to 80 μg/mL. Cytotoxicity was evaluated by RTGlo and mean (+/−SD) luminescence values shown) from four independent experiments. SKOV-3 and OVCAR-3 viability are presented in comparison with control in supplementary figure 1.

*SeNP characterization*

SeNPs were purchased from NANOCS (New York, USA) with two different coatings, BSA and chitosan. Manufacturer specifications stated 25 – 50 nm of diameter for both nanoparticles. Size shape and charge analysis was conducted by Dynamic Light Scattering and Zeta Potential measurement using a ZetaSizer Nano (Malvern Instruments, Malvern, UK) with a 173° scattering angle using SeNPs at 1μg/mL in water (reflexive index of 1.33) at 25°C.

*Cell growth and Se treatment*

Both SKOV-3 and OVCAR-3 cells were cultured in growth medium until 80% confluency, trypsinized per regular passage and seeded to sterile petri dishes (Corning, UK) at 37° C and 5% $CO_2$. After 48 h incubation culture medium was removed and 2 mL of fresh medium containing the expected concentration of aqueous Se (selenite $Se^{4+}$) or SeNPs added for a further 48 h prior to analysis, with a minimum of three biological repeats.

*Cell viability assay*

Ovarian cancer cell viability in the presence and absence of Se treatments was determined using the Real-Time Glo assay (RTGlo, PROMEGA, Southampton, UK). $1 \times 10^3$ ovarian cancer cells/well were plated within 96-well white plates (Corning, UK). After 24 h of growth, culture media was aspirated and 100 μL of fresh medium containing aqueous Se (selenite $Se^{4+}$) or SeNPs (BSA or chitosan) were added. An increasing dose range (0.06 μg/mL to 40 μg/mL) was applied by dilution in appropriate medium for 48 h. The RTGlo with RPMI-1640 medium was added 1:1 with treatment medium. A BMG Labtech Fluostar Omega was used to measure luminescence every 24 h and presented as absolute values. IC20/IC50 doses were determined as the concentration of treatment that reduced by 20%/50% the luminescence signal compared to untreated control. The IC20/IC50 values shown (average ± standard deviation) are from a minimum of four independent experiments performed with 6 technical repeats.

*Migration assay*

$2 \times 10^5$ SKOV-3 cells/per well were seeded in 12 well plates and cultured in complete culture medium until the cells reached confluence. A scratch was then introduced to the monolayers, using a sterile (20 μL pipette) tip. The media was then aspirated and a fresh, fetal bovine serum (FBS, Gibco, UK) free medium containing IC20 selenium treatment was added to each well and cultured for 48 h. The scratch was imaged at 0, 24, 48 h using a Primo Vert inverted light microscope (Zeiss, Cambridge, UK). Average scratch width measurements were measured at three random areas, in three wells for each condition, as previously reported.[22] The migration rate was calculated according to the following equation: cell motilities (%) = [1 − (distance of scratched area at 24 h/distance of scratched area at 0 h)] ×100%.

*Protein blotting*

Total cellular protein was extracted using TRIzol™ reagent (Sigma, Gillingham, UK) and quantified using the DC™ Protein Assay (BioRad, Deeside, UK). Protein from each sample was mixed with Laemmli sample buffer containing β-mercaptoethanol (5%) and boiled at 95°C for 5 min. Equal

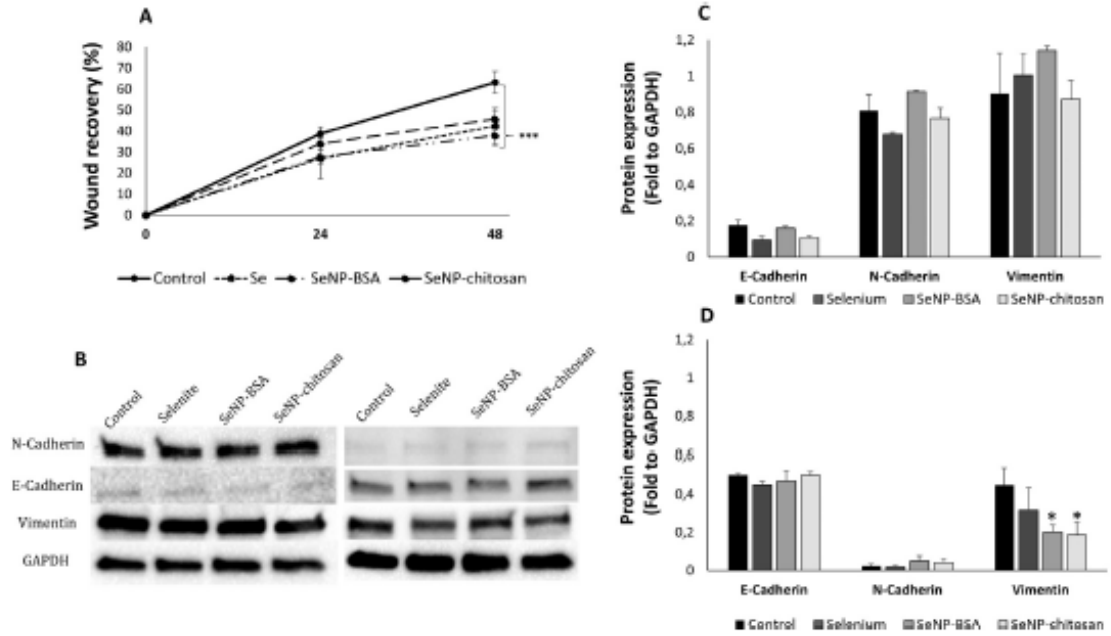


Figure 3. **Effect of SeNPs on EMT phenotype.** Scratch/wound healing assay (A) results showed that selenite, SeNP-chitosan and SeNP-BSA treatments at IC20 significantly decreased migration of SKOV-3 cells during 48 h. SeNP-BSA treatment decreases the recovery rate by 25% (+/−4.8%), SeNP-chitosan treatment by 16.5% (+/−3.8%) and selenite treatment by 18.6 (+/−8.2%) in comparison with control ($P < 0.05$). It was not possible to complete the migration assay with OVCAR-3 cells as they do not survive when depleted with FBS. Treatment for 48 h with IC20 selenite, SeNP-BSA and SeNP-chitosan resulted in no significant alteration in SKOV-3 or OVCAR-3 cells profiling of EMT markers (E-cadherin, N-cadherin, Vimentin) (C, D). In untreated SKOV-3 (C) relative vimentin expression levels were similar between conditions with respectively 0.9 (+/−0.2) for control, 1.01 (+/−0.1) for selenite, 1.14 (+/−0.02) for BSA SeNP, 0.87 (+/−0.11) for chitosan SeNP. Relative expression of E-cadherin was low (0.01 to 0.02). N-cadherin expression was similar between conditions with respectively 0.8 (+/−0.08) for control, 0.67 (+/−0.01) for selenite, 0.9 (+/−0.01) for BSA SeNP, 0.76 (+/−0.05) for chitosan SeNP. In untreated OVCAR-3 (D) relative vimentin expression levels were 0.45 (+/−0.08) while it was decreased in treated cells with 0.31 (+/−0.1) with selenite, 0.20(+/−0.03) for BSA SeNP and 0.18(+/−0.06) for chitosan SeNP. Relative expression of N-cadherin was very low (0.02 to 0.05). E-cadherin expressions were the same between the different conditions with 0.50 (+/−0.05) for control, 0.45 (+/−0.2) for selenite, 0.47 (+/−0.05) for SeNP-BSA and 0.5 (+/−0.002) for chitosan SeNP. Examples of western blots have been displayed in (B).

amounts of protein (30 µg) were separated by SDS-PAGE (4-20% gels) and subsequently transferred onto a PVDF membrane (Biorad, Deeside, UK). The membranes were blocked for 1 h in 5% BSA prepared in 0.1% Tris-buffered saline-Tween20® (TBS-T). Blots were then incubated with the corresponding primary antibody (E-cadherin: mouse monoclonal (Abcam ab1416, Cambridge, UK), vimentin: mouse monoclonal (Santa Cruz sc-6260, Wembley, UK), N-cadherin: rabbit polyclonal (Abcam ab18203, Cambridge, Wembley, UK) or GAPDH: mouse monoclonal (Santa Cruz sc-47724, Wembley, UK)) at a concentration of 200 µg/mL overnight at 4°C. Blots were then washed 3 times with TBS-T and incubated at room temperature for 1 h with the appropriate secondary antibody (goat anti-mouse Abcam ab150113 or goat anti-rabbit Abcam ab6721 HRP secondary, Cambridge, UK) at a concentration of 400 µg/mL. For signal detection, membranes were processed using the Clarity™ Western ECL Substrate kit (BioRad, Deeside, UK) according to the manufacturer's recommendations and visualized using a ChemiDoc XRS system (BioRad, Deeside, UK). Analysis of the intensity of the bands was done using Image Lab (BioRad, Deeside, UK) software tracing fixed size-limited rectangle around the bands of interest and reporting the Adjusted Volume (Intensity corrected by the background noise). Protein expression was normalized GAPDH and relative expression expressed as the mean fold induction ± standard deviation.

*qRT-PCR*

Following RNA extraction and quantification, qPCR was carried out in accordance with the manufacturers' recommendations, using the RETROscript® kit two-step method (Invitrogen Ltd., UK). Following cDNA synthesis from 100 ng of RNA, each sample was analyzed by qPCR in triplicate using iQ SYBR Green supermix (BioRad, Deeside, UK) and gene specific primers (Sigma-Aldrich, Gillingham, UK) to evaluate different gene expression GAPDH (GAPDH Forward: GTCCACTGGCGTCTTCAC, Reverse: CTTGAGGCTGTTGTCATACTTC) and GPX1 (GPX1 Forward: GTGCTCGGCTTCCCGTGCAAC, Reverse: CTCGAAGAGCATGAAGTTGGGC). Serial dilutions of cDNA were used to plot a calibration curve, and gene expression quantified

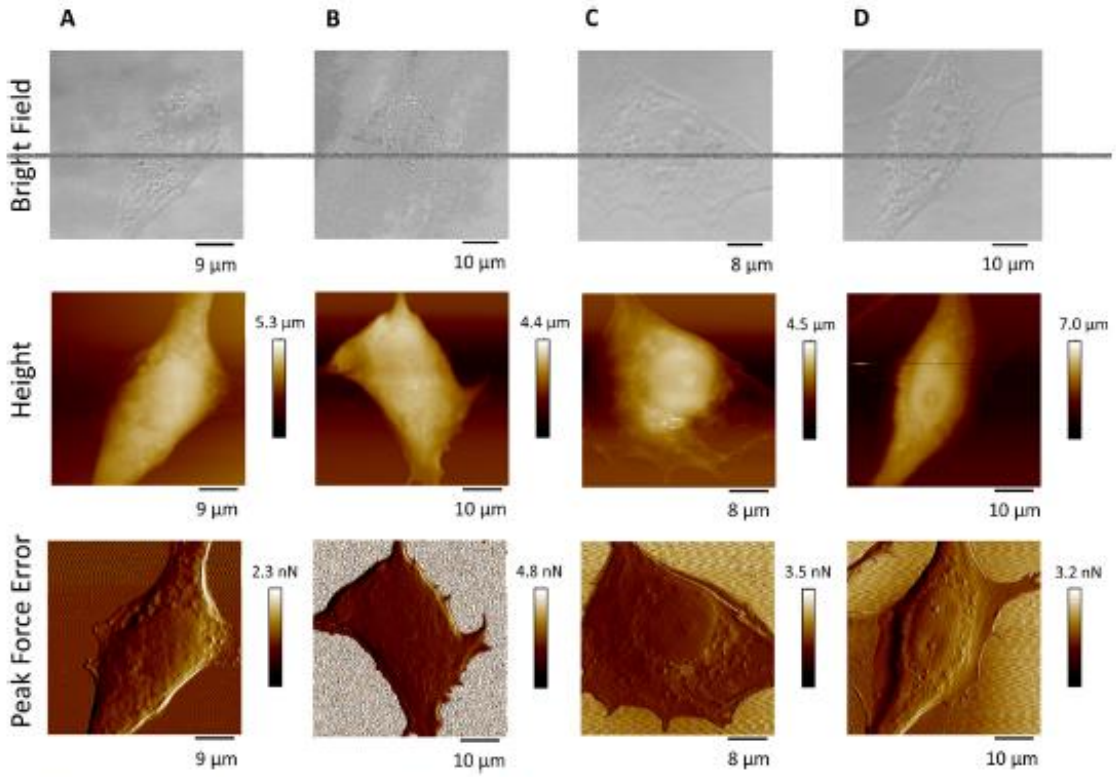


Figure 4. **Effect of SeNP on SKOV-3 morphology and topography.** SKOV-3 cells were treated with Se-NPs for 48 h and compared to selenite (IC20) and an untreated control. High resolution AFM imaging was performed and subsequent image analysis. No morphological and/or topographical cell changes were detected with stable morphological features observed in the Control (A), IC20 Selenite (B), IC20 BSA coated SeNP (C), IC20 chitosan coated SeNP (D) using bright field, AFM height and PeakForce error signal respectively. The shown image is representative of the morphology of SKOV-3, from imaging 15 cells from 3 biological repeats.

by plotting threshold cycle values. Expression levels were normalized to values obtained for the reference gene (GAPDH) and relative expression expressed as the mean fold induction ± standard deviation. Statistical differences between the treatment groups and the control were determined by analysis of variance (ANOVA) (where $P < 0.05$ was considered significant).

*AFM analysis*

*Young modulus, indentation and adhesion*

Force-indentation curves were obtained using a Nanowizard II AFM (JPK, Berlin, Germany) mounted on a ZEISS 510 confocal microscope (Zeiss, Cambridge, UK) as described in [23]. During AFM, cells were kept alive in serum free, pH indicator free culture media at 37°C in a petri dish using a standard stage heater and analyzed for a maximum of 3 h. The inverted optical microscope was used to position the tip on the cell and force volume conducted using borosilicate colloidal (Novascan, UK) cantilevers, with a nominal spring constant of 0.35 N/m with a radius of 2.5 µm. Prior to measurements, deflection sensitivity and spring constant were experimentally determined, the latter using the subroutine of the JPK software. Three individual force curves (ramp size of 6 µm) were taken on a total of 25 cells, across 3 independent biological experiments, using a maximum force indentation of 6 nN was used. JPK Data Processing program was used to process the acquired force curves. For each force curve the baseline was corrected to 0 and the approach curve in the contact regime of each force curve was fitted using the classical Hertz model according to Eq. 1. In both cases, the fitting module in the JPK software was used and only curves with a goodness of fit between 0.85 and 1 were considered for statistical analysis.

$$R_{RMS} = \sqrt{\frac{\sum Z_i^2}{N}} \quad (1)$$

In this equation, F is the force applied by the cantilever tip to the cell, E is the Young's modulus (fit parameter), υ is the Poisson's ratio (0.5), R the radius of the indenter, δ is the indentation depth and α is the half-angle of the indenter (18° for the used sharp probes).

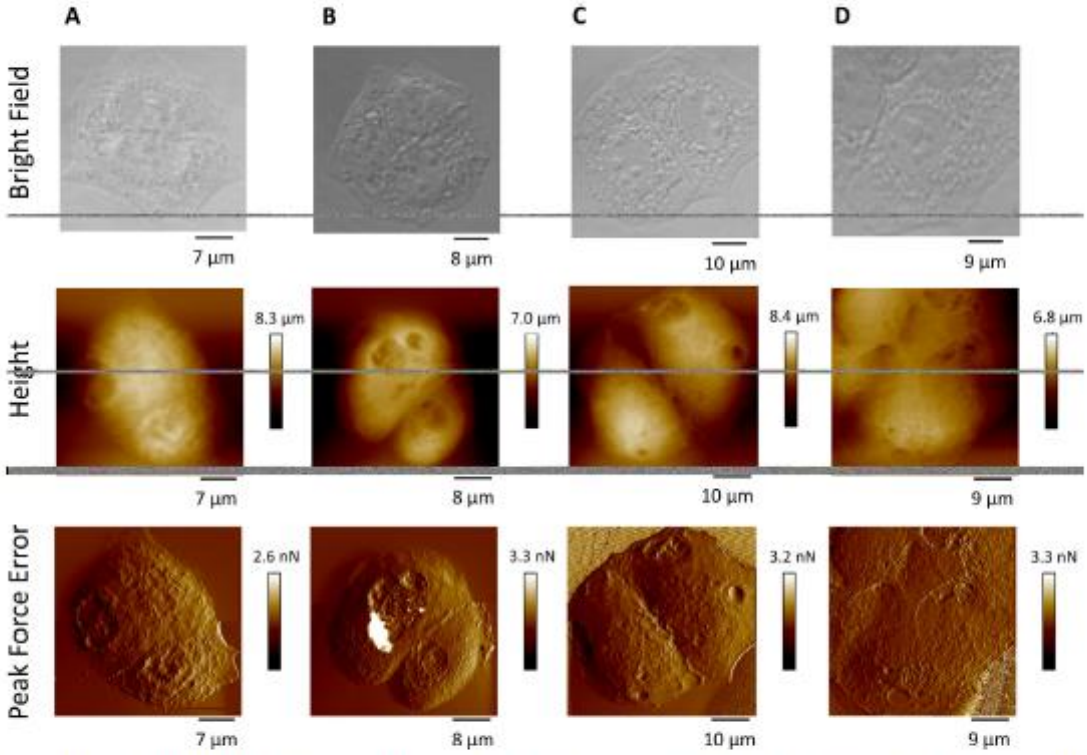


Figure 5. **Effect of SeNP on OVCAR-3 morphology and topography.** OVCAR-3 cells were treated with Se-NPs for 48 h and compared to selenite (IC20) and an untreated control. High resolution AFM imaging was performed and subsequent image analysis. No morphological and/or topographical cell changes were detected with stable morphological features observed in the Control (A), IC20 selenite (B), IC20 BSA coated SeNP (C), IC20 chitosan coated SeNP (D) using bright field, AFM height and PeakForce error signal respectively. The shown image is representative of the morphology of OVCAR-3, from imaging 15 cells from 3 biological repeats.

*Topography and surface roughness*

In order to resolve the membrane architecture, cells were fixed for imaging according to the protocols outlined in Francis et al. [24] Briefly cells were washed 2 times with PBS then fixed for 30 min in 4% PFA (Merck, UK) diluted in PBS at RT. PFA was subsequently removed and replaced by phosphate buffered saline (PBS), at RT. SKOV-3 and OVCAR-3 cell morphology and topography were analyzed using a BioScope Catalyst (Bruker Instruments, USA) mounted on a Nikon Eclipse Ti-S inverted optical microscope (Nikon Instruments, Netherlands). The inverted optical microscope was used to carefully position the tip on the desired cell and tapping mode imaging undertaken using MLCT-E silicon nitride cantilevers (Bruker-Nano, UK). Offline processing for AFM height data consisted of first-order flattening and plane fitting. The membrane roughness was measured using the subroutine in the Nanoscope Analysis software v1.50, on areas of 25 $\mu m^2$ each on five cells for control and treated, from a minimum of 3 biological repeats. Membrane roughness was calculated using Eq. 2,

$$R_{RMS} = \sqrt{\frac{\sum Z_i^2}{N}} \quad (2)$$

where N is the number of height points in the analyzed area and Zi is the vertical distance of data point i from the mean image data plane. Sixteen roughness measurements were calculated per image, with 1 $\mu m^2$ areas of measurement.

*Statistical analysis*

All data presented are calculated from a minimum of three biological repeats, with technical repeats included per sample, as denoted. Data normality was analyzed using the Kolmogorov Smirnov test, with normally distributed data analyzed with the one-way and two-way analysis of variance (ANOVA) or the Mann–Whitney pairwise test for non-parametric data. In all cases in which ANOVA was significant, multiple comparison methods were used. Differences were considered significant for $P \leq 0.05$ ($*P \leq 0.05$, $**P \leq 0.01$, $***P \leq 0.001$). All data were analyzed in MiniTab 14.

## Results

*Physicochemical and biological characterization of SeNPs*

Based on previous observations showing Se has anti-proliferative effects on ovarian cancer cells, [14,25,26] and the good tolerability of

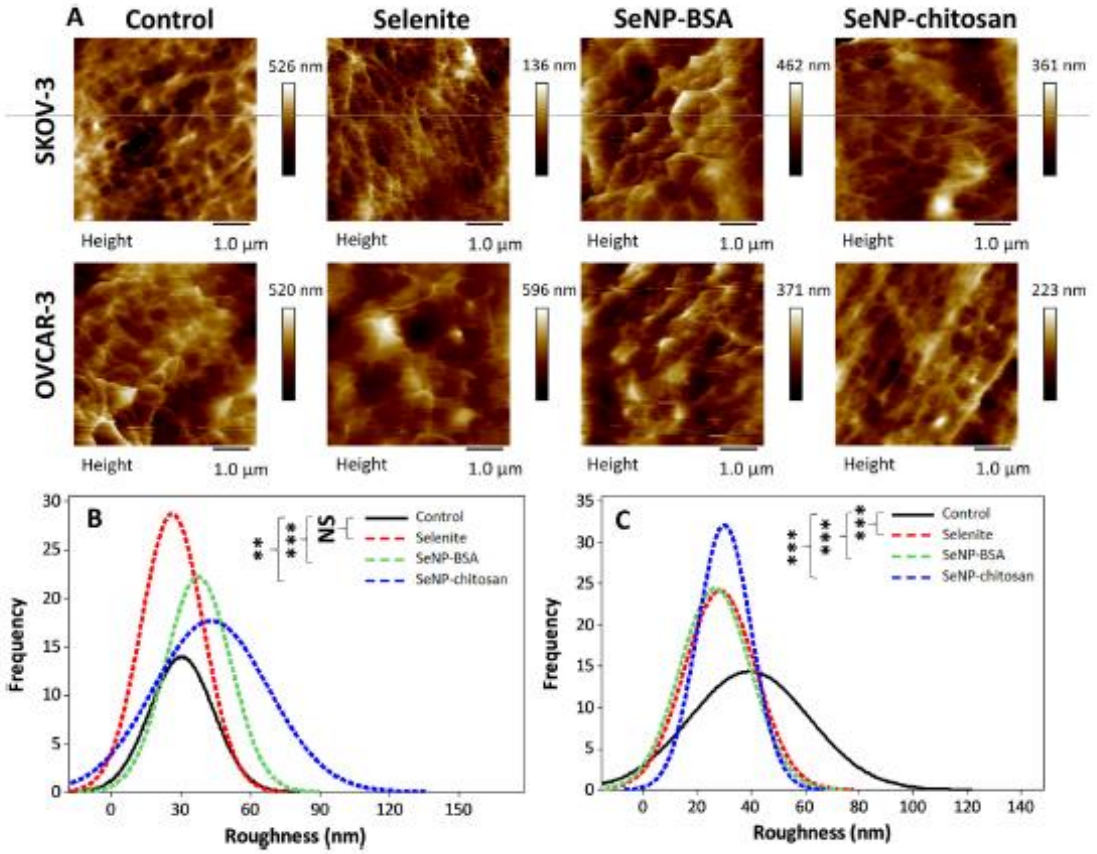


Figure 6. **Effect of SeNP on SKOV-3 and OVCAR-3 surface roughness.** Cell roughness (SKOV-3 (B) and OVCAR-3 (C)) was calculated on height cells with 25µm$^2$ areas measurement and 1µm$^2$ analysis squares in all groups. Images of example areas are displayed in A. SKOV-3 control cell surface roughness ($R_{RMS}$= 33.08 +/− 1.56 nm) was similar with selenite treated cells ($R_{RMS}$=26.41 +/− 1.15 nm) and significantly lower than observed in SeNP treated cells ($R_{RMS}$=37.31 +/− 1.58 nm for BSA and $R_{RMS}$=42.89 +/− 2.37 nm for Chitosan). OVCAR-3 control cell surface roughness ($R_{RMS}$ =39.39 +/− 2.48 nm) was significantly higher than that observed in treated cells ($R_{RMS}$=28.41 +/− 1.82 nm in selenite treated cells, $R_{RMS}$=27.92 +/− 1.75 nm in BSA coated SeNP treated cells and $R_{RMS}$= 30.05 +/− 1.11 nm in chitosan coated SeNP).

SeNPs *in vivo* in other disease models[27,28] we evaluated cytotoxicity of BSA and chitosan coated SeNP on SKOV-3 and OVCAR-3 cells. Characterization of SeNPs (see supplementary figure 2) aggregation and charge demonstrated SeNP-BSA had a negative charge (-51.2 ± 15.8 mV) and an average size of 108 ± 30 nm and PDI of 0.123 ± 0.002 which was considered monodisperse, and the 30-100 nm size range confirmed by transmission electron microscopy (TEM) (Figure 1, *A* and *B*). SeNP-chitosan had a positive charge of 16.4 ± 4.4 mV, an average size of 320 ± 221 nm and PDI of 0.220 ± 0.012 and was considered as polydisperse.[29] SeNP-chitosan size values with the ZetaSizer measurement were higher than the supplier's specification of 50nm average size however TEM images confirmed those specifications (Figure 1, *A* and *B*)

To demonstrate that SKOV3 and OVCAR3 cells were responding to Se treatments, and therefore confirming that Se had been effectively taken up by cells, GPX1 mRNA levels were measured.[30] GPX mRNA levels increased 2-2.5-fold following Se treatment in both cell types (Figure 1, *C*).

### *Ovarian cancer cell line dependent SeNP cytotoxicity*

SKOV-3 and OVCAR-3 cell monolayers were treated with increasing concentrations of SeNP-BSA, SeNP-chitosan or sodium selenite (0 – 80 µg/mL) over 48 h and cell viability measured. For SKOV-3 (Figure 2) cells selenite treatment had a greater cytotoxic than SeNP-BSA and SeNP-chitosan. The IC20 for selenite was 3 µg/mL at 48 h (Figure 2), whereas the IC20 for SeNP-BSA and SeNP-chitosan were 6 µg/mL and 13 µg/mL respectively ($P < 0.05$). Above 5µg/mL of selenite, SKOV-3 cell viability was significantly reduced compared to untreated control after 48 h ($P < 0.05$). Whereas for SeNP-BSA and SeNP-chitosan the concentration required to cause a significant reduction in cell viability was 10 µg/mL and 20 µg/mL respectively ($P < 0.05$).

In contrast, OVCAR-3 cells were more sensitive to both types of nanoparticles than selenite (Figure 2), the IC20 at 48 h was not significantly different between SeNP-BSA and SeNP-chitosan treatment at 20 μg/mL and 18 μg/mL respectively ($P > 0.05$), whereas the IC20 for selenite was 40 μg/mL (Figure 2, $P < 0.05$).

IC50 values confirmed SKOV-3 cells were more sensitive than OVCAR-3 to both selenite and SeNP-BSA treatments (8 vs 56 μg/mL and 19 vs 42 μg/mL respectively, $P< 0.05$), whereas the IC50 for SeNP-chitosan the same (40 μg/mL) for both SKOV-3 and OVCAR-3 (Figure 2, *B* and *C*). It appears that selenite has a greater cytotoxic effect on SKOV-3 cells than SeNPs, whereas the opposite was observed for OVCAR-3 cells, which are more sensitive to SeNPs than selenite. The concentrations of SeNPs required to decrease cell viability are all significantly higher in OVCAR-3 than SKOV-3 suggesting that the two cell types are responding differently to Se treatment despite the GPX stimulation being similar.

Epithelial–mesenchymal transition (EMT) is a cellular mechanism linked to differentiation during cancer progression,[31] and includes alterations in E- and N-cadherin and vimentin expression, and increased cell migration.[32] Efforts to reverse these transitions are an important consideration in treating aggressive cancers. The effect of Se on cell motility was assessed using a scratch assay, treating cells with IC20 levels of selenite and SeNPs for 48 h. Motility rates were decreased by 25% following SeNP-BSA treatment, 17% after SeNP-chitosan treatment and 19% with selenite ($P < 0.05$, Figure 3, *A*), suggesting that whilst selenite was move cytotoxic the three treatments has a similar extent in reducing cell motility. Scratch assays were not possible with OVCAR-3 cells as these cells do not survive when depleted with FBS. In SKOV-3 cells assessment of EMT markers revealed that selenite and SeNPs had no effect with E-cadherin expression remaining at very low levels, and N-cadherin and vimentin remaining highly expressed consistent with an unaltered mesenchymal phenotype. (Figure 3, *B* and *C*. In OVCAR-3 cells the E-cadherin:N-cadherin was the opposite to that observed in SKOV-3 cells suggestive of a more epithelial phenotype (Figure 3, *B* and *D*), however neither marker responded to selenium treatments. In contrast, vimentin levels significantly ($P < 0.05$) decreased following treatment with SeNPs, an effect that has previously been correlated with a decrease in cancer cell mechanical integrity.[18]

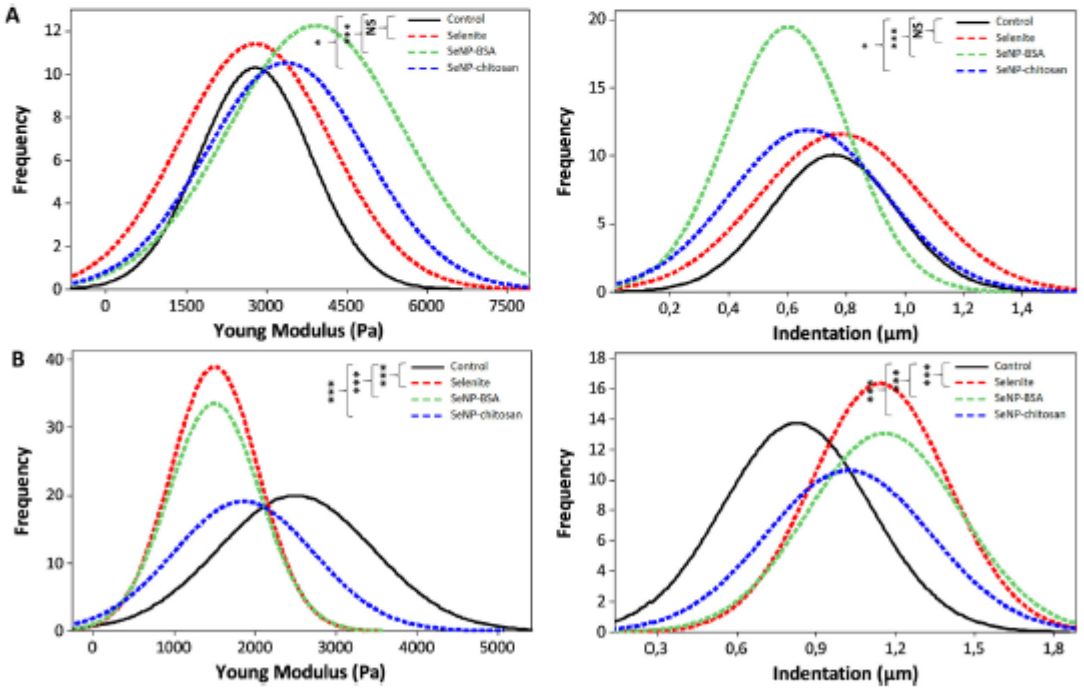


Figure 7. **Effect of SeNP on SKOV-3 and OVCAR -3 cell stiffness and nano-indentation.** AFM probe with a colloidal tip was used as a nano-indentor to monitor changes in cell elasticity following 48 h of treatment. Using Hertz mechanics, elasticity was calculated from the observed changes in the contact regime of the force curve. The 0 point in the x-axis indicates when the cantilever tip makes contact with the cell surface. Total cell elasticity values are drawn in frequency curve for control and treated cells at 48 h. Highly significant alterations in median values were detected between control and treated cells. Indentation data reported that were applying the same force results in treated OVCAR-3 (B) cells deforming more than control cells. SKOV-3 (A) cells seem to deform less after treatment. Statistical significance was determined using the Mann-Whitney test with the following used symbols NS=$P > 0.05$, *$P < 0.05$ **$P < 0.01$, ***$P < 0.001$

*Effect of SeNP treatment on surface roughness and biomechanics*

Previously ovarian cancer cell biomechanics have been shown to differ depending on the invasive potential of cells,[16] and perturbations in gene expression patterns linked to enhanced cellular movement, migration, and invasion.[17] Given the decreases in motility rates described above we reasoned that this may be linked to altered biomechanical properties following SeNP exposure. Using high-resolution tapping mode AFM we initially resolved gross cellular morphology and nanoscale surface topography.

SKOV-3 had an elongated, mesenchymal like, morphology and a smooth membrane ultrastructure that remained unaltered following treatment (Figure 4, all panels). No significant change in cell height was observed between untreated cells (2.4 ± 0.3 μm) and those treated with selenite (2.8 ± 0.6 μm), SeNP-BSA (2.7 ± 0.3 μm) or SeNP-chitosan (2.3 ± 0.8 μm).

OVCAR-3 cells had a spherical, epithelial like morphology that remained unaltered following SeNP treatment (Figure 5, all panels) consistent with the observed N-cadherin and E-cadherin expression ratios. No significant changes in the height of OVCAR-3 were observed between untreated (5.2 ± 0.6 μm) and selenite (4.8 ± 0.4 μm), SeNP-BSA (5.1 ± 0.5 μm) or SeNP-chitosan (4.0 ± 0.5 μm) treated cells ($P > 0.05$; Figure 5). An increase in intra-cellular vesicles was apparent in cells with all Se treatments in bright filed images.

Membrane topography is sensitive to changes of both physical or chemical factors, and NP exposure has been shown to modulate cell membranes.[33] To investigate any SeNP effects on membrane roughness, 1 $\mu m^2$ areas of the cell surface selected at random from a 25 $\mu m^2$ image area and analyzed for roughness. Surface roughness increased in SKOV-3 cell treated with SeNP-BSA (37.31 ± 1.58 nm) and SeNP-chitosan (42.89 ± 2.37 nm), compared to untreated cells (33.08 ± 1.56 nm), whereas no change was detected following selenite treatment (26.41 ± 1.15 nm) ($P > 0.05$, Figure 6). For OVCAR-3 cells the surface roughness of SeNP treated was significantly decreased from 39.39 ± 2.48 nm in untreated controls to 28.41 ± 1.82 nm with selenite, 27.92 ± 1.75 nm with SeNP-BSA, and 30.05 ± 1.11 nm with SeNP-chitosan treatment ($P < 0.05$). There was no significant difference in OVCAR-3 surface roughness was observed between selenite and SeNP treatments ($P > 0.05$, Figure 6).

The mechanical properties of cells change during cancer progression, with metastatic cells becoming more elastic[17] after initial transformation to enable basement membrane penetration.[34–36] To investigate whether Se treatment resulted in any changes in cell elasticity, both SKOV-3 and OVCAR-3 cells were characterized using AFM based nanoindentation, with a colloidal probe (Figure 7).

A significant increase in cell stiffness was observed for SKOV-3 cells following treatment with either SeNP-BSA (3.9 ± 0.2 kPa) or SeNP-chitosan (3.4 ± 0.1 kPa) compared to control (2.8 ± 0.1 kPa; $P < 0.05$), whereas no alterations were detectable following selenite treatment (2.8 ± 0.2 kPa; $P > 0.05$). Indentation analysis revealed a significant decrease for SeNP treated SKOV-3 cells (Figure 7, *A*) with 600 ± 20 nm ($P < 0.001$) for SeNP-BSA and 668 ± 30 nm ($P < 0.05$) for SeNP-chitosan in comparison with control (756 ± 30 nm) and selenite treated cells (780 ± 31 nm). In OVCAR-3 cells the Young's modulus was decreased following SeNP-BSA (1.5 ± 0.1kPa), SeNP-chitosan (1.9 ± 0.1kPa) or selenite (1.5 ± 0.1kPa) treatment compared to the untreated control (2.5 ± 0.1kPa; $P < 0.001$), which together with significantly increase in cell indentation (Figure 7, *B*) following each treatment (selenite 1,141 ± 25 nm, SeNP-BSA 1,157 ± 29 nm, SeNP-chitosan 1,021 ± 34 nm) demonstrated that cell membranes had become more deformable in comparison with control (825 ± 28 nm, $P < 0.001$). Example typical force curves have been collected and are shown in Supplementary Figure 3.

Cellular adhesion to the AFM probe was also analyzed, with no significant alterations in SKOV-3 or OVCAR-3 cells respectively, as shown in Supplementary Figure 4.

## Discussion

Despite the anticancer properties associated with selenium, its use as a cancer therapy has not yet been realized due to systemic toxicity when administered in an aqueous form. Here we demonstrated that, like selenite, SeNPs are effective at inducing a cytotoxic effect on two different serous ovarian cancer derived cell lines and observed distinct responses for each cell type. Both selenite and SeNPs were cytotoxic to SKOV-3 cells, with selenite having a 2.5- and 5- fold lower IC50 than SeNP-BSA and SeNP-chitosan respectively. However, given that aqueous selenium is significantly more toxic when administered systemically in murine models,[5,27,28] the use of SeNP-BSA is likely to provide an opportunity to deliver cytotoxic doses of Se *in vivo*. In addition, tumor specific delivery could occur through the enhanced permeability and retention effect,[37] further reducing toxicity. For OVCAR-3 cells SeNP-BSA and SeNP-chitosan had an approximately 2-fold greater cytotoxic effect than selenite. Given the above considerations, and that the IC50 for SeNPs in OVCAR-3 cells was almost five times greater than for SKOV-3 cells, both types of SeNP are likely to be the only safe and tolerable route for Se administration to target cancer cell growth *in vivo*.

Changes in cell mobility in SKOV-3 led us to investigate cell membrane dynamics in response to selenium treatment as we and others have previously observed differences in ovarian cancer cell biomechanics which were dependent on the invasive potential of cells,[16] and associated with genes involved in enhanced cellular movement, migration, and invasion.[17] Detailed AFM analysis revealed that SKOV-3 cells become less elastic following SeNPs treatment but remained unchanged when treated with selenite. This suggests that SeNPs are triggering a mechanism that results in a lower metastatic potential, and in agreement with the reduced migratory capacity of these cells following treatment.[20,22] In contrast, AFM analysis revealed that OVCAR-3 cells became more elastic following treatment with the higher IC20 concentrations of SeNP and selenite required to induce a cytotoxic effect with these cells. These results highlight specific differences in membrane architecture between SKOV-3 and OVCAR-3 and indicate that SeNP treatment can cause differential cell type specific cytoskeletal effects.

Further contrasting effects were seen with surface roughness, which increased following SeNP treatment in SKOV-3 cells, possibly as a result of nanoparticle internalization as previous studies have shown that BSA coated SeNPs, similar to those used in the present study, were internalized through endocytosis or clathrin mediated vesicles.[38–40] As selenite would be expected to be taken up by anion transporters[41] this difference in surface roughness was anticipated. Surprisingly, the surface roughness of OVCAR-3 cells decreased following SeNPs and selenite treatment and was accompanied by the appearance of intracellular vesicles which are likely to be autophagosomes (Figure 5, *B–D*).[42,43] This suggests that, uniquely, Se forms may induce autophagy which would act as a resistance mechanism in OVCAR-3 cells[41] and offers an explanation as to why the levels of SeNPs required to illicit a response is higher for these cells. This detailed nanomechanical assessment of two distinct ovarian cancer cell types has established that changes in the mechanical properties of ovarian cancer cells, which are likely to result from reorganization of the actin cytoskeleton induced by selenium. SeNPs are effective at preventing cell proliferation in high grade serous ovarian cancer cells, apparently through different biological pathways. High grade serous ovarian cancers continues to present obstacles to currently available treatment through the presentation of advanced and highly aggressive forms of the disease, resulting in a high rate of mortality.[8] The observations made here pave the way for further investigations into evaluating the utility of SeNPs as a pan-cancer treatment, at least in ovarian cancer, although Se is known to be effective in many other cancer types.

## Acknowledgments

This project received support from the Welsh Government ERDF SMART Expertise grant RISE (2017/COL/001), the Medical Research Council UK Confidence in Concept grant (MC_PC_19053) and the Institut National de la Santé et de la Recherche Médicale, France, grant SEDMAC (PC201607).

Benoit Toubhans received a scholarship co-funded by the Université Grenoble Alpes and Swansea University.

## Appendix A. Supplementary data

Supplementary data to this article can be found online at https://doi.org/10.1016/j.nano.2020.102258.

## References

1. Fernandes AP, Gandin V. Selenium compounds as therapeutic agents in cancer. *Biochim Biophys Acta* 1850;**2015**:1642-60.
2. Combs F. J. Biomarkers of selenium status. *Nutrients* 2015;**7**:2209-36.
3. Khurana A, Tekula S, Saifi MA, Venkatesh P, Godugu C. Therapeutic applications of selenium nanoparticles. *Biomedicine & Pharmacotherapy* 2019;**111**:802-12.
4. Sonkusre P, Cameotra SS. Biogenic selenium nanoparticles induce ROS-mediated necroptosis in PC-3 cancer cells through TNF activation. *Journal of Nanobiotechnology* 2017;**15**:43.
5. Huang G, Liu Z, He L, Luk K-H, Cheung S-T, Wong K-H, et al. Autophagy is an important action mode for functionalized selenium nanoparticles to exhibit anti-colorectal cancer activity. *Biomater Sci* 2018;**6**:2508-17.
6. Chen T, Wong Y-S. Selenocystine induces reactive oxygen species-mediated apoptosis in human cancer cells. *Biomed Pharmacother* 2009;**63**:105-13.
7. Vinceti M, Filippini T, Del Giovane C, Dennert G, Zwahlen M, Brinkman M, et al. Selenium for preventing cancer. *Cochrane Database Syst Rev* 2018;**1**CD005195.
8. Webb PM, Jordan SJ. Epidemiology of epithelial ovarian cancer. *Best Pract Res Clin Obstet Gynaecol* 2017;**41**:3-14.
9. Geoffrion LD, Hesabizadeh T, Medina-Cruz D, Kusper M, Taylor P, Vernet-Crua A, et al. Naked selenium nanoparticles for antibacterial and anticancer treatments. *ACS Omega* 2020;**5**:2660-9.
10. Song X, Chen Y, Zhao G, Sun H, Che H, Leng X. Effect of molecular weight of chitosan and its oligosaccharides on antitumor activities of chitosan-selenium nanoparticles. *Carbohydr Polym* 2020;**231**:115689.
11. Shahverdi AR, Shahverdi F, Faghfuri E, Reza Khoshayand M, Mavandadnejad F, Yazdi MH, et al. Characterization of folic acid surface-coated selenium nanoparticles and corresponding in vitro and in vivo effects against breast cancer. *Arch Med Res* 2018;**49**:10-7.
12. Zaorsky NG, Churilla TM, Egleston BL, Fisher SG, Ridge JA, Horwitz EM, et al. Causes of death among cancer patients. *Ann Oncol* 2017;**28**:400-7.
13. Bertone ER, Hankinson SE, Newcomb PA, Rosner B, Willet WC, Stampfer MJ, et al. A population-based case-control study of carotenoid and vitamin A intake and ovarian cancer (United States). *Cancer Causes Control* 2001;**12**:83-90.
14. Bao P, Chen Z, Tai R-Z, Shen H-M, Martin FL, Zhu Y-G. Selenite-induced toxicity in cancer cells is mediated by metabolic generation of endogenous selenium nanoparticles. *J Proteome Res* 2015;**14**:1127-36.
15. Pattabiraman DR, Weinberg RA. Tackling the cancer stem cells – what challenges do they pose? *Nat Rev Drug Discov* 2014;**13**:497-512.
16. Xu W, Mezencev R, Kim B, Wang L, McDonald J, Sulchek T. Cell stiffness is a biomarker of the metastatic potential of ovarian cancer cells. *PLoS One* 2012;**7**, https://doi.org/10.1371/journal.pone.0046609.
17. Quintela M, Sieglaff DH, Gazze AS, Zhang A, Gonzalez D, Francis L, et al. HBO1 directs histone H4 specific acetylation, potentiating mechano-transduction pathways and membrane elasticity in ovarian cancer cells. *Nanomedicine* 2019;**17**:254-65.
18. Fife CM, McCarroll JA, Kavallaris M. Movers and shakers: cell cytoskeleton in cancer metastasis. *Br J Pharmacol* 2014;**171**:5507-23.
19. Suresh S. Biomechanics and biophysics of cancer cells. *Acta Materialia* 2007;**55**:3989-4014.
20. Kabla Alexandre J. Collective cell migration: leadership, invasion and segregation. *Journal of The Royal Society Interface* 2012;**9**:3268-78.
21. Bidkar AP, Sanpui P, Ghosh SS. Efficient induction of apoptosis in cancer cells by paclitaxel-loaded selenium nanoparticles. *Nanomedicine (Lond)* 2017;**12**:2641-51.
22. Liang C-C, Park AY, Guan J-L. In vitro scratch assay: a convenient and inexpensive method for analysis of cell migration in vitro. *Nature Protocols* 2007;**2**:329-33.
23. Pan-Castillo B, Gazze SA, Thomas S, Lucas C, Margarit L, Gonzalez D, et al. Morphophysical dynamics of human endometrial cells during decidualization. *Nanomedicine: Nanotechnology, Biology and Medicine* 2018;**14**:2235-45.
24. Francis LW, Gonzalez D, Ryder T, Baer K, Rees M, White JO, et al. Optimized sample preparation for high-resolution AFM characterization of fixed human cells. *Journal of Microscopy* 2010;**240**:111-21.
25. Brozmanová J, Mániková D, Vlčková V, Chovanec M. Selenium: a double-edged sword for defense and offence in cancer. *Arch Toxicol* 2010;**84**:919-38.
26. Zhao G, Wu X, Chen P, Zhang L, Yang CS, Zhang J. Selenium nanoparticles are more efficient than sodium selenite in producing reactive oxygen species and hyper-accumulation of selenium nanoparticles in cancer cells generates potent therapeutic effects. *Free Radic Biol Med* 2018;**126**:55-66.

27. Bai K, Hong B, Hong Z, Sun J, Wang C. Selenium nanoparticles-loaded chitosan/citrate complex and its protection against oxidative stress in d-galactose-induced aging mice. *Journal of Nanobiotechnology* 2017;**15**:92.
28. Zhang J, Wang H, Yan X, Zhang L. Comparison of short-term toxicity between Nano-Se and selenite in mice. *Life Sci* 2005;**76**:1099-109.
29. Clayton KN, Salameh JW, Wereley ST, Kinzer-Ursem TL. Physical characterization of nanoparticle size and surface modification using particle scattering diffusometry. *Biomicrofluidics* 2016;**10**, https://doi.org/10.1063/1.4962992.
30. Zhang JS, Gao XY, Zhang LD, Bao YP. Biological effects of a nano red elemental selenium. *Biofactors* 2001;**15**:27-38.
31. Tang HM, Kuay KT, Koh PF, Asad M, Tan TZ, Chung VY, et al. An epithelial marker promoter induction screen identifies histone deacetylase inhibitors to restore epithelial differentiation and abolishes anchorage independence growth in cancers. *Cell Death Discov* 2016;**2**:16041.
32. Wheelock MJ, Shintani Y, Maeda M, Fukumoto Y, Johnson KR. Cadherin switching. *J Cell Sci* 2008;**121**:727-35.
33. Lesniak A, Salvati A, Santos-Martinez MJ, Radomski MW, Dawson KA, Åberg C. Nanoparticle adhesion to the cell membrane and its effect on nanoparticle uptake efficiency. *J Am Chem Soc* 2013;**135**:1438-44.
34. Mierke CT. Physical break-down of the classical view on cancer cell invasion and metastasis. *Eur J Cell Biol* 2013;**92**:89-104.
35. Tadeo I, Berbegall AP, Escudero LM, Alvaro T, Noguera R. Biotensegrity of the extracellular matrix: physiology, dynamic mechanical balance, and implications in oncology and mechanotherapy. *Front Oncol* 2014;**4**:39.
36. Cross SE, Kreth J, Zhu L, Sullivan R, Shi W, Qi F, et al. Nanomechanical properties of glucans and associated cell-surface adhesion of Streptococcus mutans probed by atomic force microscopy under in situ conditions. *Microbiology (Reading, Engl)* 2007;**153**:3124-32.
37. Zhai Q, Xiao Y, Li P, Tian F, Zhao J, Zhang H, et al. Varied doses and chemical forms of selenium supplementation differentially affect mouse intestinal physiology. *Food Funct* 2019;**10**:5398-412.
38. Xia Y, Chen Y, Hua L, Zhao M, Xu T, Wang C, et al. Functionalized selenium nanoparticles for targeted delivery of doxorubicin to improve non-small-cell lung cancer therapy. *Int J Nanomedicine* 2018;**13**:6929-39.
39. Lara-Cruz C, Jiménez-Salazar J, Ramón-Gallegos E, Damian-Matsumura P, Batina N. Increasing roughness of the human breast cancer cell membrane through incorporation of gold nanoparticles. *Int J Nanomedicine* 2016;**11**:5149-61.
40. Oh N, Park J-H. Endocytosis and exocytosis of nanoparticles in mammalian cells. *Int J Nanomedicine* 2014;**9**:51-63.
41. Ganye D, Self WT. High affinity selenium uptake in a keratinocyte model. *FEBS Lett* 2008;**582**:299-304.
42. Janel S, Popoff M, Barois N, Werkmeister E, Divoux S, Perez F, et al. Stiffness tomography of eukaryotic intracellular compartments by atomic force microscopy. *Nanoscale* 2019;**11**:10320-8.
43. Wang Y, Xu C, Jiang N, Zheng L, Zeng J, Qiu C, et al. Quantitative analysis of the cell-surface roughness and viscoelasticity for breast cancer cells discrimination using atomic force microscopy. *Scanning* 2016;**38**:558-63.

# Selenium nanoparticles induce global histone methylation changes in ovarian cancer cells

## I. Presentation of the article

Selenium has been proven to be useful as a potential cancer preventive agent, especially in populations with demonstrable poor intake. Despite selenium toxicity increases at doses slightly higher than nutritional requirements, clinical trials investigating selenite as an anti-cancer therapy, have revealed its protective effect against liver cancer. Null or adverse effects have been found in breast cancer. These in vivo results contrast with the promising results found in in vitro cell culture models[301]. SeNPs, have led to increased possibilities when compared to aqueous selenium, due primarily to their increased accumulation and specificity against cancer cells[257,270].

Selenium nanoparticles have been shown to induce cell death mechanisms in hepatocarcinomas and breast cancers[282, 290]. Moreover, selenium has been shown to influence the epigenome, regulating cancer development and influencing the expression of selenoproteins. High doses of selenium treatment have been shown to inhibit DNA methyltransferase activity and expression; however, the mechanism remains unclear. At low selenium doses, reduced DNA methylation has been observed, due to disrupted restoration of the S-adenosylmethionine methyl donor, as a result of redirection of homocysteine toward glutathione synthesis. High doses of selenium have also been shown to trigger DNA hypomethylation due to DNMT inhibition and competition of selenium with DNA for the methyl group. At intermediate doses, DNA methylation is increased in a dose dependent manner.

Epigenetic mechanisms are abundant, complex and altered in cancer cells. The link between selenium and other relevant post translational modifications such as histone methylation has never been studied and is an important gap in the epigenetic knowledge related to selenium. In this study we investigated the effect of sub lethal dose selenium treatment on histone H3 methylation, particularly on lysines K4, K27 and K9. These marks are gross marks of DNA compaction transcription activation. We utilized 2D and 3D culture in the presence and absence of SeNP (24 to 72 hours) and combinations of epigenetic enzyme inhibitors to reveal potential pathways for histone methylation mediated selenium mechanisms in ovarian cancer cells (see Figure below).

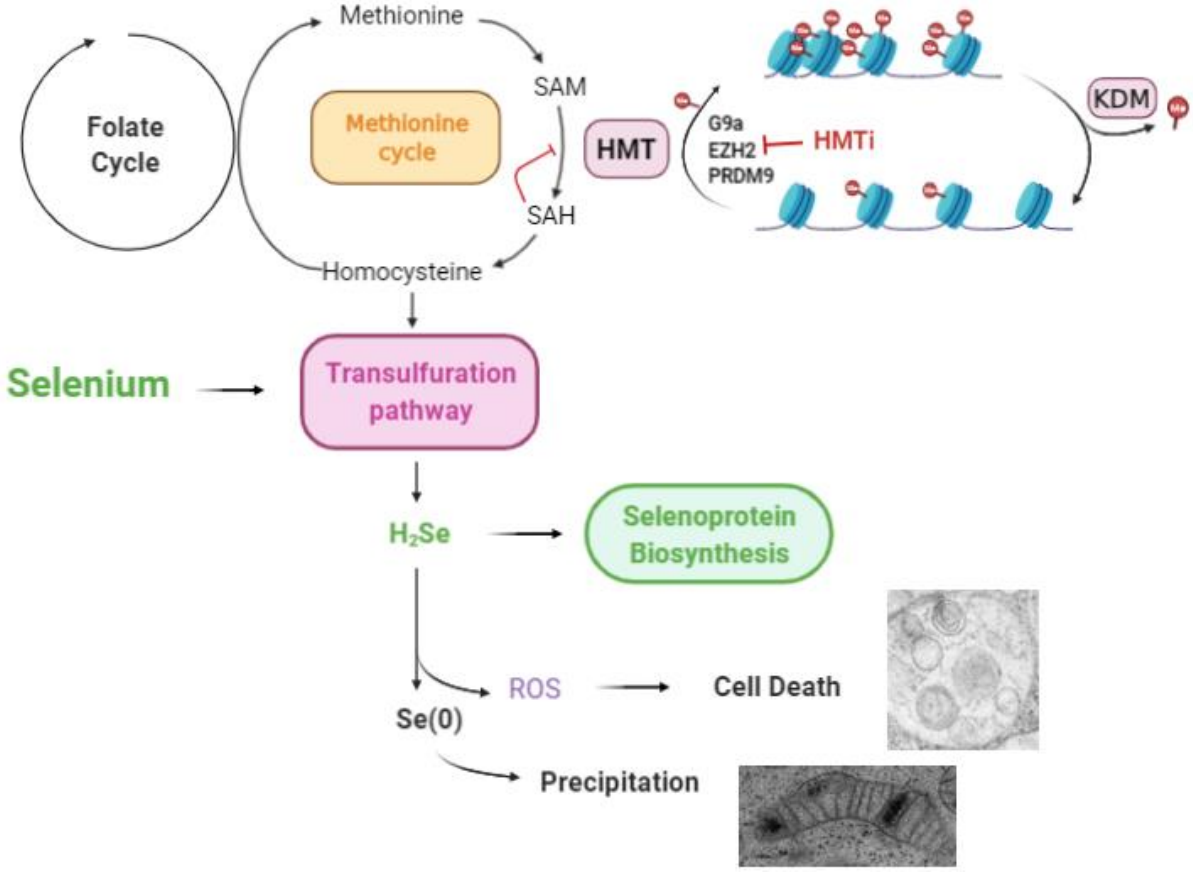


**Graphical Abstract: Simplified proposed selenium mechanisms of action for histone methylation induction in ovarian cancer cells**

*Selenium can influence histone methylation through three different pathways. The selenite from the addition of SeNPs or sodium selenite to cancer cells reacts with the glutathione GSH through the Transulfuration pathway pulling the equilibrium of the methylation SAM-SAH cycle towards the homocystein clearance into transulfuration pathway leading to the formation of selenide $H_2Se$. $H_2Se$ can then react with oxygen forming ROS damaging cells and aggregates of Se0. The increase of $H_2Se$ also increases the synthesis of SeCys through selenocysteine lyase increased expression which could enter in the Methionine cycle. Moreover, selenium increased the activity of the HMTs by increasing their level of expression.*

The lysine methyltransferase (KMT) inhibitors used were provided by the Structural Genomic Consortium. We targeted G9a which is the main histone methyltransferase allowing methylation of H3K9 which is a mark of heterochromatin. We also targeted EZH2 regulating the methylation of H3K27, associated with repression of the transcription. Finally we targeted PRDM9 regulating the methylation of H3K4, an active transcription mark. We studied the effect of selenium treatment after inhibition of those marks, showing that selenium, at sublethal doses, increased histone methylation by increasing the activity of histone methyltransferases. Treatment may also drive the clearance of S-adenosylhomocysteine through the transulfuration pathway, avoiding its inhibitory effect on histone methyltransferase, leading to increased methylation of histone lysines. Moreover when HMT were inhibited, selenium is able to increase histone methylation. This increase may be related to the increased expression of other methyltransferases, upregulated after selenium treatment. Interestingly the activated

methyltransferases were different between SKOV-3 and OVCAR-3 cell types, as shown using RNA-seq analysis, with increased autophagy in OVCAR-3 and increased apoptosis in SKOV-3. The consequence of these different phenotypes highlight an increased resistance of OVCAR-3 against SeNP treatment.

# II. Article

This paper is Under Review in Redox Biology (19/11/2020)

## Selenium nanoparticles induce global histone methylation changes in ovarian cancer cells.

Benoit Toubhans[1, 2], Marcos Quintela[1], Deyarina Gonzalez[1], Alexandra T. Gourlan[2], Laurent Charlet[2], Lewis W. Francis[1], R. Steven Conlan[1]

**Affiliations**

[1]Center for NanoHealth, **Swansea University Medical School**

[2]ISTerre **Université Grenoble Alpes**

## Abstract

The trace element selenium plays a key role in redox reactions through its incorporation in selenocysteine in antioxidant enzymes. Selenium has also been shown to affect DNA methylation through modulating the expression of DNMT1. Here we identified novel effects of selenium on histone methylation using ovarian cancer cell models treated with inorganic selenium nanoparticles (SeNP). As well as inducing oxidoreductase expression, ROS activity and cancer cell cytotoxicity, selenium caused significant increases in histone methylation. Specifically, selenium triggered an increase in the methylation of histone 3 at lysine's K4, K9 and K27, histone marks involved in both the activation and repression of gene expression, suggesting a fundamental role for selenium in these epigenetic processes. This direct function was confirmed using chemical inhibitors of the histone lysine methyltransferases EZH2 (H3K27) and G9a/EHMT2 (H3K9), both of which blocked the effect of selenium on histone methylation. This novel role for selenium supports a distinct function in histone methylation that is likely to occur though interference in the one-carbon metabolism pathway responsible for providing the methyl donor S-adenosylmethionine in both DNA and histone methylation. These observations provide important insights into the action of selenium, and the effects of SeNPs which, unlike selenite, are well tolerated in vivo. It will be important to consider both the classic antioxidant and novel methylation effects of this key redox element in its development in cancer therapy and other applications.

**Graphical Abstract: Proposed selenium mechanisms of action for histone methylation induction in ovarian cancer cells**

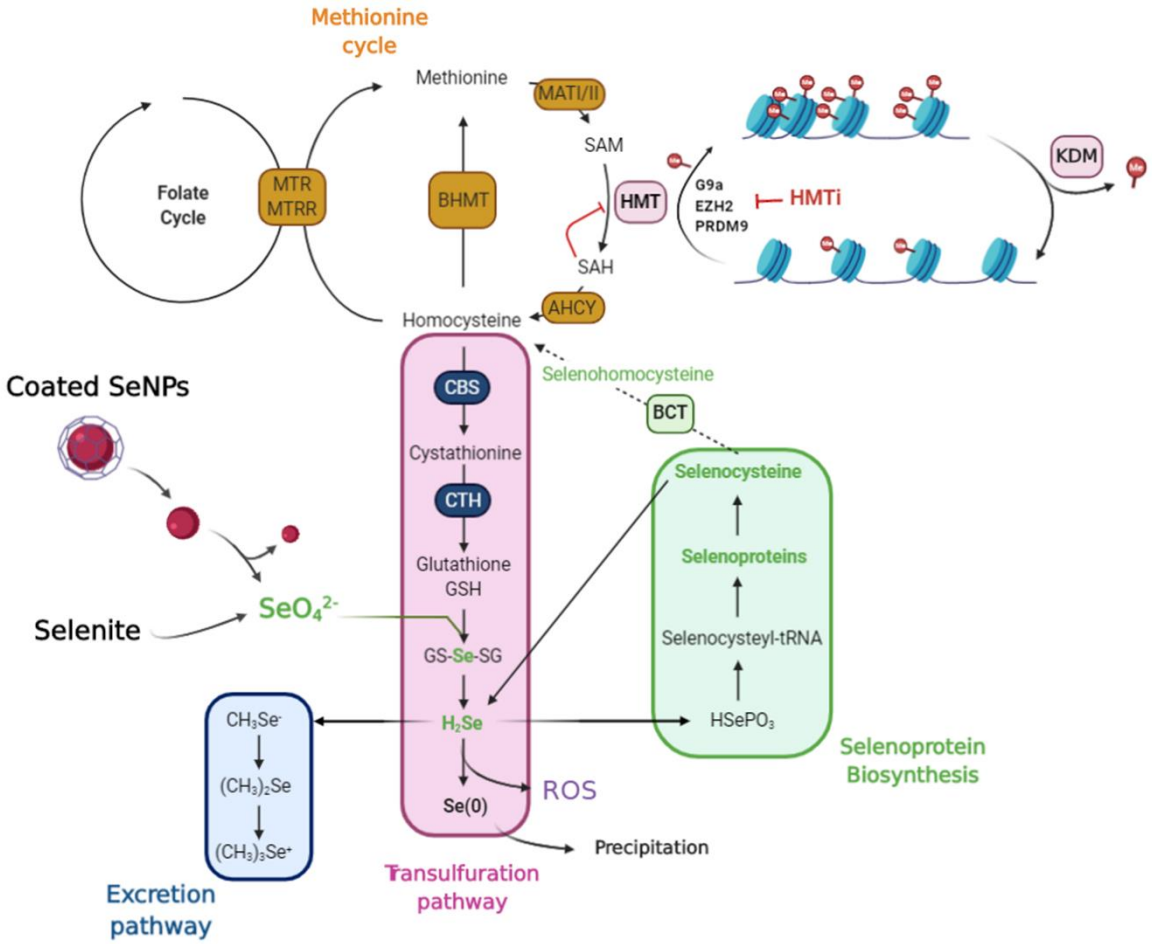


*Selenium can influence histone methylation through three different pathways. The selenite from the addition of SeNPs or sodium selenite to cancer cells reacts with the glutathione GSH forming GS-Se-SG in ovarian cancer cells pulling the equilibrium of the methylation SAM-SAH cycle towards the homocystein clearance into GSH leading to the formation of selenide $H_2Se$. $H_2Se$ can then react with oxygen forming ROS damaging cells and aggregates of Se0. The increase of $H_2Se$ is also increasing the synthesis of SeCys through selenocysteine lyase increased expression which could enter in the Methionine cycle. Moreover, selenium increased the activity of the HMTs by increasing their level of expression.*

## Introduction

Selenium compounds contribute to the maintenance and integrity of cellular systems by influencing cellular redox states and capacity to detoxify compounds, free radicals and reactive oxygen species (1).

Thioredoxin reductases for example, which contain selenocysteine, are present in the cytosol (TrxR1) and mitochondria (TrxR2) and involved in the reduction of oxidized thioredoxins, can catalyse NADPH, control ascorbate levels and regulate metabolism. Selenium is also involved in the biosynthesis of diverse molecular components that are required for important cellular functions including deoxyribonucleoside triphosphates for DNA, the reduction of oxidized proteins, and has roles in diverse regulatory mechanisms such as redox, apoptosis, immunomodulation and the formation of methyl donor compounds. In cancer increased H3K27me3, catalysed by histone lysine methyltransferases (HMTs) including EZH2, has been associated with chemoresistance (2) and demethylation linked to more aggressive phenotypes (3). Similarly knockdown of G9a/EHMT2, which catalyzes H3K9me2, is linked to ovarian cancer peritoneal metastasis and decreased invasiveness in ovarian cancer cell models (4), as is a second putative HMT SMYD3 (5). Here we show that exposure of two pathologically distinct ovarian cancer cell models to selenium results in different redox responses and effects on cell viability, and that selenium delivery via SeNP, that are well tolerated in vivo, is as effective as selenite (6, 7). Interestingly we found that selenium treatment stimulated an increase in histone methylation at the distinct epigenetic marks H3K4me3, H3K27me3 and H3K9me2. Remarkably this effect was inhibited by specific histone lysine methyltransferase inhibitors targeting EZH2 (H3K27) and G9a/EHMT2 (H3K9) demonstrating that selenium can directly modulate histone methylation, and thus cellular epigenomics. These findings highlight the importance of this micro-nutrient and that its role in redox biology should be evaluated together with its effects on epigenetic processes, particularly when considering potential applications in cancer therapy.

# Results

**SeNP penetration and response in ovarian cancer cells.**

In contrast to selenite, SeNPs are well tolerated *in vivo* and appear to offer a route to unlocking the potential of Se as a therapeutic agent (6). We compared the effect of SeNPs to selenite using two distinct 3D spheroid ovarian cancer models, OVCAR-3 and SKOV-3, and demonstrated that SeNPs were able to penetrate at least 80 µm into tumor models. 30 nm electron dense particles corresponding to selenium aggregates were observed by TEM in vacuoles and mitochondria in cells treated with SeNP-BSA (Figure 1A, Figure 1B) or SeNP-chitosan (Supplementary Figure 1) and confirmed using FITC-tagged SeNPs (Figure 1C). To determine whether the observed vacuolar structures were autophagosomes, autophagy markers were assessed (8) and ATG5 levels found to be up-regulated by SeNP-BSA, but unaffected by selenite or SeNP-chitosan in SKOV-3 (Figure 1C), whereas there was an increase of LC3B with selenite, but not with either SeNP (Figure 1C). In OVCAR-3, ATG5 expression and levels of LC3 maturation increased following all treatments, consistent with these cells being more resistant to selenium, and with constitutively activated autophagy (9).

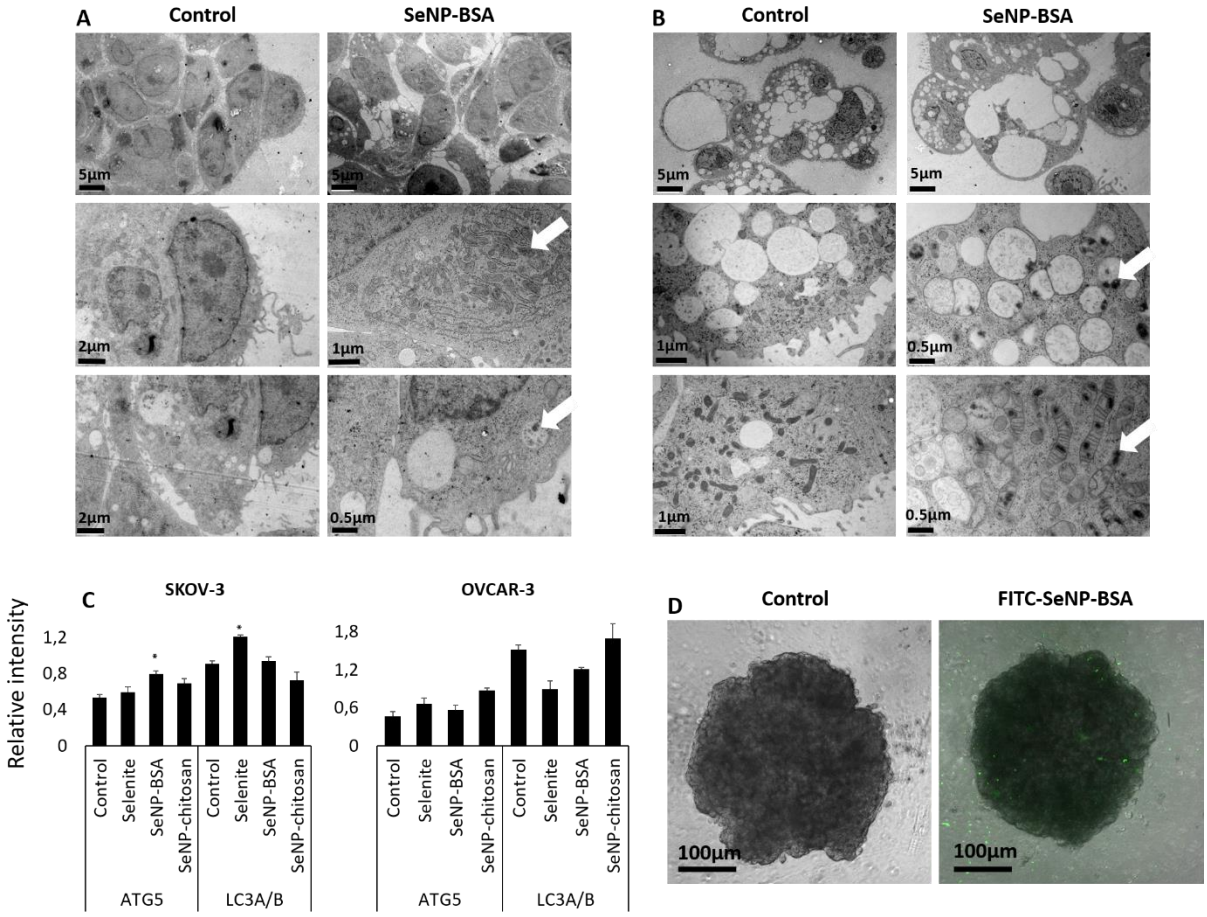


**Figure 1: SeNP accumulation in SKOV-3 and OVCAR-3**

*SeNP penetrate and accumulate in SKOV-3 and OVCAR-3 spheroids. SKOV-3 (A) and OVCAR-3 (B) cells spheroids were treated with BSA-SeNPs at sublethal doses for 24 h and imaged by TEM. Scale bars are displayed on the images (between 0.5 and 5µm). Loose contact between OVCAR-3 cells a high number of autophagosomes were observed. SeNP accumulation was observed in vesicles and mitochondria. SKOV-3 show limited accumulation of SeNPs. All images are representative of a minimum 3 biological repeats. In order to determine nanoparticle penetration, SKOV-3 cells were treated with FITC-tagged-SeNP-BSA (D) for 24 h. Confocal microscope (Ex 495nm / Em 521nm) imaging shows 50µm z-stacks of a 300µm diameter spheroid (scale bare 100µm). Local fluorescence was observed inside the spheroid demonstrating nanoparticle penetration.*

*SKOV-3 and OVCAR-3 cell spheroids treated for 24 h with selenite or SeNPs and profiling autophagy markers (C). Control and selenite treated SKOV-3 displayed similar levels of ATG5 (respectively 0.53 and 0.59), whereas SeNP-BSA treated cells showed a significant increase (0.79, $p=0.05$) of ATG5 levels. SeNP-chitosan treated SKOV-3 cells showed non-significantly elevated level of ATG5 (0.68). Selenite, but not SeNPs, significantly increased LC3B levels in SKOV-3 cells. OVCAR-3 cells displayed a general increase the expression of ATG5 in the different conditions (selenite 0.65, SeNP-BSA 0.56, SeNP-chitosan 0.87) compared to the control (0.46) but was only significant for SeNP-chitosan ($p<0.05$). Selenium treatments increased LC3A to LC3B maturation.*

*Data represent mean +/- SD of three biological replicates.*

Gene expression analysis by PCR demonstrated an expected increase in thioredoxin reductase 1 (TrxR1) expression following treatment (Figure 2A). Additionally, RNA-seq analysis identified several selenium-related genes that were differentially regulated in response to treatment (Figure 2B&C). Expression of selenoproteins I, S and T and the selenocysteine lyase (SCLY) were increased in both cell types, with increased SCLY expression suggesting the transformation of selenium to selenocysteine SeCys is likely to be occurring (10). Oxidative stress response decreased by 20-50% over the first 3 h following SeNP treatment, but steadily increased thereafter (Figure 2D&E).

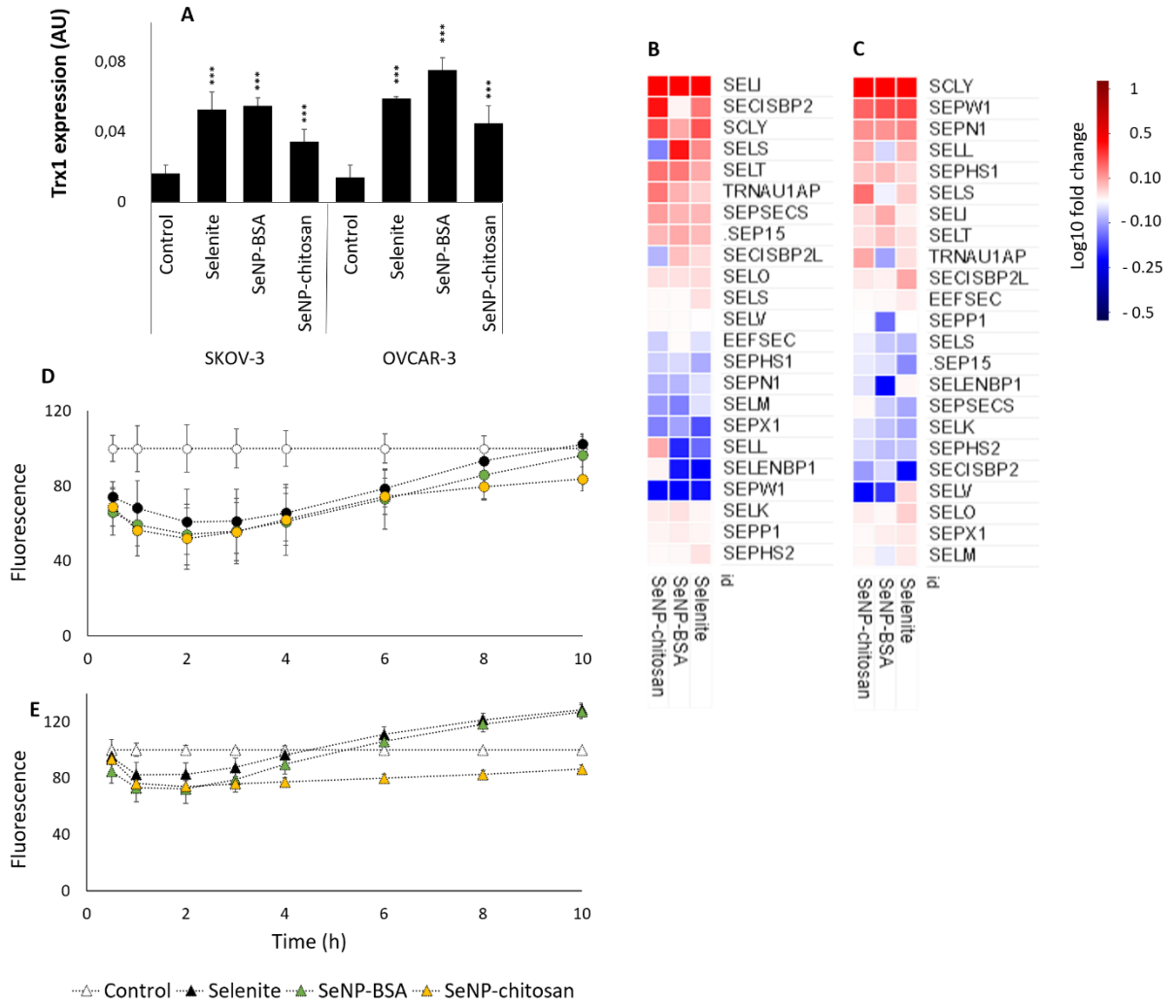


**Figure 2: Effect of selenite and coated selenium nanoparticles on selenium related gene expression and ROS production in OVCAR-3 and SKOV-3 cells**.

*Increases in expression of Trx1 (D) after 24 h of sublethal treatment with selenite or SeNPs demonstrated an expected effect of selenium on cells. Selenium treatments increased significantly ($p<0.001$) Trx1 RNA levels in SKOV-3 (Relative value of 0.01 control, 0.05 selenite and SeNP-BSA, 0.03 SeNP-chitosan) and OVCAR-3 (Relative value of 0.01 control, 0.06 selenite, 0.07 SeNP-BSA and 0.04 SeNP-chitosan).*

*SKOV-3 (A) and OVCAR-3 (B) cells were treated for 24 h with sublethal doses of selenite or coated selenium nanoparticles. RNA was extracted and sequenced by the sequencing platform of the Ecole Normale Supérieure de Lyon (IGFL). Heatmaps show the log10 of the ratio between the selenium treated and control conditions for selenium related proteins.*
*SKOV-3 (D) and OVCAR-3 (E) cells were grown as a 2D layer at 50 x $10^3$ cells per well, incubated with ROS probes, and treated IC50 concentrations of selenite, SeNP-BSA or SeNP-chitosan. ROS red fluorescent assay results showed that selenite, and SeNPs treatments at IC50 decreased the production of ROS in SKOV-3 cells. In OVCAR-3 cells, selenite and SeNP-BSA ROS production peaked above control levels after 6h. The data represents the mean +/- SD of three individual experiments.*

Treatment of spheroids resulted in significant reductions in cell viability with selenite (>0.6 µg/mL), SeNP-BSA (>1.25 µg/mL) and SeNP-chitosan (>3 µg/mL) for SKOV-3 (Figure 3A), and OVCAR-3; selenite (5 µg/mL) or SeNP-BSA or SeNP-chitosan (10 µg/mL for both). Further analysis revealed that SeNP exposure increased caspase-3 cleavage levels in SKOV-3 (2.5 fold, Figure 3C) suggesting increased apoptosis (11), whereas apoptosis was not induced in OVCAR-3 (Figure 3D). Gene ontology analysis supported these observations showing that in SKOV-3 SeNPs triggered intrinsic pathways involved in apoptotic signalling in response to DNA damage and response to oxidative stress (Table 1), whereas in OVCAR-3 exposure caused changes in cell mobility, with the activation of epithelial cell migration, epithelial to mesenchymal transition (EMT) and extracellular matrix organisation (Table 1).

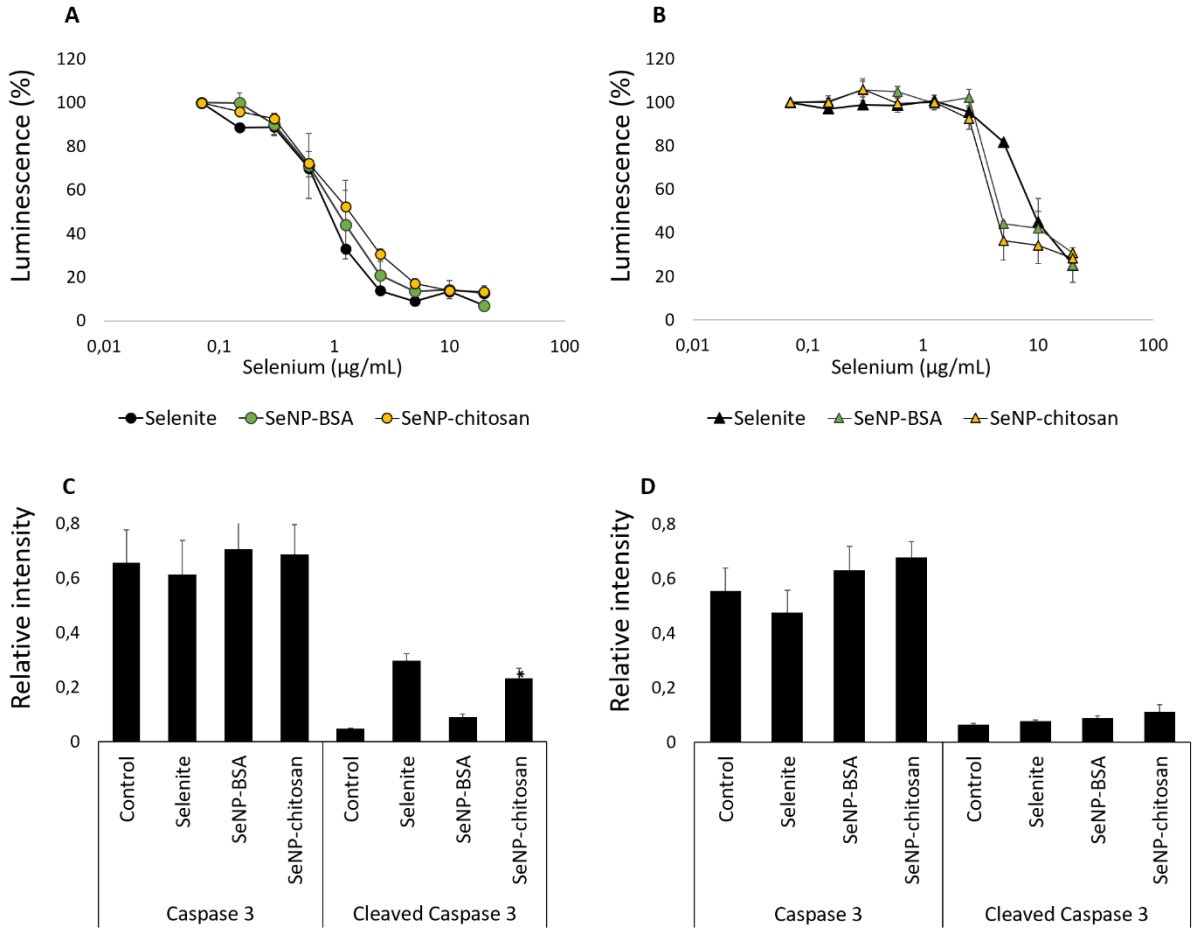


**Figure 3: Ovarian Cancer Cytotoxicity in the presence of SeNP formulations.** *SKOV-3 (A) and OVCAR-3 (B) were grown as 5 x $10^3$ cell spheroids for 24 h then treated with an increasing range of concentration (0 to 20 µg/mL) of selenite, BSA-SeNP or chitosan-SeNPs over 24 h and cellular cytotoxicity monitored. Both cell lines were treated for 24h with an. Cytotoxicity was evaluated by CellTiterGlo endpoint experiment. OVCAR-3 cells were more resistant to selenium treatment than SKOV-3 cells. Mean (+/- SD) relative to control luminescence values are shown from five independent experiments.*

*In SKOV-3 relative Caspase 3 levels (C) were similar between control and selenium treated levels, 0.65 control, 0.68 selenite, 0.70 SeNP-BSA and 0.68 SeNP-chitosan. Selenite and SeNP-chitosan treatments caused significant levels ($p<0.05$) caspase 3 cleavage with levels of 0.29 and 0.23 detected respectively. Only moderate increase in caspase 3 cleavage was observed for SeNP-BSA treatment (0.09). In OVCAR-3 no changes in caspase 3 (D) were seen for selenite (0.47), SeNP-BSA (0.62) and SeNP-chitosan (0.67) in comparison with control (0.55), and cleaved caspase levels were very low for each condition. The data represents the mean +/- SD of three individual experiments.*

**Table 1**

| | Sample | Over-representation GO biological processes | Fold Enrichment (log value) | FDR |
|---|---|---|---|---|
| SKOV-3 | Untreated | Positive regulation of cell cycle arrest | 1.83 | $4.86^{E}$-02 |
| | | Negative regulation of epithelial cell proliferation | 1.78 | $7.45^{E}$-03 |
| | | Extracellular matrix organization | 1.68 | $7.59^{E}$-06 |
| | Selenite | Intrinsic apoptotic signaling pathway in response to DNA damage | 2.50 | $3.36^{E}$-02 |
| | | Cellular response to oxidative stress | 1.87 | $7.77^{E}$-03 |
| | SeNP-BSA | Glutathione metabolic process | 2.90 | $1.36^{E}$-02 |
| | | Cellular response to oxidative stress | 1.96 | $2.22^{E}$-03 |
| | | Intrinsic apoptotic signaling pathway | 1.96 | $4.96^{E}$-02 |
| | SeNP-chitosan | DNA-dependent DNA replication maintenance of fidelity | 4.07 | $7.06^{E}$-03 |
| | | Response to oxidative stress | 1.69 | $8.10^{E}$-03 |
| | | DNA repair | 1.68 | $1.30^{E}$-03 |
| OVCAR-3 | Untreated | Positive regulation of cell cycle arrest | 1.90 | $4.78^{E}$-02 |
| | | Negative regulation of epithelial cell proliferation | 1.79 | $7.21^{E}$-03 |
| | | Extracellular matrix organization | 1.68 | $5.67^{E}$-06 |
| | | Positive regulation of autophagy | 1.66 | $4.6^{E}$-02 |
| | Selenite | Regulation of cell death | 1.31 | $3.11^{E}$-02 |
| | SeNP-BSA | Positive regulation of EMT | 2.73 | $3.86^{E}$-02 |
| | | Epithelium migration | 2.35 | $1.05^{E}$-02 |
| | | Extracellular matrix organization | 1.76 | $8.56^{E}$-04 |
| | SeNP-chitosan | Regulation of reactive oxygen species metabolic process | 2.11 | $1.72^{E}$-02 |
| | | Negative regulation of cell adhesion | 1.80 | $4.13^{E}$-02 |
| | | Regulation of cell motility | 1.44 | $1.95^{E}$-02 |

**Selenium enhances global histone methylation.**

Selenium has been shown to modulate DNA methylation, mainly through the regulation of DNMT expression; any wider involvement in epigenetic mechanisms involving methylation have yet to be explored (12, 13). We investigated whether selenium had a role in histone methylation and very interestingly observed that SeNPs triggered an increase in the levels of H3K4me3 (Figure 4A), H3K27me3 (Figure 4B) and H3K9me2 (Figure 4C), thus revealing an important role for selenium in this process. Detailed RNAseq analysis was undertaking to understand whether, as for DNA methylation, these effects were due to selenium-induced changes in HMT expression. The H3K4me3 HMT PRDM9 was not expressed in the cell lines used, whereas SETD7 (14) and SUV39H2/KMT1B (15, 16) expression was consistently upregulated by selenium. EZH2, which methylates H3K27me3 was also upregulated, whilst the expression levels of the H3K9me2 HMT EHMT2/G9a along with EHMT1/GLP were relatively unaffected (Figure 5 A&B). Changes in the expression level of other potential HMTs (as well as lysine demethylases, KDMs) were observed, although these HMTs require further

experimental validation to define their precise roles (Supplementary Figure 2), and DNMT3A and DNMT3B (18) expression was also increased.

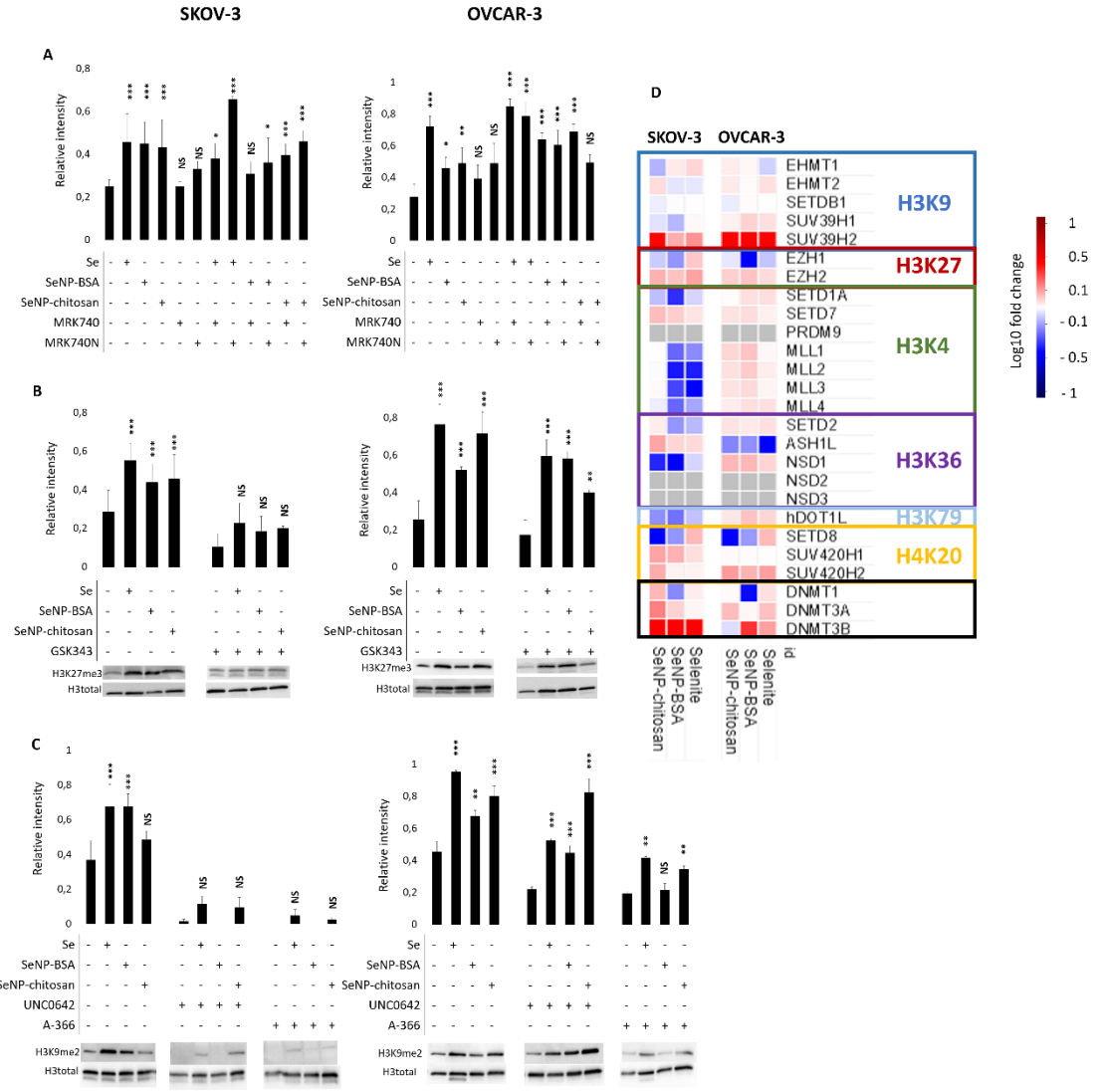


**Figure 4: Histone methylation markers in ovarian cancer cells treated with selenium and epigenetic probes.**

*SKOV-3 (left) and OVCAR-3 (right) cells were grown as a monolayer then treated for 72 h with the epigenetic probe MRK740 (A), 24h with GSK343 (B) or 72h with A366 or UNC0642 (C) then 24 h with selenium treatments.*

**Figure 4A:** *Cells were treated for 72 h with the epigenetic probe MRK740, an inhibitor of the H3K4 HMT PRDM9, followed by 24h with selenite or SeNPs. An inactive probe MRK740N was used as a control. Selenium treatment significantly ($p<0.001$) increased H3K4me3 levels in SKOV-3 by 2.5 fold. In OVCAR-3 selenite increased levels by 3 fold ($p<0.001$) and by 2 fold with SeNPs ($p<0.05$). The presence of the inhibitor MRK740 did not affect H3K4me3 levels in control or treated samples ($p<0.05$).*

**Figure 4B:** *Cells were treated for 24 h with the epigenetic probe GSK343, an inhibitor of the H3K27 HMT EZH2 followed by 24 h with selenite or SeNPs. No control probe was available for GSK343. Selenium treatments significantly ($p<0.01$) increased H3K27me3 levels by 2 fold in SKOV-3. In*

*OVCAR-3 selenite and SeNP-chitosan increased levels by 4 fold ($p<0.001$) and by 2 fold with SeNP-BSA treatment ($p<0.01$). The presence of GSK343 inhibited H3K27me3 methylation in SKOV-3 cells ($p>0.05$) but not significantly in OVCAR-3 although expression was slightly decreased.*

**Figure 4C:** *Cells were treated for 24 h with epigenetic probes A-366 or UNC0642, inhibitors of the H3K9 HMT EHMT2/G9a followed by 24 h with selenite or SeNPs. No control probe was available for A-366 or UNC0642. Selenium treatments significantly ($p<0.001$) increased H3K9me2 levels by 2 fold in SKOV-3. In OVCAR-3 selenite and SeNP-chitosan increased levels by 2 fold ($p<0.001$) and 1.5 fold with SeNP-BSA treatment ($p<0.01$). In SKOV-3 UNC0642 and A-366 decreased levels of H3K9me2 to almost undetectable levels after 24 h and blocked any effect of selenium treatments. In OVCAR-3, UNC0642 and A-366 decreased levels of H3K9me2 ($p<0.05$), and reduced the ability of selenium treatments to increase H3K9me2 levels*

**Figure 4D: Methyl transferase expression patterns in SKOV-3 and OVCAR-3 spheroids treated with sublethal doses selenium nanoparticles.**

*Heatmap of methyltransferase (D left SKOV-3, right OVCAR-3) gene expression after 24h of selenium treatments of SKOV-3 and OVCAR-3 at sublethal doses.*

**Selenium induced histone methylation occurs via histone methyltransferase activity.**

Whilst upregulation of SETD7 and EZH2 gene expression by selenium could account for increases in H3K4me3 and H3K27me3 methylation, there were no changes in EHMT2 expression. This suggested that for H3K9me2 at least selenium may also affect other histone methylation processes. To determine if this directly involved the methylation of histones, inhibitors blocking the activity of specific HMTs was investigated. As expected inhibition of PRDM9 using MRK740 (19) (or the inactive analogue MRK740N) did not result in a decrease in H3K4 tri-methylation as PRDM9 was not expressed in either cell line. Inhibition of the H3K27 methylase EZH2 using GSK343 (20) resulted in a significant decrease in H3K27me3 levels in SKOV-3 demonstrating that the effect of selenium occurs via the activity of EZH2 in these cells (Figure 4C), and likely also in OVCAR-3 cells where, whilst the effect of GSK343 was less pronounced, a decrease in H3K27me3 levels was apparent. Finally, two different EHMT2 inhibitors, UNC0642 (21) and A-366 (22), essentially ablated H3K9me2 in SeNP treated SKOV-3 (Figure 4D), and again there was a general decrease in H3K9me2 in OVCAR-3. These data support a mechanism whereby selenium-mediated increases in histone methylation occur through a biochemical process involving HMTs, as despite selenium-induced increases in expression of some HMT genes including EZH2, HMT inhibitors can abrogate this effect.

## Discussion

Selenium in the form of selenite has been explored as a mode of cancer therapy but has to date failed due to systemic toxicity (23). Here we have shown that as well as triggering enhanced redox activities, SeNPs induce cytotoxicity in ovarian cancer cell lines, with cell-type specific responses, and could therefore offer significant benefits as these nanoparticles can be delivered at cytotoxic doses *in vivo* (24, 25). In OVCAR-3 cells autophagy was constitutively activated resulting in the intracellular accumulation of SeNPs offering an explanation as to the greater resistance of these cells to high levels of selenium. In contrast, SKOV-3 cells displayed increased levels of apoptosis. To understand the mechanisms underlying the differential responses to SeNPs, we investigated the possibility of selenium inducing epigenetic effects beyond DNA methylation and identified increased levels of histone H3K4me3, H3K27me3 and H3K9me2. To understand whether this selenium induced histone methylation occurred through HMTs known to methylate each of these histone marks, specific HMT inhibitors were evaluated. The PRDM9 inhibitor MRK740 had no effect on reducing methylation H3K4 as this HMT is not expressed in the cell lines used, H3K4 methylation increases could be attributed to SeNP induced expression of SETD7 (26). Inhibition of EZH2 by GSK343 blocked SeNP induced H3K27 methylation despite associated increases in EZH2 gene expression levels, suggesting that selenium-induced H3K27 methylation may in part be due to HMTs, or mechanisms impacting EZH2 function. Increases in H3K9 methylation were effectively blocked by the EHMT2 inhibitors A-366 and UNC0642, and as EHMT2 mRNA expression was unchanged following SeNP treatment supporting the view that a mechanism distinct from the modulation of G9a/EHMT2 expression is involved in increasing histone methylation.

The inhibition of SeNP mediated methylation by HMT-specific inhibitors led to the notion that this could occur through a ubiquitous process linked to histone methylation. The methionine metabolic pathway generates SAM, the principal substrate for DNA and histone methylation (27). One possibility (Figure 5) that would result in an increased pool of SAM is the upregulation of MAT1, that synthesises SAM from methionine, by SeNP. This was effectively ruled out in the current study as no significant changes in MAT gene expression levels were observed (Figure 5). Uniquely the elements selenium and sulphur share many chemical properties, and as they are so tightly coupled it has been assumed that selenium may follow the same metabolic pathways as sulphur. More speculatively therefore, selenium could be incorporated into Se-adenosylmethionine (SeAM) and function as a SAM analogue to increase the methyl-donor pool. The synthetic SeAM analogue ProSeAM appears to be processed by

G9a/EHMT2 in a cellular context suggesting that SeAM could be used as an HMT substrate (28). However, genetic studies in yeast lacking both sam1/sam2 (MAT1/MAT2 orthologs) demonstrated whilst SeAM synthesis can occur it is highly toxic accounting for the toxicity associated with its precursor Se-methionine (SeMet) (29). Whilst SeMet was not present in the cell culture media used here, it can be synthesised from seleno-homocysteine (SeHCys) by betaine-homocysteine S-methyltransferase (BHMT) (10, 27) which is expressed in the cell lines used here (Figure 5). Another explanation is that the product of histone methylation reactions, SAH, which is an HMT inhibitor, is removed from the cellular system due to the presence of high levels of selenium. Indeed selenium supplementation in murine models has been shown to decrease the ratio of SAM/SAH suggesting that this clearance of SAH occurs in vivo (30, 31). SAH levels could be decreased following SeNP treatment, resulting in increased HMT activity, by diverting HCY into the transulfurication pathway as the introduction of selenite to this pathway leads to the formation of selenoglutathione (GS-Se-SG) and ultimately selenide ($H_2Se$) (32).

## Conclusion

We propose that selenium driven increases in histone methylation are likely to occur through distinct processes (Graphical Abstract) including 1) increasing the activity of HMT due to increasing the levels of expression of the genes encoding these enzymes and 2) clearance of SAH, likely due to a ‘pull’ of homocysteine to $H_2Se$ due to selenium activating the trans-sulfuration pathway.

The discovery that selenium, though the activity of HMTs, can directly modulate histone methylation, a key process in the regulation of global gene expression, highlights the importance of this micro-nutrient. Selenium’s pivotal role in redox biology, and its potential applications in cancer and viral therapy, should now also consider its wider role in the mechanism of action pertaining to epigenetic processes.

# Materials

## Nanoparticles

BSA and chitosan coated SeNPs were purchased from NANOCS (New York, USA) with a manufacturer defined diameter of 25 – 50 nm for both nanoparticles. SeNP characterisation and IC20 treatment levels used in 2D culture experiments have been reported previously (7).

## Cell culture

OVCAR-3 (ATCC, Maryland, US) ovarian cancer cells were cultured in RPMI-1640 (Sigma-Aldrich, UK) supplemented with 20% bovine serum albumin (BSA, Sigma-Aldrich), 5 µg/mL insulin (Sigma-Aldrich, UK), and 1% penicillin-streptomycin (v/v) solution (Sigma-Aldrich, UK). SKOV-3 (ATCC, Maryland, US) ovarian cancer cells were cultured in McCoy's 5A (Sigma-Aldrich, UK) supplemented with 10% bovine serum albumin (BSA, Sigma-Aldrich, UK), and 1% penicillin-streptomycin (v/v) (Sigma-Aldrich, UK). Cells were maintained at 37° and 5% $CO_2$ and routinely passaged using 0.25% trypsin-0,1%EDTA (v/v).

## Spheroids growth, treatment and viability assay

Cell viability was determined using a CellTiterGlo assay (PROMEGA, UK). 5,000 cells/well were plated in 96-well Ultra Low Attachment coated round bottom plates (Corning, UK). After spheroid formation (usually after 24h), 100 µL of fresh medium containing a 2X concentration of Sodium Selenite ($Na_2SeO_3$) or selenium nanoparticles (BSA or chitosan) were added. For the viability assay, an increasing dose range (0.01 µg/mL to 20 µg/mL) was applied by dilution in appropriate medium for 24, 48 or 72 h. After the treatment, 100µL of media was removed from wells and 100 µL of CellTiterGlo added. Plates were shaken for 5 min and equilibrated at room temperature for 25 min before luminescence measurements were taken (BMGLabtech Fluostar Omega, UK). IC20 and IC50 doses were determined as the concentration required to reduce the luminescence signal by 20/50%. The IC20/50 values shown are the result of a minimum of five independent experiments performed with 4 technical repeats.

## High-pressure freezing and freeze substitution

TEM sections were prepared as previously described (33). Briefly spheroids were pelleted and vitrified by high pressure freezing (HPM100, Leica Microsystems) to -90°C for 80 h in acetone with 1%OsO4. The temperature was then raised 1°C/h to 30°C and samples rinsed 4 times in acetone. Samples were infiltrated with agar low viscosity resin (LVR, Agar scientific) in

acetone for 3h. After polymerisation for 24 h at 60°, 70 to 400nm sections were obtained using an ultra-microtome (UC7, Leica Microsystems). Sections were collected on formvar-carbon-coated 100mesh copper grids and post-stained for 10min with 2% aqueous uranyl acetate, rinsed and incubated for 5 min with lead citrate. Grids were analysed using Tecnai 12 FEIMicroscope (120kV) at different magnification.

**ROS assay**

SKOV-3 and OVCAR-3 cells were seeded as monolayers at 20,000 cells per well in a dark 96-well plates and cultured overnight. Following removal of media, cells were washed once with PBS, then incubated for 1 h with the Cellular Reactive Cellular Reactive Oxygen Species Detection reagent (Red Fluorescence, Abcam186027). A 6x IC50 concentration of selenite or SeNPs was then added and the plate incubated at 37°C for the duration of the assay. Fluorescence was analysed at different time points from 30 min to 10 h (excitation filter 520nm, emission filter 605nm, BMGLabtech Fluostar Omega, UK).

**Protein blotting**

Total cellular protein was extracted, and equal amounts of protein separated by SDS-PAGE and transferred to an acrylamide membrane (BioRad, UK). After blocking in 5%BSA TBS-T for 1 h, blots were incubated with primary antibody (Caspase 3: rabbit polyclonal (CellSignal9662, UK), ATG5: rabbit polyclonal (CellSignal 2630, UK), H3K4me3: rabbit polyclonal (Thermo PA517420), H3K27me3: rabbit polyclonal (Thermo PA531817), H3K9me2: rabbit polyclonal (CellSignal 4658, UK), H3 (1B1B2): mouse monoclonal (CellSignal 14269, UK) or GAPDH: mouse monoclonal (Santa Cruz sc-47724, UK)) at a concentration of 200 μg/ml overnight, at 4°C. Blots were washed, then incubated with the appropriate secondary antibodies (goat anti-mouse Abcam ab150113 or goat anti-rabbit Abcam ab6721 HRPsecondary, UK) at a concentration of 400 μg/ml. Cross-reacting proteins were visualised (ChemiDoc XRS, BioRad, UK), and band intensities quantified using ImageLab software normalising expression to GAPDH.

**qPCR**

Following RNA extraction and quantification, qPCR was carried out in accordance with the manufacturers' recommendations, using the RETROscript® kit two-step method (Invitrogen Ltd., UK). Following cDNA synthesis from 100 ng of RNA, each sample was analysed by qPCR in triplicate using iQ SYBR Green supermix (BioRad, UK) and gene specific primers (Sigma-Aldrich, UK) to evaluate different gene expression GAPDH (GAPDH Forward:

GTCCACTGGCGTCTTCAC, Reverse: CTTGAGGCTGTTGTCATACTTC) and TrxR1 (TrxR1 Forward: CTACAGACCATTGCCTTGCT, Reverse: ACCTCCTACCCACAAGATCC). Serial dilutions of cDNA were used to plot a calibration curve, and gene expression quantified by plotting threshold cycle values. Expression levels were normalized to values obtained for the reference gene (GAPDH) and relative expression expressed as the mean fold induction ± standard deviation. Statistical differences between the treatment groups and the control were determined by analysis of variance (ANOVA) (where $p<0.05$ was considered significant).

**RNA-Sequencing**

For each condition a total of 96 independently cultured spheroids were pooled. Extracted RNA from pooled samples underwent quality control assessment using the RNA Tapestation 2200 (Agilent). cDNA libraries were prepared using the SENSE mRNA-Seq Library Prep Kit V2 (Lexogen) prior to RNA-sequencing (RNA-Seq, genomic platform, Ecole Normale Supérieure de Lyon). Raw fastq files were quality-checked using FastQC, a quality-control tool for high throughput sequencing data, prior to alignment to the hg38 indexed transcriptome using Bowtie2 (34). The eXpress software (35) was used to quantify expression from the transcriptome mapping and derive count data and the differential expression tool package DESeq2 (36), implemented within R, was used to correct for multiple hypothesis testing and determine significantly modified transcripts (FDR < 0.1) (Supplementary 1). Raw and processed RNA-Seq data is deposited in the GEO Dataset with accession number GSE149397. The PANTHER platform was used to perform statistical overrepresentation/enrichment tests (38, 39). All major PANTHER terms were tested for over-representation (GO-Biological Processes or Reactome, e.g. binomial) and gene-set enrichment comparing the lists of genes expressed in different experimental conditions. The results are displayed showing the differential distribution of significantly enriched clusters of genes compared to the overall expression tendency within samples.

## Epigenetic probes

Epigenetic probes were supplied by the Structural Genomics Consortium under an Open Science Trust Agreement: https://www.thesgc.org/click-trust. Probes were diluted in DMSO to a final concentration of 20 µM. UNC1999 and GSK343 inhibitors and an inactive control probe UNC2400 were used to evaluate EZH1/2. The inhibitor MRK-740 and inactive control probe MRK-740N were used for PRDM9. UNC0642 and A-366 were used to evaluate G9a/EHMT2. Cells were treated for 1 to 3 days with the different probes to reach IC90 of the targeted

methyltransferase. Cells were then treated for 48 h with selenite or SeNP at sub-lethal doses, protein was extracted and probed using antibodies targeting specific histone modifications as described above.

**Statistical Analysis.**

All data presented are from a minimum of three biological repeats, with technical repeats included per sample, as denoted. Data normality was analysed using the Kolmogorov Smirnov test, with normally distributed data analysed with the one-way and two-way analysis of variance (ANOVA) followed by the Mann–Whitney pairwise test for non-parametric data. In all cases in which ANOVA was significant, multiple comparison methods were used. Differences were considered significant for $P \leq 0.05$ (*$P \leq 0.05$, **$P \leq 0.01$, ***$P \leq 0.001$). All data were analysed in MiniTab 14.

## Supplementary

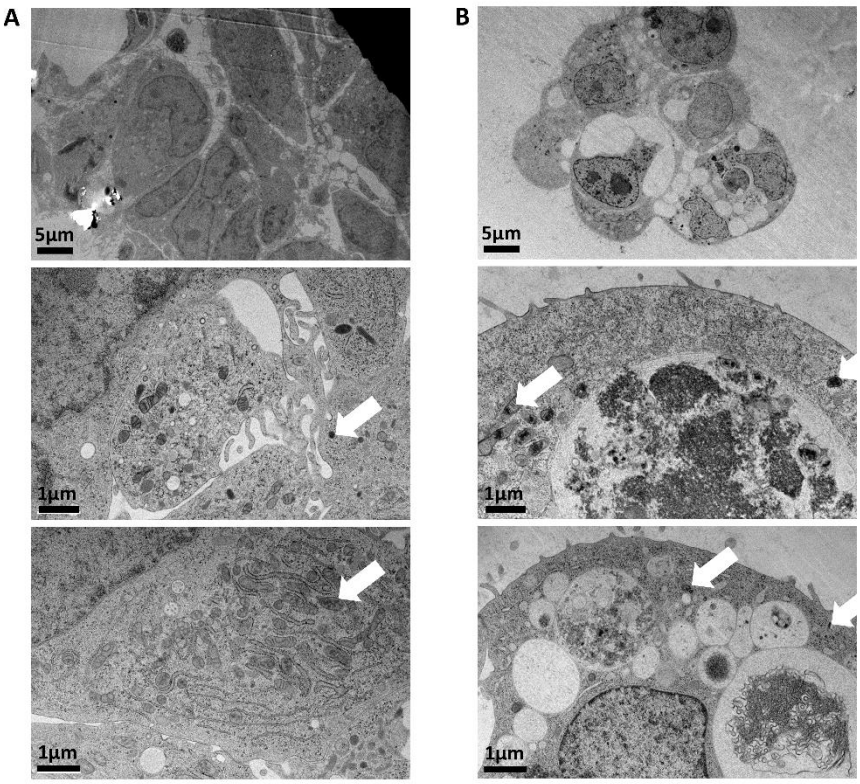


Supplementary 1: TEM images of SKOV-3 (A) and OVCAR-3 (B) treated with IC20 of SeNP-chitosan

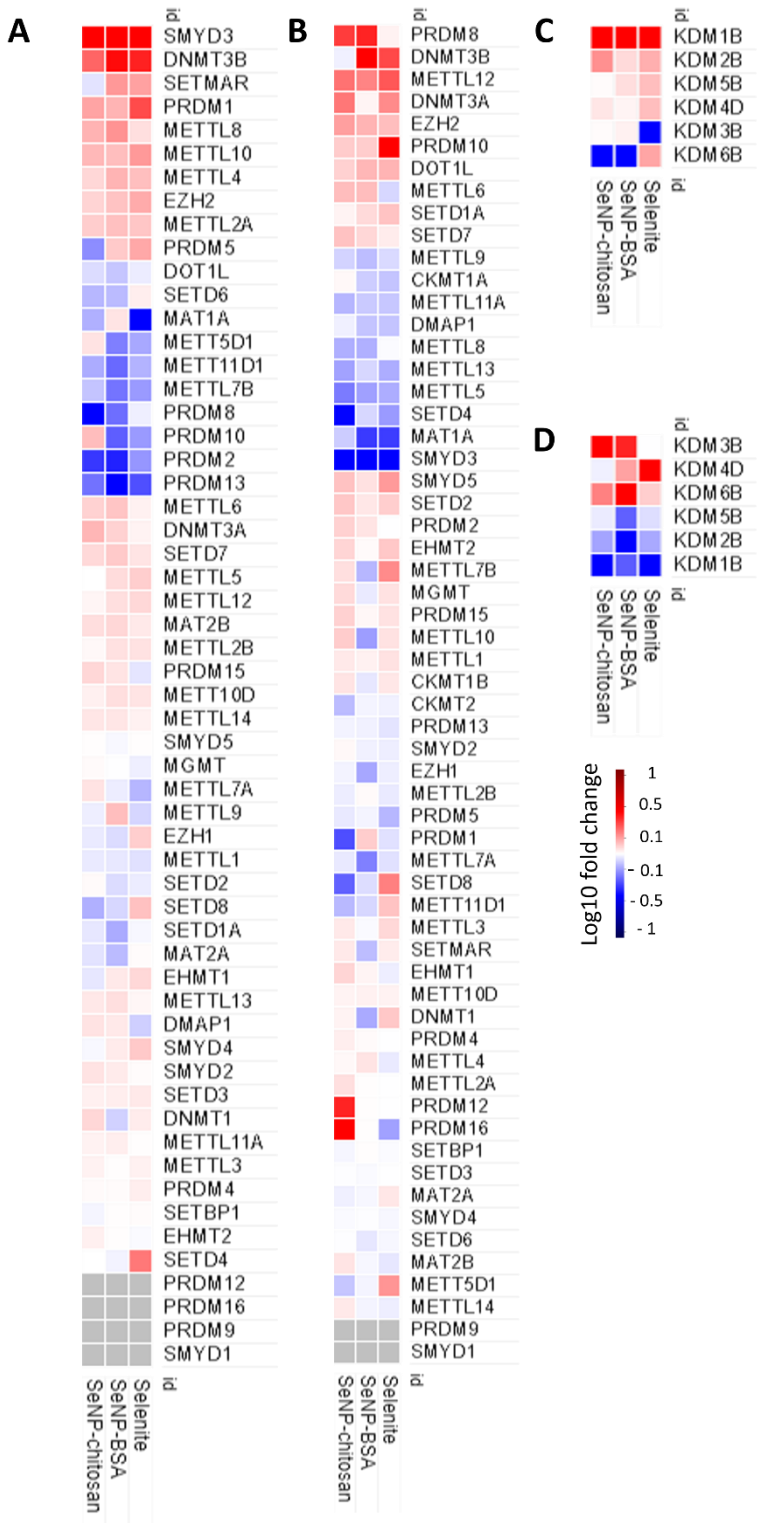


Supplementary 2 : *Heatmap of methyltransferase and demethylases (A and C SKOV-3, B and D OVCAR-3) gene expression after 24h of selenium treatments at sublethal doses.*

*Author contribution*

*Data collection, data analysis and manuscript drafting was performed by Benoit Toubhans. Marcos Quintela and Philipp Rathert analysed the RNA sequencing dataset. R Steven Conlan, and Lewis W Francis contributed to study design, critical interpretation of data and drafting of the manuscript. Deyarina Gonzalez, Laurent Charlet and Alexandra Gourlan contributed to the review of the manuscript. The authors read, amended and approved the final manuscript.*

*Acknowledgments*

*This project received financial support from Welsh Government ERDF SMART Expertise 2014-2020 West Wales and the Valleys Grant CEAT (Cluster for Epigenetics and Advanced Therapeutics, 2017/COL/004); the Medical Research Council UK Confidence in Concept grant (MC_PC_19053) s, and INSERM Grant SEDMAC (PC201607). Benoit Toubhans received a scholarship co-funded by the Université Grenoble Alpes and Swansea University.*

*TEM images:*

*The electron microscope image was supported by the Rhône-Alpes Region, FRM, FEDER, CNRS, CEA, the University Grenoble Alpes, EMBL, GIS-IBISA, the Grenoble Instruct-ERIC Centre (ISBG : UMS 3518 CNRS-CEA-UGA-EMBL) with support from FRISBI (ANR-10-INSB-05-02) and GRAL (ANR-10-LABX-49-01) within the Grenoble Partnership for Structural Biology (PSB) platform (D. Fenel , C. Moriscot, B. Gallet and G. Schoen (PSB, ISBG, UMS 3518)).*

# References


1. D. M. Townsend, K. D. Tew, H. Tapiero, Sulfur containing amino acids and human disease. *Biomed. Pharmacother.* **58**, 47–55 (2004).
2. N. Chapman-Rothe, *et al.*, Chromatin H3K27me3/H3K4me3 histone marks define gene sets in high-grade serous ovarian cancer that distinguish malignant, tumour-sustaining and chemo-resistant ovarian tumour cells. *Oncogene* **32**, 4586–4592 (2013).
3. W. P. He, *et al.*, Decreased expression of H3K27me3 in human ovarian carcinomas correlates with more aggressive tumor behavior and poor patient survival. *Neoplasma* **62**, 932–937 (2015).
4. K.-T. Hua, *et al.*, The H3K9 methyltransferase G9a is a marker of aggressive ovarian cancer that promotes peritoneal metastasis. *Mol Cancer* **13** (2014).
5. Y. Jiang, *et al.*, Overexpression of SMYD3 in Ovarian Cancer is Associated with Ovarian Cancer Proliferation and Apoptosis via Methylating H3K4 and H4K20. *J Cancer* **10**, 4072–4084 (2019).
6. A. R. Shahverdi, *et al.*, Characterization of Folic Acid Surface-Coated Selenium Nanoparticles and Corresponding In Vitro and In Vivo Effects Against Breast Cancer. *Arch. Med. Res.* **49**, 10–17 (2018).
7. B. Toubhans, *et al.*, Selenium nanoparticles trigger alterations in ovarian cancer cell biomechanics. *Nanomedicine: Nanotechnology, Biology and Medicine*, 102258 (2020).
8. X. Sui, *et al.*, Autophagy and chemotherapy resistance: a promising therapeutic target for cancer treatment. *Cell Death & Disease* **4**, e838–e838 (2013).
9. Y. Liu, *et al.*, Increased autophagy in EOC re-ascites cells can inhibit cell death and promote drug resistance. *Cell Death & Disease* **9**, 1–10 (2018).
10. M. Roman, P. Jitaru, C. Barbante, Selenium biochemistry and its role for human health. *Metallomics* **6**, 25–54 (2014).
11. H. Estevez, J. C. Garcia-Lidon, J. L. Luque-Garcia, C. Camara, Effects of chitosan-stabilized selenium nanoparticles on cell proliferation, apoptosis and cell cycle pattern in HepG2 cells: Comparison with other selenospecies. *Colloids and Surfaces B: Biointerfaces* **122**, 184–193 (2014).
12. B. Speckmann, T. Grune, Epigenetic effects of selenium and their implications for health. *Epigenetics* **10**, 179–190 (2015).
13. E. Jabłońska, E. Reszka, Selenium and Epigenetics in Cancer: Focus on DNA Methylation. *Adv. Cancer Res.* **136**, 193–234 (2017).
14. I. de A. A. Batista, L. A. Helguero, Biological processes and signal transduction pathways regulated by the protein methyltransferase SETD7 and their significance in cancer. *Signal Transduct Target Ther* **3**, 19 (2018).
15. W. Shuai, *et al.*, SUV39H2 promotes colorectal cancer proliferation and metastasis via tri-methylation of the SLIT1 promoter. *Cancer Lett* **422**, 56–69 (2018).
16. A.-R. Kim, J. Y. Sung, S. B. Rho, Y.-N. Kim, K. Yoon, Suppressor of Variegation 3-9 Homolog 2, a Novel Binding Protein of Translationally Controlled Tumor Protein, Regulates Cancer Cell Proliferation. *Biomol Ther (Seoul)* **27**, 231–239 (2019).
17. D. Husmann, O. Gozani, Histone lysine methyltransferases in biology and disease. *Nat Struct Mol Biol* **26**, 880–889 (2019).
18. L. Gao, *et al.*, Comprehensive structure-function characterization of DNMT3B and DNMT3A reveals distinctive de novo DNA methylation mechanisms. *Nature Communications* **11**, 3355 (2020).
19. A. Allali-Hassani, *et al.*, Discovery of a chemical probe for PRDM9. *Nature Communications* **10**, 1–11 (2019).
20. T. Yu, *et al.*, The EZH2 inhibitor GSK343 suppresses cancer stem-like phenotypes and reverses mesenchymal transition in glioma cells. *Oncotarget* **8**, 98348–98359 (2017).

21. Y. Cao, *et al.*, Inhibition of G9a by a small molecule inhibitor, UNC0642, induces apoptosis of human bladder cancer cells. *Acta Pharmacologica Sinica* **40**, 1076–1084 (2019).
22. W. N. Pappano, *et al.*, The Histone Methyltransferase Inhibitor A-366 Uncovers a Role for G9a/GLP in the Epigenetics of Leukemia. *PLoS ONE* **10**, e0131716 (2015).
23. M. Vinceti, *et al.*, Selenium for preventing cancer. *Cochrane Database Syst Rev* **1**, CD005195 (2018).
24. G. Huang, *et al.*, Autophagy is an important action mode for functionalized selenium nanoparticles to exhibit anti-colorectal cancer activity. *Biomater Sci* **6**, 2508–2517 (2018).
25. K. Bai, B. Hong, Z. Hong, J. Sun, C. Wang, Selenium nanoparticles-loaded chitosan/citrate complex and its protection against oxidative stress in d-galactose-induced aging mice. *Journal of Nanobiotechnology* **15**, 92 (2017).
26. S. Campaner, *et al.*, The methyltransferase Set7/9 (Setd7) is dispensable for the p53-mediated DNA damage response in vivo. *Mol. Cell* **43**, 681–688 (2011).
27. C. E. Clare, A. H. Brassington, W. Y. Kwong, K. D. Sinclair, One-Carbon Metabolism: Linking Nutritional Biochemistry to Epigenetic Programming of Long-Term Development. *Annual Review of Animal Biosciences* **7**, 263–287 (2019).
28. I. R. Bothwell, *et al.*, Se-Adenosyl-l-selenomethionine Cofactor Analogue as a Reporter of Protein Methylation (2012) https:/doi.org/10.1021/ja304782r (April 1, 2020).
29. M. G. Malkowski, *et al.*, Blocking S-adenosylmethionine synthesis in yeast allows selenomethionine incorporation and multiwavelength anomalous dispersion phasing. *Proc. Natl. Acad. Sci. U.S.A.* **104**, 6678–6683 (2007).
30. C. D. Davis, E. O. Uthus, Dietary Folate and Selenium Affect Dimethylhydrazine-Induced Aberrant Crypt Formation, Global DNA Methylation and One-Carbon Metabolism in Rats. *J Nutr* **133**, 2907–2914 (2003).
31. C. D. Davis, E. O. Uthus, J. W. Finley, Dietary Selenium and Arsenic Affect DNA Methylation In Vitro in Caco-2 Cells and In Vivo in Rat Liver and Colon. *J Nutr* **130**, 2903–2909 (2000).
32. M. Barroso, *et al.*, The Link Between Hyperhomocysteinemia and Hypomethylation: Implications for Cardiovascular Disease. *Journal of Inborn Errors of Metabolism and Screening* **5** (2017).
33. J. Decelle, *et al.*, Subcellular Chemical Imaging: New Avenues in Cell Biology. *Trends Cell Biol.* **30**, 173–188 (2020).
34. B. Langmead, S. L. Salzberg, Fast gapped-read alignment with Bowtie 2. *Nature Methods* **9**, 357–359 (2012).
35. A. Roberts, L. Pachter, Streaming fragment assignment for real-time analysis of sequencing experiments. *Nat. Methods* **10**, 71–73 (2013).
36. M. I. Love, W. Huber, S. Anders, Moderated estimation of fold change and dispersion for RNA-seq data with DESeq2. *Genome Biology* **15**, 550 (2014).
37. M. I. Love, W. Huber, S. Anders, Moderated estimation of fold change and dispersion for RNA-seq data with DESeq2. *Genome Biology* **15**, 550 (2014).
38. R. J. Cho, M. J. Campbell, Transcription, genomes, function. *Trends Genet.* **16**, 409–415 (2000).
39. P. D. Thomas, *et al.*, Applications for protein sequence-function evolution data: mRNA/protein expression analysis and coding SNP scoring tools. *Nucleic Acids Res.* **34**, W645-650 (2006).
40. R. J. Cho, M. J. Campbell, Transcription, genomes, function. *Trends in Genetics* **16**, 409–415 (2000).
41. P. D. Thomas, *et al.*, Applications for protein sequence-function evolution data: mRNA/protein expression analysis and coding SNP scoring tools. *Nucleic Acids Research* **34**, W645–W650 (2006).

# Cu isotope ratios are meaningful in ovarian cancer diagnosis

## I. Presentation of the article

Ovarian cancer detection is currently based on intraperitoneal cavity imaging and a blood test to measure the levels of circulating CA-125 concentrations. CA-125, or MUC16, is a glycoprotein secreted by the ovarian epithelium during cancer development, particularly in advanced high-grade serous sub types, with well-known limits to sensitivity and specificity for other cancer sub types. New biomarkers are required to complement CA-125 testing to increase effectiveness. However, it remains an effective approach for following patient response to chemotherapy and detecting relapse.

In the last decade, there has been significant interest in the use of blood-based metal concentration and isotopic variations in terms of their diagnostic application in oncology and other fields. Such measurements, performed using multiple-collector inductively coupled plasma mass spectrometer (MC-ICP-MS), have been growing in interest as a result of their ease of use and rapid measurement. Copper isotopes are present in the form of two ions Cu(I) and Cu(II) in cells and in blood. Transport and uptake of these two Cu ions is the cause of the selective distribution (fractionation) of the copper isotopes $^{63}$Cu(I/II) and $^{65}$Cu(I/II) between the cells and the blood. Copper isotopes are linked to fundamental biological functions such as extracellular matrix remodulation or mitochondrial metabolism. Ratios between those isotopes are determined using MC-ICP-MS and the delta value $\delta^{65}$Cu obtained is a measure of the report of Cu isotope abundances relative to a reference :

$$\partial^{65}Cu=\left[\frac{\left(^{65}Cu/^{63}Cu\right)\text{ sample - }\left(^{65}Cu/^{63}Cu\right)\text{ ref}}{\left(^{65}Cu/^{63}Cu\right)\text{ ref}}\right]\text{x}10^{3}$$

This represents the relative deviation of the $^{65}$Cu/$^{63}$Cu ratio in the measured sample from its value in the reference material NIST SRM 976 in parts per 1000 (‰).

With a typical reproducibility on $\delta^{65}$Cu at the 95 percent confidence level as determined from multiple replicates of serum samples is 0.05‰ in samples containing as low as 30ng of copper, the quantity of material needed for precise measurement is very low (200µL of serum typically) Moreover, copper turnover in the body is around 6 weeks, with a concentration of 1mg/L in blood allowing enough material to measure copper isotopes variations and being sure the differences in $\delta^{65}$Cu are due to recent copper metabolism modifications. Recent studies have focused on the evolution of copper isotopic composition in serum of breast cancer patient[100](Télouk et al., 2015)(Télouk et al., 2015). For all patients tested, a decrease of $\delta^{65}Cu_{serum}$ by 0.25 ‰, which was relative to an increase in $^{65}$Cu concentration in tumours, was observed. Measuring the temporal evolution of isotopic composition in blood demonstrated that a rapid shift in $\delta^{65}$Cu corresponded to a more advanced tumour, and correlated with CA15-3 (MUC1 blood concentration) levels in breast cancer patients[100]. Decreases in $\delta^{65}Cu_{serum}$ by 0.14

‰ have also been measured in colorectal cancer patients[100], and together indicate that $\delta^{65}$Cu could be a useful biomarker for cancer detection and progression (See Figure below).

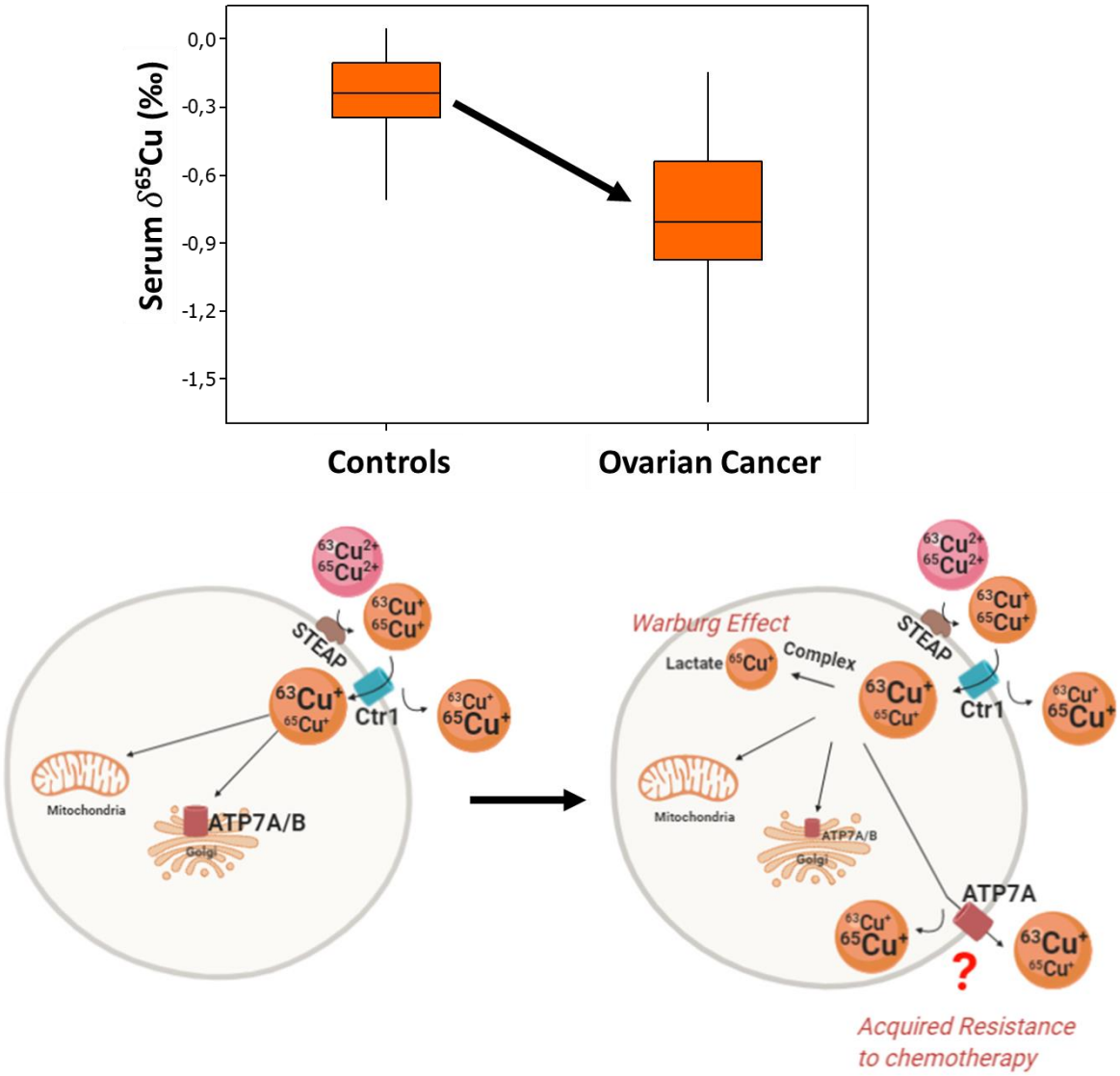


**Graphical Abstract: Proposed mechanisms of copper fractionation between normal cells and ovarian cancer cell.**

*Changes in the circulating $^{65}$Cu levels from patients with ovarian cancer may be multifactorial. The tumour environment is hypoxic and results in an increase in tumour cellular lactate metabolism leading to the preferentially chelation of heavy copper by lactate thus retaining this isoform of Cu in the tumour cells. In addition, amino acid sequence composition is selectively transporting light copper isotope $^{63}$Cu.*

*When patients are treated with platinum chemotherapy, resistance to treatment can occur. We proposed the following mechanism: In platinum treated cancer cells the copper transporter ATP7A would selectively export $^{63}$Cu. This would result in $^{65}$Cu being selectively retained in the tumour cells by lactate and increased expression of efflux copper transporter increasing the relative amount of $^{63}$Cu in blood.*

Using sample biobank of Swansea University we measured copper isotopes in the serum of 44 ovarian cancer patients and in some biopsies we have been able to obtain from the hospital. We have been able to measure a significant decrease of the $\delta^{65}$Cu in the serum of ovarian cancer patients in comparison with controls. This preliminary work brought additional results to current studies proving the efficacy of isotopic measurements to detect cancer. However a larger clinical study will be required to define $\delta^{65}$Cu thresholds that would be indicative of the presence of the disease.

# II. Article

This paper is Published in Journal of Trace Elements in Medicine and Biology
https://www.sciencedirect.com/science/article/pii/S0946672X20301760

## Cu isotope ratios are meaningful in ovarian cancer diagnosis

[12]Toubhans B., [2]Gourlan A.T, [3]Telouk P., [4]Lutchman-Singh K., [1]Francis L W., [1]Conlan R S.,[5]Margarit L., [1]Gonzalez D., [2]Charlet L.

**Affiliations:**

[1]Medical School & Centre for NanoHealth, Swansea University, Singleton Park, Swansea, SA2 8PP, UK

[2]ISTerre, Université Grenoble Alpes, CS 40700, 38058 Grenoble, France

[3]Univ Lyon, ENSL, Univ Lyon 1, CNRS, LGL-TPE, 69007 Lyon, France

[4]Swansea Bay University Health Board, Department of Gynaecology Oncology, Singleton Hospital, Swansea, SA2 8QA, UK

[5]Cwm Taf Morannwg University Health Board, Department of Obstetrics & Gynaecology, Princess of Wales Hospital, Bridgend, CF31 1RQ, UK

Journal of Trace Elements in Medicine and Biology 62 (2020) 126611

Contents lists available at ScienceDirect

Journal of Trace Elements in Medicine and Biology

journal homepage: www.elsevier.com/locate/jtemb

Pathobiochemistry

# Cu isotope ratios are meaningful in ovarian cancer diagnosis

B. Toubhans[a,b,*], A.T Gourlan[b], P. Telouk[c], K. Lutchman-Singh[d], L.W. Francis[a], R.S. Conlan[a], L. Margarit[e], D. Gonzalez[a], L. Charlet[b]

[a] Medical School & Centre for NanoHealth, Swansea University, Singleton Park, Swansea SA2 8PP, UK
[b] ISTerre, Université Grenoble Alpes, CS 40700, 38058 Grenoble, France
[c] Univ Lyon, ENSL, Univ Lyon 1, CNRS, LGL-TPE, 69007 Lyon, France
[d] Swansea Bay University Health Board, Department of Gynaecology Oncology, Singleton Hospital, Swansea SA2 8QA, UK
[e] Cwm Taf Morgannwg University Health Board, Department of Obstetrics & Gynaecology, Princess of Wales Hospital, Bridgend CF31 1RQ, UK

ARTICLE INFO

*Keywords:*
Copper
Isotopes
Ovarian cancer
Biomarker

ABSTRACT

*Background:* Ovarian cancer diagnosis is currently based on imaging and circulating CA-125 concentrations with well-known limits to sensitivity and specificity. New biomarkers are required to complement CA-125 testing to increase effectiveness. Increases in sensitivity of isotopic separation via multi collector inductively coupled plasma-mass spectrometry have recently allowed highly accurate measurement of copper (Cu) isotopic variations. Studies in breast cancer patients have revealed changes of serum copper isotopic composition demonstrating the potential for development as a cancer biomarker. Evaluating $^{65}Cu/^{63}Cu$ ratios ($\delta^{65}Cu$) in serum samples from cancer patients has revealed a strong correlation with cancer development. In this study blood samples from forty-four ovarian cancer patients, and 13 ovarian biopsies were investigated.

*Results:* Here we demonstrate that changes in Cu isotopes also occurs in ovarian cancer patients. Copper composition determined by multiple collector inductively coupled plasma mass spectrometry revealed that the copper isotopic ratio $\delta^{65}Cu$ in the plasma of 44 ovarian cancer patient cohort was significantly lower than in a group of 48 healthy donors, and indicated that serum was enriched for $^{63}Cu$. Further analysis revealed that the isotopic composition of tumour biopsies was enriched for $^{65}Cu$ compared with adjacent healthy ovarian tissues.

*Conclusions:* We propose that these changes are due to increase lactate and Cu transporter activities in the tumour. These observations demonstrate that, combined with existing strategies, $\delta^{65}Cu$ could be developed for use in ovarian cancer early detection.

## 1. Introduction

Copper (Cu) is a vital nutrient absorbed by intestinal cells and transported to the liver where it is stored thus controlling its concentration in blood [1,2]. Cu circulates mainly complexed to ceruloplasmin (60–95%) and albumin (10 %) [3,4]. In cells, Cu is complexed to metallochaperones including COX17 and ATOX1 [5] which deliver Cu to cytochrome c and ATPase 7B respectively. Modifications to Cu concentration and relative abundance of Cu isotopes (fractionation) have been linked to modified metabolic processes (oxidative phosphorylation, hypoxia, angiogenesis), and thus to health and disease [6].

Ovarian cancer diagnosis is currently based on circulating cancer antigen 125 (CA-125) concentrations where it is elevated in 50 % of early stage ovarian cancer cases [7], but is also increased in pregnancy, endometriosis [8] and other benign clinical conditions, which reduces its specificity. However it remains an effective approach for following the response to chemotherapy on patients and detecting relapse [9].

To complement clinically available diagnostic methods, new biomarkers including circulating tumour DNA, tumour serum proteins, circulating cancer cells or serum levels of metals such as Cu and zinc [10,11] are being developed due to increased sensitivity of multi collector inductively coupled plasma-mass spectrometry (MC-ICP-MS).

Copper is present in the form of two ions Cu(I) and Cu(II) in cells and in blood. Transport and uptake of these two Cu ions is the cause of the selective distribution (fractionation) of the copper isotopes $^{63}Cu$(I/II) and $^{65}Cu$(I/II) between the cells and the blood [6,12]. Recent studies have measured a strong decrease of the ratio ($\delta^{65}Cu$, see Eq. 1) of Cu isotopes in serum of breast or colorectal cancer patient [13].

The aims of the present study were to compare $\delta^{65}Cu$ ratios i) from whole blood in group of ovarian cancer patients compared to a healthy control group and ii) evaluate a small series of ovarian cancer biopsies

* Corresponding author at: ISTerre, Université Grenoble Alpes, CS 40700, 38058 Grenoble, France.
*E-mail address:* benoit.toubhans@gmail.com (B. Toubhans).

https://doi.org/10.1016/j.jtemb.2020.126611
Received 18 May 2020; Received in revised form 29 June 2020; Accepted 2 July 2020
Available online 03 July 2020

and healthy ovary tissue.

## 2. Material and methods

### 2.1. Clinical samples

Ethical approval for this study was obtained from NHS HRA Wales6 REC (15/WA/0065) to collect tissue and serum samples from ovarian cancer patients and non-cancer controls. Formal written consent was obtained from all patients at the time of recruitment into the study. Patients attending general gynaecology clinics or gynaecology oncology clinics in Swansea Bay and Cwm Taf Morgannwg NHS University Health Boards (SBUHB and CTMUHB) were recruited into this study. Forty-four women with histologically confirmed ovarian cancer were recruited in this project. These were post-menopausal patients that presented to primary care or emergency services with symptoms suggestive of ovarian pathology (pain, abdominal bloating, weight loss and change in bowel habit). An ovarian mass was subsequently identified on imaging investigations (ultrasound, CT, MRI) and tumour marker measurements [CA-125] performed. The histological evaluation of the ovarian biopsies and the cancer diagnosis was confirmed by the Pathology Department as part of the patient's routine clinical care. However, only patients with a confirmed ovarian tumour diagnosis were included in the study. Patients with infection, chronic inflammation, autoimmune disease and other cancers were excluded from this study. Amongst the patients, thirteen gave serum and biopsies and 31 gave only serum. Analysis of the CA-125 marker is reported in Table 1. Women were between 43 and 83 years old with a mean of 64.4 years old. Control serum (from the Etablissement Français du Sang, patient agreement obtained through MTA13−1728) was obtained from women between 19 and 65 years old with a mean of 33 years old were analysed. Data are included in supplementary 1 (Télouk et al., submitted to Journal of Hepatology). Blood was sampled into dry test tubes, centrifuged immediately, and stored at −80 °C. Two hundred microliters of serum were mineralized on a hot plate in a mixture of 2 mL of nitric acid and 0.5 mL of hydrogen peroxide and processed on a macroporous anion-exchange resin AGMP1 100–200 mesh (Biorad, UK) to separate Cu [14]. Biopsies (Table 2) placed into culture medium at the time of surgery were cut in pieces and one piece retained for isotopic measurements. These pieces were weighed and mineralized on a hot plate in a mixture of 2 mL nitric acid and 0.5 mL hydrogen peroxide and processed on a macroporous anion-exchange resin to separate Cu.

### 2.2. Spectrometry

Element concentrations were determined as previously described [14,15] by ICP-MS using an iCAP Q (Thermofisher Scientific, Bremen, Germany). $^{65}Cu/^{63}Cu$ ratios of the blood and biopsy samples were determined using a Nu instrument multiple-collector inductively coupled plasma mass spectrometer (MC-ICP-MS) Nu Plasma HR 500 (Wrexham, UK). As mass spectrometry isotopic measurement by MC-ICP-MS suffers from a stable bias between samples, a correction was systematically applied. For this, a constant and known standard made of zinc was systematically added in the purified samples. The Zinc acts as a mass bias corrector and standard in sample bracketing as it is measured at the same time as copper and is used as reference. This allow to reduce the MC-ICP-MS mass bias inducing wrong measurement compared to the real isotopic composition in copper.

A conventional delta value $\delta^{65}Cu$ is used throughout to report the Cu isotope abundances. $\delta^{65}Cu$ is a dimensionless parameter defined as:

$$\delta^{65}Cu = \left[\frac{(^{65}Cu/^{63}Cu)\text{sample} - (^{65}Cu/^{63}Cu)\text{ref}}{(^{65}Cu/^{63}Cu)\text{ref}}\right] \times 10^3 \text{stin}^{-1}\theta \quad (1)$$

This represents the relative deviation of the $^{65}Cu/^{63}Cu$ ratio in the measured sample from its value in the reference material NIST SRM 976 in parts per 1000 (‰). Typical reproducibility on $\delta^{65}Cu$ at the 95 percent confidence level as determined from three replicates of serum samples is 0.05‰. Natural variations of $\delta^{65}Cu$ in inorganic and organic material do not exceed +/- 3‰ [16]. These δCu variations are due to metabolic processes and biological variability.

## 3. Statistical analysis

Normality of the data was analysed using a Kolmogorov Smirnov test.

Statistically significant differences on δCu values between healthy serum vs OC serum samples were assessed using a 2-samples *t*-test as distributions of the datasets were normal. Statistically significant differences on δCu values between tumour vs non tumour ovarian biopsies were assessed using a Mann Whitney test as distributions of the datasets were not normal.

In order to evaluate the correlation between age and δCu of ovarian cancer patients, as the datasets were normally distributed we undertook a Pearson's Correlation Test. In order to evaluate the differences between number of chemotherapy and $\delta^{65}Cu$ values, we performed a Mann-Whitney test between the different groups we described in the results. Finally, the differences between cancer stage and $\delta^{65}Cu$ values was assessed using a Kruskal Wallis test between the different groups described in the results.

## 4. Results

### 4.1. Clinical diagnosis and treatment

Forty-four ovarian cancer patients were included in this study and results compared to data from 48 healthy patients (See Supplementary 1. Télouk et al. unpublished). The mean age of the women with ovarian cancer in the study was 64.4 years, and women were post-menopause (Table 1). In total 22 women were diagnosed with FIGO (Federation Internationale de Gynécologie et d'Obstétrique) stage 3 ovarian cancer, seven with FIGO stage 4 cancer and 8 FIGO stage 1 or 2 and seven benign masses.

We obtained ovarian biopsy samples from 13 patients from one or from both ovaries, 11 were tumoral and 10 were non tumoral (Table 2). The 13 patient cohort included those diagnosed with high grade serous ovarian cancer (HGSOC) (n = 6), borderline ovarian tumour (n = 1), endometrioid ovarian adenocarcinoma (n = 2) and benign tumour masses (n = 4). The levels of CA-125 were measured at diagnosis. Patients presenting before Pt chemotherapy had high levels of the marker (mean of the group = 1301 ± 1370). The effect of Pt treatment was followed by monitoring CA-125 levels. Samples were taken when the marker had significantly decreased (mean of the group = 205 ± 250).

### 4.2. Association between $\delta^{65}Cu$ and cancer

Healthy patient serum $\delta^{65}Cu$ values were compared to that of ovarian cancer patients (Fig. 1). Ovarian cancer patient serums had a copper isotope ratio ranging from -1.59 to -0.14‰ (median -0.80‰, mean -0.78‰ ± 0.05), a distribution that was significantly lower ($p < 0.001$) than the control group (between -0.71 and 0.05‰, median -0.23‰, mean -0.23‰ ± 0.02). Comparison of the copper isotope ratio in eleven ovarian tumour biopsies and ten non-tumour ovarian biopsies showed that in tumour biopsies, $\delta^{65}Cu$ values were between -0.19 and 0.59‰ (n = 11, median -0.09‰, mean 0.09‰ ± 0.08). $\delta^{65}Cu$ values were significantly lower ($p < 0.05$) in healthy ovaries with values ranging from -0.63 to 0.08‰ (n = 10, median of -0.16‰, mean of -0.16‰ ± 0.06 $p < 0.05$). Finally, no difference was found between $\delta^{65}Cu$ of the 13 patients we obtained serum and biopsies from and the 31 patients with only serum samples ($p > 0.05$).

**Table 1**
Ovarian cancer: diagnostic, stage, number of cycles of chemotherapy and analytical data on serum samples (CS = Cancer Serum, *=pre-menopausal women, N/A = not applicable, NC = non communicated).

| Sample Number | Age | Cancer Diagnosis | Stage | Nb of chemotherapy | Initial CA-125 at diagnosis | CA-125 at recruitment in the study | $\delta^{65}$Cu(‰) |
|---|---|---|---|---|---|---|---|
| CS1 | 43 | HGSOC | 4A | 3 | 1146 | 32 | −0.25 |
| CS2 | 57 | HGSOC | 4B | 4 | 363 | 19 | −0.98 |
| CS3 | 73 | Metastatic colorectal adenocarcinoma to the ovaries | 4B | NC | 202 | 202 | −0.84 |
| CS4 | 68 | HGSOC | 4A | 3 | > 25,000 | 517 | −0.57 |
| CS5 | 71 | HGSOC | 4B | 4 | 1857 | 21 | −0.59 |
| CS6 | 71 | HGSOC | 4B | 6 | 4248 | 500 | −0.47 |
| CS7 | 76 | HGSOC | 4A | 4 | 1656 | 35 | −0.81 |
| CS8 | 74 | HGSOC | 3C | 3 | 198 | 53 | −0.79 |
| CS9 | 62 | HGSOC | 3C | 3 | 3682 | 1154 | −0.6 |
| CS10 | 60 | HGSOC | 3C | 6 | 3150 | 30 | −0.87 |
| CS11 | 50 | HGSOC | 3C | 6 | 721 | 22 | −1.36 |
| CS12 | 82 | HGSOC | 3C | 6 | 2085 | 57 | −0.53 |
| CS13 | 60 | HGS Primary Peritoneal disease | 3C | 4 | 227 | < 6 | −0.9 |
| CS14 | 69 | HGSOC | 3C | 6 | 796 | 20 | −0.97 |
| CS15 | 59 | HGSOC | 3C | 6 | 11,450 | 59 | −0.8 |
| CS16 | 71 | HGSOC | 3C | 5 | 423 | 14 | −0.65 |
| CS17 | 78 | HGSOC | 3C | 9 | 2429 | 2227 | −0.89 |
| CS18 | 67 | HGSOC | 3C | 6 | 81 | 19 | −0.39 |
| CS19 | 78 | Ovarian Carcinosarcoma (Tubo) | 3C | None | 160 | 160 | −0.97 |
| CS20 | 44 | HGSOC | 3C | None | 785 | 785 | −0.67 |
| CS21 | 55 | Ovarian Carcinosarcoma | 3C | 3 | 831 | 122 | −0.61 |
| CS22 | 82 | HGSOC | 3C | 4 | 836 | 155 | −0.69 |
| CS23 | 71 | HGSOC | 3C | None | 1161 | 1613 | −1.22 |
| CS24 | 83 | HGSOC | 3C | 3 | 2538 | 206 | −1.01 |
| CS25 | 58 | HGSOC | 3C | 4 | 634 | 231 | −0.53 |
| CS26 | 80 | HGSOC | 3C | 4 | 58 | 35 | −1.13 |
| CS27 | 66 | HGSOC | 3C | 6 | 340 | 35 | −0.19 |
| CS28 | 73 | HGSOC | 3C | 4 | 204 | 37 | −1.56 |
| CS29 | 82 | HGSOC | 3C | 4 | 634 | 231 | −1.6 |
| CS30 | 56 | HGSOC | 2C | 4 | 302 | 24 | −1.1 |
| CS31 | 47 | Endometrioid adenocarcinoma ovary | 2A | None | 492 | 492 | −0.14 |
| CS32 | 62 | Ovarian Clear Cell | 1C2 | None | 241 | 431 | −0.82 |
| CS33 | 67 | Ovarian Granulosa cell tumour | 1C2 | None | 38 | 38 | −0.98 |
| CS34 | 68 | Ovarian Borderline Serous Cystadenoma | 1C2 | None | 37 | 18 | −0.68 |
| CS35 | 54 | Endometrioid adenocarcinoma ovary | 1A | None | 74 | 74 | −0.53 |
| CS36 | 57 | Borderline Serous Carcinoma | 1A | None | 67 | 67 | −0.91 |
| CS37 | 60 | Borderline Ovarian Serous tumour | 1A | None | 64 | 52 | −0.84 |
| CS38 | 60 | Ovarian Fibroma | Benign | N/A | 55 | 68 | −0.49 |
| CS39 | 55 | Mucinous Cystadenoma | Benign | N/A | 54 | 54 | −1.05 |
| CS40 | 51 | Ovarian Fibroma | Benign | N/A | 73 | 64 | −0.76 |
| CS41 | 64 | Ovarian Fibroma | Benign | N/A | 13 | 13 | −1.17 |
| CS42 | 51 | Mucinous Cystadenoma | Benign | N/A | 52 | 52 | −0.16 |
| CS43 | 46 | HGSOC | N/A | None | 12 | 12 | −0.93 |
| CS44 | 74 | Ovarian Fibroma | Benign | N/A | 37 | 37 | −0.38 |

### 4.3. Association between $\delta^{65}$Cu and cancer status

Serum $\delta^{65}$Cu values were compared based on stage of the cancer disease. Using a Kruskal Wallis test, no association was found between cancer stage and $\delta^{65}$Cu in blood, with a median of -0.58‰ (mean -0.61‰ ± 0.10) for stage 4, -0.83‰ (mean -0.86‰ ± 0.07) for stage 3, -0.87‰ (mean -0.79‰ ± 0.08) for stage 2 and -0.80‰ (mean -0.72‰ ± 0.12) for stage 1 patients ($p = 0.95$). Moreover, no association was found between stage in the disease and $\delta^{65}$Cu in tumour mass. The low number of tumour mass samples from stage 4 patients may explain the lack of correlation.

The number of cycles of chemotherapy appeared to influence the $\delta^{65}$Cu value in the biopsies. Patients receiving at least four cycles of chemotherapy had a significantly ($p = 0.05$) higher $\delta^{65}$Cu ($n = 6$, median = -0.01, mean = 0.12‰ ± 0.08) than patients receiving no chemotherapy ($n = 7$, median = -0.10, mean = -0.15‰ ± 0.06).

Finally we decided to evaluate if the differences on $\delta^{65}$Cu levels between patients were dependent on the patients age at the time of sample collection using a Pearson's Correlation Test. No significant association was observed between the patient's age and $\delta^{65}$Cu (p-value = 0,115, r = -0272).

## 5. Discussion

In the present study the degree of copper fractionation was measured in blood and tissue samples obtained from ovarian cancer patients, and $\delta^{65}$Cu was used to determine the ratio of the two stable copper isotopes. A positive $\delta^{65}$Cu indicated depletion of circulating $^{63}$Cu isotope, possibly due to an uptake by tumour cells, and conversely a negative value indicated an enrichment of the lighter $^{63}$Cu isotope in serum. We observed that $\delta^{65}$Cu was lower in the serum of ovarian cancer patient compared to that from healthy donors. Thus, as in breast and colorectal cancer [13], we observed that patients with ovarian tumours have higher levels of $^{65}$Cu in the tumour mass than in blood. No correlation was made between the stage of cancer and serum $\delta^{65}$Cu. Thus, whilst $\delta^{65}$Cu correlates with ovarian cancer diagnosis it displays no specificity for cancer type or stage [13,17].

The mechanism behind the decrease of $\delta^{65}$Cu in the serum of cancer patients has been suggested to be a consequence of the hypoxic tumour environment that increases the relative level of lactate compared to normal tissue and thus of an increased carboxyl group concentrations available for complexation with Cu [13]. Since the heavy $^{65}$Cu copper Cu(I) isotope forms more stable bonds with carboxyl groups of lactate

**Table 2**
Ovarian cancer: diagnostic, stage, number of cycle of chemotherapy and analytical data on biopsy samples (CB = Cancer biopsy, *=pre-menopausal women, N/A = not applicable).

| Sample Number | | Age | Cancer Diagnosis | Stage | Nb of chemotherapy | Tumour δCu (‰) | Non Tumour δCu(‰) | Comments |
|---|---|---|---|---|---|---|---|---|
| CB6 | Right | 71 | HGSOC | 4B | 6 | −0.09 | | HGSOC |
| | Left | | HGSOC | | | 0.01 | | HGSOC |
| CB17 | Right | 78 | HGSOC | 3C | 9 | 0.33 | | HGSOC |
| | Left | | | | | | | Not sampled |
| CB18 | Right | 67 | HGSC of L fallopian tube | 3C | 6 | −0.06 | | Benign |
| | Left | | | | | 0.26 | | Benign |
| CB25 | Right | 58 | HGSOC | 3C | 4 | 0.57 | | HGSOC |
| | Left | | | | | 0.59 | | HGSOC |
| CB27 | Right | 66 | HGSC of L fallopian tube | 3C | 6 | −0.13 | | HGSOC |
| | Left | | | | | −0.11 | | HGSOC |
| CB28 | Right | 73 | HGSC of L fallopian tube | 3 | 4 | | −0.28 | Benign |
| | Left | | | | | 0.29 | | HGSOC |
| CB31 | Right | 47 | Grade 3 endometrioid type | 2A | None | | −0.09 | Normal |
| | Left | | | | | | | Endometrioid adenocarcinoma |
| CB34 | Right | 68 | Borderline R Ovarian serous cystadenoma | 1C2 | None | −0.09 | | Borderline R Ovarian serous cystadenoma |
| | Left | | | | | | 0.08 | Several serous inclusion cysts |
| CB35 | Right | 54 | L Ovarian endometrioid adenocarcinoma | 1A | None | | −0.02 | Endometriosis foci |
| | Left | | | | | | | Endometrioid adenocarcinoma with big endometriosis and cystadenoma |
| CB39 | Right | 55 | Benign L mucinous cystadenoma | Not cancer | N/A | | −0.22 | Normal |
| | Left | | | | | | −0.26 | Benign L mucinous cystadenoma |
| CB41 | Right | 64 | Benign R fibroma | Not cancer | N/A | | | Benign R fibroma |
| | Left | | | | | | 0.06 | Normal |
| CB42 | Right | 51 | Benign R mucinous cystadenoma | Not cancer | N/A | | −0.22 | Benign mucinous cystadenoma |
| | Left | | | | | | | Normal |
| CB43 | Right | 46 | Leiomyosarcoma favoured to be of broad ligament origin | N/A | None | | −0.63 | Cellular spindle cell tumour with fascicular growth pattern w/ moderate to severe atypia |
| | Left | | | | | | −0.11 | Normal |

than lighter Cu isotopes it would be preferentially chelated and thus retained in cancer cells, resulting in an apparent decrease of serum $\delta^{65}$Cu [17]. In cells, copper is present predominantly as Cu(I) and is always complexed with transport proteins to overcome its reactivity, therefore avoiding the production of reactive oxygen species that can cause cellular damage. Ab initio calculations on the ability of organic molecules to coordinate with copper have been undertaken [18,19]. O donor (glutamine, threonine), N donor (histidine) and S donor (cysteine, methionine) amino acids19] were found to be preferentially bind $^{63}$Cu light copper isotopes of Cu(II), and can also be assumed to fractionate as Cu(I) [20].

In ovarian cancer, patients often relapse following an initial positive response to platinum chemotherapy, developing resistance and thus reducing subsequent therapeutic options [9]. The most common mechanisms for resistance are the overexpression of ATP-dependent efflux pumps such as MDR1 and ATPases 7A and B [21,22]. The ATP-dependent copper transporter ATPases 7A and 7B supplies the Golgi with copper needed for enzyme synthesis. While ATPases 7A and 7B allows fine control of copper concentration in cells, its activity also allows tumour cells to detoxify platinum-based drugs which increase the resistance of the cells to treatment [23–25]. It seems likely therefore that copper fractionation in ovarian cancer following chemotherapy could occur due to the overexpression of ATP7ase A drug efflux pump [26,27] to detoxify Pt treated patients (Fig. 2). This is supported by our mass spectrometric analysis that revealed a decrease in the $\delta^{65}$Cu value in ovarian cancer patients corresponding to a decrease in circulating $^{65}$Cu in these patients ($\delta^{65}$Cu = -0.80‰), and an increase $\delta^{65}$Cu value in tumours ($\delta^{65}$Cu = -0.01‰) compared to healthy tissue.

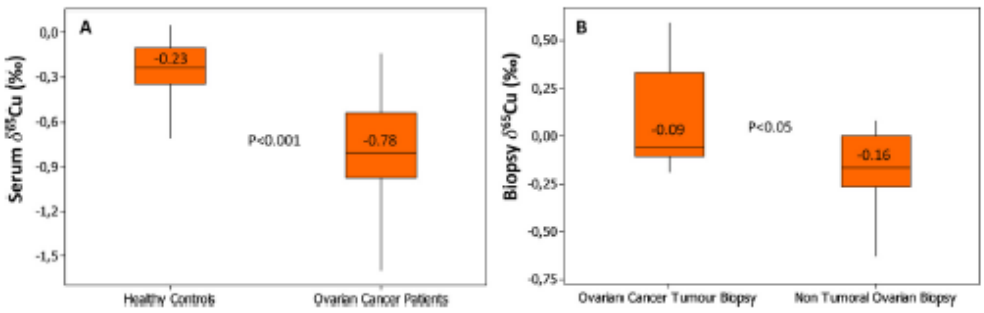


**Fig. 1.** Comparison of $\delta^{65}$Cu between healthy blood donor and ovarian cancer blood and between ovarian cancer mass and non-tumour ovarian biopsy.
A) Whisker plot of serum $\delta^{65}$Cu values for healthy women (48) compared to ovarian cancer patients (44). Boxes represent the 75 percent middle quantile and the whiskers 95 percent quantiles. Horizontal line: median. Separation between ovarian cancer patients and healthy women is significant ($p < 0.001$).
B) Whisker plot of 11 ovarian cancer mass and 10 contra-lateral ovaries that are either healthy either withdraw to be checked for cancer development. Significant difference has been measured between the two conditions ($p < 0.05$).

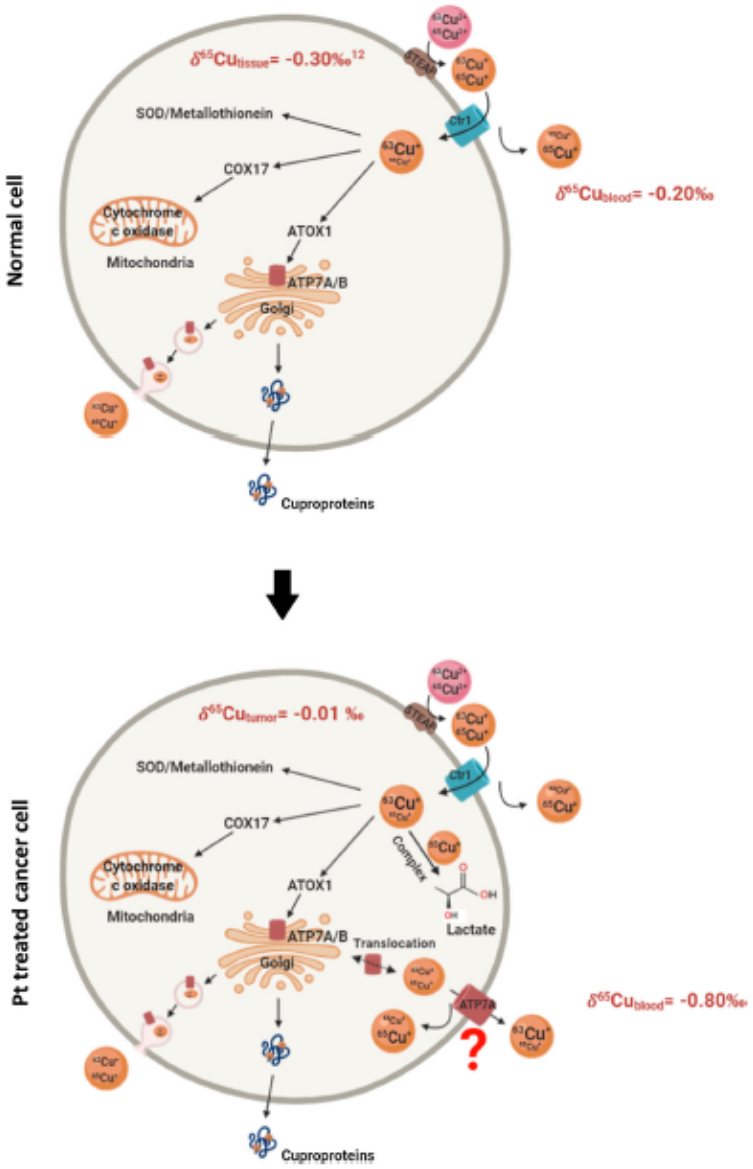


**Fig. 2.** Proposed mechanisms of copper fractionation between normal cells and platinum treated cancer cells.
Changes in the circulating $^{65}Cu$ levels from patients who have received chemotherapy may be multifactorial. The tumour environment is hypoxic and results in an increase in tumour cellular lactate metabolism leading to the preferentially chelation of heavy copper by lactate thus retaining this isoform of Cu in the tumour cells. In addition, selectivity of copper transporter toward light copper isotopes $^{63}Cu$ occurs due to transporter amino acid sequence composition [20]. In platinum treated cancer cells the copper transporter ATP7A would selectively export $^{63}Cu$. This would result in $^{65}Cu$ being selectively retained in the tumour cells by lactate and increased expression of efflux copper transporter increasing the relative amount of $^{63}Cu$ in blood.

## 6. Conclusion

Here we have demonstrated that Cu serum $\delta^{65}Cu$ levels are lower in ovarian cancer patients than in healthy donors. Conversely, ovarian cancer biopsies display a higher $\delta^{65}Cu$ than serum from healthy volunteers. Our study highlights the potential of Cu as a functional biomarker for the detection of ovarian cancer. Current development of new automatized tools to perform the chemistry on biological samples and increased performance of measurement of MC-ICP-MS will allow the future implementation of $\delta^{65}Cu$ to aid ovarian cancer detection when CA-125 and other imaging techniques are not conclusive. A larger clinical study is now required to define $\delta^{65}Cu$ thresholds that would be indicative of the presence of the disease.

## Ethics approval and consent to participate

This research was approved by NHS HRA Wales6REC (15/WA/0065) for collection of tissues and serum samples from ovarian cancer patients and non-cancer controls. Formal written consent was obtained from all patients at the time of recruitment into the study. Patients attending general gynaecology clinics or gynaecology oncology clinics in Swansea Bay and Cwm Taf Morgannwg NHS University Health Boards (SBUHB and CTMUHB) were recruited into this study. For control samples, blood samples were obtained by the Etablissement Français du Sang after patient agreement obtained through MTA13-1728.

### Consent for publication

Not applicable.

### Availability of data and materials

Not applicable.

### Funding

This project has received financial support from the Centre National de la Recherche Scientifique, France, through the MITI interdisciplinary programs and by Intitut National de la Santé Et de la Recherche Medicale, France, Grant SEDMAC (PC201607).

### Authors' contributions

Data collection, data analysis and manuscript drafting was performed by Benoit Toubhans. Alexandra T Gourlan, Laurent Charlet and Philippe Télouk contributed to the study conception and design. Clinical samples and data collection/analysis was performed by Lavinia Margarit and Kerryn Lutchman-Singh. R Steven Conlan, Deyarina Gonzalez and Lewis W Francis contributed to study design, critical interpretation of data and drafting of the manuscript. The authors read, amended and approved the final manuscript.

### Declaration of Competing Interest

All authors declare no conflict of interest.

### Acknowledgments

Cu measurements were performed at the INSU/CNRS MC-ICP-MS national facility at ENS-LYON with the help of Eloïse Godfroy.

Benoit Toubhans received a scholarship co-funded by the Université Grenoble Alpes and Swansea University.

### Appendix A. Supplementary data

Supplementary material related to this article can be found, in the online version, at doi:https://doi.org/10.1016/j.jtemb.2020.126611.

### References

[1] M. Olivares, R. Uauy, Limits of metabolic tolerance to copper and biological basis for present recommendations and regulations, Am. J. Clin. Nutr. 63 (5) (1996) 846S–852S, https://doi.org/10.1093/ajcn/63.5.846.
[2] J.R. Turnlund, Human whole-body copper metabolism, Am. J. Clin. Nutr. 67 (5 Suppl) (1998) 960S–964S, https://doi.org/10.1093/ajcn/67.5.960S.
[3] E. Frieden, H.S. Hsieh, Ceruloplasmin: the copper transport protein with essential oxidase activity, Adv. Enzymol. Relat. Areas Mol. Biol. 44 (1976) 187–236, https://doi.org/10.1002/9780470122891.ch6.
[4] A. Krężel, W. Maret, The functions of metamorphic metallothioneins in zinc and copper metabolism, Int. J. Mol. Sci. 18 (6) (2017), https://doi.org/10.3390/ijms18061237.
[5] S. Lutsenko, Copper trafficking to the secretory pathway, Met. Integr. Biometal. Sci. 8 (9) (2016) 840–852, https://doi.org/10.1039/c6mt00176a.
[6] F. Albarède, P. Télouk, V. Balter, Medical applications of isotope metallomics, Rev Mineral Geochem 82 (1) (2017) 851–885, https://doi.org/10.2138/rmg.2017.82.20.
[7] N. Scholler, N. Urban, CA125 in ovarian Cancer, Biomark. Med. 1 (4) (2007) 513–523, https://doi.org/10.2217/17520363.1.4.513.
[8] K. Al-Musalhi, M. Al-Kindi, F. Ramadhan, T. Al-Rawahi, K. Al-Hatali, W.-A. Mula-Abed, Validity of Cancer antigen-125 (CA-125) and risk of malignancy index (RMI) in the diagnosis of ovarian Cancer, Oman Med. J. 30 (6) (2015) 428–434, https://doi.org/10.5001/omj.2015.85.
[9] R.C. Bast, CA 125 and the detection of recurrent ovarian cancer: a reasonably accurate biomarker for a difficult disease, Cancer 116 (12) (2010) 2850–2853, https://doi.org/10.1002/cncr.25203.
[10] M. Zowczak, M. Iskra, L. Torliński, S. Cofta, Analysis of serum copper and zinc concentrations in cancer patients, Biol. Trace Elem. Res. 82 (1) (2001) 1, https://doi.org/10.1385/BTER:82:1-3:001.
[11] Y. Wang, Z. Sun, A. Li, Y. Zhang, Association between serum zinc levels and lung cancer: a meta-analysis of observational studies, World J. Surg. Oncol. (2019) 17, https://doi.org/10.1186/s12957-019-1617-5.
[12] F. Albarède, Metal stable isotopes in the human body: a tribute of geochemistry to medicine, Elements 11 (4) (2015) 265–269, https://doi.org/10.2113/gselements.11.4.265.
[13] P. Télouk, A. Puisieux, T. Fujii, et al., Copper isotope effect in serum of cancer patients. A pilot study, Met. Integr. Biometal. Sci. 7 (2) (2015) 299–308, https://doi.org/10.1039/c4mt00269e.
[14] F. Albarède, P. Télouk, A. Lamboux, K. Jaouen, V. Balter, Isotopic evidence of unaccounted for Fe and Cu erythropoietic pathways, Metallomics 3 (9) (2011) 926–933, https://doi.org/10.1039/C1MT00025J.
[15] C.N. Maréchal, P. Télouk, F. Albarède, Precise analysis of copper and zinc isotopic compositions by plasma-source mass spectrometry, Chem. Geol. 156 (1) (1999) 251–273, https://doi.org/10.1016/S0009-2541(98)00191-0.
[16] K. Sullivan, D. Layton-Matthews, M. Leybourne, J. Kidder, Z. Mester, L. Yang, Copper isotopic analysis in geological and biological reference materials by MC-ICP-MS, Geostand Geoanalytical Res 44 (2) (2020) 349–362, https://doi.org/10.1111/ggr.12315.
[17] V. Balter, A. Nogueira da Costa, V.P. Bondanese, et al., Natural variations of copper and sulfur stable isotopes in blood of hepatocellular carcinoma patients, Proc. Natl. Acad. Sci. U. S. A. 112 (4) (2015) 982–985, https://doi.org/10.1073/pnas.1415151112.
[18] T. Fujii, F. Moynier, M. Abe, K. Nemoto, F. Albarède, Copper isotope fractionation between aqueous compounds relevant to low temperature geochemistry and biology, Geochim. Cosmochim. Acta 110 (2013) 29–44, https://doi.org/10.1016/j.gca.2013.02.007.
[19] T. Fujii, F. Moynier, J. Blichert-Toft, F. Albarède, Density functional theory estimation of isotope fractionation of Fe, Ni, Cu, and Zn among species relevant to geochemical and biological environments, Geochim. Cosmochim. Acta 140 (2014) 553–576, https://doi.org/10.1016/j.gca.2014.05.051.
[20] J.-L. Cadiou, S. Pichat, V.P. Bondanese, et al., Copper transporters are responsible for copper isotopic fractionation in eukaryotic cells, Sci. Rep. 7 (1) (2017) 1–10, https://doi.org/10.1038/srep44533.
[21] R.W. Robey, K.M. Pluchino, M.D. Hall, A.T. Fojo, S.E. Bates, M.M. Gottesman, Revisiting the role of efflux pumps in multidrug-resistant cancer, Nat. Rev. Cancer 18 (7) (2018) 452–464, https://doi.org/10.1038/s41568-018-0005-8.
[22] A.-M. Patch, E.L. Christie, D. Etemadmoghadam, et al., Whole-genome characterization of chemoresistant ovarian cancer, Nature 521 (7553) (2015) 489–494, https://doi.org/10.1038/nature14410.
[23] R. Petruzzelli, R.S. Polishchuk, Activity and trafficking of copper-transporting ATPases in tumor development and defense against platinum-based drugs, Cells 8 (9) (2019), https://doi.org/10.3390/cells8091080.
[24] M.T. Kuo, H.H.W. Chen, I.-S. Song, N. Savaraj, T. Ishikawa, The roles of copper transporters in cisplatin resistance, Cancer Metastasis Rev. 26 (1) (2007) 71–83, https://doi.org/10.1007/s10555-007-9045-3.
[25] R. Safaei, S.B. Howell, Copper transporters regulate the cellular pharmacology and sensitivity to Pt drugs, Crit. Rev. Oncol. Hematol. 53 (1) (2005) 13–23, https://doi.org/10.1016/j.critrevonc.2004.09.007.
[26] G. Samimi, N.M. Varki, S. Wilczynski, R. Safaei, D.S. Alberts, S.B. Howell, Increase in expression of the copper transporter ATP7A during platinum drug-based treatment is associated with poor survival in ovarian Cancer patients, Clin. Cancer Res. 9 (16) (2003) 5853–5859.
[27] L.S. Mangala, V. Zuzel, R. Schmandt, et al., Therapeutic Targeting of ATP7B in Ovarian Carcinoma, Clin Cancer Res Off J Am Assoc Cancer Res 15 (11) (2009) 3770–3780, https://doi.org/10.1158/1078-0432.CCR-08-2306.

# Conclusion and Perspectives

## I. Conclusions

The close relationship between the environment and human health is well known, with geo-medical links furthering our understanding of trace element bioavailability, leading to innovative therapeutics in a range of diseases. Selenium, a crucial trace element available to humans through soil, has long been postulated to have anti-cancer properties despite its narrow toxicity window. This project utilises the principles of geochemistry and biochemistry to test and develop the use of selenium, in nanoparticulate form, in the treatment of ovarian cancer. The multidisciplinary approach utilised here, highlights the potential benefits of SeNP for ovarian cancer treatment, identifying novel histone methylation associated mechanisms of action and optimal nanoparticle coatings for increased cellular uptake and spheroid penetration. In ovarian cancer research, SeNP have been used only once as a carrier of doxorubicin *in vitro*[302] and never as a stand alone chemotherapeutic despite their high bioavailability and proved inhibition of tumour cancer cell growth. To determine the role of SeNPs in ovarian cancer we adopted a multiscale approach. We have been able to reproduce results from other cancer research groups proving the anticancer effect of SeNPs in different cancer cell line. We have also been able to measure cell physical properties after selenium treatment and, for the first time, the effect of selenium on histone modifications in cancer cells and overall impact on ovarian cancer.

In this Ph.D. dissertation we evaluated the effect of two types of coated SeNP (chitosan-coated and albumin-coated) on two ovarian cancer cell lines, OVCAR-3 and SKOV-3. These cell lines were selected as they represent metastatic and non metastatic phenotypes of high-grade serous cancer. In addition they have distinctly different cellular phenotypes with regard to growth characteristics and resistant phenotypes, prevalent in heterogenous in vivo context. SKOV-3 cells are epithelial cells derived from the ascitic fluid, they are metastatic cancer cells. OVCAR-3 are epithelial cancer cells from slow growing adenocarcinoma. Both SeNPs are cytotoxic in the two cell lines, however SKOV-3 is more sensitive than OVCAR-3. Moreover, cell monolayers (2D models) were less sensitive to selenium treatments than cell spheroids (3D models). Analysis of the mechanical cell membrane properties by AFM revealed an increased cell surface roughness and cellular stiffness in SKOV-3, while with OVCAR-3 cells, a decreased cellular stiffness is observed, indicative of altered cytoskeletal dynamics, alongside decreased vimentin expression level. SeNPs triggered early production of ROS, and a cell line dependent induction of apoptosis (in SKOV-3) or autophagy (in OVCAR-3), indicative of an enhanced resistance to SeNP in this cell type. SeNPs stimulated a global increase in histone methylation, as shown by elevated levels of H3K4me3, H3K27me3 and H3K9me2, involved in both gene activation and repression. Transcriptome analysis revealed SeNPs had a limited effect on pathways involved in the metabolism of the ubiquitous methyl-group donor S-adenosylmethionine (SAM). Whilst some effects appeared to be due to modulation of HMT activity, a clearance route for the HMT inhibitor S-adenosyl-homocysteine (SAH), possibly due to enhanced activity of the transulfuration pathway, also appears likely. It appears that reduction in cell viability following SeNP exposure occurs through different mechanisms that result in contrasting perturbations in cellular mechanics in serous ovarian cancer subtypes.

As well as the development of new, advanced therapeutics for ovarian cancer, there is additional need for the development of new or additional diagnostic procedures. Currently diagnosed via a blood test for elevated CA-125; Ovarian cancer diagnosis lacks specificity and sensitivity and is limited to the detection of advanced disease. Numerous attempts are being made to source alternative or complimentary diagnostics. Copper metabolism is affected in a large range of disease in human and in mammals. Cancer development have been related to increase of copper concentration in blood and modification of the copper isotope ratios in liver, colon and breast cancer patients. Blood copper ratio indicate enrichment in light copper isotopes. On the other hand, heavy copper isotopes are found preferentially in tumoral cells in comparison with surrounding tissues. We hypothesized the role of intracellular oxidative conditions and cancer adaptations to explain the modifications of copper ratios. The accumulation of lactate would explain the chelation of heavy copper. Moreover copper transporters would also be involved in the process. Following copper isotopes ratio in blood would give good tool to detect cancer and follow its treatment.

# II. Perspectives

The potential impact of Selenium on cancer is the topic of intense discussion. Understanding novel SeNP mechanisms of action on cancer cells will enable more effective SeNP-based treatment to be developed against cancer, not least in ovarian cancer, a complex and multifaceted disease with a very poor prognostic outcome. As shown in this study, the inclusion of advanced cell culture models in pre-clinical evaluation, such as the spheroid cultures used here, will provide significant added value in terms of clinical translation. This project could be expanded with further explorative work, enhancing our understanding of Selenium speciation, functional genomics and further establishing links to cell and tissue mechanical properties. Amongst a myriad of future research lines, I would recommend the following;

**Mapping the speciation of selenium in tumours**

Conducting 2D or 3D selenium elemental (and speciation) mapping in spheroids and tumours would enable the nature of the selenium aggregates observed in the cells to be determined. Extra- and intracellular speciation would to reveal whether assimilatory selenate reduction occurs, in analogy to S, and whether blood SeMet is preferentially taken up by tumours in humans. Such a quantitative understanding of S/Se metabolism and its intracellular localisation would allow known S species, metabolites (sulphate, Cys, Met, SAM, APS and PAPS) and (potential) Se analogues to be targeted using standard commercially available or newly synthesised compounds. The identity of the synthesized organic Se compounds will be determined in situ by XAS technique, and could be compared to ex-situ determination, after extraction by LC-ICP-MS/MS and - if required - high resolution LC-ESI-MS/MS, for identification of species for which no analytical standards are available. Synchrotron-based XAS techniques (HERFD-XAS and µ-XANES) could fingerprint *in-situ* the presence of S/Se organic or inorganic forms in tissues close to the natural, hydrated state. The recent upgrade (30 times X-ray brilliance increase) at the European Synchrotron Radiation Facility (ESRF) will

allow bulk speciation tomography to be performed with 30 nm and 0.3 pm spatial resolution and detection limit, respectively, and in very short times. Larger sections of ovarian tissue can be exposed to $^{76}Se$, and NanoSIMS maps obtained after their metabolism (with a 100 nm, 10 ppm spatial resolution and detection limit). In addition, spatial speciation of S or Se in a thin layer of flat tissue surface or within a cell, both down to 100 nm thickness, can be obtained at LBNL, Berkeley, CA, with prototype NMR imaging system using confocal imaging.

Overall, µ-XRF and µ-XAS around the Se K-edge will be used to distinguish between Se(IV) or Se°NP uptake by spheroids and their distribution within cell compartments. Moreover it would allow to decipher the mechanism of aggregation of selenium inside the mitochondria and vacuoles we observed in the paper entitled "Selenium nanoparticles induce global histone methylation changes in ovarian cancer cells" whether it is native SeNPs or secondary aggregated forms.

**Expanding knowledge of selenium nanoparticle effect on the genome**

We have been able to prove the increase of histone 3 lysine methylation through selenium nanoparticles treatment in ovarian cancer cells. We also used the RNAseq dataset in order to determine gross modifications of hallmarks through selenium treatment. We tried to combine treatment of selenium with DNMT inhibitor (5-aza) and HDAC inhibitor (SAHA) and haven't been able to prove any additive cytotoxic effect. This first approach needs to be complemented with gene expression screening as drug resistance is dependent from chromatin regulators that cannot be analysed only with genomic analysis but need the help of functional genomic. We preferentially would study the effect of SeNPs on DNA methylation as it has been done only with aqueous selenium.

The genetic screening using RNAi of specific epigenetic complexes such as KRAB, GLP, EED, LSD1 or DNMT3A would lead us to increase the knowledge of the effect of selenium on transcription factors and the most essential amongst them in drug resistance. Epigenetic and genetic mediators are influenced by selenium and lead cells to death. We would use this RNAi genetic screen in order to determine the main cell death actors that are regulated through selenium treatment. For example, the transient KO experiments of autophagy would lead us to determine which factors are leading cells to greater cell death. Moreover we would target genes associated with histone modifications based on stable knockdown cell lines from sensitive and resistant to selenium ovarian cancer cells. RNAi screening would lead to identify regulatory molecules responsible for epigenetic modifications in those cell lines.
Increasing our ability to systematically screen gene expression affected by selenium treatment would lead us to draw a precise pathway of action of selenium within cancer cells and normal cells.

**Better models for ovarian cancer study**

The environment surrounding a tumour influences the evolution of this tumour in many cancers and especially ovarian cancer. In comparison with the surrounding environment of solid tumours, the malignant ascitic fluid accumulating in the peritoneal cavity during ovarian cancer

progression constitutes a unique form of highly inflammatory environment. The ascitic fluid is constantly evolving with the evolution of the pathology and plays a major role in tumour progression, spheroid formation, tumour dissemination. Ascitic fluid is constituted of a high cell density fluid with high concentration of growth factors such as vascular endothelial growth factors (VEGF), transforming growth factors (TGFB, IL6, CXCL2). Dissemination of epithelial ovarian cancer is mediated through the ascitic fluid which is circulating around the ovaries and allow the detachment and the survival of ovarian cancer cells leading to the formation of spheroids, and then tumours, on secondary sites, notably on the peritoneal cavity epithelium (highly receptive to ovarian cancer seeding) which further lead to ovarian cancer metastasis to other organs when the epithelial ovarian cancer undergo epithelial-to-mesenchymal- transition through the peritoneal cavity. However during the dispersion from the primary site to the peritoneum, epithelial ovarian cancer cells must undergo adaptative changes in tumour to progress to the next step and most of the time only a fraction of cancer cells are circulating in the intraperitoneum before landing to the secondary site. This led us to develop a microfluidic model of the circulation of fluid surrounding a spheroid and assess the effect of selenium on the structure of the spheroid.

**Improving mechanical properties investigation**

Importantly, in vivo, tissue shaping, tissue repair and cancer invasion is done through collective movement of cells. This is possible thanks to the orientation of migration of the cells and made possible thanks to coordination between the cells that require the cytoskeleton. This coordination is regulated by multiscale process of mechanical changes within cells occurring at different timescales.

Following the monolayer mechanical properties analysis we performed, building a nanomechanical model on 3D spheroids would make these mechanical measurement closer to the tumoral reality. We applied a Cell-Tak coating as a thin layer on glass slides. The Cell-Tak is a polyphenolic protein from marine mussels which can bind to the sugar coating of the human cells in order to immobilize them (https://pubmed.ncbi.nlm.nih.gov/17779975/). The stiffness of the slide is greater than the spheroid allowing us to be sure we measure the modification of stiffness of the spheroid without parasite effect of the substrate. It also allows us to place securely the spheroid avoiding its movement while measuring. We have been able to assess the effect of selenite on SKOV-3 spheroids measuring a decrease of the overall stiffness of 5,000 cell spheroids. A decrease of the spheroid stiffness is interpreted as a decrease of the interactions between the cells leading to an erosion of the spheroid structure liberating single cells which are easier to treat than aggregates and are more prone to anoïkis due to lost interactions with other cells. These types of measurements are giving us insights on what would be the effect of intraperitoneal selenium treatment and further development might lead to combined treatment with other intraperitoneal injected drugs to kill cancer cells.

Finally combining AFM and confocal we would be able to draw the relationship between cell structure, cell mechanics and functions of those parameters. It would allow us to link changes in cell stiffness following selenium treatment and the metastatic potential of ovarian cancer cells. We would also be able to draw the relation between changes in nanomechanical properties and cell death or loss of viability.

**Improving Ovarian Cancer detection**

In order to improve the detection of ovarian cancer development, we would also improve our pilot study on copper isotopes. With only 11 paired serum-biopsy we haven't been able to find any correlation between the $\delta$Cu of serum and $\delta$Cu of the tumoral biopsies. Going further would involve increasing the number of tumoral biopsy samples paired with serum. Moreover we would track copper ratio in blood over time through treatment process and assess if the copper biomarker can detect relapse of cancer. Finally on a biochemistry part it would be interesting to decipher the mechanism underlying this shift of copper isotopes which remains hypothetical.

# References


(1) Hanahan, D.; Weinberg, R. A. Hallmarks of Cancer: The Next Generation. *Cell* **2011**, *144* (5), 646–674. https://doi.org/10.1016/j.cell.2011.02.013.

(2) Fernald, K.; Kurokawa, M. Evading Apoptosis in Cancer. *Trends Cell Biol.* **2013**, *23* (12), 620–633. https://doi.org/10.1016/j.tcb.2013.07.006.

(3) Bray, F.; Ferlay, J.; Soerjomataram, I.; Siegel, R. L.; Torre, L. A.; Jemal, A. Global Cancer Statistics 2018: GLOBOCAN Estimates of Incidence and Mortality Worldwide for 36 Cancers in 185 Countries. *CA Cancer J Clin* **2018**, *68* (6), 394–424. https://doi.org/10.3322/caac.21492.

(4) Testa, U.; Petrucci, E.; Pasquini, L.; Castelli, G.; Pelosi, E. Ovarian Cancers: Genetic Abnormalities, Tumor Heterogeneity and Progression, Clonal Evolution and Cancer Stem Cells. *Medicines (Basel)* **2018**, *5* (1). https://doi.org/10.3390/medicines5010016.

(5) Gajjar, K.; Ogden, G.; Mujahid, M. I.; Razvi, K. Symptoms and Risk Factors of Ovarian Cancer: A Survey in Primary Care. *ISRN Obstet Gynecol* **2012**, *2012*, 754197. https://doi.org/10.5402/2012/754197.

(6) Matsumoto, K.; Onda, T.; Yaegashi, N. Pharmacotherapy for Recurrent Ovarian Cancer: Current Status and Future Perspectives. *Jpn. J. Clin. Oncol.* **2015**, *45* (5), 408–410. https://doi.org/10.1093/jjco/hyv014.

(7) Engelberth, S. A.; Hempel, N.; Bergkvist, M. Development of Nanoscale Approaches for Ovarian Cancer Therapeutics and Diagnostics. *Crit Rev Oncog* **2014**, *19* (3–4), 281–315. https://doi.org/10.1615/critrevoncog.2014011455.

(8) Siegel, R. L.; Miller, K. D.; Jemal, A. Cancer Statistics, 2018. *CA Cancer J Clin* **2018**, *68* (1), 7–30. https://doi.org/10.3322/caac.21442.

(9) Siegel, R. L.; Miller, K. D.; Jemal, A. Cancer Statistics, 2020. *CA: A Cancer Journal for Clinicians* **2020**, *70* (1), 7–30. https://doi.org/10.3322/caac.21590.

(10) Torre, L. A.; Trabert, B.; DeSantis, C. E.; Miller, K. D.; Samimi, G.; Runowicz, C. D.; Gaudet, M. M.; Jemal, A.; Siegel, R. L. Ovarian Cancer Statistics, 2018. *CA Cancer J Clin* **2018**, *68* (4), 284–296. https://doi.org/10.3322/caac.21456.

(11) McLemore, M. R.; Miaskowski, C.; Aouizerat, B. E.; Chen, L.-M.; Dodd, M. J. Epidemiological and Genetic Factors Associated with Ovarian Cancer. *Cancer Nurs* **2009**, *32* (4), 281–288; quiz 289–290. https://doi.org/10.1097/NCC.0b013e31819d30d6.

(12) Murdoch, W. J.; Murphy, C. J.; Van Kirk, E. A.; Shen, Y. Mechanisms and Pathobiology of Ovulation. *Soc Reprod Fertil Suppl* **2010**, *67*, 189–201. https://doi.org/10.7313/upo9781907284991.017.

(13) Richards, J. S.; Russell, D. L.; Ochsner, S.; Espey, L. L. Ovulation: New Dimensions and New Regulators of the Inflammatory-like Response. *Annu. Rev. Physiol.* **2002**, *64*, 69–92. https://doi.org/10.1146/annurev.physiol.64.081501.131029.

(14) Mehra, K.; Mehrad, M.; Ning, G.; Drapkin, R.; McKeon, F. D.; Xian, W.; Crum, C. P. STICS, SCOUTs and P53 Signatures; a New Language for Pelvic Serous Carcinogenesis. *Front Biosci (Elite Ed)* **2011**, *3*, 625–634. https://doi.org/10.2741/e275.

(15) Casagrande, J. T.; Pike, M. C.; Ross, R. K.; Louie, E. W.; Roy, S.; Henderson, B. E. "INCESSANT OVULATION" AND OVARIAN CANCER. *The Lancet* **1979**, *314* (8135), 170–173. https://doi.org/10.1016/S0140-6736(79)91435-1.

(16) Mungenast, F.; Thalhammer, T. Estrogen Biosynthesis and Action in Ovarian Cancer. *Front Endocrinol (Lausanne)* **2014**, *5*, 192. https://doi.org/10.3389/fendo.2014.00192.

(17) Salehi, F.; Dunfield, L.; Phillips, K. P.; Krewski, D.; Vanderhyden, B. C. Risk Factors for Ovarian Cancer: An Overview with Emphasis on Hormonal Factors. *J Toxicol*

*Environ Health B Crit Rev* **2008**, *11* (3–4), 301–321. https://doi.org/10.1080/10937400701876095.
(18) Siiteri, P. K. Adipose Tissue as a Source of Hormones. *Am. J. Clin. Nutr.* **1987**, *45* (1 Suppl), 277–282. https://doi.org/10.1093/ajcn/45.1.277.
(19) Sundar, S.; Neal, R. D.; Kehoe, S. Diagnosis of Ovarian Cancer. *BMJ* **2015**, *351*, h4443. https://doi.org/10.1136/bmj.h4443.
(20) Gorodetska, I.; Kozeretska, I.; Dubrovska, A. BRCA Genes: The Role in Genome Stability, Cancer Stemness and Therapy Resistance. *J Cancer* **2019**, *10* (9), 2109–2127. https://doi.org/10.7150/jca.30410.
(21) Moorman, P. G.; Havrilesky, L. J.; Gierisch, J. M.; Coeytaux, R. R.; Lowery, W. J.; Peragallo Urrutia, R.; Dinan, M.; McBroom, A. J.; Hasselblad, V.; Sanders, G. D.; Myers, E. R. Oral Contraceptives and Risk of Ovarian Cancer and Breast Cancer among High-Risk Women: A Systematic Review and Meta-Analysis. *J. Clin. Oncol.* **2013**, *31* (33), 4188–4198. https://doi.org/10.1200/JCO.2013.48.9021.
(22) Kurman, R. J.; Shih, I.-M. Seromucinous Tumors of the Ovary. What's in a Name? *Int. J. Gynecol. Pathol.* **2016**, *35* (1), 78–81. https://doi.org/10.1097/PGP.0000000000000266.
(23) Cancer Genome Atlas Research Network. Integrated Genomic Analyses of Ovarian Carcinoma. *Nature* **2011**, *474* (7353), 609–615. https://doi.org/10.1038/nature10166.
(24) Ibanez de Caceres, I.; Battagli, C.; Esteller, M.; Herman, J. G.; Dulaimi, E.; Edelson, M. I.; Bergman, C.; Ehya, H.; Eisenberg, B. L.; Cairns, P. Tumor Cell-Specific BRCA1 and RASSF1A Hypermethylation in Serum, Plasma, and Peritoneal Fluid from Ovarian Cancer Patients. *Cancer Res.* **2004**, *64* (18), 6476–6481. https://doi.org/10.1158/0008-5472.CAN-04-1529.
(25) Wei, S. H.; Balch, C.; Paik, H. H.; Kim, Y.-S.; Baldwin, R. L.; Liyanarachchi, S.; Li, L.; Wang, Z.; Wan, J. C.; Davuluri, R. V.; Karlan, B. Y.; Gifford, G.; Brown, R.; Kim, S.; Huang, T. H.-M.; Nephew, K. P. Prognostic DNA Methylation Biomarkers in Ovarian Cancer. *Clin Cancer Res* **2006**, *12* (9), 2788–2794. https://doi.org/10.1158/1078-0432.CCR-05-1551.
(26) Lengyel, E. Ovarian Cancer Development and Metastasis. *Am. J. Pathol.* **2010**, *177* (3), 1053–1064. https://doi.org/10.2353/ajpath.2010.100105.
(27) Tan, D. S.; Agarwal, R.; Kaye, S. B. Mechanisms of Transcoelomic Metastasis in Ovarian Cancer. *The Lancet Oncology* **2006**, *7* (11), 925–934. https://doi.org/10.1016/S1470-2045(06)70939-1.
(28) Burleson, K. M.; Boente, M. P.; Pambuccian, S. E.; Skubitz, A. P. N. Disaggregation and Invasion of Ovarian Carcinoma Ascites Spheroids. *J Transl Med* **2006**, *4*, 6. https://doi.org/10.1186/1479-5876-4-6.
(29) Ahmed, N.; Stenvers, K. Getting to Know Ovarian Cancer Ascites: Opportunities for Targeted Therapy-Based Translational Research. *Front. Oncol.* **2013**, *3*. https://doi.org/10.3389/fonc.2013.00256.
(30) Moffitt, L.; Karimnia, N.; Stephens, A.; Bilandzic, M. Therapeutic Targeting of Collective Invasion in Ovarian Cancer. *International Journal of Molecular Sciences* **2019**, *20* (6), 1466. https://doi.org/10.3390/ijms20061466.
(31) Patel, I. S.; Madan, P.; Getsios, S.; Bertrand, M. A.; MacCalman, C. D. Cadherin Switching in Ovarian Cancer Progression. *International Journal of Cancer* **2003**, *106* (2), 172–177. https://doi.org/10.1002/ijc.11086.
(32) Elloul, S.; Silins, I.; Tropé, C. G.; Benshushan, A.; Davidson, B.; Reich, R. Expression of E-Cadherin Transcriptional Regulators in Ovarian Carcinoma. *Virchows Arch* **2006**, *449* (5), 520–528. https://doi.org/10.1007/s00428-006-0274-6.
(33) Yeung, T.-L.; Leung, C. S.; Yip, K.-P.; Au Yeung, C. L.; Wong, S. T. C.; Mok, S. C. Cellular and Molecular Processes in Ovarian Cancer Metastasis. A Review in the

Theme: Cell and Molecular Processes in Cancer Metastasis. *Am. J. Physiol., Cell Physiol.* **2015**, *309* (7), C444-456. https://doi.org/10.1152/ajpcell.00188.2015.

(34) Sawada, K.; Mitra, A. K.; Radjabi, A. R.; Bhaskar, V.; Kistner, E. O.; Tretiakova, M.; Jagadeeswaran, S.; Montag, A.; Becker, A.; Kenny, H. A.; Peter, M. E.; Ramakrishnan, V.; Yamada, S. D.; Lengyel, E. Loss of E-Cadherin Promotes Ovarian Cancer Metastasis via Alpha 5-Integrin, Which Is a Therapeutic Target. *Cancer Res.* **2008**, *68* (7), 2329–2339. https://doi.org/10.1158/0008-5472.CAN-07-5167.

(35) Cannistra, S. A.; Kansas, G. S.; Niloff, J.; DeFranzo, B.; Kim, Y.; Ottensmeier, C. Binding of Ovarian Cancer Cells to Peritoneal Mesothelium in Vitro Is Partly Mediated by CD44H. *Cancer Res.* **1993**, *53* (16), 3830–3838.

(36) Casey, R. C.; Burleson, K. M.; Skubitz, K. M.; Pambuccian, S. E.; Oegema, T. R.; Ruff, L. E.; Skubitz, A. P. N. B1-Integrins Regulate the Formation and Adhesion of Ovarian Carcinoma Multicellular Spheroids. *The American Journal of Pathology* **2001**, *159* (6), 2071–2080. https://doi.org/10.1016/S0002-9440(10)63058-1.

(37) Arlt, M. J. E.; Novak-Hofer, I.; Gast, D.; Gschwend, V.; Moldenhauer, G.; Grünberg, J.; Honer, M.; Schubiger, P. A.; Altevogt, P.; Krüger, A. Efficient Inhibition of Intra-Peritoneal Tumor Growth and Dissemination of Human Ovarian Carcinoma Cells in Nude Mice by Anti-L1-Cell Adhesion Molecule Monoclonal Antibody Treatment. *Cancer Res.* **2006**, *66* (2), 936–943. https://doi.org/10.1158/0008-5472.CAN-05-1818.

(38) Robinson-Smith, T. M.; Isaacsohn, I.; Mercer, C. A.; Zhou, M.; Van Rooijen, N.; Husseinzadeh, N.; McFarland-Mancini, M. M.; Drew, A. F. Macrophages Mediate Inflammation-Enhanced Metastasis of Ovarian Tumors in Mice. *Cancer Res.* **2007**, *67* (12), 5708–5716. https://doi.org/10.1158/0008-5472.CAN-06-4375.

(39) Sehouli, J.; Senyuva, F.; Fotopoulou, C.; Neumann, U.; Denkert, C.; Werner, L.; Gülten, O.-O. Intra-Abdominal Tumor Dissemination Pattern and Surgical Outcome in 214 Patients with Primary Ovarian Cancer. *J Surg Oncol* **2009**, *99* (7), 424–427. https://doi.org/10.1002/jso.21288.

(40) Scotton, C. J.; Wilson, J. L.; Scott, K.; Stamp, G.; Wilbanks, G. D.; Fricker, S.; Bridger, G.; Balkwill, F. R. Multiple Actions of the Chemokine CXCL12 on Epithelial Tumor Cells in Human Ovarian Cancer. *Cancer Res* **2002**, *62* (20), 5930–5938.

(41) Xu, L.; Yoneda, J.; Herrera, C.; Wood, J.; Killion, J. J.; Fidler, I. J. Inhibition of Malignant Ascites and Growth of Human Ovarian Carcinoma by Oral Administration of a Potent Inhibitor of the Vascular Endothelial Growth Factor Receptor Tyrosine Kinases. *Int. J. Oncol.* **2000**, *16* (3), 445–454. https://doi.org/10.3892/ijo.16.3.445.

(42) Rosen, D. G.; Yang, G.; Liu, G.; Mercado-Uribe, I.; Chang, B.; Xiao, X. S.; Zheng, J.; Xue, F.-X.; Liu, J. Ovarian Cancer: Pathology, Biology, and Disease Models. *Front Biosci (Landmark Ed)* **2009**, *14*, 2089–2102. https://doi.org/10.2741/3364.

(43) Kroeger, P. T.; Drapkin, R. Pathogenesis and Heterogeneity of Ovarian Cancer. *Curr. Opin. Obstet. Gynecol.* **2017**, *29* (1), 26–34. https://doi.org/10.1097/GCO.0000000000000340.

(44) Erickson, B. K.; Conner, M. G.; Landen, C. N. The Role of the Fallopian Tube in the Origin of Ovarian Cancer. *Am J Obstet Gynecol* **2013**, *209* (5), 409–414. https://doi.org/10.1016/j.ajog.2013.04.019.

(45) Koshiyama, M.; Matsumura, N.; Konishi, I. Recent Concepts of Ovarian Carcinogenesis: Type I and Type II. *Biomed Res Int* **2014**, *2014*, 934261. https://doi.org/10.1155/2014/934261.

(46) Karst, A. M.; Drapkin, R. Ovarian Cancer Pathogenesis: A Model in Evolution https://www.hindawi.com/journals/jo/2010/932371/ (accessed Jan 24, 2020). https://doi.org/10.1155/2010/932371.

(47) Labidi-Galy, S. I.; Papp, E.; Hallberg, D.; Niknafs, N.; Adleff, V.; Noe, M.; Bhattacharya, R.; Novak, M.; Jones, S.; Phallen, J.; Hruban, C. A.; Hirsch, M. S.; Lin, D. I.; Schwartz, L.; Maire, C. L.; Tille, J.-C.; Bowden, M.; Ayhan, A.; Wood, L. D.; Scharpf, R. B.; Kurman, R.; Wang, T.-L.; Shih, I.-M.; Karchin, R.; Drapkin, R.; Velculescu, V. E. High Grade Serous Ovarian Carcinomas Originate in the Fallopian Tube. *Nat Commun* **2017**, *8* (1), 1093. https://doi.org/10.1038/s41467-017-00962-1.

(48) Kohn, E. C.; Ivy, S. P. Whence High-Grade Serous Ovarian Cancer. *Am Soc Clin Oncol Educ Book* **2017**, *37*, 443–448. https://doi.org/10.1200/EDBK_174718.

(49) Bavle, R. M. Mitosis at a Glance. *J Oral Maxillofac Pathol* **2014**, *18* (Suppl 1), S2-5. https://doi.org/10.4103/0973-029X.141175.

(50) Malpica, A.; Deavers, M. T.; Lu, K.; Bodurka, D. C.; Atkinson, E. N.; Gershenson, D. M.; Silva, E. G. Grading Ovarian Serous Carcinoma Using a Two-Tier System. *Am. J. Surg. Pathol.* **2004**, *28* (4), 496–504. https://doi.org/10.1097/00000478-200404000-00009.

(51) Mahadevappa, A.; Krishna, S. M.; Vimala, M. G. Diagnostic and Prognostic Significance of Ki-67 Immunohistochemical Expression in Surface Epithelial Ovarian Carcinoma. *J Clin Diagn Res* **2017**, *11* (2), EC08-EC12. https://doi.org/10.7860/JCDR/2017/24350.9381.

(52) Ovarian Cancers Research Guide http://resources.nationalacademies.org/Infographics/OvarianCancers/Research-Guide.html (accessed May 23, 2020).

(53) Yamaguchi, H.; Condeelis, J. Regulation of the Actin Cytoskeleton in Cancer Cell Migration and Invasion. *Biochim. Biophys. Acta* **2007**, *1773* (5), 642–652. https://doi.org/10.1016/j.bbamcr.2006.07.001.

(54) Ramos, J. R.; Pabijan, J.; Garcia, R.; Lekka, M. The Softening of Human Bladder Cancer Cells Happens at an Early Stage of the Malignancy Process. *Beilstein J. Nanotechnol.* **2014**, *5* (1), 447–457. https://doi.org/10.3762/bjnano.5.52.

(55) Cross, S. E.; Kreth, J.; Zhu, L.; Sullivan, R.; Shi, W.; Qi, F.; Gimzewski, J. K. Nanomechanical Properties of Glucans and Associated Cell-Surface Adhesion of Streptococcus Mutans Probed by Atomic Force Microscopy under in Situ Conditions. *Microbiology (Reading, Engl.)* **2007**, *153* (Pt 9), 3124–3132. https://doi.org/10.1099/mic.0.2007/007625-0.

(56) Cross, S. E.; Jin, Y.-S.; Tondre, J.; Wong, R.; Rao, J.; Gimzewski, J. K. AFM-Based Analysis of Human Metastatic Cancer Cells. *Nanotechnology* **2008**, *19* (38), 384003. https://doi.org/10.1088/0957-4484/19/38/384003.

(57) Guck, J.; Schinkinger, S.; Lincoln, B.; Wottawah, F.; Ebert, S.; Romeyke, M.; Lenz, D.; Erickson, H. M.; Ananthakrishnan, R.; Mitchell, D.; Käs, J.; Ulvick, S.; Bilby, C. Optical Deformability as an Inherent Cell Marker for Testing Malignant Transformation and Metastatic Competence. *Biophys. J.* **2005**, *88* (5), 3689–3698. https://doi.org/10.1529/biophysj.104.045476.

(58) Rebelo, L. M.; Sousa, J. S. de; Filho, J. M.; Radmacher, M. Comparison of the Viscoelastic Properties of Cells from Different Kidney Cancer Phenotypes Measured with Atomic Force Microscopy. *Nanotechnology* **2013**, *24* (5), 055102. https://doi.org/10.1088/0957-4484/24/5/055102.

(59) Levental, I.; Georges, P. C.; Janmey, P. A. Soft Biological Materials and Their Impact on Cell Function. *Soft Matter* **2007**, *3* (3), 299–306. https://doi.org/10.1039/B610522J.

(60) Krouskop, T. A.; Wheeler, T. M.; Kallel, F.; Garra, B. S.; Hall, T. Elastic Moduli of Breast and Prostate Tissues under Compression: *Ultrasonic Imaging* **2016**. https://doi.org/10.1177/016173469802000403.

(61) Paszek, M. J.; Zahir, N.; Johnson, K. R.; Lakins, J. N.; Rozenberg, G. I.; Gefen, A.; Reinhart-King, C. A.; Margulies, S. S.; Dembo, M.; Boettiger, D.; Hammer, D. A.;

Weaver, V. M. Tensional Homeostasis and the Malignant Phenotype. *Cancer Cell* **2005**, *8* (3), 241–254. https://doi.org/10.1016/j.ccr.2005.08.010.

(62) Baker, E. L.; Lu, J.; Yu, D.; Bonnecaze, R. T.; Zaman, M. H. Cancer Cell Stiffness: Integrated Roles of Three-Dimensional Matrix Stiffness and Transforming Potential. *Biophys. J.* **2010**, *99* (7), 2048–2057. https://doi.org/10.1016/j.bpj.2010.07.051.

(63) Gang, Z.; Qi, Q.; Jing, C.; Wang, C. Measuring Microenvironment Mechanical Stress of Rat Liver during Diethylnitrosamine Induced Hepatocarcinogenesis by Atomic Force Microscope. *Microsc. Res. Tech.* **2009**, *72* (9), 672–678. https://doi.org/10.1002/jemt.20716.

(64) Lekka, M.; Gil, D.; Pogoda, K.; Dulińska-Litewka, J.; Jach, R.; Gostek, J.; Klymenko, O.; Prauzner-Bechcicki, S.; Stachura, Z.; Wiltowska-Zuber, J.; Okoń, K.; Laidler, P. Cancer Cell Detection in Tissue Sections Using AFM. *Archives of Biochemistry and Biophysics* **2012**, *518* (2), 151–156. https://doi.org/10.1016/j.abb.2011.12.013.

(65) Coceano, G.; Yousafzai, M. S.; Ma, W.; Ndoye, F.; Venturelli, L.; Hussain, I.; Bonin, S.; Niemela, J.; Scoles, G.; Cojoc, D.; Ferrari, E. Investigation into Local Cell Mechanics by Atomic Force Microscopy Mapping and Optical Tweezer Vertical Indentation. *Nanotechnology* **2015**, *27* (6), 065102. https://doi.org/10.1088/0957-4484/27/6/065102.

(66) Faria, E. C.; Ma, N.; Gazi, E.; Gardner, P.; Brown, M.; Clarke, N. W.; Snook, R. D. Measurement of Elastic Properties of Prostate Cancer Cells Using AFM. *Analyst* **2008**, *133* (11), 1498–1500. https://doi.org/10.1039/b803355b.

(67) Xu, W.; Mezencev, R.; Kim, B.; Wang, L.; McDonald, J.; Sulchek, T. Cell Stiffness Is a Biomarker of the Metastatic Potential of Ovarian Cancer Cells. *PLOS ONE* **2012**, *7* (10), e46609. https://doi.org/10.1371/journal.pone.0046609.

(68) Bergfeldt, K.; Rydh, B.; Granath, F.; Grönberg, H.; Thalib, L.; Adami, H.-O.; Hall, P. Risk of Ovarian Cancer in Breast-Cancer Patients with a Family History of Breast or Ovarian Cancer: A Population-Based Cohort Study. *Lancet* **2002**, *360* (9337), 891–894. https://doi.org/10.1016/S0140-6736(02)11023-3.

(69) Scholler, N.; Urban, N. CA125 in Ovarian Cancer. *Biomark Med* **2007**, *1* (4), 513–523. https://doi.org/10.2217/17520363.1.4.513.

(70) Al-Musalhi, K.; Al-Kindi, M.; Ramadhan, F.; Al-Rawahi, T.; Al-Hatali, K.; Mula-Abed, W.-A. Validity of Cancer Antigen-125 (CA-125) and Risk of Malignancy Index (RMI) in the Diagnosis of Ovarian Cancer. *Oman Med J* **2015**, *30* (6), 428–434. https://doi.org/10.5001/omj.2015.85.

(71) Yurkovetsky, Z.; Skates, S.; Lomakin, A.; Nolen, B.; Pulsipher, T.; Modugno, F.; Marks, J.; Godwin, A.; Gorelik, E.; Jacobs, I.; Menon, U.; Lu, K.; Badgwell, D.; Bast, R. C.; Lokshin, A. E. Development of a Multimarker Assay for Early Detection of Ovarian Cancer. *J. Clin. Oncol.* **2010**, *28* (13), 2159–2166. https://doi.org/10.1200/JCO.2008.19.2484.

(72) Vaughan, S.; Coward, J. I.; Bast, R. C.; Berchuck, A.; Berek, J. S.; Brenton, J. D.; Coukos, G.; Crum, C. C.; Drapkin, R.; Etemadmoghadam, D.; Friedlander, M.; Gabra, H.; Kaye, S. B.; Lord, C. J.; Lengyel, E.; Levine, D. A.; McNeish, I. A.; Menon, U.; Mills, G. B.; Nephew, K. P.; Oza, A. M.; Sood, A. K.; Stronach, E. A.; Walczak, H.; Bowtell, D. D.; Balkwill, F. R. Rethinking Ovarian Cancer: Recommendations for Improving Outcomes. *Nat. Rev. Cancer* **2011**, *11* (10), 719–725. https://doi.org/10.1038/nrc3144.

(73) Bast, R. C. CA 125 and the Detection of Recurrent Ovarian Cancer: A Reasonably Accurate Biomarker for a Difficult Disease. *Cancer* **2010**, *116* (12), 2850–2853. https://doi.org/10.1002/cncr.25203.

(74) Mathieu, K. B.; Bedi, D. G.; Thrower, S. L.; Qayyum, A.; Bast, R. C. Screening for Ovarian Cancer: Imaging Challenges and Opportunities for Improvement. *Ultrasound Obstet Gynecol* **2018**, *51* (3), 293–303. https://doi.org/10.1002/uog.17557.
(75) Iyer, V. R.; Lee, S. I. MRI, CT, and PET/CT for Ovarian Cancer Detection and Adnexal Lesion Characterization. *AJR Am J Roentgenol* **2010**, *194* (2), 311–321. https://doi.org/10.2214/AJR.09.3522.
(76) Weber, S.; McCann, C. K.; Boruta, D. M.; Schorge, J. O.; Growdon, W. B. Laparoscopic Surgical Staging of Early Ovarian Cancer. *Rev Obstet Gynecol* **2011**, *4* (3–4), 117–122.
(77) Prat, J.; FIGO Committee on Gynecologic Oncology. Staging Classification for Cancer of the Ovary, Fallopian Tube, and Peritoneum. *Int J Gynaecol Obstet* **2014**, *124* (1), 1–5. https://doi.org/10.1016/j.ijgo.2013.10.001.
(78) Balter, V.; Nogueira da Costa, A.; Bondanese, V. P.; Jaouen, K.; Lamboux, A.; Sangrajrang, S.; Vincent, N.; Fourel, F.; Télouk, P.; Gigou, M.; Lécuyer, C.; Srivatanakul, P.; Bréchot, C.; Albarède, F.; Hainaut, P. Natural Variations of Copper and Sulfur Stable Isotopes in Blood of Hepatocellular Carcinoma Patients. *Proc. Natl. Acad. Sci. U.S.A.* **2015**, *112* (4), 982–985. https://doi.org/10.1073/pnas.1415151112.
(79) Albarède, F. Metal Stable Isotopes in the Human Body: A Tribute of Geochemistry to Medicine. *Elements* **2015**, *11* (4), 265–269. https://doi.org/10.2113/gselements.11.4.265.
(80) Chamel, G.; Gourlan, A. T.; Télouk, P.; Sayag, D.; Milliard, V.; Loiseau, C.; Simon, M.; Buff, S.; Ponce, F. Retrospective Evaluation of Blood Copper Stable Isotopes Ratio 65Cu/63Cu as a Biomarker of Cancer in Dogs. *Veterinary and Comparative Oncology* **2017**, *15* (4), 1323–1332. https://doi.org/10.1111/vco.12273.
(81) Gourlan, A. T.; Douay, G.; Telouk, P. Copper Isotopes as Possible Neoplasia Biomarkers in Captive Wild Felids. *Zoo Biology* **2019**, *38* (4), 371–383. https://doi.org/10.1002/zoo.21504.
(82) WHO | JECFA http://apps.who.int/food-additives-contaminants-jecfa-database/chemical.aspx?chemID=2824 (accessed Jan 27, 2020).
(83) Micronutrients, I. of M. (US) P. on. *Copper*; National Academies Press (US), 2001.
(84) Knutson, M. D. Steap Proteins: Implications for Iron and Copper Metabolism. *Nutr. Rev.* **2007**, *65* (7), 335–340. https://doi.org/10.1111/j.1753-4887.2007.tb00311.x.
(85) Kim, B.-E.; Nevitt, T.; Thiele, D. J. Mechanisms for Copper Acquisition, Distribution and Regulation. *Nat. Chem. Biol.* **2008**, *4* (3), 176–185. https://doi.org/10.1038/nchembio.72.
(86) Gil-Bea, F. J.; Aldanondo, G.; Lasa-Fernández, H.; Munain, A. L. de; Vallejo-Illarramendi, A. Insights into the Mechanisms of Copper Dyshomeostasis in Amyotrophic Lateral Sclerosis. *Expert Reviews in Molecular Medicine* **2017**, *19*. https://doi.org/10.1017/erm.2017.9.
(87) Turnlund, J. R. Human Whole-Body Copper Metabolism. *Am. J. Clin. Nutr.* **1998**, *67* (5 Suppl), 960S-964S. https://doi.org/10.1093/ajcn/67.5.960S.
(88) Olivares, M.; Uauy, R. Limits of Metabolic Tolerance to Copper and Biological Basis for Present Recommendations and Regulations. *Am. J. Clin. Nutr.* **1996**, *63* (5), 846S-52S. https://doi.org/10.1093/ajcn/63.5.846.
(89) Frieden, E.; Hsieh, H. S. Ceruloplasmin: The Copper Transport Protein with Essential Oxidase Activity. *Adv. Enzymol. Relat. Areas Mol. Biol.* **1976**, *44*, 187–236. https://doi.org/10.1002/9780470122891.ch6.
(90) Fox, P. L.; Mukhopadhyay, C.; Ehrenwald, E. Structure, Oxidant Activity, and Cardiovascular Mechanisms of Human Ceruloplasmin. *Life Sci.* **1995**, *56* (21), 1749–1758. https://doi.org/10.1016/0024-3205(95)00146-w.

(91) Iwata, S.; Ostermeier, C.; Ludwig, B.; Michel, H. Structure at 2.8 Å Resolution of Cytochrome c Oxidase from Paracoccus Denitrificans. *Nature* **1995**, *376* (6542), 660–669. https://doi.org/10.1038/376660a0.

(92) Albarède, F.; Télouk, P.; Balter, V. Medical Applications of Isotope Metallomics. *Reviews in Mineralogy and Geochemistry* **2017**, *82* (1), 851–885. https://doi.org/10.2138/rmg.2017.82.20.

(93) Nasulewicz, A.; Mazur, A.; Opolski, A. Role of Copper in Tumour Angiogenesis--Clinical Implications. *J Trace Elem Med Biol* **2004**, *18* (1), 1–8. https://doi.org/10.1016/j.jtemb.2004.02.004.

(94) Hordyjewska, A.; Popiołek, Ł.; Kocot, J. The Many "Faces" of Copper in Medicine and Treatment. *Biometals* **2014**, *27* (4), 611–621. https://doi.org/10.1007/s10534-014-9736-5.

(95) Babich, P. S.; Skvortsov, A. N.; Rusconi, P.; Tsymbalenko, N. V.; Mutanen, M.; Puchkova, L. V.; Broggini, M. Non-Hepatic Tumors Change the Activity of Genes Encoding Copper Trafficking Proteins in the Liver. *Cancer Biol Ther* **2013**, *14* (7), 614–624. https://doi.org/10.4161/cbt.24594.

(96) Wang, Z.; Chen, J.; Zhang, T. Cu Isotopic Composition in Surface Environments and in Biological Systems: A Critical Review. *International Journal of Environmental Research and Public Health* **2017**, *14* (5), 538. https://doi.org/10.3390/ijerph14050538.

(97) Albarède, F.; Telouk, P.; Lamboux, A.; Jaouen, K.; Balter, V. Isotopic Evidence of Unaccounted for Fe and Cu Erythropoietic Pathways. *Metallomics* **2011**, *3* (9), 926–933. https://doi.org/10.1039/C1MT00025J.

(98) Fujii, T.; Moynier, F.; Blichert-Toft, J.; Albarède, F. Density Functional Theory Estimation of Isotope Fractionation of Fe, Ni, Cu, and Zn among Species Relevant to Geochemical and Biological Environments. *Geochimica et Cosmochimica Acta* **2014**, *140*, 553–576. https://doi.org/10.1016/j.gca.2014.05.051.

(99) Iyengar, G. V. Reevaluation of the Trace Element Content in Reference Man. *Radiation Physics and Chemistry* **1998**, *51* (4), 545–560. https://doi.org/10.1016/S0969-806X(97)00202-8.

(100) Télouk, P.; Puisieux, A.; Fujii, T.; Balter, V.; Bondanese, V. P.; Morel, A.-P.; Clapisson, G.; Lamboux, A.; Albarede, F. Copper Isotope Effect in Serum of Cancer Patients. A Pilot Study. *Metallomics* **2015**, *7* (2), 299–308. https://doi.org/10.1039/c4mt00269e.

(101) Lauwens, S.; Costas-Rodríguez, M.; Van Vlierberghe, H.; Vanhaecke, F. Cu Isotopic Signature in Blood Serum of Liver Transplant Patients: A Follow-up Study. *Sci Rep* **2016**, *6*. https://doi.org/10.1038/srep30683.

(102) Bondanese, V. P.; Lamboux, A.; Simon, M.; Lafont, J. E.; Albalat, E.; Pichat, S.; Vanacker, J.-M.; Telouk, P.; Balter, V.; Oger, P.; Albarède, F. Hypoxia Induces Copper Stable Isotope Fractionation in Hepatocellular Carcinoma, in a HIF-Independent Manner. *Metallomics* **2016**, *8* (11), 1177–1184. https://doi.org/10.1039/c6mt00102e.

(103) Doubeni, C. A.; Doubeni, A. R.; Myers, A. E. Diagnosis and Management of Ovarian Cancer. *Am Fam Physician* **2016**, *93* (11), 937–944.

(104) Armstrong, D. K.; Bundy, B.; Wenzel, L.; Huang, H. Q.; Baergen, R.; Lele, S.; Copeland, L. J.; Walker, J. L.; Burger, R. A.; Gynecologic Oncology Group. Intraperitoneal Cisplatin and Paclitaxel in Ovarian Cancer. *N. Engl. J. Med.* **2006**, *354* (1), 34–43. https://doi.org/10.1056/NEJMoa052985.

(105) Raja, F. A.; Chopra, N.; Ledermann, J. A. Optimal First-Line Treatment in Ovarian Cancer. *Ann. Oncol.* **2012**, *23 Suppl 10*, x118-127. https://doi.org/10.1093/annonc/mds315.

(106) Orr, B.; Edwards, R. P. Diagnosis and Treatment of Ovarian Cancer. *Hematol. Oncol. Clin. North Am.* **2018**, *32* (6), 943–964. https://doi.org/10.1016/j.hoc.2018.07.010.
(107) Pignata, S.; Scambia, G.; Ferrandina, G.; Savarese, A.; Sorio, R.; Breda, E.; Gebbia, V.; Musso, P.; Frigerio, L.; Del Medico, P.; Lombardi, A. V.; Febbraro, A.; Scollo, P.; Ferro, A.; Tamberi, S.; Brandes, A.; Ravaioli, A.; Valerio, M. R.; Aitini, E.; Natale, D.; Scaltriti, L.; Greggi, S.; Pisano, C.; Lorusso, D.; Salutari, V.; Legge, F.; Di Maio, M.; Morabito, A.; Gallo, C.; Perrone, F. Carboplatin plus Paclitaxel versus Carboplatin plus Pegylated Liposomal Doxorubicin as First-Line Treatment for Patients with Ovarian Cancer: The MITO-2 Randomized Phase III Trial. *J. Clin. Oncol.* **2011**, *29* (27), 3628–3635. https://doi.org/10.1200/JCO.2010.33.8566.
(108) Salani, R.; Backes, F. J.; Fung, M. F. K.; Holschneider, C. H.; Parker, L. P.; Bristow, R. E.; Goff, B. A. Posttreatment Surveillance and Diagnosis of Recurrence in Women with Gynecologic Malignancies: Society of Gynecologic Oncologists Recommendations. *Am. J. Obstet. Gynecol.* **2011**, *204* (6), 466–478. https://doi.org/10.1016/j.ajog.2011.03.008.
(109) Mantia-Smaldone, G. M.; Edwards, R. P.; Vlad, A. M. Targeted Treatment of Recurrent Platinum-Resistant Ovarian Cancer: Current and Emerging Therapies. *Cancer Manag Res* **2011**, *3*, 25–38. https://doi.org/10.2147/CMR.S8759.
(110) Raja, F. A.; Counsell, N.; Colombo, N.; Pfisterer, J.; du Bois, A.; Parmar, M. K.; Vergote, I. B.; Gonzalez-Martin, A.; Alberts, D. S.; Plante, M.; Torri, V.; Ledermann, J. A. Platinum versus Platinum-Combination Chemotherapy in Platinum-Sensitive Recurrent Ovarian Cancer: A Meta-Analysis Using Individual Patient Data. *Ann. Oncol.* **2013**, *24* (12), 3028–3034. https://doi.org/10.1093/annonc/mdt406.
(111) Pfisterer, J.; Plante, M.; Vergote, I.; du Bois, A.; Hirte, H.; Lacave, A. J.; Wagner, U.; Stähle, A.; Stuart, G.; Kimmig, R.; Olbricht, S.; Le, T.; Emerich, J.; Kuhn, W.; Bentley, J.; Jackisch, C.; Lück, H.-J.; Rochon, J.; Zimmermann, A. H.; Eisenhauer, E.; AGO-OVAR; NCIC CTG; EORTC GCG. Gemcitabine plus Carboplatin Compared with Carboplatin in Patients with Platinum-Sensitive Recurrent Ovarian Cancer: An Intergroup Trial of the AGO-OVAR, the NCIC CTG, and the EORTC GCG. *J. Clin. Oncol.* **2006**, *24* (29), 4699–4707. https://doi.org/10.1200/JCO.2006.06.0913.
(112) Patch, A.-M.; Christie, E. L.; Etemadmoghadam, D.; Garsed, D. W.; George, J.; Fereday, S.; Nones, K.; Cowin, P.; Alsop, K.; Bailey, P. J.; Kassahn, K. S.; Newell, F.; Quinn, M. C. J.; Kazakoff, S.; Quek, K.; Wilhelm-Benartzi, C.; Curry, E.; Leong, H. S.; Australian Ovarian Cancer Study Group; Hamilton, A.; Mileshkin, L.; Au-Yeung, G.; Kennedy, C.; Hung, J.; Chiew, Y.-E.; Harnett, P.; Friedlander, M.; Quinn, M.; Pyman, J.; Cordner, S.; O'Brien, P.; Leditschke, J.; Young, G.; Strachan, K.; Waring, P.; Azar, W.; Mitchell, C.; Traficante, N.; Hendley, J.; Thorne, H.; Shackleton, M.; Miller, D. K.; Arnau, G. M.; Tothill, R. W.; Holloway, T. P.; Semple, T.; Harliwong, I.; Nourse, C.; Nourbakhsh, E.; Manning, S.; Idrisoglu, S.; Bruxner, T. J. C.; Christ, A. N.; Poudel, B.; Holmes, O.; Anderson, M.; Leonard, C.; Lonie, A.; Hall, N.; Wood, S.; Taylor, D. F.; Xu, Q.; Fink, J. L.; Waddell, N.; Drapkin, R.; Stronach, E.; Gabra, H.; Brown, R.; Jewell, A.; Nagaraj, S. H.; Markham, E.; Wilson, P. J.; Ellul, J.; McNally, O.; Doyle, M. A.; Vedururu, R.; Stewart, C.; Lengyel, E.; Pearson, J. V.; Waddell, N.; deFazio, A.; Grimmond, S. M.; Bowtell, D. D. L. Whole-Genome Characterization of Chemoresistant Ovarian Cancer. *Nature* **2015**, *521* (7553), 489–494. https://doi.org/10.1038/nature14410.
(113) Norquist, B.; Wurz, K. A.; Pennil, C. C.; Garcia, R.; Gross, J.; Sakai, W.; Karlan, B. Y.; Taniguchi, T.; Swisher, E. M. Secondary Somatic Mutations Restoring BRCA1/2 Predict Chemotherapy Resistance in Hereditary Ovarian Carcinomas. *J. Clin. Oncol.* **2011**, *29* (22), 3008–3015. https://doi.org/10.1200/JCO.2010.34.2980.

(114) Kayl, A. E.; Meyers, C. A. Side-Effects of Chemotherapy and Quality of Life in Ovarian and Breast Cancer Patients. *Curr. Opin. Obstet. Gynecol.* **2006**, *18* (1), 24–28. https://doi.org/10.1097/01.gco.0000192996.20040.24.

(115) Coleman, R. L.; Sill, M. W.; Bell-McGuinn, K.; Aghajanian, C.; Gray, H. J.; Tewari, K. S.; Rubin, S. C.; Rutherford, T. J.; Chan, J. K.; Chen, A.; Swisher, E. M. A Phase II Evaluation of the Potent, Highly Selective PARP Inhibitor Veliparib in the Treatment of Persistent or Recurrent Epithelial Ovarian, Fallopian Tube, or Primary Peritoneal Cancer in Patients Who Carry a Germline BRCA1 or BRCA2 Mutation - An NRG Oncology/Gynecologic Oncology Group Study. *Gynecol. Oncol.* **2015**, *137* (3), 386–391. https://doi.org/10.1016/j.ygyno.2015.03.042.

(116) Drew, Y. The Development of PARP Inhibitors in Ovarian Cancer: From Bench to Bedside. *Br. J. Cancer* **2015**, *113 Suppl 1*, S3-9. https://doi.org/10.1038/bjc.2015.394.

(117) Mirza, M. R.; Monk, B. J.; Herrstedt, J.; Oza, A. M.; Mahner, S.; Redondo, A.; Fabbro, M.; Ledermann, J. A.; Lorusso, D.; Vergote, I.; Ben-Baruch, N. E.; Marth, C.; Mądry, R.; Christensen, R. D.; Berek, J. S.; Dørum, A.; Tinker, A. V.; du Bois, A.; González-Martín, A.; Follana, P.; Benigno, B.; Rosenberg, P.; Gilbert, L.; Rimel, B. J.; Buscema, J.; Balser, J. P.; Agarwal, S.; Matulonis, U. A.; ENGOT-OV16/NOVA Investigators. Niraparib Maintenance Therapy in Platinum-Sensitive, Recurrent Ovarian Cancer. *N. Engl. J. Med.* **2016**, *375* (22), 2154–2164. https://doi.org/10.1056/NEJMoa1611310.

(118) Kalli, K. R.; Oberg, A. L.; Keeney, G. L.; Christianson, T. J. H.; Low, P. S.; Knutson, K. L.; Hartmann, L. C. Folate Receptor Alpha as a Tumor Target in Epithelial Ovarian Cancer. *Gynecol. Oncol.* **2008**, *108* (3), 619–626. https://doi.org/10.1016/j.ygyno.2007.11.020.

(119) Elnakat, H.; Ratnam, M. Role of Folate Receptor Genes in Reproduction and Related Cancers. *Front. Biosci.* **2006**, *11*, 506–519. https://doi.org/10.2741/1815.

(120) Luo, H.; Xu, X.; Ye, M.; Sheng, B.; Zhu, X. The Prognostic Value of HER2 in Ovarian Cancer: A Meta-Analysis of Observational Studies. *PLoS One* **2018**, *13* (1). https://doi.org/10.1371/journal.pone.0191972.

(121) Guastalla, J. P.; Allouache, D.; Combe, M.; Weber, B.; Cretin, J.; Curé, H.; Mousseau, M.; Paraiso, D.; Camilleri-Broët, S.; Pujade-Lauraine, E. HER2 Overexpression and Amplification in Advanced Ovarian Cancer (AOC): Treatment with Trastuzumab—A GINECO Study. *JCO* **2007**, *25* (18_suppl), 5559–5559. https://doi.org/10.1200/jco.2007.25.18_suppl.5559.

(122) Conklin, K. A. Chemotherapy-Associated Oxidative Stress: Impact on Chemotherapeutic Effectiveness. *Integr Cancer Ther* **2004**, *3* (4), 294–300. https://doi.org/10.1177/1534735404270335.

(123) Stylianopoulos, T.; Jain, R. K. Combining Two Strategies to Improve Perfusion and Drug Delivery in Solid Tumors. *PNAS* **2013**, *110* (46), 18632–18637. https://doi.org/10.1073/pnas.1318415110.

(124) Ashikbayeva, Z.; Tosi, D.; Balmassov, D.; Schena, E.; Saccomandi, P.; Inglezakis, V. Application of Nanoparticles and Nanomaterials in Thermal Ablation Therapy of Cancer. *Nanomaterials (Basel)* **2019**, *9* (9). https://doi.org/10.3390/nano9091195.

(125) Decuzzi, P.; Pasqualini, R.; Arap, W.; Ferrari, M. Intravascular Delivery of Particulate Systems: Does Geometry Really Matter? *Pharm. Res.* **2009**, *26* (1), 235–243. https://doi.org/10.1007/s11095-008-9697-x.

(126) Gupta, S.; Pathak, Y.; Gupta, M. K.; Vyas, S. P. Nanoscale Drug Delivery Strategies for Therapy of Ovarian Cancer: Conventional vs Targeted. *Artificial Cells, Nanomedicine, and Biotechnology* **2019**, *47* (1), 4066–4088. https://doi.org/10.1080/21691401.2019.1677680.

(127) Nowotnik, D. P.; Cvitkovic, E. ProLindac$^{TM}$ (AP5346): A Review of the Development of an HPMA DACH Platinum Polymer Therapeutic. *Advanced Drug Delivery Reviews* **2009**, *61* (13), 1214–1219. https://doi.org/10.1016/j.addr.2009.06.004.

(128) Slingerland, M.; Guchelaar, H.-J.; Rosing, H.; Scheulen, M. E.; van Warmerdam, L. J. C.; Beijnen, J. H.; Gelderblom, H. Bioequivalence of Liposome-Entrapped Paclitaxel Easy-To-Use (LEP-ETU) Formulation and Paclitaxel in Polyethoxylated Castor Oil: A Randomized, Two-Period Crossover Study in Patients with Advanced Cancer. *Clin Ther* **2013**, *35* (12), 1946–1954. https://doi.org/10.1016/j.clinthera.2013.10.009.

(129) Park, J. W.; Kirpotin, D. B.; Hong, K.; Shalaby, R.; Shao, Y.; Nielsen, U. B.; Marks, J. D.; Papahadjopoulos, D.; Benz, C. C. Tumor Targeting Using Anti-Her2 Immunoliposomes. *J Control Release* **2001**, *74* (1–3), 95–113. https://doi.org/10.1016/s0168-3659(01)00315-7.

(130) McDonagh, C. F.; Huhalov, A.; Harms, B. D.; Adams, S.; Paragas, V.; Oyama, S.; Zhang, B.; Luus, L.; Overland, R.; Nguyen, S.; Gu, J.; Kohli, N.; Wallace, M.; Feldhaus, M. J.; Kudla, A. J.; Schoeberl, B.; Nielsen, U. B. Antitumor Activity of a Novel Bispecific Antibody That Targets the ErbB2/ErbB3 Oncogenic Unit and Inhibits Heregulin-Induced Activation of ErbB3. *Mol. Cancer Ther.* **2012**, *11* (3), 582–593. https://doi.org/10.1158/1535-7163.MCT-11-0820.

(131) Suzuki, R.; Takizawa, T.; Kuwata, Y.; Mutoh, M.; Ishiguro, N.; Utoguchi, N.; Shinohara, A.; Eriguchi, M.; Yanagie, H.; Maruyama, K. Effective Anti-Tumor Activity of Oxaliplatin Encapsulated in Transferrin-PEG-Liposome. *Int J Pharm* **2008**, *346* (1–2), 143–150. https://doi.org/10.1016/j.ijpharm.2007.06.010.

(132) Derakhshandeh, K.; Fathi, S. Role of Chitosan Nanoparticles in the Oral Absorption of Gemcitabine. *Int J Pharm* **2012**, *437* (1–2), 172–177. https://doi.org/10.1016/j.ijpharm.2012.08.008.

(133) Mohammed, M. A.; Syeda, J. T. M.; Wasan, K. M.; Wasan, E. K. An Overview of Chitosan Nanoparticles and Its Application in Non-Parenteral Drug Delivery. *Pharmaceutics* **2017**, *9* (4). https://doi.org/10.3390/pharmaceutics9040053.

(134) Ross, R. W.; Zietman, A. L.; Xie, W.; Coen, J. J.; Dahl, D. M.; Shipley, W. U.; Kaufman, D. S.; Islam, T.; Guimaraes, A. R.; Weissleder, R.; Harisinghani, M. Lymphotropic Nanoparticle-Enhanced Magnetic Resonance Imaging (LNMRI) Identifies Occult Lymph Node Metastases in Prostate Cancer Patients Prior to Salvage Radiation Therapy. *Clin Imaging* **2009**, *33* (4), 301–305. https://doi.org/10.1016/j.clinimag.2009.01.013.

(135) Rivera Gil, P.; Hühn, D.; del Mercato, L. L.; Sasse, D.; Parak, W. J. Nanopharmacy: Inorganic Nanoscale Devices as Vectors and Active Compounds. *Pharmacol. Res.* **2010**, *62* (2), 115–125. https://doi.org/10.1016/j.phrs.2010.01.009.

(136) Libutti, S. K.; Paciotti, G. F.; Byrnes, A. A.; Alexander, H. R.; Gannon, W. E.; Walker, M.; Seidel, G. D.; Yuldasheva, N.; Tamarkin, L. Phase I and Pharmacokinetic Studies of CYT-6091, a Novel PEGylated Colloidal Gold-RhTNF Nanomedicine. *Clin. Cancer Res.* **2010**, *16* (24), 6139–6149. https://doi.org/10.1158/1078-0432.CCR-10-0978.

(137) Allis, C. D.; Jenuwein, T. The Molecular Hallmarks of Epigenetic Control. *Nature Reviews Genetics* **2016**, *17* (8), 487–500. https://doi.org/10.1038/nrg.2016.59.

(138) Biswas, S.; Rao, C. M. Epigenetics in Cancer: Fundamentals and Beyond. *Pharmacology & Therapeutics* **2017**, *173*, 118–134. https://doi.org/10.1016/j.pharmthera.2017.02.011.

(139) Kornberg, R. D. Chromatin Structure: A Repeating Unit of Histones and DNA. *Science* **1974**, *184* (4139), 868–871. https://doi.org/10.1126/science.184.4139.868.

(140) Luger, K.; Mäder, A. W.; Richmond, R. K.; Sargent, D. F.; Richmond, T. J. Crystal Structure of the Nucleosome Core Particle at 2.8 A Resolution. *Nature* **1997**, *389* (6648), 251–260. https://doi.org/10.1038/38444.

(141) Henikoff, S.; Smith, M. M. Histone Variants and Epigenetics. *Cold Spring Harb Perspect Biol* **2015**, *7* (1), a019364. https://doi.org/10.1101/cshperspect.a019364.

(142) Rothbart, S. B.; Strahl, B. D. Interpreting the Language of Histone and DNA Modifications. *Biochim. Biophys. Acta* **2014**, *1839* (8), 627–643. https://doi.org/10.1016/j.bbagrm.2014.03.001.

(143) Rice, J. C.; Briggs, S. D.; Ueberheide, B.; Barber, C. M.; Shabanowitz, J.; Hunt, D. F.; Shinkai, Y.; Allis, C. D. Histone Methyltransferases Direct Different Degrees of Methylation to Define Distinct Chromatin Domains. *Mol. Cell* **2003**, *12* (6), 1591–1598. https://doi.org/10.1016/s1097-2765(03)00479-9.

(144) Scheer, S.; Ackloo, S.; Medina, T. S.; Schapira, M.; Li, F.; Ward, J. A.; Lewis, A. M.; Northrop, J. P.; Richardson, P. L.; Kaniskan, H. Ü.; Shen, Y.; Liu, J.; Smil, D.; McLeod, D.; Zepeda-Velazquez, C. A.; Luo, M.; Jin, J.; Barsyte-Lovejoy, D.; Huber, K. V. M.; De Carvalho, D. D.; Vedadi, M.; Zaph, C.; Brown, P. J.; Arrowsmith, C. H. A Chemical Biology Toolbox to Study Protein Methyltransferases and Epigenetic Signaling. *Nature Communications* **2019**, *10* (1), 1–14. https://doi.org/10.1038/s41467-018-07905-4.

(145) Spellmon, N.; Holcomb, J.; Trescott, L.; Sirinupong, N.; Yang, Z. Structure and Function of SET and MYND Domain-Containing Proteins. *Int J Mol Sci* **2015**, *16* (1), 1406–1428. https://doi.org/10.3390/ijms16011406.

(146) Marchesi, I.; Bagella, L. Role of Enhancer of Zeste Homolog 2 Polycomb Protein and Its Significance in Tumor Progression and Cell Differentiation. *Chromatin Remodelling* **2013**. https://doi.org/10.5772/55370.

(147) Chen, K.; Chen, Z.; Wu, D.; Zhang, L.; Lin, X.; Su, J.; Rodriguez, B.; Xi, Y.; Xia, Z.; Chen, X.; Shi, X.; Wang, Q.; Li, W. Broad H3K4me3 Is Associated with Increased Transcription Elongation and Enhancer Activity at Tumor-Suppressor Genes. *Nat. Genet.* **2015**, *47* (10), 1149–1157. https://doi.org/10.1038/ng.3385.

(148) Ng, H. H.; Robert, F.; Young, R. A.; Struhl, K. Targeted Recruitment of Set1 Histone Methylase by Elongating Pol II Provides a Localized Mark and Memory of Recent Transcriptional Activity. *Mol. Cell* **2003**, *11* (3), 709–719. https://doi.org/10.1016/s1097-2765(03)00092-3.

(149) Li, S.; Shen, L.; Chen, K. Association between H3K4 Methylation and Cancer Prognosis: A Meta-analysis. *Thorac Cancer* **2018**, *9* (7), 794–799. https://doi.org/10.1111/1759-7714.12647.

(150) Seligson, D. B.; Horvath, S.; McBrian, M. A.; Mah, V.; Yu, H.; Tze, S.; Wang, Q.; Chia, D.; Goodglick, L.; Kurdistani, S. K. Global Levels of Histone Modifications Predict Prognosis in Different Cancers. *Am J Pathol* **2009**, *174* (5), 1619–1628. https://doi.org/10.2353/ajpath.2009.080874.

(151) Liu, B.; Cheng, J.; Zhang, X.; Wang, R.; Zhang, W.; Lin, H.; Xiao, X.; Cai, S.; Chen, X.; Cheng, H. Global Histone Modification Patterns as Prognostic Markers to Classify Glioma Patients. *Cancer Epidemiol. Biomarkers Prev.* **2010**, *19* (11), 2888–2896. https://doi.org/10.1158/1055-9965.EPI-10-0454.

(152) Shilatifard, A. The COMPASS Family of Histone H3K4 Methylases: Mechanisms of Regulation in Development and Disease Pathogenesis. *Annu. Rev. Biochem.* **2012**, *81* (1), 65–95. https://doi.org/10.1146/annurev-biochem-051710-134100.

(153) Fog, C. K.; Galli, G. G.; Lund, A. H. PRDM Proteins: Important Players in Differentiation and Disease. *BioEssays* **2012**, *34* (1), 50–60. https://doi.org/10.1002/bies.201100107.

(154) Di Zazzo, E.; De Rosa, C.; Abbondanza, C.; Moncharmont, B. PRDM Proteins: Molecular Mechanisms in Signal Transduction and Transcriptional Regulation. *Biology (Basel)* **2013**, *2* (1), 107–141. https://doi.org/10.3390/biology2010107.
(155) Lyu, T.; Jiang, Y.; Jia, N.; Che, X.; Li, Q.; Yu, Y.; Hua, K.; Bast, R. C.; Feng, W. SMYD3 Promotes Implant Metastasis of Ovarian Cancer via H3K4 Trimethylation of Integrin Promoters. *International Journal of Cancer* **2020**, *146* (6), 1553–1567. https://doi.org/10.1002/ijc.32673.
(156) McCabe, M. T.; Creasy, C. L. EZH2 as a Potential Target in Cancer Therapy. *Epigenomics* **2014**, *6* (3), 341–351. https://doi.org/10.2217/epi.14.23.
(157) Czermin, B.; Melfi, R.; McCabe, D.; Seitz, V.; Imhof, A.; Pirrotta, V. Drosophila Enhancer of Zeste/ESC Complexes Have a Histone H3 Methyltransferase Activity That Marks Chromosomal Polycomb Sites. *Cell* **2002**, *111* (2), 185–196. https://doi.org/10.1016/s0092-8674(02)00975-3.
(158) Müller, J.; Hart, C. M.; Francis, N. J.; Vargas, M. L.; Sengupta, A.; Wild, B.; Miller, E. L.; O'Connor, M. B.; Kingston, R. E.; Simon, J. A. Histone Methyltransferase Activity of a Drosophila Polycomb Group Repressor Complex. *Cell* **2002**, *111* (2), 197–208. https://doi.org/10.1016/s0092-8674(02)00976-5.
(159) Varambally, S.; Dhanasekaran, S. M.; Zhou, M.; Barrette, T. R.; Kumar-Sinha, C.; Sanda, M. G.; Ghosh, D.; Pienta, K. J.; Sewalt, R. G. A. B.; Otte, A. P.; Rubin, M. A.; Chinnaiyan, A. M. The Polycomb Group Protein EZH2 Is Involved in Progression of Prostate Cancer. *Nature* **2002**, *419* (6907), 624–629. https://doi.org/10.1038/nature01075.
(160) He, L.-R.; Liu, M.-Z.; Li, B.-K.; Jia, W.-H.; Zhang, Y.; Liao, Y.-J.; Chen, Y.-C.; Zhang, L.-J.; Guan, X.-Y.; Zeng, Y.-X.; Kung, H.-F.; Xie, D. High Expression of EZH2 Is Associated with Tumor Aggressiveness and Poor Prognosis in Patients with Esophageal Squamous Cell Carcinoma Treated with Definitive Chemoradiotherapy. *Int. J. Cancer* **2010**, *127* (1), 138–147. https://doi.org/10.1002/ijc.25031.
(161) Kleer, C. G.; Cao, Q.; Varambally, S.; Shen, R.; Ota, I.; Tomlins, S. A.; Ghosh, D.; Sewalt, R. G. A. B.; Otte, A. P.; Hayes, D. F.; Sabel, M. S.; Livant, D.; Weiss, S. J.; Rubin, M. A.; Chinnaiyan, A. M. EZH2 Is a Marker of Aggressive Breast Cancer and Promotes Neoplastic Transformation of Breast Epithelial Cells. *Proc. Natl. Acad. Sci. U.S.A.* **2003**, *100* (20), 11606–11611. https://doi.org/10.1073/pnas.1933744100.
(162) Cardenas, H.; Zhao, J.; Vieth, E.; Nephew, K. P.; Matei, D. EZH2 Inhibition Promotes Epithelial-to-Mesenchymal Transition in Ovarian Cancer Cells. *Oncotarget* **2016**, *7* (51), 84453–84467. https://doi.org/10.18632/oncotarget.11497.
(163) Campbell, S.; Ismail, I. H.; Young, L. C.; Poirier, G. G.; Hendzel, M. J. Polycomb Repressive Complex 2 Contributes to DNA Double-Strand Break Repair. *Cell Cycle* **2013**, *12* (16), 2675–2683. https://doi.org/10.4161/cc.25795.
(164) O'Hagan, H. M.; Mohammad, H. P.; Baylin, S. B. Double Strand Breaks Can Initiate Gene Silencing and SIRT1-Dependent Onset of DNA Methylation in an Exogenous Promoter CpG Island. *PLOS Genetics* **2008**, *4* (8), e1000155. https://doi.org/10.1371/journal.pgen.1000155.
(165) Chou, D. M.; Adamson, B.; Dephoure, N. E.; Tan, X.; Nottke, A. C.; Hurov, K. E.; Gygi, S. P.; Colaiácovo, M. P.; Elledge, S. J. A Chromatin Localization Screen Reveals Poly (ADP Ribose)-Regulated Recruitment of the Repressive Polycomb and NuRD Complexes to Sites of DNA Damage. *PNAS* **2010**, *107* (43), 18475–18480. https://doi.org/10.1073/pnas.1012946107.
(166) Cheng, M.-F.; Lee, C.-H.; Hsia, K.-T.; Huang, G.-S.; Lee, H.-S. Methylation of Histone H3 Lysine 27 Associated with Apoptosis in Osteosarcoma Cells Induced by Staurosporine. *Histol. Histopathol.* **2009**, *24* (9), 1105–1111. https://doi.org/10.14670/HH-24.1105.

(167) Gong, F.; Miller, K. M. Histone Methylation and the DNA Damage Response. *Mutation Research/Reviews in Mutation Research* **2019**, *780*, 37–47. https://doi.org/10.1016/j.mrrev.2017.09.003.
(168) Shi, Y.; Whetstine, J. R. Dynamic Regulation of Histone Lysine Methylation by Demethylases. *Mol. Cell* **2007**, *25* (1), 1–14. https://doi.org/10.1016/j.molcel.2006.12.010.
(169) Barski, A.; Cuddapah, S.; Cui, K.; Roh, T.-Y.; Schones, D. E.; Wang, Z.; Wei, G.; Chepelev, I.; Zhao, K. High-Resolution Profiling of Histone Methylations in the Human Genome. *Cell* **2007**, *129* (4), 823–837. https://doi.org/10.1016/j.cell.2007.05.009.
(170) Rosenfeld, J. A.; Wang, Z.; Schones, D. E.; Zhao, K.; DeSalle, R.; Zhang, M. Q. Determination of Enriched Histone Modifications in Non-Genic Portions of the Human Genome. *BMC Genomics* **2009**, *10*, 143. https://doi.org/10.1186/1471-2164-10-143.
(171) Guelen, L.; Pagie, L.; Brasset, E.; Meuleman, W.; Faza, M. B.; Talhout, W.; Eussen, B. H.; de Klein, A.; Wessels, L.; de Laat, W.; van Steensel, B. Domain Organization of Human Chromosomes Revealed by Mapping of Nuclear Lamina Interactions. *Nature* **2008**, *453* (7197), 948–951. https://doi.org/10.1038/nature06947.
(172) Wei, L.; Chiu, D. K.-C.; Tsang, F. H.-C.; Law, C.-T.; Cheng, C. L.-H.; Au, S. L.-K.; Lee, J. M.-F.; Wong, C. C.-L.; Ng, I. O.-L.; Wong, C.-M. Histone Methyltransferase G9a Promotes Liver Cancer Development by Epigenetic Silencing of Tumor Suppressor Gene RARRES3. *Journal of Hepatology* **2017**, *67* (4), 758–769. https://doi.org/10.1016/j.jhep.2017.05.015.
(173) Zhang, J.; Wang, Y.; Shen, Y.; He, P.; Ding, J.; Chen, Y. G9a Stimulates CRC Growth by Inducing P53 Lys373 Dimethylation-Dependent Activation of Plk1. *Theranostics* **2018**, *8* (10), 2884–2895. https://doi.org/10.7150/thno.23824.
(174) Wang, Y.-F.; Zhang, J.; Su, Y.; Shen, Y.-Y.; Jiang, D.-X.; Hou, Y.-Y.; Geng, M.-Y.; Ding, J.; Chen, Y. G9a Regulates Breast Cancer Growth by Modulating Iron Homeostasis through the Repression of Ferroxidase Hephaestin. *Nat Commun* **2017**, *8* (1), 274. https://doi.org/10.1038/s41467-017-00350-9.
(175) Shankar, S. R.; Bahirvani, A. G.; Rao, V. K.; Bharathy, N.; Ow, J. R.; Taneja, R. G9a, a Multipotent Regulator of Gene Expression. *Epigenetics* **2013**, *8* (1), 16–22. https://doi.org/10.4161/epi.23331.
(176) Kondo, Y.; Shen, L.; Ahmed, S.; Boumber, Y.; Sekido, Y.; Haddad, B. R.; Issa, J.-P. J. Downregulation of Histone H3 Lysine 9 Methyltransferase G9a Induces Centrosome Disruption and Chromosome Instability in Cancer Cells. *PLoS ONE* **2008**, *3* (4), e2037. https://doi.org/10.1371/journal.pone.0002037.
(177) Gaspar-Maia, A.; Alajem, A.; Meshorer, E.; Ramalho-Santos, M. Open Chromatin in Pluripotency and Reprogramming. *Nat Rev Mol Cell Biol* **2011**, *12* (1), 36–47. https://doi.org/10.1038/nrm3036.
(178) Steffensen, K. D.; Alvero, A. B.; Yang, Y.; Waldstrøm, M.; Hui, P.; Holmberg, J. C.; Silasi, D.-A.; Jakobsen, A.; Rutherford, T.; Mor, G. Prevalence of Epithelial Ovarian Cancer Stem Cells Correlates with Recurrence in Early-Stage Ovarian Cancer. *J Oncol* **2011**, *2011*. https://doi.org/10.1155/2011/620523.
(179) Chapman-Rothe, N.; Curry, E.; Zeller, C.; Liber, D.; Stronach, E.; Gabra, H.; Ghaem-Maghami, S.; Brown, R. Chromatin H3K27me3/H3K4me3 Histone Marks Define Gene Sets in High-Grade Serous Ovarian Cancer That Distinguish Malignant, Tumour-Sustaining and Chemo-Resistant Ovarian Tumour Cells. *Oncogene* **2013**, *32* (38), 4586–4592. https://doi.org/10.1038/onc.2012.477.
(180) Bernstein, B. E.; Mikkelsen, T. S.; Xie, X.; Kamal, M.; Huebert, D. J.; Cuff, J.; Fry, B.; Meissner, A.; Wernig, M.; Plath, K.; Jaenisch, R.; Wagschal, A.; Feil, R.;

Schreiber, S. L.; Lander, E. S. A Bivalent Chromatin Structure Marks Key Developmental Genes in Embryonic Stem Cells. *Cell* **2006**, *125* (2), 315–326. https://doi.org/10.1016/j.cell.2006.02.041.

(181) Jiang, Y.; Lyu, T.; Che, X.; Jia, N.; Li, Q.; Feng, W. Overexpression of SMYD3 in Ovarian Cancer Is Associated with Ovarian Cancer Proliferation and Apoptosis via Methylating H3K4 and H4K20. *J Cancer* **2019**, *10* (17), 4072–4084. https://doi.org/10.7150/jca.29861.

(182) Wei, S.; Li, C.; Yin, Z.; Wen, J.; Meng, H.; Xue, L.; Wang, J. Histone Methylation in DNA Repair and Clinical Practice: New Findings during the Past 5-Years. *J Cancer* **2018**, *9* (12), 2072–2081. https://doi.org/10.7150/jca.23427.

(183) He, W. P.; Li, Q.; Zhou, J.; H, Z. S.; Kung, H. F.; Guan, X. Y.; Xie, D.; Yang, G. F. Decreased Expression of H3K27me3 in Human Ovarian Carcinomas Correlates with More Aggressive Tumor Behavior and Poor Patient Survival. *Neoplasma* **2015**, *62* (6), 932–937. https://doi.org/10.4149/neo_2015_113.

(184) Tang, G.; Guo, J.; Zhu, Y.; Huang, Z.; Liu, T.; Cai, J.; Yu, L.; Wang, Z. Metformin Inhibits Ovarian Cancer via Decreasing H3K27 Trimethylation. *International Journal of Oncology* **2018**, *52* (6), 1899–1911. https://doi.org/10.3892/ijo.2018.4343.

(185) Hua, K.-T.; Wang, M.-Y.; Chen, M.-W.; Wei, L.-H.; Chen, C.-K.; Ko, C.-H.; Jeng, Y.-M.; Sung, P.-L.; Jan, Y.-H.; Hsiao, M.; Kuo, M.-L.; Yen, M.-L. The H3K9 Methyltransferase G9a Is a Marker of Aggressive Ovarian Cancer That Promotes Peritoneal Metastasis. *Mol Cancer* **2014**, *13*. https://doi.org/10.1186/1476-4598-13-189.

(186) Rayman, M. P.; Infante, H. G.; Sargent, M. Food-Chain Selenium and Human Health: Spotlight on Speciation. *Br. J. Nutr.* **2008**, *100* (2), 238–253. https://doi.org/10.1017/S0007114508922522.

(187) Fordyce, F. M. Selenium Deficiency and Toxicity in the Environment. In *Essentials of Medical Geology: Revised Edition*; Selinus, O., Ed.; Springer Netherlands: Dordrecht, 2013; pp 375–416. https://doi.org/10.1007/978-94-007-4375-5_16.

(188) *Encyclopedia of Human Nutrition*; Academic Press, 2012.

(189) Letavayová, L.; Vlcková, V.; Brozmanová, J. Selenium: From Cancer Prevention to DNA Damage. *Toxicology* **2006**, *227* (1–2), 1–14. https://doi.org/10.1016/j.tox.2006.07.017.

(190) Fraga, C. G. Relevance, Essentiality and Toxicity of Trace Elements in Human Health. *Mol. Aspects Med.* **2005**, *26* (4–5), 235–244. https://doi.org/10.1016/j.mam.2005.07.013.

(191) Whanger, P. D. Selenium and Its Relationship to Cancer: An Update. *Br. J. Nutr.* **2004**, *91* (1), 11–28. https://doi.org/10.1079/bjn20031015.

(192) Medical Definition of SELENOSIS https://www.merriam-webster.com/medical/selenosis (accessed Jun 1, 2020).

(193) Vinceti, M.; Filippini, T.; Del Giovane, C.; Dennert, G.; Zwahlen, M.; Brinkman, M.; Zeegers, M. P.; Horneber, M.; D'Amico, R.; Crespi, C. M. Selenium for Preventing Cancer. *Cochrane Database Syst Rev* **2018**, *1*, CD005195. https://doi.org/10.1002/14651858.CD005195.pub4.

(194) Schwarz, K.; Foltz, C. M. SELENIUM AS AN INTEGRAL PART OF FACTOR 3 AGAINST DIETARY NECROTIC LIVER DEGENERATION. *J. Am. Chem. Soc.* **1957**, *79* (12), 3292–3293. https://doi.org/10.1021/ja01569a087.

(195) Combs, G. F.; Combs, S. B. The Nutritional Biochemistry of Selenium. *Annual Review of Nutrition* **1984**, *4* (1), 257–280. https://doi.org/10.1146/annurev.nu.04.070184.001353.

(196) Hazane-Puch, F.; Arnaud, J.; Trocmé, C.; Faure, P.; Laporte, F.; Champelovier, P. Sodium Selenite Decreased HDAC Activity, Cell Proliferation and Induced Apoptosis

in Three Human Glioblastoma Cells. *Anticancer Agents Med Chem* **2016**, *16* (4), 490–500. https://doi.org/10.2174/1871520615666150819095426.

(197) Vinceti, M.; Filippini, T.; Cilloni, S.; Bargellini, A.; Vergoni, A. V.; Tsatsakis, A.; Ferrante, M. Health Risk Assessment of Environmental Selenium: Emerging Evidence and Challenges. *Mol Med Rep* **2017**, *15* (5), 3323–3335. https://doi.org/10.3892/mmr.2017.6377.

(198) Mandrioli, J.; Michalke, B.; Solovyev, N.; Grill, P.; Violi, F.; Lunetta, C.; Conte, A.; Sansone, V. A.; Sabatelli, M.; Vinceti, M. Elevated Levels of Selenium Species in Cerebrospinal Fluid of Amyotrophic Lateral Sclerosis Patients with Disease-Associated Gene Mutations. *Neurodegener Dis* **2017**, *17* (4–5), 171–180. https://doi.org/10.1159/000460253.

(199) Wallenberg, M.; Misra, S.; Björnstedt, M. Selenium Cytotoxicity in Cancer. *Basic Clin. Pharmacol. Toxicol.* **2014**, *114* (5), 377–386. https://doi.org/10.1111/bcpt.12207.

(200) Cherest, H.; Davidian, J. C.; Thomas, D.; Benes, V.; Ansorge, W.; Surdin-Kerjan, Y. Molecular Characterization of Two High Affinity Sulfate Transporters in Saccharomyces Cerevisiae. *Genetics* **1997**, *145* (3), 627–635.

(201) Lazard, M.; Blanquet, S.; Fisicaro, P.; Labarraque, G.; Plateau, P. Uptake of Selenite by Saccharomyces Cerevisiae Involves the High and Low Affinity Orthophosphate Transporters. *J. Biol. Chem.* **2010**, *285* (42), 32029–32037. https://doi.org/10.1074/jbc.M110.139865.

(202) Haratake, M.; Hongoh, M.; Ono, M.; Nakayama, M. Thiol-Dependent Membrane Transport of Selenium through an Integral Protein of the Red Blood Cell Membrane. *Inorg. Chem.* **2009**, *48* (16), 7805–7811. https://doi.org/10.1021/ic900988j.

(203) Burk, R. F.; Hill, K. E. Regulation of Selenium Metabolism and Transport. *Annu. Rev. Nutr.* **2015**, *35*, 109–134. https://doi.org/10.1146/annurev-nutr-071714-034250.

(204) Ross, A. C.; Caballero, B. H.; Cousins, R. J.; Tucker, K. L.; Ziegler, T. R. *Modern Nutrition in Health and Disease: Eleventh Edition*; Wolters Kluwer Health Adis (ESP), 2012.

(205) Roman, M.; Jitaru, P.; Barbante, C. Selenium Biochemistry and Its Role for Human Health. *Metallomics* **2014**, *6* (1), 25–54. https://doi.org/10.1039/c3mt00185g.

(206) *Selenium: Its Molecular Biology and Role in Human Health*, 3rd ed.; Hatfield, D. L., Berry, M. J., Gladyshev, V. N., Eds.; Springer-Verlag: New York, 2012. https://doi.org/10.1007/978-1-4614-1025-6.

(207) Speckmann, B.; Grune, T. Epigenetic Effects of Selenium and Their Implications for Health. *Epigenetics* **2015**, *10* (3), 179–190. https://doi.org/10.1080/15592294.2015.1013792.

(208) Skalickova, S.; Milosavljevic, V.; Cihalova, K.; Horky, P.; Richtera, L.; Adam, V. Selenium Nanoparticles as a Nutritional Supplement. *Nutrition* **2017**, *33*, 83–90. https://doi.org/10.1016/j.nut.2016.05.001.

(209) Nakamuro, K.; Okuno, T.; Hasegawa, T. Metabolism of Selenoamino Acids and Contribution of Selenium Methylation to Their Toxicity. *Journal of Health Science* **2000**, *46* (6), 418–421. https://doi.org/10.1248/jhs.46.418.

(210) Papp, L. V.; Lu, J.; Holmgren, A.; Khanna, K. K. From Selenium to Selenoproteins: Synthesis, Identity, and Their Role in Human Health. *Antioxid. Redox Signal.* **2007**, *9* (7), 775–806. https://doi.org/10.1089/ars.2007.1528.

(211) Rayman, M. P. Selenium in Cancer Prevention: A Review of the Evidence and Mechanism of Action. *Proceedings of the Nutrition Society* **2005**, *64* (4), 527–542. https://doi.org/10.1079/PNS2005467.

(212) Brozmanová, J.; Mániková, D.; Vlčková, V.; Chovanec, M. Selenium: A Double-Edged Sword for Defense and Offence in Cancer. *Arch Toxicol* **2010**, *84* (12), 919–938. https://doi.org/10.1007/s00204-010-0595-8.

(213) Yu, Y. P.; Yu, G.; Tseng, G.; Cieply, K.; Nelson, J.; Defrances, M.; Zarnegar, R.; Michalopoulos, G.; Luo, J.-H. Glutathione Peroxidase 3, Deleted or Methylated in Prostate Cancer, Suppresses Prostate Cancer Growth and Metastasis. *Cancer Research* **2007**, *67* (17), 8043–8050. https://doi.org/10.1158/0008-5472.CAN-07-0648.

(214) Shetty, S.; Marsicano, J. R.; Copeland*, P. R. Uptake and Utilization of Selenium from Selenoprotein P. *Biol Trace Elem Res* **2018**, *181* (1), 54–61. https://doi.org/10.1007/s12011-017-1044-9.

(215) Klein, E. A.; Thompson, I. M.; Lippman, S. M.; Goodman, P. J.; Albanes, D.; Taylor, P. R.; Coltman, C. SELECT: The Selenium and Vitamin E Cancer Prevention Trial: Rationale and Design. *Prostate Cancer Prostatic Dis.* **2000**, *3* (3), 145–151. https://doi.org/10.1038/sj.pcan.4500412.

(216) Hurst, R.; Fairweather-Tait, S. Selenium and Vitamin E Supplementation for Cancer Prevention. *JAMA* **2009**, *301* (18), 1876–1877; author reply 1877. https://doi.org/10.1001/jama.2009.626.

(217) Jabłońska, E.; Reszka, E. Selenium and Epigenetics in Cancer: Focus on DNA Methylation. *Adv. Cancer Res.* **2017**, *136*, 193–234. https://doi.org/10.1016/bs.acr.2017.07.002.

(218) Mehdi, Y.; Hornick, J.-L.; Istasse, L.; Dufrasne, I. Selenium in the Environment, Metabolism and Involvement in Body Functions. *Molecules* **2013**, *18* (3), 3292–3311. https://doi.org/10.3390/molecules18033292.

(219) Davis, C. D.; Tsuji, P. A.; Milner, J. A. Selenoproteins and Cancer Prevention. *Annu. Rev. Nutr.* **2012**, *32*, 73–95. https://doi.org/10.1146/annurev-nutr-071811-150740.

(220) Chan, J. M.; Darke, A. K.; Penney, K. L.; Tangen, C. M.; Goodman, P. J.; Lee, G.-S. M.; Sun, T.; Peisch, S.; Tinianow, A. M.; Rae, J. M.; Klein, E. A.; Thompson, I. M.; Kantoff, P. W.; Mucci, L. A. Selenium- or Vitamin E-Related Gene Variants, Interaction with Supplementation, and Risk of High-Grade Prostate Cancer in SELECT. *Cancer Epidemiol. Biomarkers Prev.* **2016**, *25* (7), 1050–1058. https://doi.org/10.1158/1055-9965.EPI-16-0104.

(221) Zu, K.; Bihani, T.; Lin, A.; Park, Y.-M.; Mori, K.; Ip, C. Enhanced Selenium Effect on Growth Arrest by BiP/GRP78 Knockdown in P53-Null Human Prostate Cancer Cells. *Oncogene* **2006**, *25* (4), 546–554. https://doi.org/10.1038/sj.onc.1209071.

(222) Geyikoglu, F.; Türkez, H. Protective Effect of Sodium Selenite against the Genotoxicity of Aflatoxin B1 in Human Whole Blood Cultures. *Brazilian Archives of Biology and Technology* **2006**, *49* (3), 393–398. https://doi.org/10.1590/S1516-89132006000400006.

(223) Pourkhalili, N.; Hosseini, A.; Nili-Ahmadabadi, A.; Rahimifard, M.; Navaei-Nigjeh, M.; Hassani, S.; Baeeri, M.; Abdollahi, M. Improvement of Isolated Rat Pancreatic Islets Function by Combination of Cerium Oxide Nanoparticles/Sodium Selenite through Reduction of Oxidative Stress. *Toxicology Mechanisms and Methods* **2012**, *22* (6), 476–482. https://doi.org/10.3109/15376516.2012.673093.

(224) Ghosh, J. Rapid Induction of Apoptosis in Prostate Cancer Cells by Selenium: Reversal by Metabolites of Arachidonate 5-Lipoxygenase. *Biochem. Biophys. Res. Commun.* **2004**, *315* (3), 624–635. https://doi.org/10.1016/j.bbrc.2004.01.100.

(225) Kim, E. H.; Sohn, S.; Kwon, H. J.; Kim, S. U.; Kim, M.-J.; Lee, S.-J.; Choi, K. S. Sodium Selenite Induces Superoxide-Mediated Mitochondrial Damage and Subsequent Autophagic Cell Death in Malignant Glioma Cells. *Cancer Res.* **2007**, *67* (13), 6314–6324. https://doi.org/10.1158/0008-5472.CAN-06-4217.

(226) Řezáčová, K.; Čáňová, K.; Bezrouk, A.; Rudolf, E. Selenite Induces DNA Damage and Specific Mitochondrial Degeneration in Human Bladder Cancer Cells. *Toxicol In Vitro* **2016**, *32*, 105–114. https://doi.org/10.1016/j.tiv.2015.12.011.
(227) Wang, Z.; Jiang, C.; Lü, J. Induction of Caspase-Mediated Apoptosis and Cell-Cycle G1 Arrest by Selenium Metabolite Methylselenol. *Mol. Carcinog.* **2002**, *34* (3), 113–120. https://doi.org/10.1002/mc.10056.
(228) Zeng, H.; Briske-Anderson, M.; Idso, J. P.; Hunt, C. D. The Selenium Metabolite Methylselenol Inhibits the Migration and Invasion Potential of HT1080 Tumor Cells. *J. Nutr.* **2006**, *136* (6), 1528–1532. https://doi.org/10.1093/jn/136.6.1528.
(229) Zhu, Z.; Jiang, W.; Ganther, H. E.; Thompson, H. J. Mechanisms of Cell Cycle Arrest by Methylseleninic Acid. *Cancer Res.* **2002**, *62* (1), 156–164.
(230) Liu, Y.; Tang, J.; Liu, D.; Zhang, L.; He, Y.; Li, J.; Gao, L.; Tang, D.; Jin, X.; Kong, D. Increased Autophagy in EOC Re-Ascites Cells Can Inhibit Cell Death and Promote Drug Resistance. *Cell Death & Disease* **2018**, *9* (4), 1–10. https://doi.org/10.1038/s41419-018-0449-5.
(231) Xiang, N.; Zhao, R.; Zhong, W. Sodium Selenite Induces Apoptosis by Generation of Superoxide via the Mitochondrial-Dependent Pathway in Human Prostate Cancer Cells. *Cancer Chemother. Pharmacol.* **2009**, *63* (2), 351–362. https://doi.org/10.1007/s00280-008-0745-3.
(232) Liu, J.; Li, J.; Zhang, J.-F.; Xin, X.-Y. Combination of Fenretinide and Selenite Inhibits Proliferation and Induces Apoptosis in Ovarian Cancer Cells. *Int J Mol Sci* **2013**, *14* (11), 21790–21804. https://doi.org/10.3390/ijms141121790.
(233) Berthier, S.; Arnaud, J.; Champelovier, P.; Col, E.; Garrel, C.; Cottet, C.; Boutonnat, J.; Laporte, F.; Faure, P.; Hazane-Puch, F. Anticancer Properties of Sodium Selenite in Human Glioblastoma Cell Cluster Spheroids. *Journal of Trace Elements in Medicine and Biology* **2017**, *44*, 161–176. https://doi.org/10.1016/j.jtemb.2017.04.012.
(234) Fischer, J. L.; Mihelc, E. M.; Pollok, K. E.; Smith, M. L. Chemotherapeutic Selectivity Conferred by Selenium: A Role for P53-Dependent DNA Repair. *Mol Cancer Ther* **2007**, *6* (1), 355–361. https://doi.org/10.1158/1535-7163.MCT-06-0472.
(235) de Rosa, V.; Erkekoğlu, P.; Forestier, A.; Favier, A.; Hincal, F.; Diamond, A. M.; Douki, T.; Rachidi, W. Low Doses of Selenium Specifically Stimulate the Repair of Oxidative DNA Damage in LNCaP Prostate Cancer Cells. *Free Radic. Res.* **2012**, *46* (2), 105–116. https://doi.org/10.3109/10715762.2011.647009.
(236) Baliga, M. S.; Wang, H.; Zhuo, P.; Schwartz, J. L.; Diamond, A. M. Selenium and GPx-1 Overexpression Protect Mammalian Cells against UV-Induced DNA Damage. *Biol Trace Elem Res* **2007**, *115* (3), 227–242. https://doi.org/10.1007/BF02685998.
(237) Cui, J.; Yan, M.; Liu, X.; Yin, S.; Lu, S.; Fan, L.; Hu, H. Inorganic Selenium Induces Nonapoptotic Programmed Cell Death in PC-3 Prostate Cancer Cells Associated with Inhibition of Glycolysis. *J. Agric. Food Chem.* **2019**, *67* (38), 10637–10645. https://doi.org/10.1021/acs.jafc.9b03875.
(238) Forman, H. J.; Fukuto, J. M.; Torres, M. Redox Signaling: Thiol Chemistry Defines Which Reactive Oxygen and Nitrogen Species Can Act as Second Messengers. *Am. J. Physiol., Cell Physiol.* **2004**, *287* (2), C246-256. https://doi.org/10.1152/ajpcell.00516.2003.
(239) Dröge, W. Free Radicals in the Physiological Control of Cell Function. *Physiol. Rev.* **2002**, *82* (1), 47–95. https://doi.org/10.1152/physrev.00018.2001.
(240) Tarze, A.; Dauplais, M.; Grigoras, I.; Lazard, M.; Ha-Duong, N.-T.; Barbier, F.; Blanquet, S.; Plateau, P. Extracellular Production of Hydrogen Selenide Accounts for Thiol-Assisted Toxicity of Selenite against Saccharomyces Cerevisiae. *J. Biol. Chem.* **2007**, *282* (12), 8759–8767. https://doi.org/10.1074/jbc.M610078200.

(241) Morrison, D. G.; Berdan, R. C.; Pauly, D. F.; Turner, D. S.; Oborn, C. J.; Medina, D. Selenium Distribution in Mammary Epithelial Cells Reveals Its Possible Mechanism of Inhibition of Cell Growth. *Anticancer Res.* **1988**, *8* (1), 51–63.

(242) Kumar, S.; Björnstedt, M.; Holmgren, A. Selenite Is a Substrate for Calf Thymus Thioredoxin Reductase and Thioredoxin and Elicits a Large Non-Stoichiometric Oxidation of NADPH in the Presence of Oxygen. *Eur. J. Biochem.* **1992**, *207* (2), 435–439. https://doi.org/10.1111/j.1432-1033.1992.tb17068.x.

(243) Petronilli, V.; Costantini, P.; Scorrano, L.; Colonna, R.; Passamonti, S.; Bernardi, P. The Voltage Sensor of the Mitochondrial Permeability Transition Pore Is Tuned by the Oxidation-Reduction State of Vicinal Thiols. Increase of the Gating Potential by Oxidants and Its Reversal by Reducing Agents. *J. Biol. Chem.* **1994**, *269* (24), 16638–16642.

(244) Peyroche, G.; Saveanu, C.; Dauplais, M.; Lazard, M.; Beuneu, F.; Decourty, L.; Malabat, C.; Jacquier, A.; Blanquet, S.; Plateau, P. Sodium Selenide Toxicity Is Mediated by O2-Dependent DNA Breaks. *PLoS One* **2012**, *7* (5). https://doi.org/10.1371/journal.pone.0036343.

(245) Spallholz, J. E. On the Nature of Selenium Toxicity and Carcinostatic Activity. *Free Radical Biology and Medicine* **1994**, *17* (1), 45–64. https://doi.org/10.1016/0891-5849(94)90007-8.

(246) Shen, H. M.; Yang, C. F.; Ding, W. X.; Liu, J.; Ong, C. N. Superoxide Radical-Initiated Apoptotic Signalling Pathway in Selenite-Treated HepG(2) Cells: Mitochondria Serve as the Main Target. *Free Radic. Biol. Med.* **2001**, *30* (1), 9–21. https://doi.org/10.1016/s0891-5849(00)00421-4.

(247) Herrero, E.; Wellinger, R. E. Yeast as a Model System to Study Metabolic Impact of Selenium Compounds. *Microb Cell 2* (5), 139–149. https://doi.org/10.15698/mic2015.05.200.

(248) Zhang, Y.; Li, X.; Huang, Z.; Zheng, W.; Fan, C.; Chen, T. Enhancement of Cell Permeabilization Apoptosis-Inducing Activity of Selenium Nanoparticles by ATP Surface Decoration. *Nanomedicine: Nanotechnology, Biology and Medicine* **2013**, *9* (1), 74–84. https://doi.org/10.1016/j.nano.2012.04.002.

(249) Sun, D.; Liu, Y.; Yu, Q.; Zhou, Y.; Zhang, R.; Chen, X.; Hong, A.; Liu, J. The Effects of Luminescent Ruthenium(II) Polypyridyl Functionalized Selenium Nanoparticles on BFGF-Induced Angiogenesis and AKT/ERK Signaling. *Biomaterials* **2013**, *34* (1), 171–180. https://doi.org/10.1016/j.biomaterials.2012.09.031.

(250) Huang, G.; Liu, Z.; He, L.; Luk, K.-H.; Cheung, S.-T.; Wong, K.-H.; Chen, T. Autophagy Is an Important Action Mode for Functionalized Selenium Nanoparticles to Exhibit Anti-Colorectal Cancer Activity. *Biomater Sci* **2018**, *6* (9), 2508–2517. https://doi.org/10.1039/c8bm00670a.

(251) Czabotar, P. E.; Lessene, G.; Strasser, A.; Adams, J. M. Control of Apoptosis by the BCL-2 Protein Family: Implications for Physiology and Therapy. *Nature Reviews Molecular Cell Biology* **2014**, *15* (1), 49–63. https://doi.org/10.1038/nrm3722.

(252) Khurana, A.; Tekula, S.; Saifi, M. A.; Venkatesh, P.; Godugu, C. Therapeutic Applications of Selenium Nanoparticles. *Biomedicine & Pharmacotherapy* **2019**, *111*, 802–812. https://doi.org/10.1016/j.biopha.2018.12.146.

(253) Sonkusre, P.; Cameotra, S. S. Biogenic Selenium Nanoparticles Induce ROS-Mediated Necroptosis in PC-3 Cancer Cells through TNF Activation. *J Nanobiotechnology* **2017**, *15* (1), 43. https://doi.org/10.1186/s12951-017-0276-3.

(254) Zhao, S.; Yu, Q.; Pan, J.; Zhou, Y.; Cao, C.; Ouyang, J.-M.; Liu, J. Redox-Responsive Mesoporous Selenium Delivery of Doxorubicin Targets MCF-7 Cells and Synergistically Enhances Its Anti-Tumor Activity. *Acta Biomaterialia* **2017**, *54*, 294–306. https://doi.org/10.1016/j.actbio.2017.02.042.

(255) Fulda, S.; Debatin, K.-M. Extrinsic versus Intrinsic Apoptosis Pathways in Anticancer Chemotherapy. *Oncogene* **2006**, *25* (34), 4798–4811. https://doi.org/10.1038/sj.onc.1209608.

(256) Huang, Y.; He, L.; Liu, W.; Fan, C.; Zheng, W.; Wong, Y.-S.; Chen, T. Selective Cellular Uptake and Induction of Apoptosis of Cancer-Targeted Selenium Nanoparticles. *Biomaterials* **2013**, *34* (29), 7106–7116. https://doi.org/10.1016/j.biomaterials.2013.04.067.

(257) Wang, X.; Sun, K.; Tan, Y.; Wu, S.; Zhang, J. Efficacy and Safety of Selenium Nanoparticles Administered Intraperitoneally for the Prevention of Growth of Cancer Cells in the Peritoneal Cavity. *Free Radical Biology and Medicine* **2014**, *72*, 1–10. https://doi.org/10.1016/j.freeradbiomed.2014.04.003.

(258) Wang, Y.; Chen, P.; Zhao, G.; Sun, K.; Li, D.; Wan, X.; Zhang, J. Inverse Relationship between Elemental Selenium Nanoparticle Size and Inhibition of Cancer Cell Growth in Vitro and in Vivo. *Food and Chemical Toxicology* **2015**, *85*, 71–77. https://doi.org/10.1016/j.fct.2015.08.006.

(259) Srivastava, P.; Kowshik, M. Anti-Neoplastic Selenium Nanoparticles from Idiomarina Sp. PR58-8. *Enzyme and Microbial Technology* **2016**, *95*, 192–200. https://doi.org/10.1016/j.enzmictec.2016.08.002.

(260) Fu, X.; Yang, Y.; Li, X.; Lai, H.; Huang, Y.; He, L.; Zheng, W.; Chen, T. RGD Peptide-Conjugated Selenium Nanoparticles: Antiangiogenesis by Suppressing VEGF-VEGFR2-ERK/AKT Pathway. *Nanomedicine: Nanotechnology, Biology and Medicine* **2016**, *12* (6), 1627–1639. https://doi.org/10.1016/j.nano.2016.01.012.

(261) Degenhardt, K.; Mathew, R.; Beaudoin, B.; Bray, K.; Anderson, D.; Chen, G.; Mukherjee, C.; Shi, Y.; Gélinas, C.; Fan, Y.; Nelson, D. A.; Jin, S.; White, E. Autophagy Promotes Tumor Cell Survival and Restricts Necrosis, Inflammation, and Tumorigenesis. *Cancer Cell* **2006**, *10* (1), 51–64. https://doi.org/10.1016/j.ccr.2006.06.001.

(262) Kang, R.; Zeh, H. J.; Lotze, M. T.; Tang, D. The Beclin 1 Network Regulates Autophagy and Apoptosis. *Cell Death Differ* **2011**, *18* (4), 571–580. https://doi.org/10.1038/cdd.2010.191.

(263) Králová, V.; Benešová, S.; Červinka, M.; Rudolf, E. Selenite-Induced Apoptosis and Autophagy in Colon Cancer Cells. *Toxicology in Vitro* **2012**, *26* (2), 258–268. https://doi.org/10.1016/j.tiv.2011.12.010.

(264) YANG, Y.; LUO, H.; HUI, K.; CI, Y.; SHI, K.; CHEN, G.; SHI, L.; XU, C. Selenite-Induced Autophagy Antagonizes Apoptosis in Colorectal Cancer Cells in Vitro and in Vivo. *Oncol Rep* **2016**, *35* (3), 1255–1264. https://doi.org/10.3892/or.2015.4484.

(265) Xiang, N.; Zhao, R.; Song, G.; Zhong, W. Selenite Reactivates Silenced Genes by Modifying DNA Methylation and Histones in Prostate Cancer Cells. *Carcinogenesis* **2008**, *29* (11), 2175–2181. https://doi.org/10.1093/carcin/bgn179.

(266) de Miranda, J. X.; Andrade, F. de O.; Conti, A. de; Dagli, M. L. Z.; Moreno, F. S.; Ong, T. P. Effects of Selenium Compounds on Proliferation and Epigenetic Marks of Breast Cancer Cells. *J Trace Elem Med Biol* **2014**, *28* (4), 486–491. https://doi.org/10.1016/j.jtemb.2014.06.017.

(267) Ganther, H. E. Selenium Metabolism, Selenoproteins and Mechanisms of Cancer Prevention: Complexities with Thioredoxin Reductase. *Carcinogenesis* **1999**, *20* (9), 1657–1666. https://doi.org/10.1093/carcin/20.9.1657.

(268) Zeng, H.; Combs, G. F. Selenium as an Anticancer Nutrient: Roles in Cell Proliferation and Tumor Cell Invasion. *The Journal of Nutritional Biochemistry* **2008**, *19* (1), 1–7. https://doi.org/10.1016/j.jnutbio.2007.02.005.

(269) Liu, W.; Li, X.; Wong, Y.-S.; Zheng, W.; Zhang, Y.; Cao, W.; Chen, T. Selenium Nanoparticles as a Carrier of 5-Fluorouracil to Achieve Anticancer Synergism. *ACS Nano* **2012**, *6* (8), 6578–6591. https://doi.org/10.1021/nn202452c.

(270) Chen, T.; Wong, Y.-S.; Zheng, W.; Bai, Y.; Huang, L. Selenium Nanoparticles Fabricated in Undaria Pinnatifida Polysaccharide Solutions Induce Mitochondria-Mediated Apoptosis in A375 Human Melanoma Cells. *Colloids and Surfaces B: Biointerfaces* **2008**, *67* (1), 26–31. https://doi.org/10.1016/j.colsurfb.2008.07.010.

(271) Zhang, J.; Wang, X.; Xu, T. Elemental Selenium at Nano Size (Nano-Se) as a Potential Chemopreventive Agent with Reduced Risk of Selenium Toxicity: Comparison with Se-Methylselenocysteine in Mice. *Toxicol. Sci.* **2008**, *101* (1), 22–31. https://doi.org/10.1093/toxsci/kfm221.

(272) Wang, H.; Zhang, J.; Yu, H. Elemental Selenium at Nano Size Possesses Lower Toxicity without Compromising the Fundamental Effect on Selenoenzymes: Comparison with Selenomethionine in Mice. *Free Radic. Biol. Med.* **2007**, *42* (10), 1524–1533. https://doi.org/10.1016/j.freeradbiomed.2007.02.013.

(273) Zhang, E.; Xing, R.; Liu, S.; Qin, Y.; Li, K.; Li, P. Advances in Chitosan-Based Nanoparticles for Oncotherapy. *Carbohydr Polym* **2019**, *222*, 115004. https://doi.org/10.1016/j.carbpol.2019.115004.

(274) Huang, B.; Zhang, J.; Hou, J.; Chen, C. Free Radical Scavenging Efficiency of Nano-Se in Vitro. *Free Radical Biology and Medicine* **2003**, *35* (7), 805–813. https://doi.org/10.1016/S0891-5849(03)00428-3.

(275) Zhang, J.; Wang, H.; Yan, X.; Zhang, L. Comparison of Short-Term Toxicity between Nano-Se and Selenite in Mice. *Life Sci.* **2005**, *76* (10), 1099–1109. https://doi.org/10.1016/j.lfs.2004.08.015.

(276) Zhai, X.; Zhang, C.; Zhao, G.; Stoll, S.; Ren, F.; Leng, X. Antioxidant Capacities of the Selenium Nanoparticles Stabilized by Chitosan. *Journal of Nanobiotechnology* **2017**, *15* (1), 4. https://doi.org/10.1186/s12951-016-0243-4.

(277) Bai, Y.; Wang, Y.; Zhou, Y.; Li, W.; Zheng, W. Modification and Modulation of Saccharides on Elemental Selenium Nanoparticles in Liquid Phase. *Materials Letters* **2008**, *15* (62), 2311–2314. https://doi.org/10.1016/j.matlet.2007.11.098.

(278) Peng, D.; Zhang, J.; Liu, Q.; Taylor, E. W. Size Effect of Elemental Selenium Nanoparticles (Nano-Se) at Supranutritional Levels on Selenium Accumulation and Glutathione S-Transferase Activity. *J. Inorg. Biochem.* **2007**, *101* (10), 1457–1463. https://doi.org/10.1016/j.jinorgbio.2007.06.021.

(279) Zhang, J.-S.; Gao, X.-Y.; Zhang, L.-D.; Bao, Y.-P. Biological Effects of a Nano Red Elemental Selenium. *BioFactors* **2001**, *15* (1), 27–38. https://doi.org/10.1002/biof.5520150103.

(280) Rinaudo, M. Chitin and Chitosan: Properties and Applications. *Progress in Polymer Science* **2006**, *31* (7), 603–632. https://doi.org/10.1016/j.progpolymsci.2006.06.001.

(281) Yu, B.; Zhang, Y.; Zheng, W.; Fan, C.; Chen, T. Positive Surface Charge Enhances Selective Cellular Uptake and Anticancer Efficacy of Selenium Nanoparticles. *Inorg. Chem.* **2012**, *51* (16), 8956–8963. https://doi.org/10.1021/ic301050v.

(282) Estevez, H.; Garcia-Lidon, J. C.; Luque-Garcia, J. L.; Camara, C. Effects of Chitosan-Stabilized Selenium Nanoparticles on Cell Proliferation, Apoptosis and Cell Cycle Pattern in HepG2 Cells: Comparison with Other Selenospecies. *Colloids and Surfaces B: Biointerfaces* **2014**, *122*, 184–193. https://doi.org/10.1016/j.colsurfb.2014.06.062.

(283) Cummings, J.; McArdle, C. S. Studies on the in Vivo Disposition of Adriamycin in Human Tumours Which Exhibit Different Responses to the Drug. *British Journal of Cancer* **1986**, *53* (6), 835–838. https://doi.org/10.1038/bjc.1986.141.

(284) Yoo, H. S.; Park, T. G. Folate-Receptor-Targeted Delivery of Doxorubicin Nano-Aggregates Stabilized by Doxorubicin–PEG–Folate Conjugate. *Journal of Controlled Release* **2004**, *100* (2), 247–256. https://doi.org/10.1016/j.jconrel.2004.08.017.
(285) Shahverdi, A. R.; Shahverdi, F.; Faghfuri, E.; Reza Khoshayand, M.; Mavandadnejad, F.; Yazdi, M. H.; Amini, M. Characterization of Folic Acid Surface-Coated Selenium Nanoparticles and Corresponding In Vitro and In Vivo Effects Against Breast Cancer. *Arch. Med. Res.* **2018**, *49* (1), 10–17. https://doi.org/10.1016/j.arcmed.2018.04.007.
(286) Luesakul, U.; Puthong, S.; Neamati, N.; Muangsin, N. PH-Responsive Selenium Nanoparticles Stabilized by Folate-Chitosan Delivering Doxorubicin for Overcoming Drug-Resistant Cancer Cells. *Carbohydr Polym* **2018**, *181*, 841–850. https://doi.org/10.1016/j.carbpol.2017.11.068.
(287) Pi, J.; Jin, H.; Liu, R.; Song, B.; Wu, Q.; Liu, L.; Jiang, J.; Yang, F.; Cai, H.; Cai, J. Pathway of Cytotoxicity Induced by Folic Acid Modified Selenium Nanoparticles in MCF-7 Cells. *Appl Microbiol Biotechnol* **2013**, *97* (3), 1051–1062. https://doi.org/10.1007/s00253-012-4359-7.
(288) Unsoy, G.; Khodadust, R.; Yalcin, S.; Mutlu, P.; Gunduz, U. Synthesis of Doxorubicin Loaded Magnetic Chitosan Nanoparticles for PH Responsive Targeted Drug Delivery. *European Journal of Pharmaceutical Sciences* **2014**, *62*, 243–250. https://doi.org/10.1016/j.ejps.2014.05.021.
(289) Bidkar, A. P.; Sanpui, P.; Ghosh, S. S. Efficient Induction of Apoptosis in Cancer Cells by Paclitaxel-Loaded Selenium Nanoparticles. *Nanomedicine (Lond)* **2017**, *12* (21), 2641–2651. https://doi.org/10.2217/nnm-2017-0189.
(290) Rezvanfar, M. A.; Rezvanfar, M. A.; Shahverdi, A. R.; Ahmadi, A.; Baeeri, M.; Mohammadirad, A.; Abdollahi, M. Protection of Cisplatin-Induced Spermatotoxicity, DNA Damage and Chromatin Abnormality by Selenium Nano-Particles. *Toxicology and Applied Pharmacology* **2013**, *266* (3), 356–365. https://doi.org/10.1016/j.taap.2012.11.025.
(291) Vekariya, K. K.; Kaur, J.; Tikoo, K. Alleviating Anastrozole Induced Bone Toxicity by Selenium Nanoparticles in SD Rats. *Toxicology and Applied Pharmacology* **2013**, *268* (2), 212–220. https://doi.org/10.1016/j.taap.2013.01.028.
(292) Hassanin, K. M. A.; Abd El-Kawi, S. H.; Hashem, K. S. The Prospective Protective Effect of Selenium Nanoparticles against Chromium-Induced Oxidative and Cellular Damage in Rat Thyroid. *International Journal of Nanomedicine* **2013**, *8*, 1713–1720. https://doi.org/10.2147/IJN.S42736.
(293) Sun, F.; Wang, J.; Wu, X.; Yang, C. S.; Zhang, J. Selenium Nanoparticles Act as an Intestinal P53 Inhibitor Mitigating Chemotherapy-Induced Diarrhea in Mice. *Pharmacol. Res.* **2019**, *149*, 104475. https://doi.org/10.1016/j.phrs.2019.104475.
(294) Xu, C.; Qiao, L.; Ma, L.; Guo, Y.; Dou, X.; Yan, S.; Zhang, B.; Roman, A. Biogenic Selenium Nanoparticles Synthesized by Lactobacillus Casei ATCC 393 Alleviate Intestinal Epithelial Barrier Dysfunction Caused by Oxidative Stress via Nrf2 Signaling-Mediated Mitochondrial Pathway. *Int J Nanomedicine* **2019**, *14*, 4491–4502. https://doi.org/10.2147/IJN.S199193.
(295) Sadek, K. M.; Lebda, M. A.; Abouzed, T. K.; Nasr, S. M.; Shoukry, M. Neuro- and Nephrotoxicity of Subchronic Cadmium Chloride Exposure and the Potential Chemoprotective Effects of Selenium Nanoparticles. *Metab Brain Dis* **2017**, *32* (5), 1659–1673. https://doi.org/10.1007/s11011-017-0053-x.
(296) Luo, H.; Wang, F.; Bai, Y.; Chen, T.; Zheng, W. Selenium Nanoparticles Inhibit the Growth of HeLa and MDA-MB-231 Cells through Induction of S Phase Arrest. *Colloids and Surfaces B: Biointerfaces* **2012**, *94*, 304–308. https://doi.org/10.1016/j.colsurfb.2012.02.006.

(297) Vekariya, K. K.; Kaur, J.; Tikoo, K. ERα Signaling Imparts Chemotherapeutic Selectivity to Selenium Nanoparticles in Breast Cancer. *Nanomedicine: Nanotechnology, Biology and Medicine* **2012**, *8* (7), 1125–1132. https://doi.org/10.1016/j.nano.2011.12.003.

(298) Zheng, J.-S.; Zheng, S.-Y.; Zhang, Y.-B.; Yu, B.; Zheng, W.; Yang, F.; Chen, T. Sialic Acid Surface Decoration Enhances Cellular Uptake and Apoptosis-Inducing Activity of Selenium Nanoparticles. *Colloids Surf B Biointerfaces* **2011**, *83* (1), 183–187. https://doi.org/10.1016/j.colsurfb.2010.11.023.

(299) Gao, F.; Yuan, Q.; Gao, L.; Cai, P.; Zhu, H.; Liu, R.; Wang, Y.; Wei, Y.; Huang, G.; Liang, J.; Gao, X. Cytotoxicity and Therapeutic Effect of Irinotecan Combined with Selenium Nanoparticles. *Biomaterials* **2014**, *35* (31), 8854–8866. https://doi.org/10.1016/j.biomaterials.2014.07.004.

(300) Fife, C. M.; McCarroll, J. A.; Kavallaris, M. Movers and Shakers: Cell Cytoskeleton in Cancer Metastasis. *Br. J. Pharmacol.* **2014**, *171* (24), 5507–5523. https://doi.org/10.1111/bph.12704.

(301) Bao, P.; Chen, Z.; Tai, R.-Z.; Shen, H.-M.; Martin, F. L.; Zhu, Y.-G. Selenite-Induced Toxicity in Cancer Cells Is Mediated by Metabolic Generation of Endogenous Selenium Nanoparticles. *J. Proteome Res.* **2015**, *14* (2), 1127–1136. https://doi.org/10.1021/pr501086e.

(302) Nasrolahi Shirazi, A.; Tiwari, R. K.; Oh, D.; Sullivan, B.; Kumar, A.; Beni, Y. A.; Parang, K. Cyclic Peptide–Selenium Nanoparticles as Drug Transporters. *Mol. Pharmaceutics* **2014**, *11* (10), 3631–3641. https://doi.org/10.1021/mp500364a.